

New Strategies in Bioconjugation -
Chemical Modification of Nucleic Acids and Peptides

Inauguraldissertation

zur

Erlangung der Würde eines Doktors der Philosophie

vorgelegt der

Philosophisch-Naturwissenschaftlichen Fakultät

der Universität Basel



von

Pascal Jarno Schmidt

aus Eimeldingen, Deutschland

Basel, 2016

Originaldokument gespeichert auf dem Dokumentenserver der Universität Basel

edoc.unibas.ch

Genehmigt von der Philosophisch-Naturwissenschaftlichen Fakultät auf Antrag
von:

Prof. Dr. Dennis G. Gillingham

Prof. Dr. Florian P. Seebeck

Basel, den 15. September 2015

Prof. Dr. Jörg Schibler

Dekan der Philosophisch-
Naturwissenschaftlichen
Fakultät

For the past.....

This work is dedicated to my wonderful girlfriend **Stefanie Geigle**, the person whom I love from the bottom of my heart and stood by my side for almost four very hard years. Without her constant love, support and passion this would not have been possible for me. I am deeply grateful to her for standing by my side in all the hard times we had and I hope our love will have a collective future. We managed everything so far – we will manage the forthcoming, whatever it is. Love never dies...

.....and the future!

Acknowledgements

During the past 10 years at the University of Basel I have met many people who contributed to my personal development in many different ways and to whom I'd like to address a few words as a sign of appreciation.

First of all, I'd like to express my deepest gratitude to **Prof. Dr. Dennis Gillingham** for being one of his pioneers in the Gillingham research group and for the trust in me, my skills and my passion for scientific research. I would like to say *thank you* for all the fruitful discussions of my research, the exchange of valuable knowledge to me and the ever-open door for any business. I am very thankful for the freedom and the independence he gave me on my projects from which I learned so much over the past years. I highly appreciated to work under the supervision of a friend-like boss as he is and I am also very proud on everything I learned from him on my way to become a PhD. For his scientific career and family I deeply wish him all the best and hope his stay at the University of Basel will continue – it was a pleasure for me to be part of *your* research group. I also hope our future relationship will continue as a good and long-living friendship no matter where science will place us.

I would like to thank **Prof. Dr. Florian Seebeck** for accepting the co-examination of my PhD thesis and the good relationship between our neighboring research groups and the great BBQ's we had together.

In addition, I'd like to thank **Prof. Wolf-Dietrich Woggon** for his fundamental contributions on the dirhodium project and for accepting to chair my PhD defense.

On the way of becoming a PhD there is nothing more important than the working atmosphere and the people contributing to it on a daily basis. Therefore I'd like to address my special gratitude to the best labmates “The Gillis” in Lab 308 (**Daniel Bachman, Na Fei, Cedric Stress** and **Linna Zhou**) and 210 (**Kiril Tishinov** and **Stefanie Geigle**) for all the chemical discussions, advices and help on any subjects. Thank you for all the great time we spent together in the legendary “Heavy Metal” lab, for the delicious cheese lunches, paper and birthday apéros and of course for all the unforgettable time we spent outside the lab on trips, BBQ's or festivals (thanks for your support at the Baden in Blut Open Air). I hope our moments and friendship will hold on and we'll be proud to be the first Gillingham alumnis – I am.

In addition I'd like also to thank **Stefanie Geigle** and **Cedric Stress** for proofreading this thesis.

Special thanks also go to **Dr. Daniel Häussinger** and his group for their excellent NMR services, to **Dr. Heinz Nadig** for many discussions and his great service on high resolution mass spectrometry. The entire Werkstatt team, the secretaries as well as **Roy Lips** and **Markus Hauri** are acknowledged for maintaining laboratory devices, taking care of administrative tasks, ordering consumables and running the Chemikaliensammlung.

For the constant support, freedom and sympathy throughout my studies I am grateful to my parents (**Chantal** and **Karl-Heinz Schmidt**), grandparents, friends and relatives. In particular I'd like to thank **Florian Menacher**, **Marie** and **Charles Wicky**, **Max Schmidt** and **Ingrid Heidt** for their accompaniment on my way – I wish we could have shared this moment. Moreover I'd like to thank my wonderful girlfriend **Stefanie Geigle** for her warm-hearted support and love throughout the time we spent together – thank you for standing by my side and loving me; I love you too. I also would like to acknowledge the whole Geigle Family (**Detlef**, **Friederike**, **Franziska**, **Tobias** and **Sebastian**) for being a big part of my life and for all the love, trust and security I have experienced – you keep me grounded. I'm also grateful to my soulmates **Judith** and **Georg Menacher** for being my second family and for all the good and hard times we experienced together. Thanks for the great friend- and relationship we had during the past ten years and for everything you did for me without hesitation – I highly appreciate that. We'll never forget the origins of our collective roots...

In addition I am grateful to all the numerous professors, post Docs, PhD students, practical students, Wahlpraktikum students of the University of Basel who contributed to my personal development and the great experience I have made on my way. I can't name all of you – but I will remember all of you.

For funding I'd like to thank the Swiss National Science Foundation as well as the University of Basel.

Table of contents

List of abbreviations	IX
1 Thesis Outline	1
1.1 Introducing the concept of bioconjugation	2
1.2 Direct reactions with natural functional groups	3
1.2.1 Chemical modifications of DNA	3
1.2.2 Modification of amino acids in proteins and peptides	8
1.2.2.1 Cysteine modifications	8
1.2.2.2 Lysine modifications	10
1.2.2.3 Tyrosine modifications	11
1.2.2.4 Reactions of C- and N-termini	12
1.3 “Bioorthogonal” bioconjugation using unnatural functional groups	14
1.3.1 Staudinger Ligation	14
1.3.2 “Click” Chemistry	15
1.3.3 Inverse electron demand Diels-Alder reaction	17
1.3.4 Hydrazone and Oxime condensations	18
1.4 Challenges and remaining problems	19
2 Guided catalyst to selectively target nucleic acids	20
2.1 Peptide Nucleic Acids	20
2.1.1 Peptide Nucleic Acids and their properties	20
2.1.2 Peptide Nucleic Acids in templated chemistry	22
2.1.3 Applications of Peptide Nucleic Acids in chemical biology	23
2.1.4 PNA monomers and their chemical assembly	25
2.2 Dirhodium catalysis and its applications in chemical biology	29
2.3 Results and discussion	34
2.3.1 Nucleic acid alkylation using template PNA-dirhodium conjugates	34
2.3.1.1 Design of the PNA catalyst template – a retrosynthetic analysis	35
2.3.2 Synthesis of 1 st generation PNA and its conjugation to dirhodium	36
2.3.3 Retrosynthesis of 2 nd generation PNA catalyst	39
2.3.4 Synthesis of modular dicarboxylate ligands and dirhodium catalysts	40
2.3.5 Dirhodium catalyzed nitrene-, C-H and O-H insertion	42
2.3.6 Synthesis of 2 nd generation PNA and its bioconjugation to dirhodium	44
2.3.7 Initial alkylation of ssDNA using template PNA-dirhodium carbenoids	49
2.3.8 Conclusion and outlook	54

3	Novel methods for oxime bioconjugations in chemical biology	57
3.1	Introduction	57
3.2	Characteristics and challenges of oxime condensations.....	57
3.3	Present methods for the optimization of oxime condensations	60
3.4	Results and discussion - Rapid oxime condensations using dialdehydes.....	63
3.4.1	Substrate synthesis.....	64
3.4.2	HPLC studies.....	67
3.4.3	Probing the effect of biological interfering additives	70
3.4.4	¹ H-NMR studies – a mechanistic and kinetic insight	71
3.4.5	Fluorescence quench assay – determining k_1	77
3.4.6	Bioconjugation with a complex DNA substrate	81
3.4.7	Conclusion and outlook.....	82
3.5	Results and discussion - Rapid oxime condensations using boronic acids	85
3.5.1	¹ H-NMR studies – initial findings	86
3.5.2	HPLC studies.....	87
3.5.3	Fluorescence quench assay: determining k_1	91
3.5.3.1	Synthesis.....	91
3.5.3.2	Kinetic assay.....	95
3.5.4	Probing the effect of biological interfering additives	98
3.5.5	Stability and reversibility tests	99
3.5.6	Conclusions and outlook	104
4	Experimental	106
4.1	General Information	106
4.2	Chemical synthesis	108
4.2.1	Guided catalysts studies	108
4.2.1.1	Synthesis of small molecules and dirhodium catalysts	108
4.2.1.2	Substrate synthesis and experimental details for dirhodium catalyzed nitrene, C-H and O-H insertion	123
4.2.1.3	Synthesis of PNA, PNA-Rh ₂ catalysts and oligonucleotides	128
4.2.1.4	Alkylation studies using PNA-dirhodium carbenoids	139
4.2.1.5	Circular dichroism studies.....	142
4.2.2	Dialdehyde studies.....	143
4.2.2.1	Synthesis of small molecules and dirhodium catalysts	143
4.2.2.2	Synthesis of LYRAG pentapeptide hydroxylamine substrates	151
4.2.2.3	HPLC assays.....	153
4.2.2.4	¹ H-NMR studies	156

4.2.2.5	Fluorescence quenching assay	160
4.2.2.6	DNA bioconjugation	163
4.2.3	Boronic acid studies	165
4.2.3.1	Synthesis of small molecules.....	165
4.2.3.2	¹ H-NMR studies	176
4.2.3.3	HPLC studies.....	180
4.2.3.4	Fluorescence quenching assay.....	184
4.3	Appendix	189
4.3.1	X-ray data.....	189
4.3.2	License details for reference #173.....	191
4.3.3	License details for reference #213.....	192
5	References	194
	Curriculum Vitae.....	207

List of abbreviations

(v/v) or (w/w)	volume or weight percent
2-FPBA	2-formylphenylboronic acid
A	adenine
Å	Ångström 10^{-10} m
AA	amino acid
Ac ₂ O	acetic acid anhydride
aeg	(2-aminoethyl)glycine
Bhoc	benzhydryloxycarbonyl
Boc	<i>tert</i> -butoxycarbonyl
Boc ₂ O	di- <i>tert</i> -butyl dicarbonate
C	cytosine
CDI	1,1'-carbonyldiimidazole
CV	column volume(s)
Da	dalton(s)
DBU	1,8-Diazabicyclo[5.4.0]undec-7-en
DCC	dicyclohexylcarbodiimide
DCI	deuterated hydrochloric acid
DEAD	diethyl azodicarboxylate
DIPEA	<i>N,N</i> -diisopropylethylamine
DMAP	4-(<i>N,N</i> -Dimethylamino)pyridine
DMF	<i>N,N</i> -dimethylformamide
DMSO	dimethyl sulfoxide
dsDNA or RNA	double-stranded deoxyribonucleic or ribonucleic acid
ϵ	extinction coefficient [$L \text{ mol}^{-1} \text{ cm}^{-1}$]
EDC	1-ethyl-3-(3-dimethylaminopropyl)carbodiimide hydrochloride
eq.	equivalent(s)
ESI-MS	electron spray ionization mass spectrometry
Et ₂ O	diethylether
EtOAc	ethyl acetate
EtOH	ethanol
FAB	fast atom bombardment
FG	functional group
Fmoc	fluorenylmethoxycarbonyl
G	guanine
HATU	<i>N,N,N',N'</i> -tetramethyl- <i>O</i> -(7-azabenzotriazol-1-yl)uronium hexafluorophosphate
HCTU	<i>O</i> -(6-chlorobenzotriazol-1-yl)- <i>N,N,N',N'</i> -tetramethyluronium hexafluorophosphate
HOBt	1-hydroxybenzotriazole
HRMS	high resolution mass spectrometry
HV	high vacuum
IBHA	isoindole bis(hemiaminal)
K	degree Kelvin
KMnO ₄	potassium permanganate
KP _i	potassium phosphate
LC	liquid chromatography

LRMS	low resolution mass spectrometry
LYRAG	leucine-tyrosine-arginine-alanine-glycine
MALDI-TOF-MS	matrix-assisted laser desorption ionization time of flight mass spectrometry
Me ₂ S	dimethyl sulfide
MeCN	acetonitrile
MeOH	methanol
MES	2-(<i>N</i> -morpholino)ethanesulfonic acid
MHz	megahertz
MMT	monomethoxytrityl
mRNA	messenger ribonucleic acid
MS/MS	tandem mass spectrometry
NaBH ₃ CN	sodium cyanoborohydride
NaIO ₄	sodium periodate
NEt ₃	triethylamine
NMM	<i>N</i> -methylmorpholine
NMP	<i>N</i> -methylpyrrolidinone
NMR	nuclear magnetic resonance (spectroscopy)
O ₃	ozone
OAc	acetate
OPA	<i>ortho</i> -phthaldehyde
PAGE	polyacrylamide gel electrophoresis
Pd(dppf)Cl ₂	[1,1'-Bis(diphenylphosphino)ferrocene]dichloropalladium(II)
Pd(PPh ₃) ₂ Cl ₂	bis(triphenylphosphine)dichloropalladium(II)
Pin	pinacol ester
PNA	peptide nucleic acid
ppm	parts per million
PyBrop	bromo-tris-pyrrolidino phosphoniumhexafluorophosphate
R _f	retention factor
RP-HPLC	reverse phase high performance liquid chromatography
S/N	signal to noise ratio
Sc(OTf) ₃	scandium(III) triflate
Si60	Silica Gel with 60 Å pore size
ssDNA or RNA	single-stranded deoxyribonucleic or ribonucleic acid
T	thymine
TBE	Tris/Borate/EDTA buffer
TFA	trifluoroacetic acid
TFMSA	trifluoromethanesulfonic acid
THF	tetrahydrofuran
TIS	triisopropylsilane
TLC	thin layer chromatography
T _m	temperature at which 50% of double stranded DNA is denatured
TMS	trimethyl silyl
TMSOTf	trimethylsilyl trifluoromethanesulfonate
t _R	retention time [min]
TSTU	2-succinimide-1,1,3,3-tetramethyluronium tetrafluoroborate
UPLC-MS	ultra high performance liquid chromatography

Abstract

One of the open challenges in chemical biology is to identify reactions that proceed with large rate constants in water at neutral pH values. Once assembled, these conjugates may be used for a broad variety of applications (*e.g.*, therapeutics, imaging probes or as a catalytic system). Herein we describe a novel approach for the chemical modification of nucleic acids using guided organometallic-catalysts. Customized dirhodium complexes were prepared using modular ligands bearing various functional groups and connected to peptide nucleic acids through stable oxime linkages. The final constructs have been optimized for aqueous catalysis and were tested in preliminary alkylation studies of single-stranded DNA *via* dirhodium-carbenoids generated from α -diazocarbonyl compounds. During the course of optimizing the rather slow kinetics of oxime formation, we have developed two highly efficient methods for rapid oxime-based bioconjugations. (1) Dialdehydes were found to react with *O*-alkylhydroxylamines at rates of $500 \text{ M}^{-1} \text{ s}^{-1}$ in neutral aqueous buffer in the absence of a catalyst. The key to these conjugations is an unusually stable cyclic intermediate, which ultimately undergoes dehydration to yield an oxime. The scope and limitations of this method are outlined, as well as its application in bioconjugation with a DNA 41-mer and a mechanistic interpretation that will facilitate further developments of reactions with *O*-alkylhydroxylamines at low substrate concentrations. (2) Oximes proximal to boronic acids form in neutral aqueous buffer with rate constants of more than $10^4 \text{ M}^{-1} \text{ s}^{-1}$, the largest to date for any oxime condensation. The reaction tolerates a variety of biological interfering additives and is suitable for the rapid modification of short peptide sequences. Once formed, the oxime products are stable for days and undergo slow interconversion through a hydrolysis-based mechanism. Boron's dynamic coordination chemistry confers an adaptability that seems to aid a number of elementary steps in the oxime condensation.

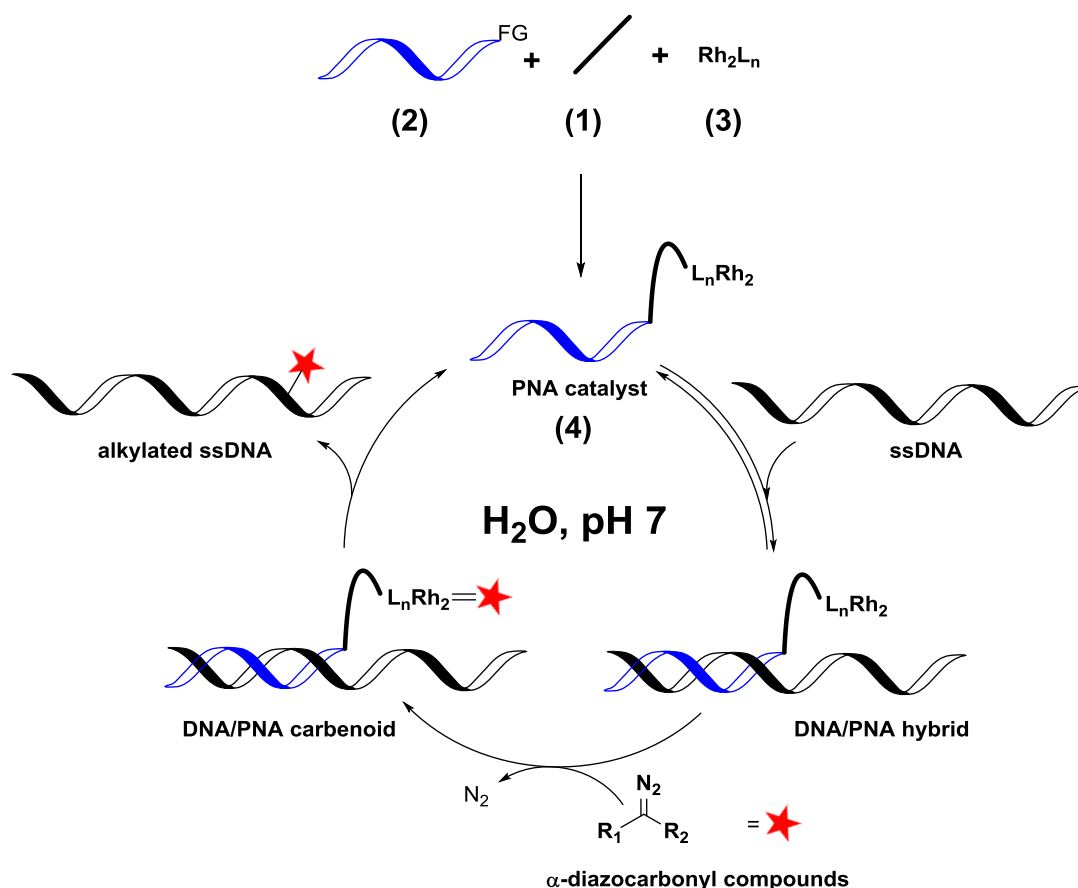
In conclusion both methods represent important improvements for oxime-based bioconjugations in water (pH 7) at low equimolar concentrations. The high reaction kinetics are achieved without the need for additional reagents, catalysts or variations of the reaction conditions. In addition, the possibility of using reacting pairs that are commercially available will greatly enhance the applicability of these methods for efficient conjugations of precious biomolecules in the future.

1 Thesis Outline

The main goal of the present thesis was to develop a new method for the catalytic, structure-selective nucleic acid modification using guided organometallic-catalysts in aqueous media under neutral conditions. This architecture was planned to be constructed from short peptide nucleic acid (PNA) sequences which are covalently connected to a dirhodium catalyst through a rapid and robust bioconjugation technique. Once assembled, these organometallic-catalysts will WATSON-CRICK base-pair to complementary nucleic acid sequences in a dynamic fashion. The addition of α -diazocarbonyl compounds will generate a reactive organometallic-carbenoid catalyst which is able to undergo site-specific insertion reactions with the target's functional groups present in close proximity.

This strategy was pursued by addressing the following aspects:

- (1) choosing a suitable conjugation method to build the organometallic-catalyst
- (2) synthesis of short peptide nucleic acid sequences equipped with modifiable functional groups
- (3) developing dirhodium catalysts with suitable functional groups for conjugation
- (4) assembling of the organometallic-catalyst and probing its ability in nucleic acid modification



1.1 Introducing the concept of bioconjugation

Bioconjugation is a powerful chemical method used for the covalent derivatization of biomolecules to form stable conjugates comprising the combined properties of their individual components.¹ Its development allows the direct access to a broad range of natural or synthetically valuable compounds (*e.g.*, nucleic acids and proteins) exceeding the molecular complexity accessible by stepwise chemical synthesis.² The ability to perform such conjugations through a selective and facile chemical transformation also has practical applications in therapeutics³ or diagnostics⁴. Applying bioconjugation in the field of chemical biology⁵ has helped scientists to understand biochemical pathways and mechanisms, and also enabled true structure-activity relationship (SAR) of biomolecular processes. Ideally a bioconjugation reaction should be chemoselective, robust and biocompatible (neutral pH in water, tolerant to other interfering functional groups) proceeding with high rate constants at low concentrations (*e.g.*, nM- μ M regime) with substrate stoichiometries near unity (**Figure 1.1**).^{6,7} Therefore it is necessary to develop and design new chemical methods which meet these challenging requirements to generate molecules with carefully engineered characteristics. Several techniques are reported in the literature and include labeling⁸, ligation⁹ as well as the use of heterobifunctional¹⁰ and trifunctional¹¹ crosslinkers to study protein-protein interactions for example. The crosslinking of such monofunctional components to create multifunctional molecules can be accessed either by direct reaction of natural functional groups (FGs) or through bioorthogonal conjugation¹² with unnatural FGs (*vide infra*).

This clearly underlines the importance of exploring **NEW STRATEGIES IN BIOCONJUGATION**, an important component in today's life science research.

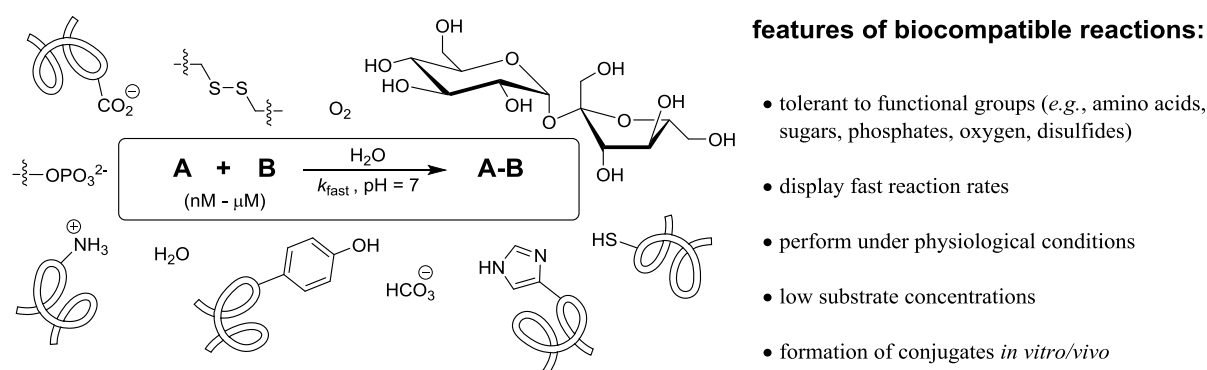


Figure 1.1: A bioconjugation reaction between two chemical species A and B bearing bioorthogonal functional groups. The reaction is biocompatible and proceeds in a complex environment of competing functionalities as found in living systems.

1.2 Direct reactions with natural functional groups

Nature provides a sea of FGs which have a broad range of reactivity based on their chemical properties in different environments. Covalent and non-covalent interactions of FGs are the core of metabolism (*e.g.*, ATP, NADH) and biological molecular recognition (*e.g.*, DNA double helix, signalling proteins).¹³ If chemists are able to selectively target and modify these functional groups, then perhaps it would be possible to build on Nature's designs and get access to new molecules applicable in the field of chemical biology.

Since our research goal was to directly target and modify native FGs present in biopolymers, particularly nucleic acids, it is of importance to present an overview of selected and established methods covering this research area. Within the following section focus is laid on the use of natural FGs present in biomolecules for their modification through bioconjugation chemistry.

1.2.1 Chemical modifications of DNA

Targeting native DNA sequences with chemical probes is a challenging task which requires reagents that are reactive enough to form a covalent bond with one of the various functional groups present in the oligonucleotides. Of major interest are therefore activated electrophiles capable to react with nucleophilic phosphates or nucleobase heteroatoms in DNA. These reagents are mainly classified into two classes depending on their alkylation pathways; S_N1 and S_N2 -type alkylation agents.¹⁴ Although the sites of DNA modification are the same for these reagents, they differ by their percental occurrence. The use of methyl methanesulfonate (MMS), a S_N2 -type reagent, was found to alkylate N-1_A and N-3_C in ssDNA while *N*-methyl-*N'*-nitrosourea (NMU), a S_N1 -type reagent, alkylates the phosphodiester backbone of ssDNA (**Figure 1.2**).¹⁵ When tested with dsDNA both reagents perform similar with major preferences for the N-7_G site which is located in the major groove of DNA, thus allowing for a greater accessibility.¹⁶ Guanine *O*-alkylations are less significant since the oxygen atom is involved in WATSON-CRICK base pairing and normally lacks reactivity to be modified efficiently.

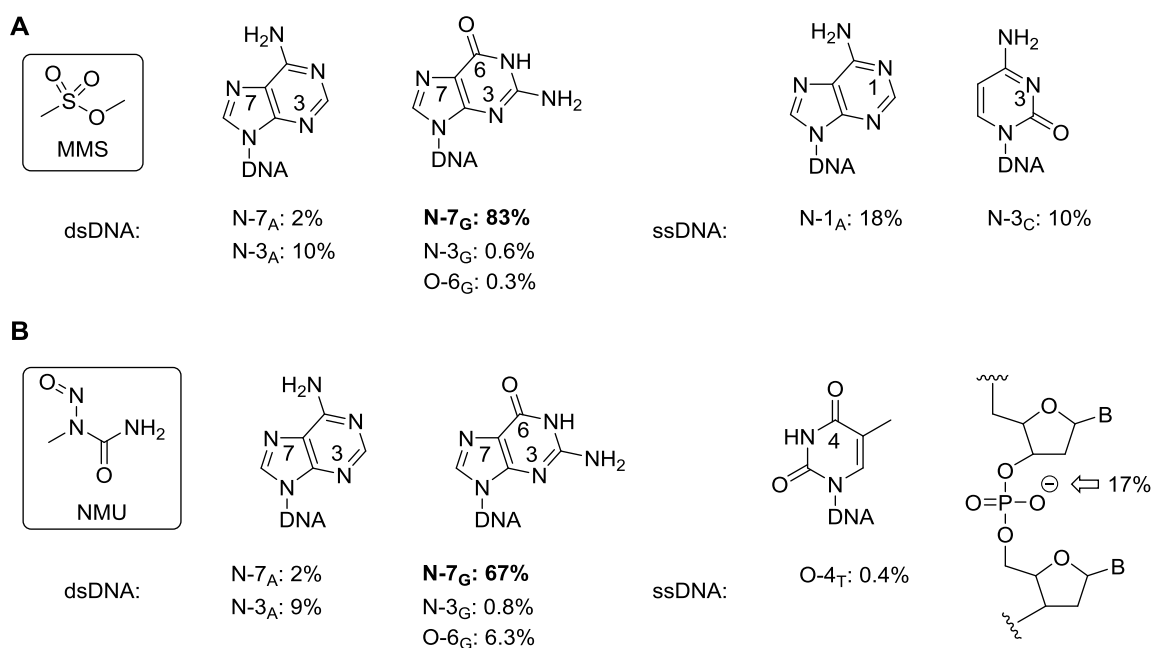
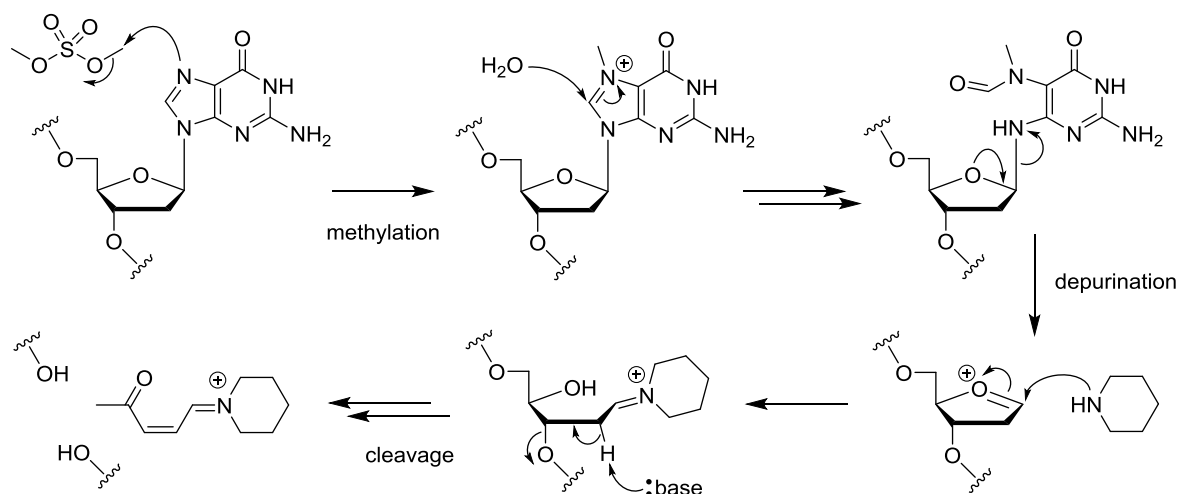


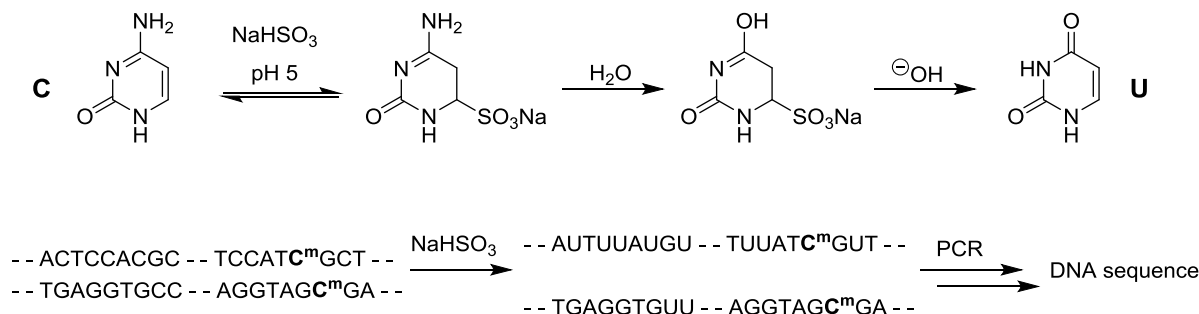
Figure 1.2: DNA alkylating agents and their sites of modification on nucleobases and phosphodiester backbone. (A) Methyl methane sulfonate (MMS) alkylations of A/G in dsDNA and A/C in ssDNA. (B) *N*-methyl-*N*⁷-nitrosourea (NMU) alkylations of A/G in dsDNA and T/phosphodiester backbone in ssDNA.

Another very similar alkylating agent, dimethyl sulfate (DMS), was investigated in the early sixties by LAWLEY and BROOKES as an efficient mutagen. Treatment of RNA with ¹⁴C-labeled DMS followed by acidic hydrolysis was found to deliver four isotopically labeled products, the major being N-7_G.¹⁷ Later GILBERT and MAXAM could exploit this finding by developing a new technique for DNA sequencing based on DMS-mediated guanine alkylation and subsequent depurination followed by alkaline cleavage at the abasic site (**Scheme 1.1**).^{18,19} A high resolution gel electrophoresis could reveal the cleaved fragments, resulting in a ladder with characteristic bands corresponding to each guanine present in the DNA. This reaction was part of one of the earliest sequencing technologies.



Scheme 1.1: Dimethyl sulfate-initiated methylation pathway of the N-7_G with subsequent depurination and piperidine-mediated DNA cleavage used for sequencing.

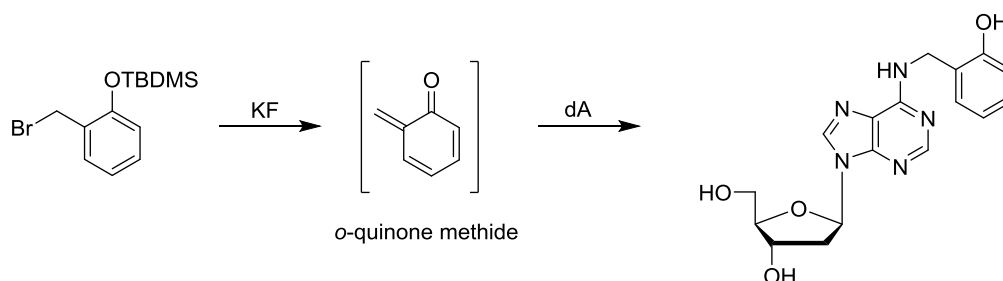
Another important sequencing method relies on the principle of selective bisulfite-initiated conversion of intact cytidines to uracils (**Scheme 1.2**).^{20,21} This method is primarily used to reveal 5-methylcytosine residues in individual DNA strands upon bisulfite treatment, polymerase chain reaction (PCR) amplification and sequencing.^{22,23}



Scheme 1.2: Selective bisulfite conversion pathway of cytidine to uracil used for the detection of 5-methylcytosines in DNA.

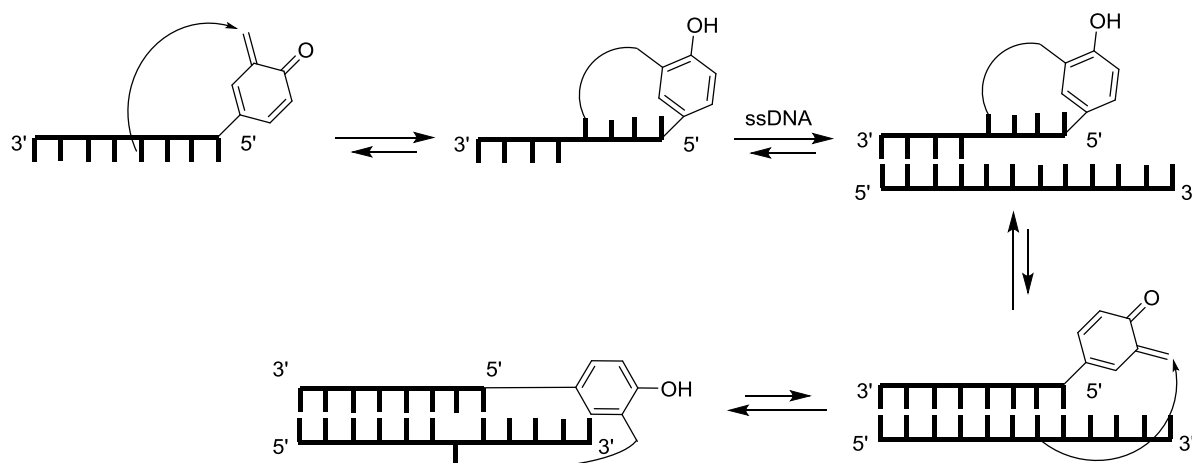
In 1985, SEGAL and SOLOMON showed the potential of acrylonitrile (AN) as a direct mutagen in their alkylation studies with calf thymus DNA. Initial and separate treatment of AN with deoxynucleosides under physiological conditions resulted in site-specific cyanoethylation as confirmed by MS/MS studies. Probing the alkylating agent with calf thymus DNA showed various modifications of all nucleobases to different extents.²⁴ *In situ* generated AN is also known to react with thymines during the deprotection step of oligonucleotide synthesis and results in cyanoethyl-alkylated N-3_T species *via* MICHAEL addition.^{25,26}

ROKITA *et al.* developed an important method for direct nucleic acid modification which uses a reactive, *in situ* generated, *ortho*-quinone methide (QM) as alkylating agent.²⁷ This species is quickly obtained through fluoride deprotection of an *o*-(bromomethyl)phenol derivative and susceptible to nucleophilic attack by the exocyclic amino groups of deoxynucleosides (**Scheme 1.3**).²⁸



Scheme 1.3: Representative *o*-quinone methide alkylation of the exocyclic amino group in deoxyadenine initiated by *O*-deprotection with potassium fluoride. Further examples (dG and dC) are also reported.²⁸

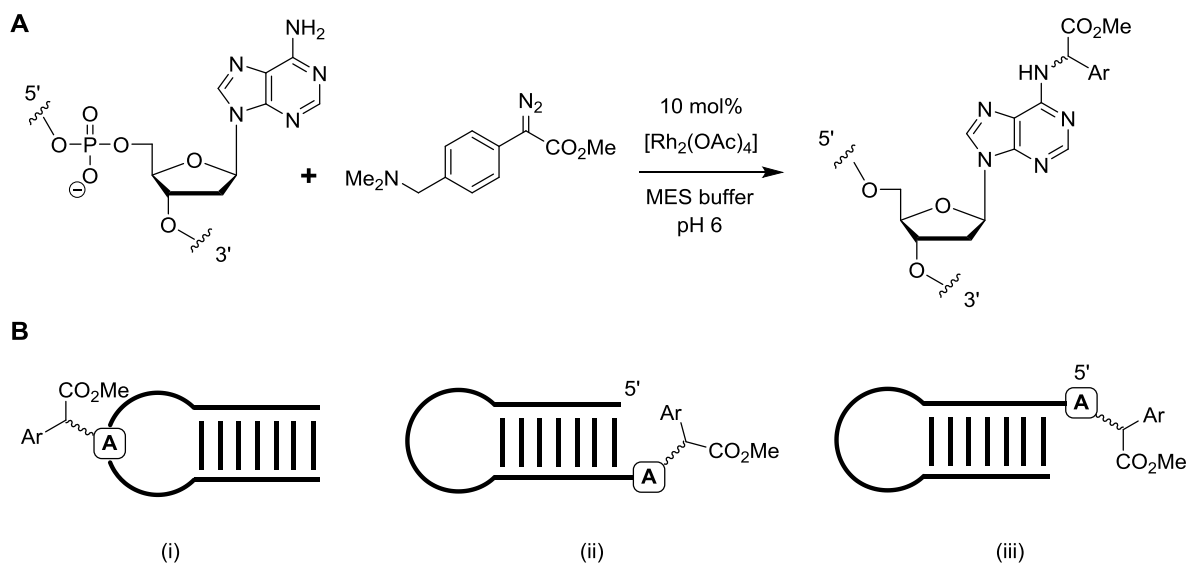
Later, in 2003 they could show that an acridine-functionalized QM is able to cross-link dsDNA as shown by denaturing gel electrophoresis. Monoalkylations were found to be rare and their presence explained by the ability of the QM to “walk” from unfavorable to favorable cross-links while generating this intermediate.²⁹ Recently it was shown that the terminal attachment of a QM to an unnatural nucleic acid is effective in cross-linking a complementary DNA strand through a reversible process. Although self-adducts were found to be the kinetically dominating species, the system equilibrated to the thermodynamically favored interstrand product (**Scheme 1.4**).³⁰



Scheme 1.4: Pathway of interstrand cross-linkage using an unnatural nucleic acid equipped with a terminal QM. The reaction proceeds through a reversible self-adduct delivering the covalently linked product upon hybridization to a complementary ssDNA sequence.

A variety of DNA cross-linking agents are known, some of which have even reached clinical application as cancer treatments.³¹ Among those, prominent examples are *cis*-platin and carboplatin³², nitrogen mustards like mustine, melphalan and chlorambucil³³ as well as Mitomycin C³⁴ and psoralens³⁵, the latter which crosslinks DNA upon irradiation. For a full and detailed review on DNA interstrand cross-linking and potential cancer treatment the reader is redirected to DEANS and WEST.³¹

A more recent approach for the structure-selective catalytic nucleic acid modification was described by our research group in 2012.³⁶ DR. KIRIL TISHINOV could demonstrate that aqueous dirhodium-carbenoid catalysis can be used as a direct method for the alkylation of native DNA. NMR experiments revealed that exocyclic amino groups are the only sites for modification while thymine and uracil were completely unreactive. Since dsDNA could not be targeted with this method, a single reactive adenine in a hairpin turn region or as a 3' or 5' overhang could be selectively alkylated as confirmed separately by MS/MS experiments (**Scheme 1.5**).



Scheme 1.5: Structure-selective catalytic nucleic acid modifications of the adenine nucleobase. **(A)** Reaction pathway for the alkylation of the exocyclic amino group using aqueous dirhodium-carbenoid catalysis. **(B)** Alkylation of a hairpin (i) turn region, (ii) 3' overhang and (iii) 5' overhang.

1.2.2 Modification of amino acids in proteins and peptides

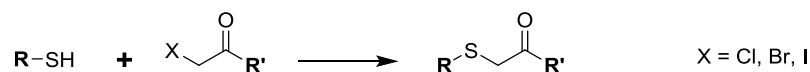
Since peptide modifications and their use in bioconjugation are presented at a later stage, I will introduce this concept now as a subsection of “Direct reactions with natural FGs”.

Proteins and peptides are key components of life. These biomolecules are essential for the structure, function and regulation of the body’s tissues and organs. Composed by a unique sequence of short amino acid fragments, proteins and peptides play a key role in intra- and extracellular events. The activity and function of proteins are often regulated by specific chemical changes on amino acid side-chains. These chemical modifications, termed post-translational modifications (PTMs), are natively introduced by enzymes or cofactors and include glycosylations, phosphorylations, acetylations or ubiquitinations, to mention only a few.³⁷ These supremely complex and selective processes for the covalent modification of highly functional molecules is a key step in most biological processes. They are responsible for the generation of proteome complexity and thus great effort has been invested in understanding these processes in detail. Drawing inspiration from Nature, chemists and biologists have begun to develop methods for selective protein and peptide modifications. These bioconjugations are mainly based on the reactivity of particular amino acid residues within the biomolecule towards a specific chemical FG. Techniques that enable such artificial chemical modifications of amino acids are therefore of major interest in chemical biology.

The following subsections will give the reader a brief overview of some selected and established methods available for the selective modification of reactive amino acids and their bioconjugation to other molecules.

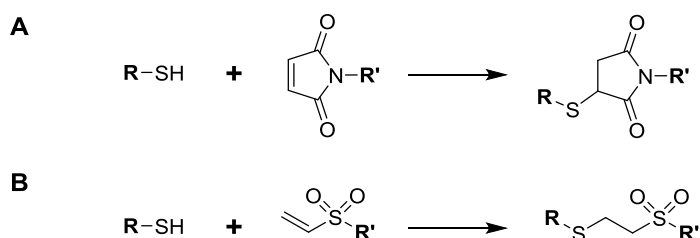
1.2.2.1 Cysteine modifications

Reactions on cysteine are the most common chemical approach to direct protein modification due to its low natural abundance in proteins and the highly nucleophilic character of the sulfhydryl group compared to the side chains of other amino acids. Alkylation agents are widely used for covalent modifications, but sometimes off-target reactions with histidine, methionine, lysine as well as *N*-terminal amino groups can be observed.³⁸ Iodoacetic acid was early found to deliver selective cysteine modification in human hemoglobin as concluded by COLE *et al.*³⁹ Similarly, papain was later shown to be modified at the sulfhydryl group of the active site cysteine residue (Cys²⁵) using a α -halocarbonyl-containing flavin compound.⁴⁰ Another alkylating reagent for the selective modification of cysteine is iodoacetamide which was first reported 1935 by GODDARD and MICHAELIS.⁴¹ The acetamide derivative of cysteine has found applications for peptide mapping of proteins containing cysteine residues.^{42,43} A schematic representation of the general mode of cysteine bioconjugation through alkylation is depicted in **Scheme 1.6**.



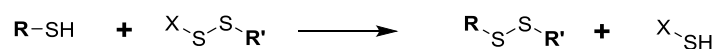
Scheme 1.6: Cysteine bioconjugation approach using α -haloacetyl compounds forming a thioether linkage.

Another important class of molecules for cysteine bioconjugation comprises maleimides^{44,45} and vinyl sulfones⁴⁶ (**Scheme 1.7**). These MICHAEL acceptors undergo conjugate additions with sulfhydryl residues in proteins to give thioethers. A polyethylene glycol (PEG) equipped vinyl sulfone was shown to selectively modify reduced RNase at its cysteine residues depending on the pH. While this reaction with sulfhydryls was found to be fast and selective at pH 7-9, lysine residues were slowly modified at elevated pH values.⁴⁷ This method is a suitable alternative to introduce a post-translational PEGylation into hydrophobic proteins which demand a water solubilizing agent. Similarly, BELL *et al.* reported that selective maleimide PEGylation of a α -interferon based protein drug at its cysteine side chains resulted in enhanced circulating half-time and antitumor activity.⁴⁸ Other maleimide-based bioconjugations comprise antibody affinity-labeling with biotin⁴⁹ or with maleimide-activated enzymes², the formation of mixed bis-thioethers^{50,51} and maleimide fluorophores for protein imaging.⁵² However, maleimide and its conjugates were found to be hydrolytically unstable and ring opening with subsequent elimination of the cysteine residue is a problem at alkaline pH and should be considered when planning such a reaction.⁵³



Scheme 1.7: Conjugate additions of cysteine for bioconjugation. (A) Sulfhydryl addition to maleimides. (B) Sulfhydryl addition to vinylsulfones.

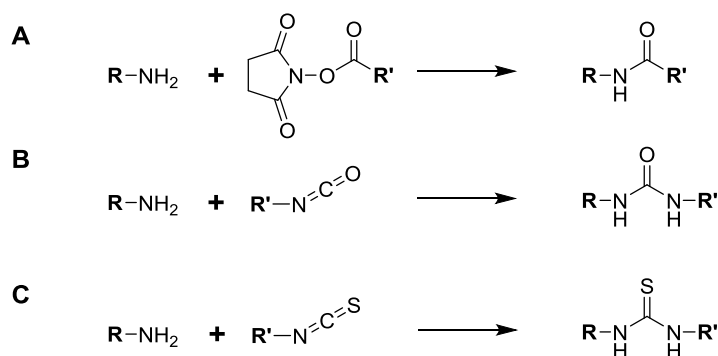
When oxidized, cysteines are present as disulfides and play an important role in protein folding and stability. Interstrand disulfide bonds can be reduced by *e.g.*, tris(2-carboxyethyl)phosphine (TCEP) or dithiothreitol (DTT) to unmask the cysteines and exploit their reactivities. In turn a suitable method for the covalent modification of reduced thiols is their conversion into mixed disulfides *via* disulfide exchange (**Scheme 1.8**). Reagents which can be used for these transformations comprise pyridyl disulfides⁵⁴ and the more prominent ELLMAN'S reagent which was developed for the spectrophotometric quantification of protein thiols.^{55,56}



Scheme 1.8: Disulfide exchange as a bioconjugation method for cysteine modification.

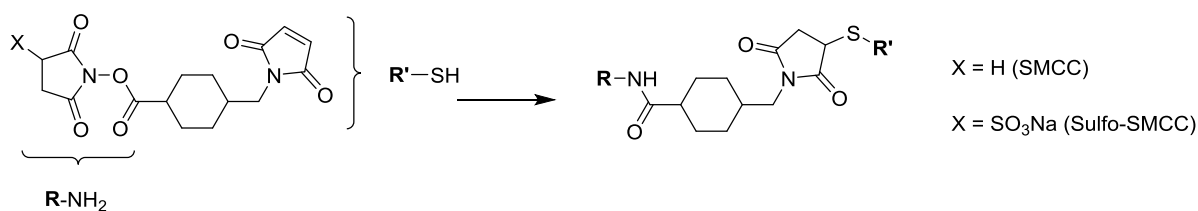
1.2.2.2 Lysine modifications

Lysines contribute to the overall net positive charge of proteins because they are protonated under physiological conditions. Above its pK_a of 9.3-9.5 the ϵ -amino group becomes nucleophilic and a potential target for the modification with potent electrophilic reagents. Among those are *e.g.*, *N*-hydroxysuccinimide (NHS) activated esters for the formation of amide bonds, urea formation with isocyanates and thiourea formation with isothiocyanates (**Scheme 1.9**).



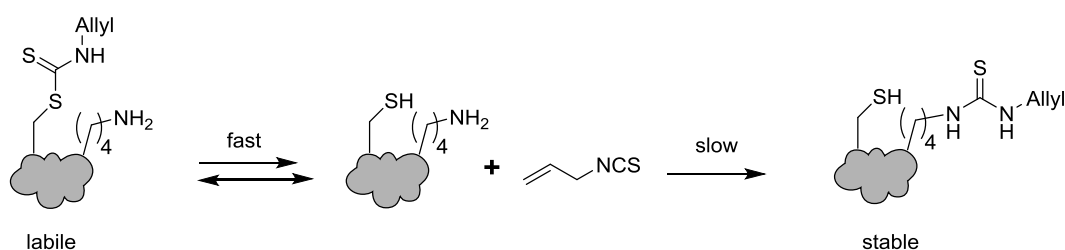
Scheme 1.9: Selected bioconjugation strategies for lysine residues. (A) Amide bond formation through NHS esters. (B) Urea formation with isocyanates. (C) Thiourea formation with isothiocyanates.

NHS esters are a widely used activation method for carboxylates in the formation of a stable amide bond and have been established as one of the most general bioconjugation techniques for lysine side chain modifications. Prior to the reaction, stable NHS esters have to be prepared synthetically through their carboxylates and a condensing agent such as *N,N'*-dicyclohexylcarbodiimid (DCC). Upon conjugation with the ϵ -amine of lysine the NHS acts as a leaving group while forming a stable amide conjugate. Prominent examples for this activation and lysine modification are the sulfo-NHS-mediated biotinylation^{57,58}, the NHS-mediated introduction of fluorescent labels or the use as a heterobifunctional NHS ester-maleimide crosslinker (**Scheme 1.10**).¹⁰



Scheme 1.10: Heterobifunctional sulfo- and succinimidyl-4-(*N*-maleimidomethyl)cyclohexane-1-carboxylate (Sulfo-SMCC and SMCC) crosslinkers. A lysine-containing biomolecule can be connected to a cysteine target.

Isocyanates have only limited applications for bioconjugation since these reagents were found to be too unstable and result in amines when exposed to moisture. Nevertheless some examples exist, one of them being the selective lysine side chain modification in horse cytochrome *c* with *m*-trifluoromethylphenyl isocyanate as detected by ^{19}F -NMR, trypsin digest and peptide mapping.^{59,60} The less reactive isothiocyanates were found to deliver almost exclusively stable lysine conjugates but are also able to react with *N*-terminal α -amines depending on the pH of the reaction media.² TULS *et al.* demonstrated the selective labeling of Lys³³⁸ in cytochrome P-450 with fluorescein isothiocyanate⁶¹ while NAKAMURA *et al.* used allyl isothiocyanate (AITC) which modifies lysines in bovine serum albumin through an intermediate AITC-cysteine adduct.⁶² This transfer was confirmed by synthetic probes which were subjected to detailed LC-MS analysis. The mechanism is not clarified yet and is proposed to happen through a fast but reversible AITC-cysteine intermediate delivering the thermodynamically favored AITC-lysine over time (**Scheme 1.11**).

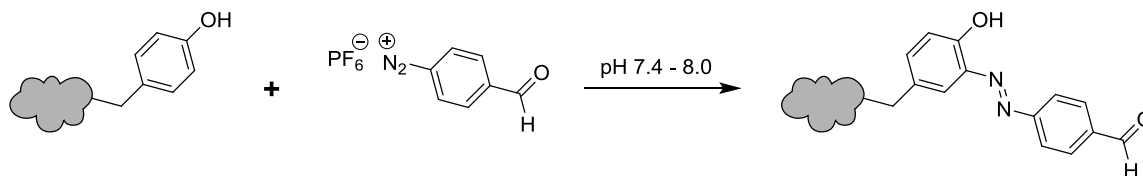


Scheme 1.11: Proposed mechanism by NAKAMURA for the reaction of AITC with a cys/lys-containing protein under physiological conditions.⁶²

1.2.2.3 Tyrosine modifications

Tyrosine modifications are rather rare due to its low reactivity under physiological conditions. Nonetheless the resonance donation effect of the phenolic group allows tyrosine to be selectively modified at the *ortho*-position with suitable electrophiles. The most popular among tyrosine

modifications is the diazo bond formation with a diazonium reagent.¹⁰ Recently, a very elegant example was published for tyrosine-selective modification of proteins using formylbenzene diazonium hexafluorophosphate (FBDP) which introduces additionally a bioorthogonal aldehyde for further functionalization (**Scheme 1.12**).⁶³

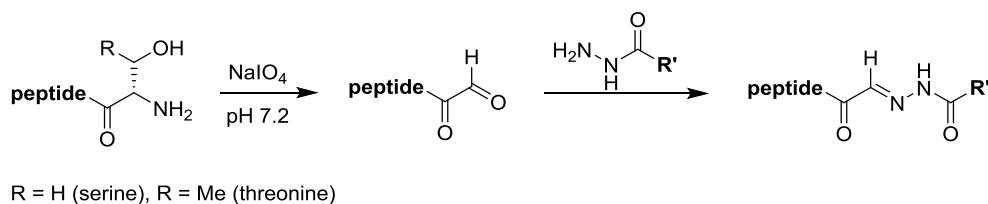


Scheme 1.12: Selective tyrosine modification with FBDP under physiological conditions to give a functionalized, bioorthogonal conjugate.

Modifications on tyrosine though were primarily chosen to obtain information on their binding properties within proteins and include also *O*-acetylations or nitrations of the phenyl ring.¹⁰

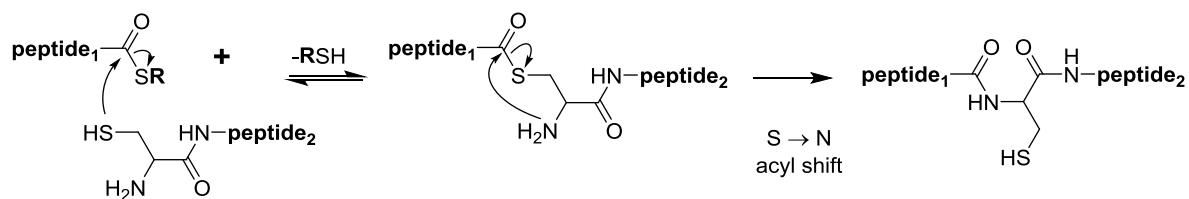
1.2.2.4 Reactions of C- and N-termini

The selective reaction of C- or N-terminal amino acids is also of great interest for PTM and strategies targeting one specific residue at the end of a peptide or protein have been successfully developed. Although direct methods for modification exist, some amino acids have to be converted first into different, reactive groups which are then able to be used in further bioconjugation reactions. N-terminal serine⁶⁴ or threonine⁶⁵ can be oxidized with NaIO₄ to glyoxal groups which can be further reacted to form a stable bioconjugate as shown by KAWAKAMI or CHELIUS (**Scheme 1.13**). Similarly FRANCIS *et al.* could show that pyridoxal 5'-phosphate is able to oxidize the α -amino group into a ketone or an aldehyde which can then be condensed with a hydroxylamine-bearing dye.⁶⁶ Other chemoselective strategies comprise oxazolidine (serine) and thiazolidine (cysteine) formation with aldehydes as well as N-terminal tryptophan modification through PICTET-SPENGLER reaction.^{67,68}



Scheme 1.13: N-terminal serine and threonine oxidation with subsequent bioconjugation to a hydrazone derivative.

Certainly the most prominent example which exploits various reactivities in a stepwise fashion for selective protein modification is native chemical ligation (NCL). In 1993, DAWSON *et al.* applied this ligation method to peptide fragments containing a C-terminal α -thioester whereas the second one was equipped with an unprotected *N*-terminal cysteine residue.⁶⁹ The reaction is initiated by nucleophilic attack of the cysteine thiol (Scheme 1.14, peptide₂) on the α -thioester (peptide₁) to give the kinetic transthioesterification intermediate. The final thermodynamic and enlarged peptide product is obtained by subsequent S \rightarrow N acyl shift and connected through a robust amide bond, providing a powerful method for the chemoselective ligation of peptide fragments in a smart way.



Scheme 1.14: Native chemical ligation strategy used for the formation of larger peptides from smaller peptide fragments containing a C-terminal α -thioester and an unprotected *N*-terminal cysteine. The ligated product is connected *via* native (amide) bond next to the cysteine.

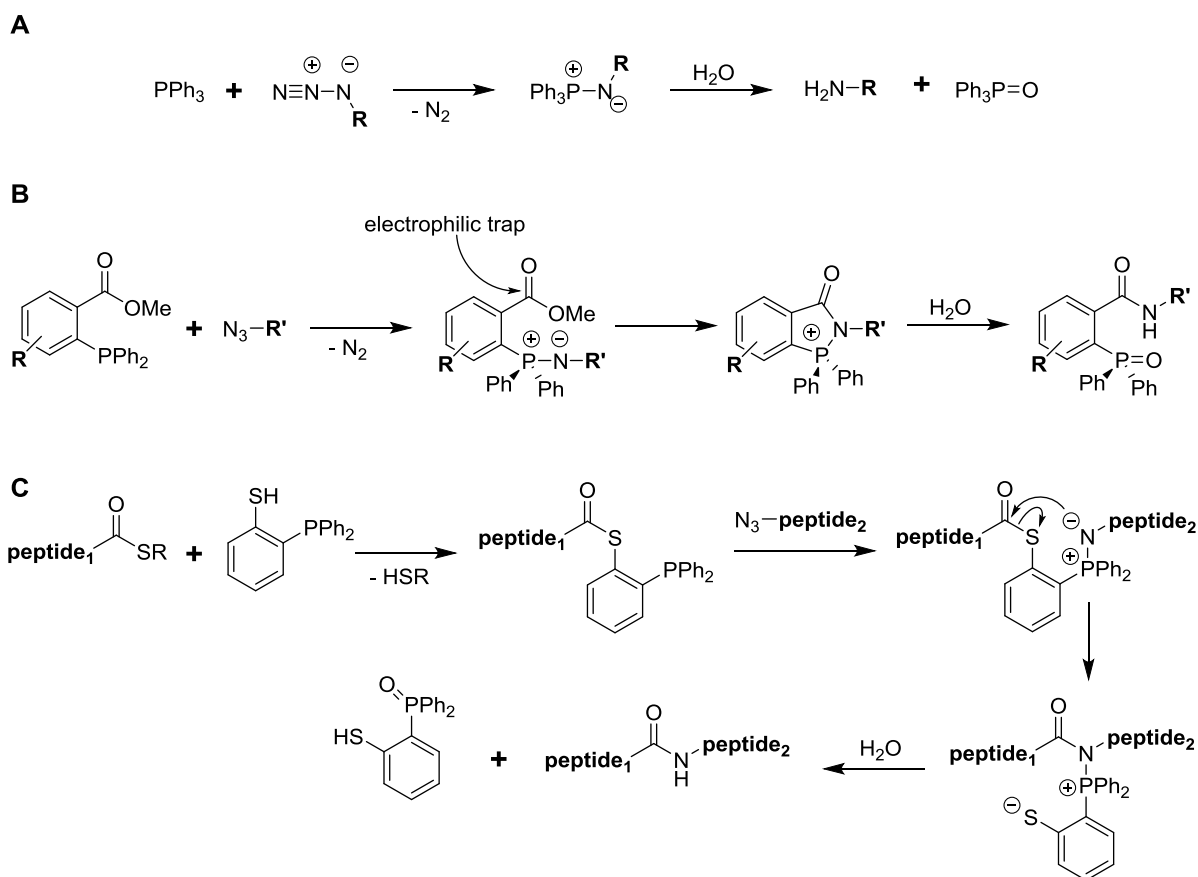
1.3 “Bioorthogonal” bioconjugation using unnatural functional groups

Nature provides a defined but limited toolbox of FGs (*e.g.*, hydroxyls, acids, amines, thiols, phosphates, phenols etc.) which can be used for molecular conjugation. Amide bonds in peptides can be formed by condensing amines with carboxylic acids and are amongst the most important bonds found in biology (*vide supra*). Scientists however have extended this toolbox by developing unnatural but highly useful FGs (*e.g.*, alkyl halides, azides, alkynes, boronic acids, phosphorous(III), diazo compounds etc.) which can be used for bioorthogonal bioconjugation reactions. In general, a bioorthogonal transformation is a reaction that does not interfere with biological processes but displays chemoselectivity and high reactivities under physiological conditions.⁶ The development of such reactions remains important not only to study natural processes, but to potentially expand on them.

Because the bioconjugation strategies used for the presented work relied on unnatural FGs the reader is given a brief overview of selected and important methods developed in the past and applied in this field.

1.3.1 Staudinger Ligation

Almost 100 years ago, in 1919 STAUDINGER and MEYER discovered the irreversible reaction of a phosphine with an azide to yield an amine under aqueous conditions (**Scheme 1.15**, panel A).⁷⁰ In 2000, BERTOZZI *et al.* could further develop the STAUDINGER reaction by a modification using a phosphine reagent containing an internal electrophilic trap (**Scheme 1.15**, panel B).⁷¹ This method termed “STAUDINGER ligation” enables the covalent coupling reaction between complex reaction partners and is the artificial counterpart of the NCL for bioconjugation using unnatural FGs. Shortly after, BERTOZZI and RAINES independently turned this reaction into a “traceless” STAUDINGER ligation by the use of phosphinothiols.^{72,73} The latter being first reacted with a peptide containing a C-terminal thioester reacts afterwards with an azide to give an aza-ylide intermediate. Upon reaction with the activated thioester a stable peptide bond is formed, with the phosphinoyl released as the sole by-product (**Scheme 1.15**, panel C). Compared to NCL where an *N*-terminal cysteine residue is essential for a successful connection, this method allows the synthesis of long peptides which may contain any amino acid at the ligation junction. Unfortunately this method is of limited applicability due to its rather slow kinetics and the use of easily oxidized phosphines under aerobic conditions. For a detailed overview on the bioconjugation *via* azide-STAUDINGER ligation the reader is referred to the reviews of VAN HEST and BRÄSE.^{74,75}

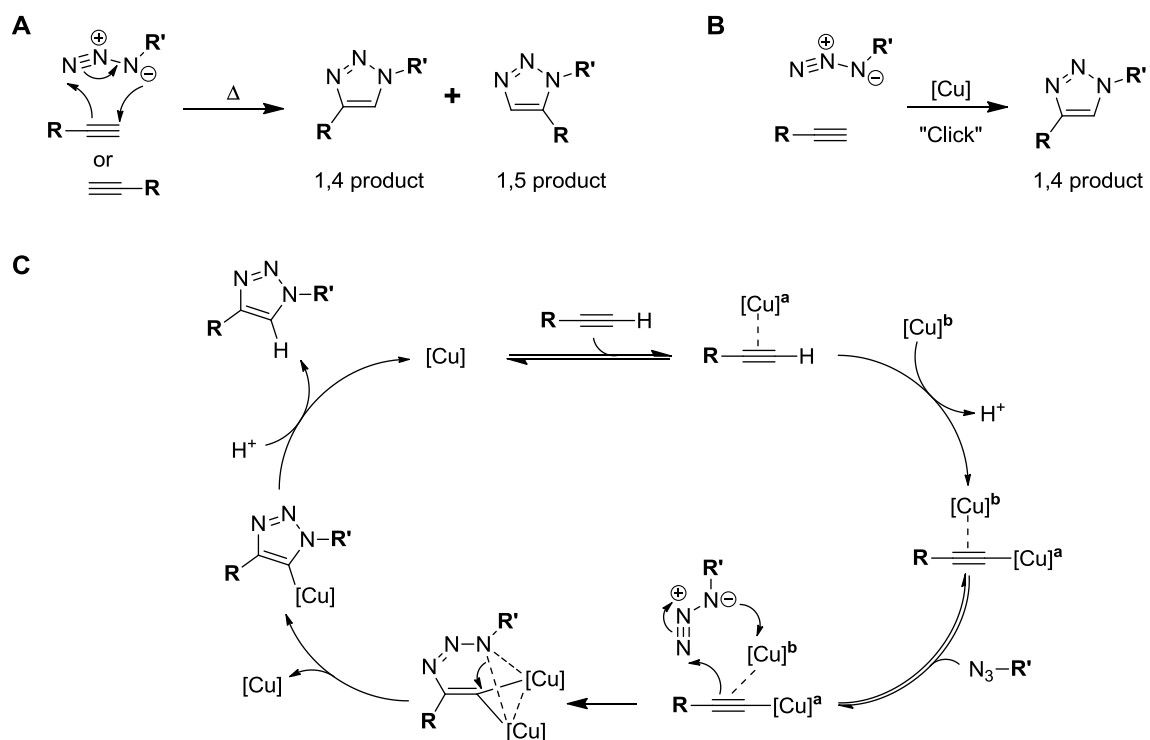


Scheme 1.15: (A) STAUDINGER reduction of azides with triphenylphosphine to yield primary amines. (B) Staudinger ligation using an electrophilic trap for the conjugation of the azide moiety to the phosphine. (C) Traceless STAUDINGER ligation using a phosphinothiol as the ligating mediator.

1.3.2 “Click” Chemistry

The origin of “click” chemistry goes back to the mid sixties where HUISGEN *et al.* presented the concept of 1,3-dipolar cycloaddition reactions between a dipolarophile (*e.g.*, alkene, alkyne) and a dipolar species (*e.g.*, nitrile, azide) to give five-membered heterocycles.⁷⁶ In particular, the addition of azides to alkynes or olefins is nowadays known as the HUISGEN 1,3-dipolar cycloaddition and still one of the classic reactions in organic chemistry. Although the reaction connects two substrates with excellent atom economy, it was found to be slow and elevated temperatures were essential for acceptable product yields (**Scheme 1.16**, panel A). In addition, the concerted mechanism usually results in mixtures of 1,4 and 1,5-regioisomers and is difficult to control. In 2001, US scientists KOLB, FINN and SHARPLESS introduced the term “click” chemistry which relies on the use of a Cu(I) catalyst for the efficient synthesis of such triazoles.⁷⁷ This method turned out to be very powerful, selective and modular delivering the products in high yields under mild reaction conditions and with broad FG tolerance. Using a Cu(I) catalyst was found not only to accelerate the reaction, but also to deliver

regiospecifically the 1,4-disubstituted 1,2,3-triazoles (**Scheme 1.16**, panel B). These observations were independently reported in 2002 by FOKIN and SHARPLESS, and MELDAL as separate publications.^{78,79} The proposed mechanism of the Cu(I)-catalyzed azide-alkyne cycloaddition (CuAAC) was recently revisited by FOKIN and describes the involvement of a dinuclear Cu(I) species which was supported by isotopic crossover experiments (**Scheme 1.16**, panel C).⁸⁰



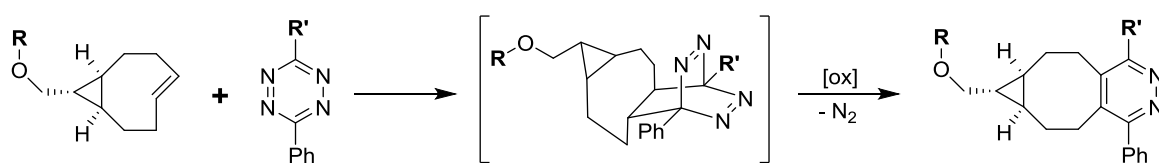
Scheme 1.16: (A) HUISGEN 1,3-dipolar cycloaddition delivering mixtures of 1,4 and 1,5 regioisomers upon heating. (B) General Cu(I)-catalyzed azide-alkyne cycloaddition; “click” reaction. (C) Revisited mechanistic cycle of CuAAC involving two copper atoms.

The revised mechanism of CuAAC involves initial formation of a π -coordinated copper/acetylene species which is transformed into a copper acetylide upon addition of a second copper atom. The added azide is able to coordinate the dinuclear copper acetylide species in a reversible fashion. Upon cycloaddition and C-N bond formation with subsequent elimination of one copper atom from the catalytic cycle, a five-membered copper triazolide is formed delivering the 1,4-disubstituted 1,2,3-triazole after protonation.

Since its discovery, the CuAAC reaction has found considerable applications in organic synthesis, materials chemistry and for bioconjugation of larger constructs.⁸¹ The main advantage of this method is the bioorthogonal nature of these two synthetic FGs and the tolerance of aqueous and oxygen rich conditions when Cu(I) is formed *in situ* by reduction of copper(II) salts (*e.g.*, $\text{CuSO}_4 \cdot 5 \text{H}_2\text{O}$).⁸² Its major limit for *in vivo* applications is the need for a catalyst (which is often toxic) and the rather slow kinetics. For a detailed overview on click bioconjugation the reader is referred to the reviews of BEST and FINN.^{83,84}

1.3.3 Inverse electron demand Diels-Alder reaction

Originally designed as a “Click” substitution avoiding a toxic copper catalyst, inverse electron demand DIELS-ALDER (IEDDA) reactions have shown to display unusually fast reactions kinetics. First reported in the sixties⁸⁵, FOX and HILDERBRAND introduced this reaction separately in 2008 as an efficient method for the bioconjugation of tetrazines and olefins, and has attracted high attention in the field of chemical biology ever since.^{86,87} FOX *et al.* demonstrated later an unusually fast tetrazine-*trans*-cyclooctene ligation, also known as strain-promoted inverse electron demand DIELS-ALDER cycloaddition (SPIEDAC).⁸⁸ Through a smart design of a highly strained alkene dieneophile, they report initial reaction rates of $>20,000 \text{ M}^{-1} \text{ s}^{-1}$ (Scheme 1.17).

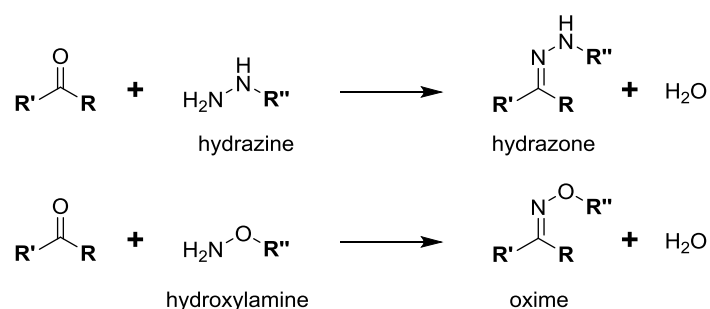


Scheme 1.17: Representative SPIEDAC bioconjugation with fast reaction kinetics between a tetrazine and a *trans*-cyclooctene. The intermediate undergoes a retro DIELS-ALDER reaction upon release of nitrogen and delivers the re-aromatized product after a separate oxidation step.

Recently a number of researchers have introduced genetically encoded tetrazine amino acids into proteins. In one case green fluorescent protein was expressed in bacteria and then rapidly conjugated to a strained olefin for fluorogenic labeling. In the same study they also identified a water soluble substrate pair for SPIEDAC which displays second order rate constants of $>3,000,000 \text{ M}^{-1} \text{ s}^{-1}$, the fastest rate known for a bioconjugation reaction to date.⁸⁹ These remarkable findings display again the potential of bioorthogonal FGs in chemical biology as useful tools for the selective and fast connection of large biomolecules. However IEDDA reactions have the obvious drawback of relatively complex starting materials which limits their use for quick assembly. Nonetheless, if high reaction rates are key criteria, this technique is certainly the most interesting one and further examples as well as their biomedical applications have been reviewed in several scientific publications.^{90,91}

1.3.4 Hydrazone and Oxime condensations

Probably one of the oldest class of FGs used for bioorthogonal bioconjugations are aldehydes and ketones.⁹² If condensed with hydrazines they deliver hydrazones whereas their reaction with *O*-alkylhydroxylamines results in the formation of oximes (**Scheme 1.18**). Compared to the rather labile Schiff bases obtained from carbonyls and primary or secondary amines, these strong α -effect amines form significantly more stable conjugates under physiological conditions.¹ Both, hydrazones and oximes have found broad applications in the field of chemical biology as bioconjugation strategies. Oximes have been used for the fluorescent labeling of proteins⁹³, synthesis of antibody-drug conjugates⁹⁴, surface-functionalization of nanoparticles⁹⁵ or as fluorescence quenchers⁹⁶ to mention a few examples. In industry oximes are used as intermediates in the production of ϵ -caprolactam which can be polymerized for the large scale synthesis of polycaprolactam (Nylon 6), a material with high tensile strength and elasticity.⁹⁷ The hydrazone formation has also been exploited for the modification of cell surfaces with affinity tags⁹⁸, for immobilizing protein capture agents⁹⁹ or for the construction of biocompatible and exchangeable linkers¹⁰⁰. Although widely applied, the kinetics of these condensations are generally slow and require fine tuning of the reaction conditions.⁹² Nonetheless the readily available starting materials and the bioorthogonal nature of these transformations has made hydrazone and oxime condensations a mainstay in chemical biology.



Scheme 1.18: Condensation of carbonyl compounds with α -effect nucleophiles like hydrazines and *O*-alkylhydroxylamines to form hydrazones and oximes, respectively.

1.4 Challenges and remaining problems

As described in the previous sections, many methods have been successfully developed for the selective modification of nucleic acids, peptides, proteins and other large biomolecules. Many of them have found broad applications in research laboratories, medical clinics and industrial facilities but are still rare and call for further development.¹ Each of the individual methods have their limitations like slow reaction kinetics, water incompatibility, the use of toxic or easily oxidized reagents, complex starting material syntheses, additional catalysts or high substrate concentrations. Therefore research is a necessary task to circumvent, minimize, or even exclude those limits. An extended overview of various established bioorthogonal reactions for bioconjugation classified by their reaction kinetics, which spans almost 10 orders of magnitude, is shown in **Figure 1.3**. Their general limitations are indicated below the respective reaction schemes.⁹²

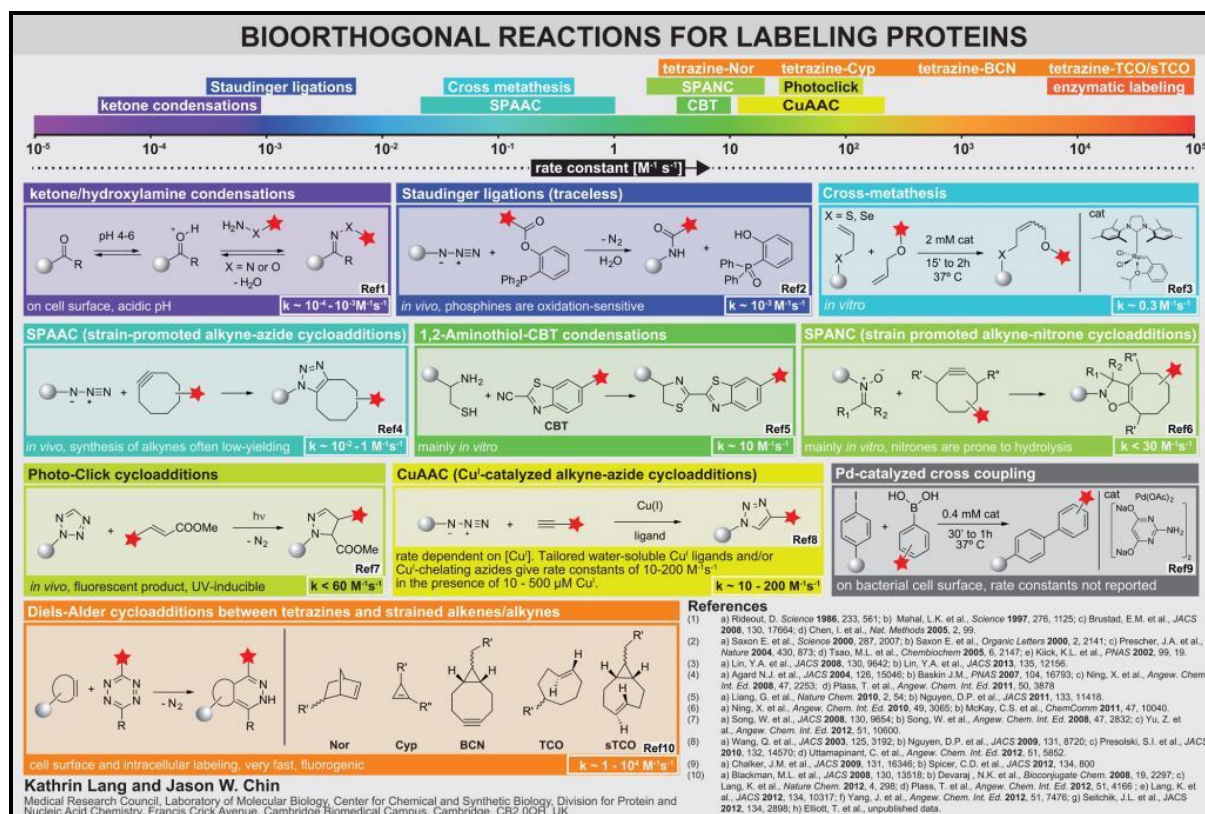


Figure 1.3: A collection of bioorthogonal reactions used in the field of bioconjugation and their limitations asserted by their rate constants.⁹² With personal permission of Prof. Dr. Jason W. Chin.

Taken together, the existing tools for the chemical modification of biomolecules (*vide supra*) have proven fruitful, combining chemical reactivity with natural or artificial functionalities and has delivered methods to explore Nature's secrets. Nonetheless these techniques require further development or even new innovations.

2 Guided catalyst to selectively target nucleic acids

To achieve our research goal for the catalytic, structure-selective nucleic acid modification using guided organometallic-catalysts, a short peptide nucleic acid (PNA) sequence was envisioned as template linked to a dirhodium catalyst. PNA has been widely used as a DNA counterpart for many applications based on its superior properties whereas dirhodium catalysis has been commonly used for carbenoid-based chemistry. Within the following sections focus is laid first on the introduction of PNA, its applications in templated chemistry and assembly through PNA monomers followed by a brief overview of dirhodium catalysis in chemical biology.

2.1 Peptide Nucleic Acids

2.1.1 Peptide Nucleic Acids and their properties

Peptide Nucleic Acids are an artificial DNA mimic which specifically recognizes complementary ssDNA, dsDNA as well as mRNA through WATSON-CRICK base pairing.¹⁰¹ PNA, first termed polyamide nucleic acid, was introduced by the Danish scientist PETER EGIL NIELSEN and co-workers in 1991.¹⁰² These unnatural nucleic acids were originally designed as potential ligands which should be able to recognize dsDNA in a sequence specific manner. It was first built by using computer-assisted models to determine proper bond distances and structural similarities (*e.g.*, hydrogen donor-acceptor properties) to the natural archetype. In addition, the inspiration for a synthetic analog came from earlier work by MOSER and DERVAN in which they investigated the possibility of triplex formation of dsDNA with a homopyrimidine-containing ssDNA.¹⁰³ Unlike dsDNA they found that the third ssDNA binds to the major groove of the pre-formed double helix through HOOGSTEEEN base pairing thus forming a stable triple helical structure (**Figure 2.1**).^{104,105}

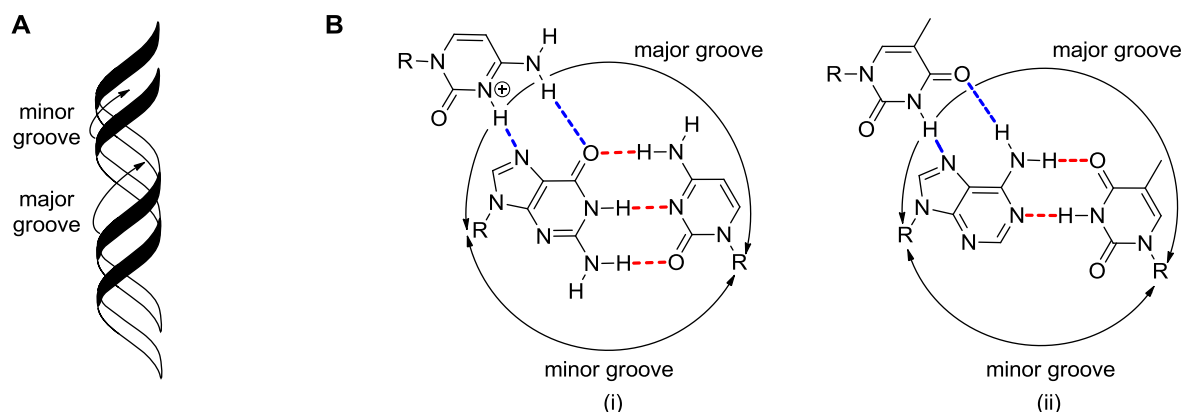


Figure 2.1: (A) Schematic front view of a dsDNA containing a major and minor groove. Both twist around their common helix axis and are opposite to each other. (B) Major groove binding modes of an isomorphous C⁺GC (i) and a TAT (ii) DNA triplex (helical top view). HOOGSTEEEN base pairing of C⁺GC and TAT is indicated through hydrogen bonds (blue) whereas the WATSON-CRICK duplex is highlighted in red.

This observation was the driving force for the development of a concept in which an oligonucleotide mimic is able to bind to dsDNA through this alternative hydrogen-bonding pattern within the major groove. Replacement of the deoxyribose phosphodiester backbone of DNA with repeating units of *N*-(2-aminoethyl)glycine (aeg) to which the nucleobases are attached *via* a methylenecarbonyl group were found to fit best to the structural requirements needed (**Figure 2.2**).¹⁰⁶

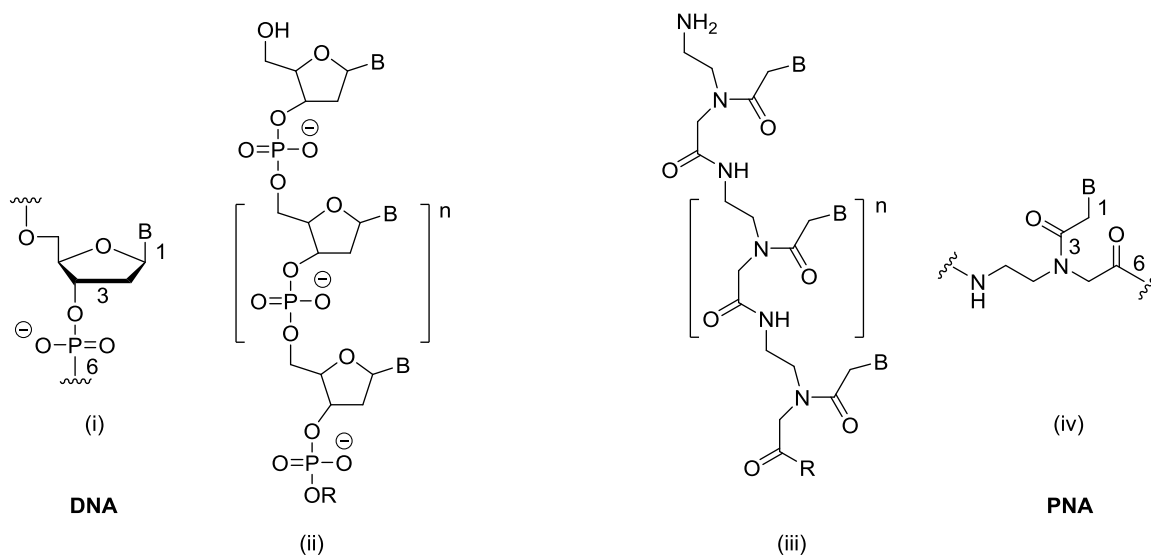


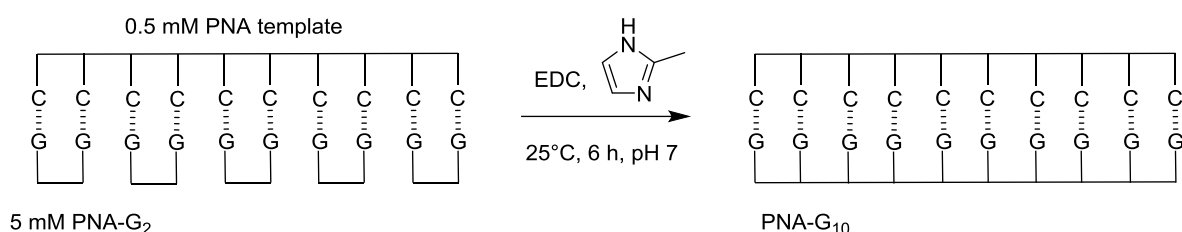
Figure 2.2: Schematic structural comparison of the deoxyribose phosphodiester backbone in DNA (i) and (ii) and the *N*-(2-aminoethyl)glycine backbone of its PNA analog (iii) and (iv). Both structures contain a six bond distance between the nucleobase and their respective repeating unit as well as a three bond distance to their backbone (indicated through bond numbering 1, 3 and 6 in (i) and (iv)).

While the structural differences of PNA compared to DNA were obvious (achiral, acyclic, more flexible, uncharged) and considered as potential drawbacks its synthetic challenge was less of a problem. Once a suitable monomer synthesis was established the pseudo-peptides were readily accessible through MERRIFIELD'S SPPS approach established in the early sixties.¹⁰⁷ Due to its synthetic nature PNA was found to be chemically stable and resistant to enzymatic degradation, which makes it attractive for *in vivo* applications as a nucleic acid analog.¹⁰⁸ Many studies on PNA/DNA or RNA systems revealed that PNA had superior helical binding properties at low to medium ionic strength compared to DNA that set them apart from traditional nucleic acid analogues (*e.g.*, LNA, TNA or GNA).¹⁰⁹ These findings are mainly attributed to the uncharged nature of PNA which allows short sequences to bind complementary DNA in a quick and sequence selective fashion. In particular, thermal denaturation studies demonstrated that antiparallel PNA/DNA and PNA/RNA duplexes were more stable than the corresponding dsDNA and dsRNA duplexes.¹⁰¹ In addition the stability of PNA was also found to be highly affected by the presence of base pair mismatches compared to DNA or RNA as reported by JENSEN *et al.*¹¹⁰ Besides the ability of PNA to form stable PNA/DNA or RNA duplexes¹¹¹, NIELSEN and others revealed the existence of several dsDNA-PNA systems like triplex-

invasion¹¹², duplex-invasion¹¹³, double duplex-invasion¹¹⁴ or tail-clamp complexes which could be used for various applications.^{115,116} In summary, the ability of PNA to sequence-specifically bind to complementary DNA/RNA forming highly stable helical structures has attracted many scientist's attentions to exploit these systems for a particular research problem in *e.g.*, chemical biology, material science, diagnostics and therapeutics. Some of these examples will be discussed in more detail in the following sections.

2.1.2 Peptide Nucleic Acids in templated chemistry

In 1995 BÖHLER, NIELSEN and ORGEL reported the first example of a PNA-templated reaction. They demonstrated that a PNA C₁₀ oligomer could either act itself as a template for the synthesis of a RNA-containing oligomer using a primer for extension, or it can be assembled from its PNA G₂ dimers by template-directed synthesis on a d(C)₁₀ template (**Scheme 2.1**).¹¹⁷



Scheme 2.1: PNA template-directed synthesis of a PNA-G₁₀ oligomer by the assembly of five PNA-G₂ units using an EDC/2-methyl imidazole coupling protocol at neutral pH.

Later LIU *et al.* used a hairpin DNA template for the oligomerization of PNA aldehydes up to 20 base-pairs and showed additionally high discrimination when base pair mismatches were present.¹¹⁸ A homothymine PNA decamer was used by JANSSEN and co-workers for the size-controlled templated assembly of chiral *p*-phenylenevinylene oligomers into functional nanostructures.¹¹⁹ As mentioned in section 1.2.1 (*vide supra*), the ROKITA group was able to use an *ortho*-quinone methide (QM) strategy for templated nucleic acid crosslinking (see **Scheme 1.3** in section 1.2.1). For this purpose they used a QM-containing PNA template which upon hybridization to ssDNA was able to deliver the quinone methide alkylating agent forming a stable PNA-DNA conjugate.³⁰ Until today several methods were published which show the potential of PNA-templated reactions for *e.g.*, chimeric DNA/PNA ligation¹²⁰, carbodiimide-mediated ligation of short PNA fragments¹²¹ or more recently the self-assembly of Fab (fragment antigen binding) antibody fragments.¹²²

2.1.3 Applications of Peptide Nucleic Acids in chemical biology

As described before, PNA was initially created as potential sequence-specific DNA analog which can be used as gene silencing agent at the level of transcription or translation. Preventing gene modulation is essential if an organism (in particular a human being) comprises a genetic defect and a regulatory system for the over expression of specific proteins is needed. Due to its property to break up DNA duplexes PNAs are considered as potential antigene and antisense agents for blocking either translation or transcription (Figure 2.3).¹²³

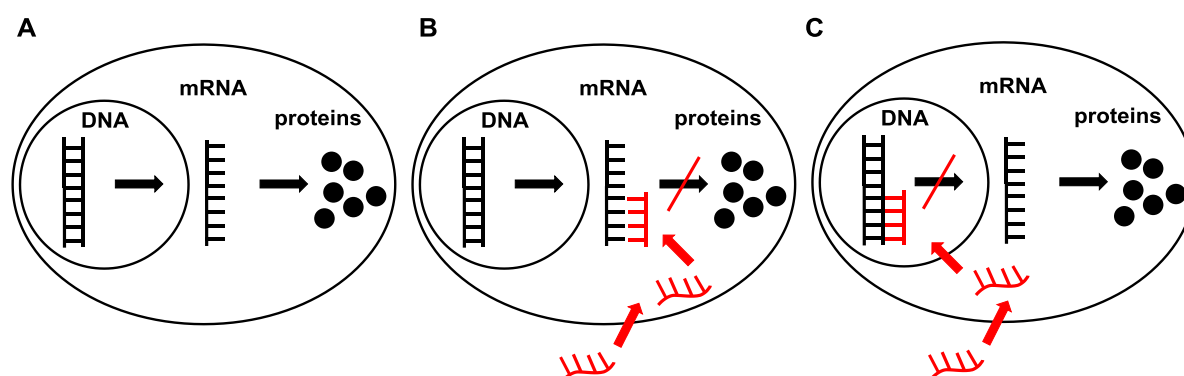


Figure 2.3: (A) The central dogma of molecular biology¹²⁴: cellular dsDNA is transcribed into mRNA which is translated into proteins. (B) Treatment of the cell with a complementary antisense oligonucleotide inhibits protein expression at the level of mRNA translation. (C) Treatment of the cell with a complementary antigene oligonucleotide inhibits gene expression.

A more recent *in vivo* study which also relies on the principle of RNA interference through antisense PNA showed promising results on the basis of reactivating proteins needed for a specific function. In particular WOOD and LU could demonstrate that muscular dystrophy, which is a genetic disease caused by point mutations, can be treated by applying a PNA-based drug. The PNA is delivered into the cell of a mouse where it binds to the defect pre-mRNA intron22/exon23 junction containing a stop codon, thereby skipping exon23 during the process of splicing. The shortened dystrophin protein generated was found to have sufficient activity and restored its muscular functionality (Figure 2.4).¹²⁵ This shows the potential of RNA interfering PNAs to be used in drug discovery by fine-tuning conditions and the structural characteristics.

Compared to DNA and RNA, PNAs in general have poor penetration properties that limit their application for *in vivo* studies. To enhance the cellular uptake of uncharged PNA it is typically conjugated to cationic cell-penetrating peptides (CPPs) like TAT or penetratin which are additionally equipped with oligo-arginine residues.¹²⁶ Using phosphonate-peptide PNA conjugates were found to

show enhanced cellular delivery through cationic lipids and exhibit antisense activity in a luciferase splicing redirection system in the low nanomolar concentration range.¹²⁷

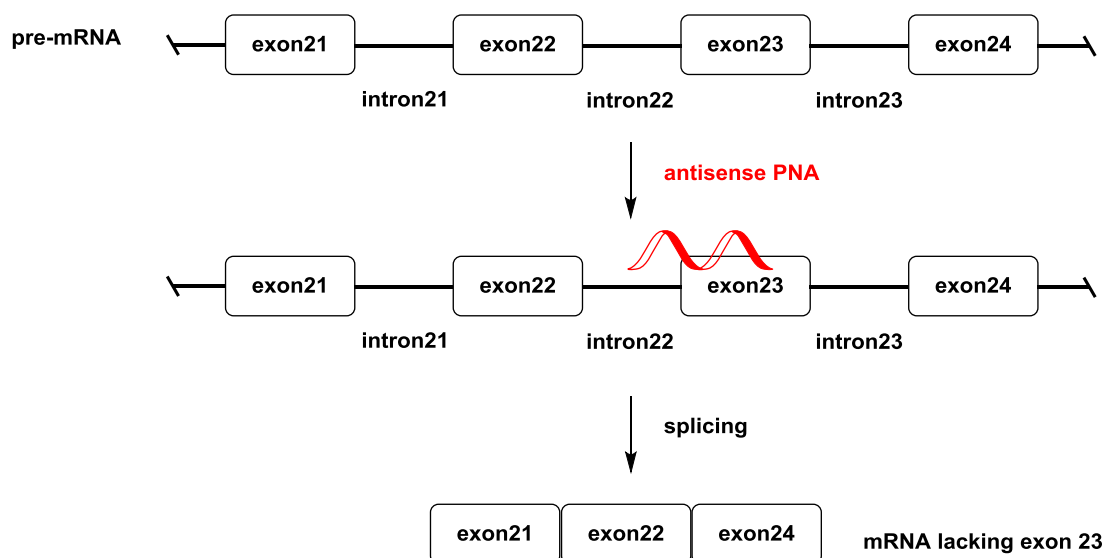


Figure 2.4: Schematic representation of the antisense PNA blocking the intron22/exon23 junction in pre-mRNA. The splicing process generates mRNA lacking exon23 but can be transcribed into a protein which restores muscular function.

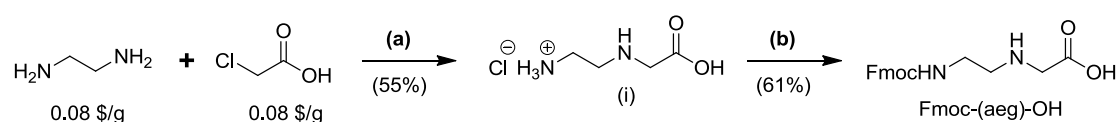
Other examples where PNA has been successfully applied so far comprise PCR clamping¹²⁸ for the selective amplification of a mutated sequence for early stage genetic diagnostics (*e.g.*, detection of a few cancer cells in a tissue), as fluorescent *in situ* hybridization probes (FISH) for the detection and visualization of infective agents in clinical microbiology¹²⁹ or as an antibacterial agent against multi-resistant microbes.¹³⁰

These applications demonstrate the power of chemical modification in enabling life science research. It is at the stage of synthesis where functionality and compatibility can be introduced and many methods have been developed over the past years introducing chemical modifications into PNAs to enhance their SAR. It is clear however that prior to the modification of a PNA, monomers have to be synthesized in a simple and effective way which can be scaled up easily. The following section will focus on the synthesis of standard PNA monomers which are generally used for assembling the PNA oligomers.

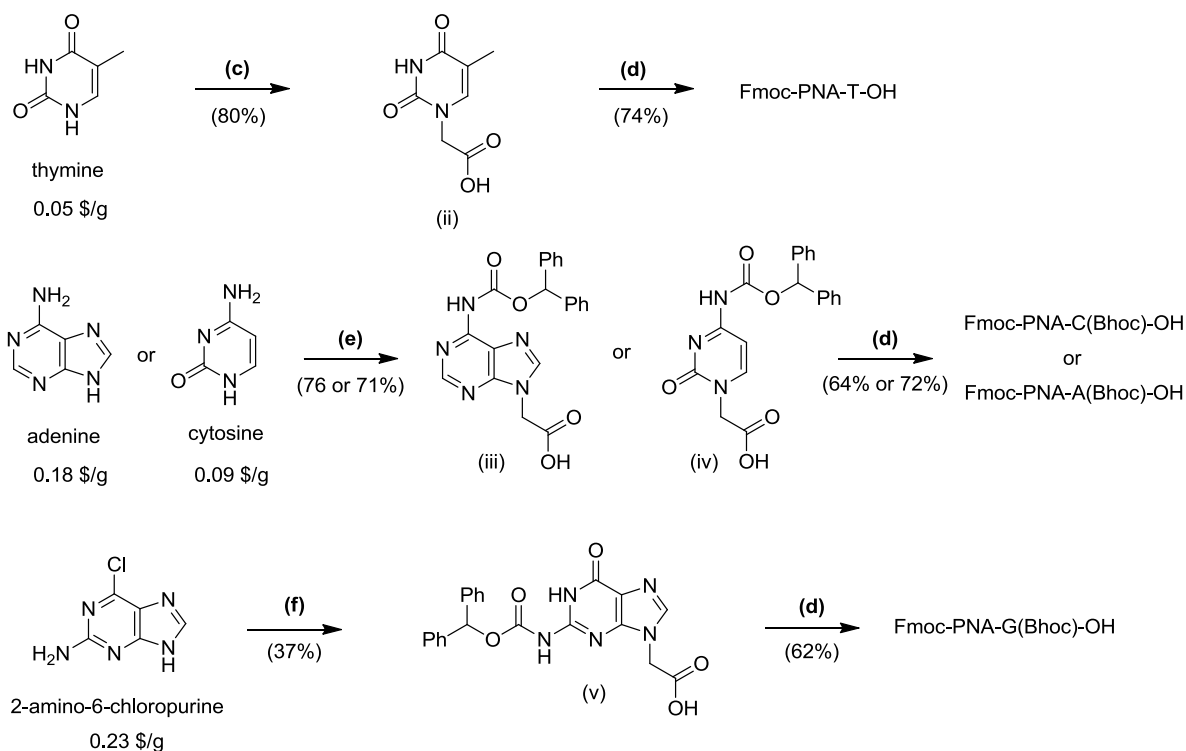
2.1.4 PNA monomers and their chemical assembly

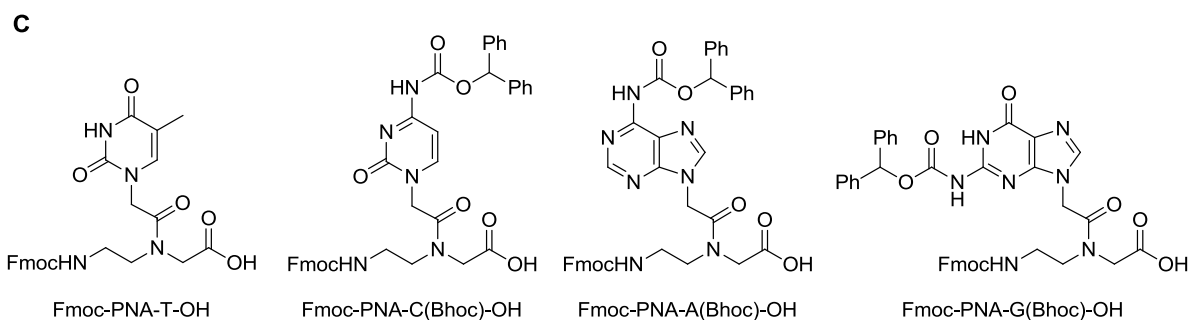
The routinely used PNA monomers for SPPS are the products of multistep synthesis and scalable up to several grams. Although the Fmoc/Bhoc-protected monomers are available from several suppliers (*e.g.*, Link, Panagene or PolyOrg, Inc.; starting at ± 200 \$/g) the synthetic pathway commonly used for academic research is presented in this section. If affordable in terms of time, the synthesis of multigram quantities of PNA monomers is easily achieved through robust and easy chemistry starting from very cheap starting materials (*e.g.*, adenine, thymine, cytosine; 0.05-0.18 \$/g). An overview of the synthetic steps for the synthesis of Fmoc-B(PG)-OH PNA monomers is presented in **Scheme 2.2**.

A



B

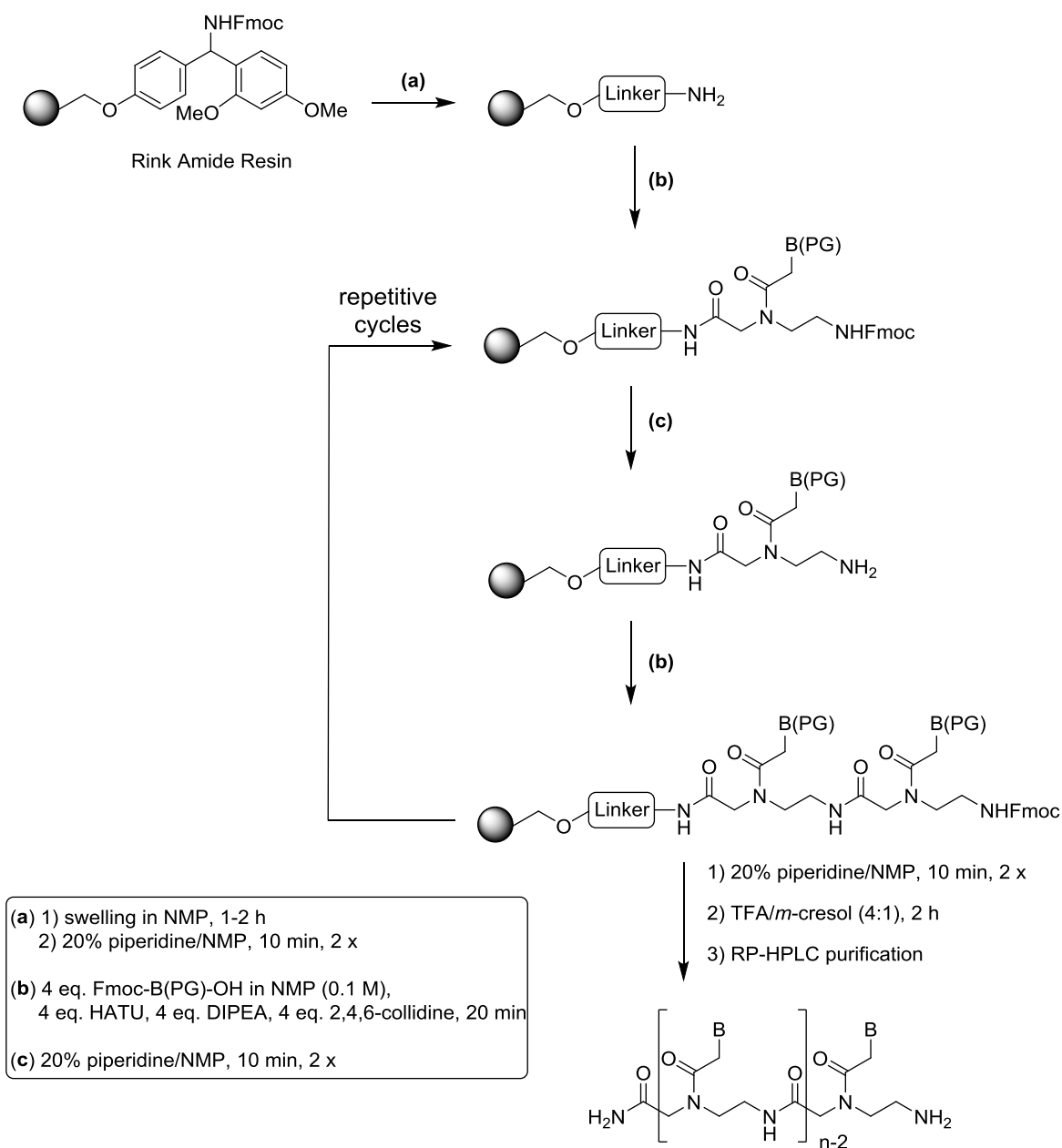




Scheme 2.2: (A) Synthesis of the PNA backbone Fmoc-(aeg)-OH; (a) neat ethylenediamine; (b) TMS-Cl, Fmoc-OSu, NMM. (B) Synthesis of the final PNA monomers starting from their nucleobases T/A/C and G precursor; (c) KOH, bromoacetic acid; (d) Fmoc-(aeg)-OH, TSTU, DIPEA (this procedure is used for the monomers containing Boc protecting groups – the yields for step d in all cases are also related to Boc protected monomers); (e) KO^tBu, benzyl bromoacetate followed by CDI, benzhydryol followed by LiOH; (f) K₂CO₃, benzyl bromoacetate followed by triphosgene, DIPEA, benzhydryol followed by NaH, 3-hydroxypropionitrile. (C) Chemical structures of the four Fmoc-PNA-B(PG)-OH monomers.

The monomer synthesis is divided into two parts which are the synthesis of the PNA backbone and the synthesis of the four protected nucleobases containing a free carboxylic acid. The backbone is constructed starting from chloroacetic acid reacting with neat ethylenediamine to give the amine salt (i) which is then Fmoc protected at its *N*-terminus affording the PNA backbone scaffold (Fmoc-(aeg)-OH) in 34% overall yield (Scheme 2.2, panel A).^{131,132} In the second synthetic part the carboxylic acid moiety at N-1 (T/C) and N-9 (A/G) is first introduced, followed by protection of the exocyclic amino groups of the nucleobases A/C and G-precursor with *N*-benzhydryloxycarbonyl (Bhoc) to give the acids (ii-v) ready to be coupled.^{133,134} The final PNA monomers are obtained by an amide coupling between the backbone and the protected nucleobases in yields ranging from 62-74% (Scheme 2.2, panel B and C).¹³⁵

The monomers, once successfully synthesized or obtained from commercial sources, can be used either for automated or manual SPPS on the same resins employed for the coupling of amino acids. Depending on the final functionality of the oligonucleotide suitable resins have to be selected which allow either a C-terminal amide (*e.g.*, MBHA, rink amide resin) or carboxylic acid (*e.g.*, Wang, 2-Chlorotrityl resin). A general protocol for the manual assembly of short PNA sequences is outlined in Scheme 2.3 and follows a published procedure by GOODWIN *et al.*¹³⁶

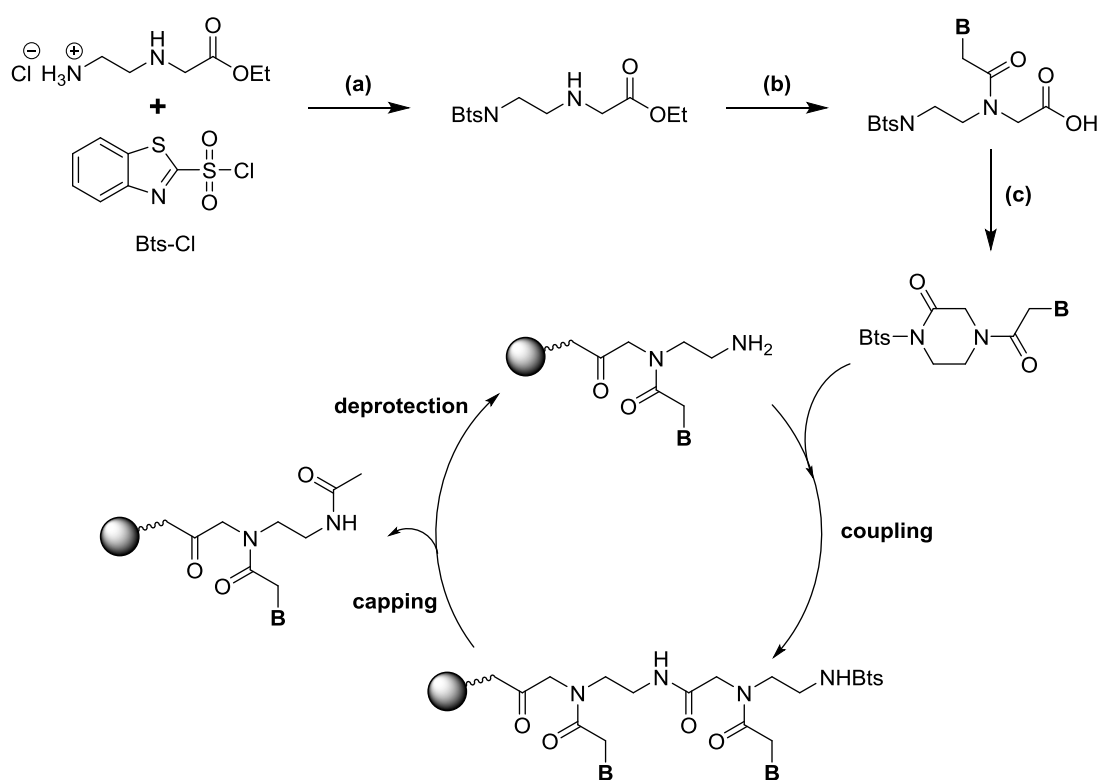


Scheme 2.3: General synthetic cycle for the SPPS of short PNA sequences containing a C-terminal amide.

To allow a high degree of FG accessibility the polystyrene-based solid phase needs to be swollen in a suitable solvent for one to several hours.^{137,138} This is followed by a repetitive piperidine deprotection step if a Fmoc protected amine-based resin is used. After each step a washing cycle is included which uses $\text{CH}_2\text{Cl}_2/\text{NMP}$ (1:1, 1 min, 3 x) to remove excess reagents. A pre-activated reaction cocktail containing 4 eq. of each Fmoc-PNA(PG)-OH, HATU, DIPEA and 2,4,6-collidine is then reacted with the free amine for 20 min at room temperature followed by a washing cycle. From this stage on the deprotection/coupling cycles are repeated until the desired PNA sequence is assembled and is ready for a final Fmoc removal. Treating the resin with high TFA concentrations and a thiol-based cation scavenger removes all Bhoc protecting groups and liberates the crude PNA which is then precipitated from cold ether and purified preparatively employing acidic RP-HPLC. After lyophilizing the pure

PNA oligonucleotide aqueous stock solutions are prepared and quantified by UV spectrophotometry at 260 nm using molar extinction coefficients ϵ_{260} for the bases reported in the literature or supplied from companies.^{139,140}

Although the above described conditions are well-established, they require harsh conditions during the oligomer synthesis and possible side reactions can lead to undesired products hampering the purification. An alternative to the Fmoc/Bhoc strategy was reported in 2007 by co-workers of Panagene Inc. which uses self-activating PNA monomers and the Bts (benzothiazole-2-sulfonyl) strategy (**Scheme 2.4**).¹⁴¹ The process was found to deliver excellent purities of PNA products without the need for additional coupling reagents and a straightforward monomer synthesis with high yields.



Bts PNA synthesis cycles

1) coupling	2) capping	3) deprotection
0.3 M PNA monomer (20 eq.) and 0.2 M DIPEA solution in DMF (120 min, 40°C)	(1) 5% Ac ₂ O and 6% lutidine solution in DMF (3 min, rt); (2) 10% piperidine in DMF (3 min, rt)	0.8 M 4-methoxybenzenethiol and 0.4 M DIPEA in DMF (10 min, 40°C)

Scheme 2.4: Synthesis of self-activating PNA monomers using the Bts strategy and their assembly by SPPS through repetitive coupling, capping and deprotection cycles. (a) NEt₃; (b) DCC, HOBT, nucleobase acetic acid followed by LiOH; (c) EDC.

2.2 Dirhodium catalysis and its applications in chemical biology

Many of the reactions used to introduce new functionality into biomolecules are slow and unspecific. To improve these potential drawbacks, catalysts are commonly implied which can overcome these limits. Within this section focus is laid on the use of dirhodium catalysis (acronym: Rh(II)) for the transformation of specific FGs and the formation of new bonds connecting the reaction partners.

In the early 1970s, TEYSSIE *et al.* could demonstrate the first documented example of a dirhodium-catalyzed carbenoid O-H insertion reaction of ethyldiazoacetate using substoichiometric amounts of dirhodium tetracarboxylate [$\text{Rh}_2(\text{OAc})_4$] achieving ~600 turnovers in 4 h (**Figure 2.5**, panel A).¹⁴² This finding was the basic principle for transition-metal catalyzed carbene chemistry using Rh(II) species. In general the two axial d^7 Rh(II) centers are bridged by four equatorial ligands to give a stable, paddlewheel-like $18e^-$ complex (**Figure 2.5**, panel B). The two vacant axial positions are used for the formation of electrophilic dirhodium(II)-stabilized carbenoids with *e.g.*, α -diazocarbonyl compounds which readily insert into polar X-H bonds (X = O, N, C, S).

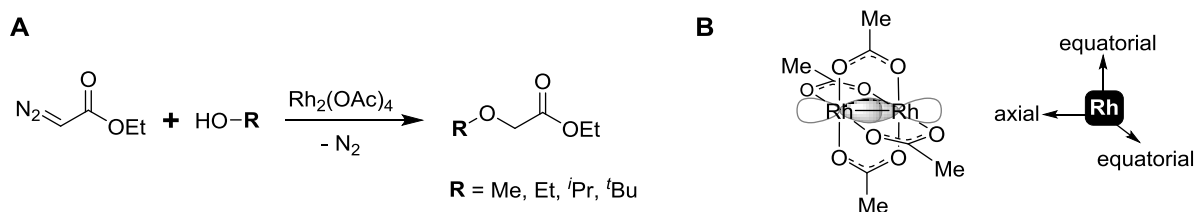
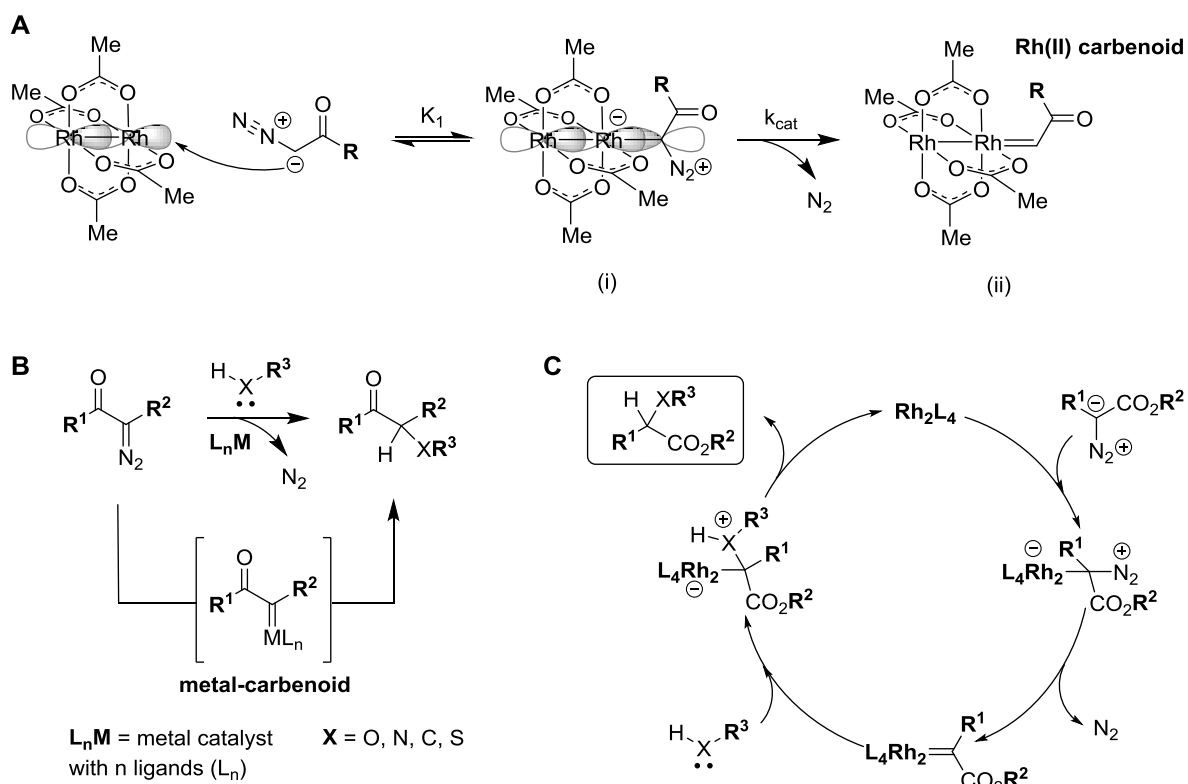


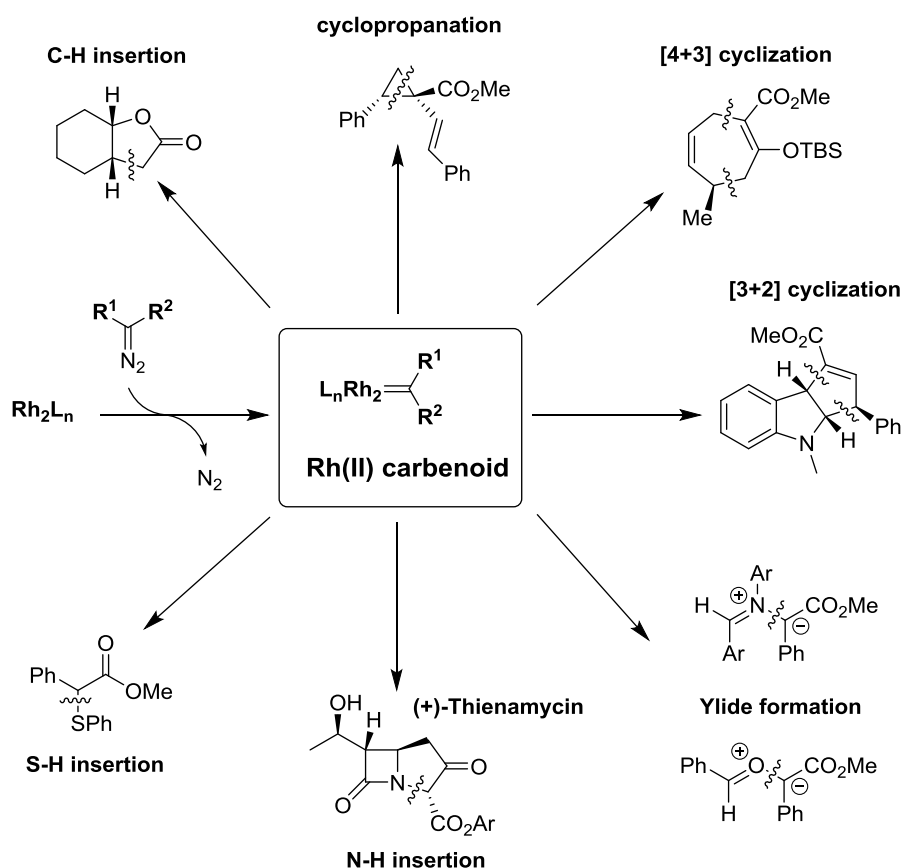
Figure 2.5: (A) $\text{Rh}_2(\text{OAc})_4$ catalyzed O-H insertion reaction of ethyldiazoacetate with various alcohols. (B) Three-dimensional “paddlewheel” structure of $\text{Rh}_2(\text{OAc})_4$ containing four equatorial acetate ligands bridging the two central Rh atoms while two vacant axial positions are available for catalysis.

A mechanistic model proposed by YATES for the copper-catalyzed decomposition of diazoketones is generally accepted for the formation of dirhodium carbenoids (**Scheme 2.5**, panel A).¹⁴³ It is initiated by the complexation of the negatively-polarized carbon atom of the α -diazocarbonyl compound to one of the axial positions forming a Rh-C σ -bond with negative charge transfer to the Rh atom. Subsequent release of N_2 forms the final electrophilic dirhodium(II) carbenoid species. Several decades later, MOREHEAD was able to show that the addition step is in a pre-equilibrium whereas the carbenoid forming step is rate-determining.¹⁴⁴ A general pathway for X-H insertions using metal-carbenoids and its concerted mechanistic steps using a Rh(II) catalyst and α -diazocarbonyl compounds is presented in **Scheme 2.5**, panel B and C.¹⁴⁵



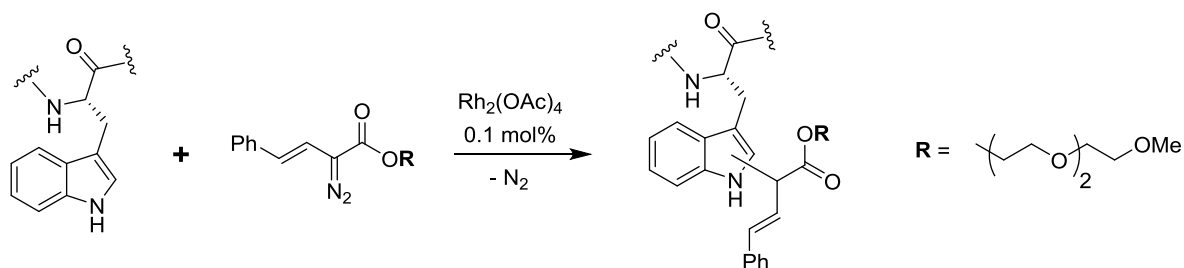
Scheme 2.5: (A) Generally accepted mechanism of Rh(II) carbenoid formation illustrated with an example: $Rh_2(OAc)_4$ reacts reversibly with an α -diazocarbonyl compound to give the covalent Rh-C species (i) which after irreversible loss of one equivalent N_2 results in the catalytically active $Rh_2(OAc)_4$ carbenoid species (ii). (B) General schematic representation of X-H insertion reactions involving transition-metal catalysts equipped with ligands. (C) Concerted mechanistic pathway of an X-H insertion reaction using $Rh_2(L)_4$ as catalyst.

Rhodium(II) carbenoid chemistry can be exploited in a variety of bond-forming methods to generate molecular diversity, expand substrate scopes and simplify or allow new key transformations in natural product synthesis (*e.g.*, total synthesis of (-)-serotobenine).¹⁴⁶ Until today many useful reactions were published on the basis of rhodium(II) carbenoids from α -diazocarbonyl substrates and comprise S-H insertions¹⁴⁷, N-H insertions used for example in Merck's synthesis of (+)-Thienamycin¹⁴⁸, *O*- and *N*-ylide formations with appropriate carbonyls and imines¹⁴⁹, [3+2]¹⁵⁰ and [4+3]¹⁵¹ cyclizations of alkenes and dienes, cyclopropanation of alkenes¹⁵² or alkynes¹⁵³ and C-H insertions on a variety of substrates (*e.g.*, intramolecular cyclization)¹⁵⁴. A collective overview of Rh(II) carbenoid chemistries is presented in **Scheme 2.6**.



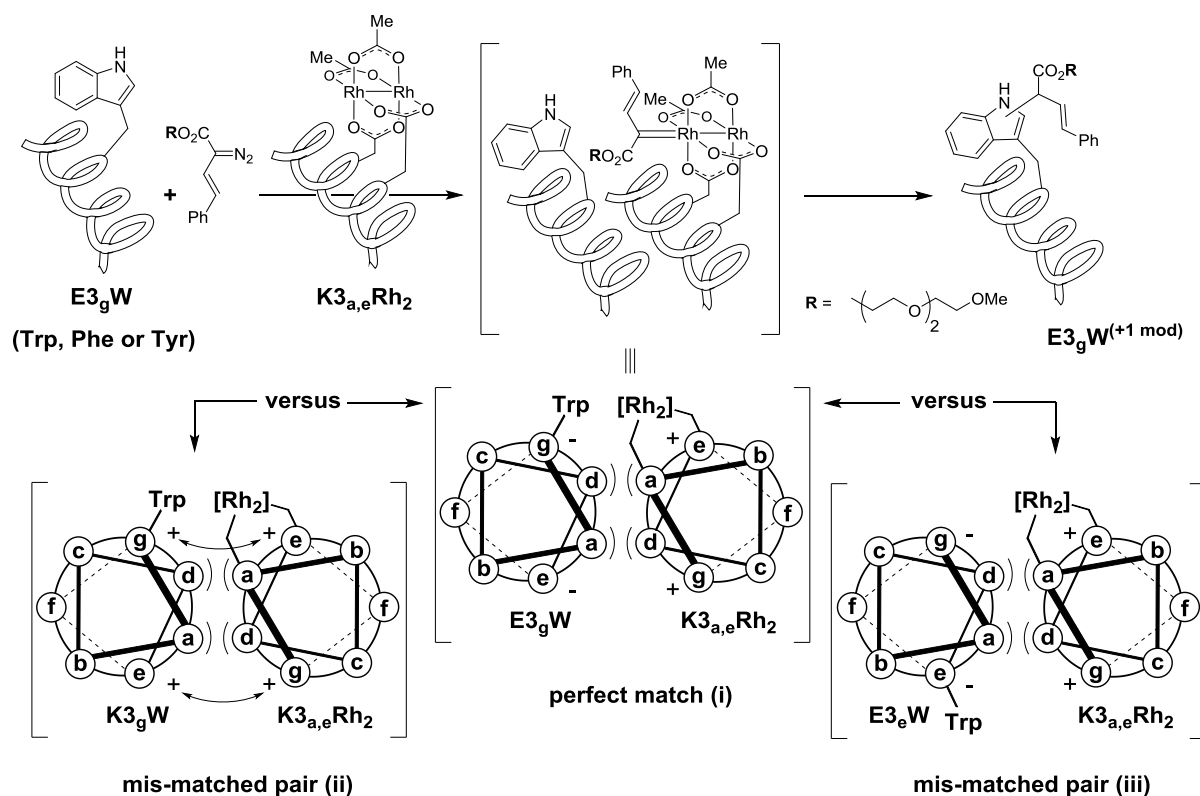
Scheme 2.6: Overview of Rh(II) carbenoid reactions from α -diazo carbonyl precursors with different substrates delivering a variety of products. R^1 and R^2 are general placeholders and unrelated to the products illustrated.

Almost a decade ago, FRANCIS *et al.* reported the first example of using Rh(II) carbenoid chemistry in aqueous solution for potential applications in chemical biology. They demonstrated a method for the selective modification of tryptophan residues using α -diazocarbonyl compounds on various protein substrates (*e.g.*, myoglobin and subtilisin) which was expanded a few years later to include lysozyme, melittin and human FKBP (**Scheme 2.7**).^{155,156}



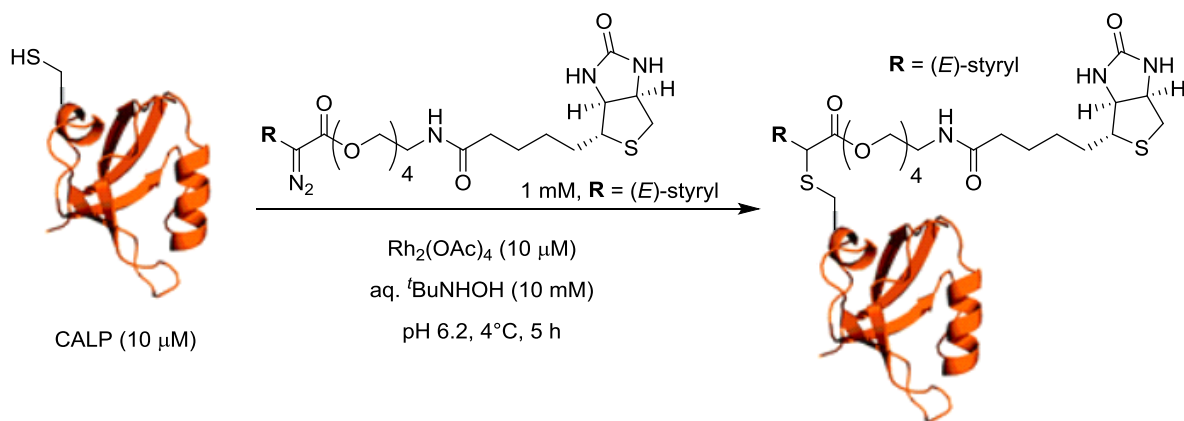
Scheme 2.7: Selective tryptophan modification on proteins in aqueous media using Rh(II) carbenoid chemistry. Modifications were found to occur at the indole nitrogen and C-2 position in a 1:1.4 ratio in 51% overall yield using a catalyst loading as low as 0.1 mol%.¹⁵⁵

These findings established the possibility of using biocompatible and chemoselective metallocarbene-based reactions on large biomolecules. In 2010, BALL and POPP extended the target of amino acid side chains to other aromatic residues (*e.g.*, phenylalanine and tyrosine) using dirhodium metallopeptide catalysis (**Scheme 2.8**).¹⁵⁷ A year later they expanded the scope and utility of the method while several buffer systems at physiological pH were tested along with a biotin-diazo conjugate allowing affinity tagging of target proteins.¹⁵⁸



Scheme 2.8: Dirhodium metallopeptide catalysis illustrated on a tryptophan-containing peptide. The reaction is enabled by an intermediate coiled-coil interaction of the peptide and carbenoid metallopeptide strands only when a perfect facial match (i) is present promoted by electrostatic attraction between opposing glutamate/lysine residues. The rate of modification drops when electrostatic repulsions (both lys-lys) of opposing strands are introduced (ii) or if a facial mis-matched pair is present (iii).

In 2012, BALL demonstrated a chemoselective cysteine modification in CALP protein using the same Rh(II) carbenoid chemistry based on a biotin-diazo compound but without using a protein template (**Scheme 2.9**).¹⁵⁹ They confirmed the site of protein modification by trypsin digest followed by MS/MS fragmentation studies and verified these results separately by modifying a series of peptides derived from that particular CALP sequence. The covalent linkage was additionally found to be stable in human serum over several hours thus promising potential for applications under biological conditions.



Scheme 2.9: Chemoselective cysteine modification using Rh(II) carbenoid chemistry using a biotin-diazo compound at near neutral pH in aqueous media. Tryptophan or other amino acid side chains were found to be untouched under these reaction conditions.

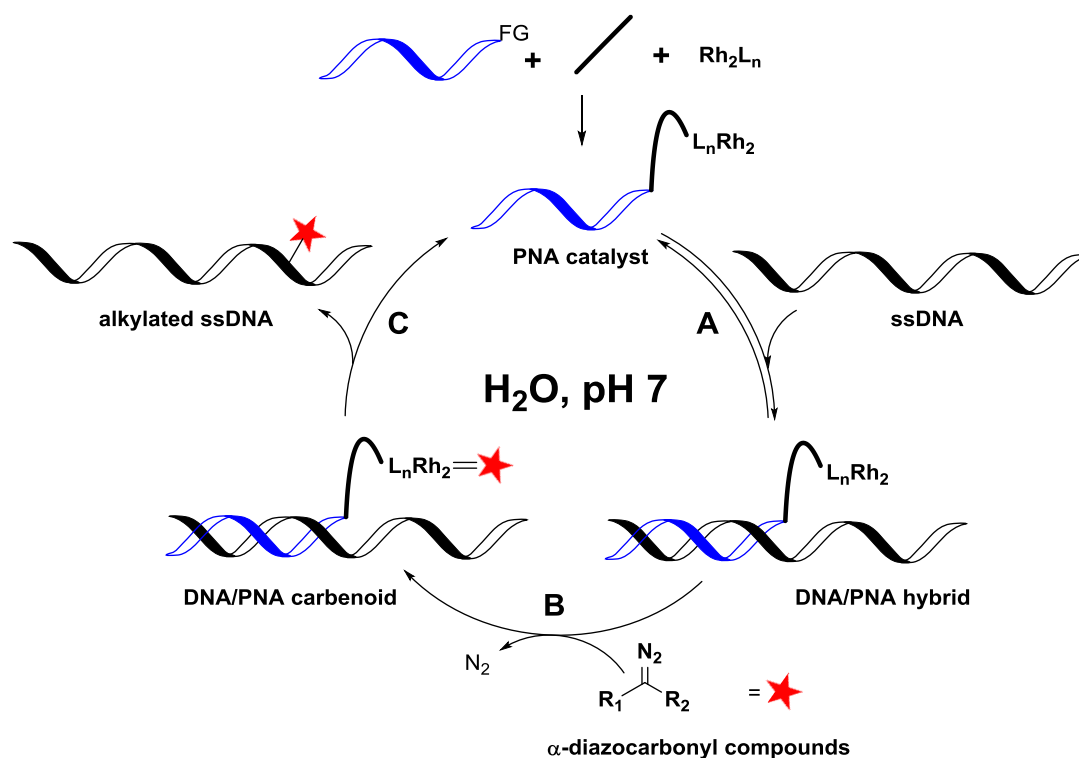
For a detailed summary on dirhodium metalloptides described by BALL, the reader is referred to the publication entitled “Designing Enzyme-like Catalysts: A Rhodium(II) Metallopeptide Case Study”.¹⁶⁰

2.3 Results and discussion

Note: For clarity many molecular structures are represented only schematically; their entire skeletal formulas are illustrated in the experimental section 4.2.1.3.

2.3.1 Nucleic acid alkylation using template PNA-dirhodium conjugates

The aim of the work discussed in this chapter was to develop a short PNA-based self-assembling catalyst for the direct, sequence-specific alkylation of ssDNA using Rh(II)-stabilized carbenoids in aqueous media under neutral conditions. The catalytic system was envisioned to contain a templating PNA sequence which is covalently linked to a Rh(II) catalyst through a rapid bioconjugation reaction. Once the organometallic catalyst is assembled, substrate selectivity is achieved through dynamic WATSON-CRICK base-pairing (annealing) with the complementary ssDNA target. Reaction with a α -diazocarbonyl compound forms a Rh(II)-stabilized PNA carbenoid *in situ* which is able to alkylate the nucleobases of DNA by subsequent N-H insertion as previously shown by TISHINOV *et al.*³⁶ Once modification is achieved and after denaturation of the hybrid duplex, the Rh(II)-containing PNA is envisioned to re-enter the catalytic cycle achieving high turnovers (**Scheme 2.10**).



Scheme 2.10: Proposed catalytic cycle for nucleic acid modification using a pre-formed templating PNA catalyst. **Step A:** PNA catalyst and complementary ssDNA anneal through WATSON-CRICK base-pairing to form a dynamic DNA/PNA hybrid. **Step B:** Addition of a α -diazocarbonyl compound generates a reactive DNA/PNA carbenoid species which is able to undergo an insertion reaction on the DNA complement. **Step C:** Denaturation of the product liberates the active and unmodified PNA catalyst ready for the next cycle.

2.3.1.1 Design of the PNA catalyst template – a retrosynthetic analysis

For a successful design of the envisioned PNA sequence it was essential to consider some general rules reported in the literature or directly supplied from companies and their webpages.^{161,162} It is known that longer PNA oligomers tend to aggregate in solution, are difficult to purify and characterize and participate in non-specific binding of other nucleic acids.^{163,164} It was therefore essential to answer two major questions which come along with the proposed catalytic system shown in section 2.3.1:

- (1) what is a reasonable PNA length to allow a dynamic hybridization to ssDNA?
- (2) which PNA sequence should be chosen?

A detailed literature search could quickly give information on the required PNA length allowing a dynamic system. In their early studies on PNA, NIELSEN *et al.* determined the thermal stability of PNA/DNA hybrid duplexes of varying lengths.¹⁰⁶ An oligothymine PNA hexamer was found to have a melting temperature (T_m) of 31°C whereas its octamer is significantly more stable ($T_m = 52^\circ\text{C}$). For comparison, an oligothymine DNA hexamer was shown to have a T_m below 10°C.¹⁶⁵ Therefore it seemed reasonable to choose a hexameric sequence based on these findings since a T_m close to room temperature would be ideal for the required abilities of the final system.

Next, the sequence of the PNA template had to be selected which was done according to a complementary commercial ssDNA d(GCG TAT CCG GCA CGT CGA) (BioTeZ, Berlin-Buch) in the strongly preferred antiparallel orientation (amino terminus of the PNA facing the 3'-end of the ssDNA) (**Figure 2.6**).

Thus the desired PNA hexamer contained the following base sequence: **pna(CGC ATA)**



Figure 2.6: Antiparallel PNA sequence pna(CGC ATA) designed on the basis of a ssDNA d(GCG TAT CCG GCA CGA).

Inspired by previous work of BALL *et al.*, the covalent linkage of a Rh(II) species was envisioned to be achieved through simple carboxylate ligand exchange in water using an appropriate dicarboxylate linker installed at the PNA *N*-terminus and *cis*-Rh₂(OAc)₂(TFA)₂. This strategy was imagined to be highly efficient since peptide couplings on PNA are achieved with ease and final dirhodium ligations have been shown to be readily achieved in good yields with short reaction times.¹⁶⁶ A retrosynthetic analysis of the hexameric PNA catalyst **1.1** is outlined in **Figure 2.7**.

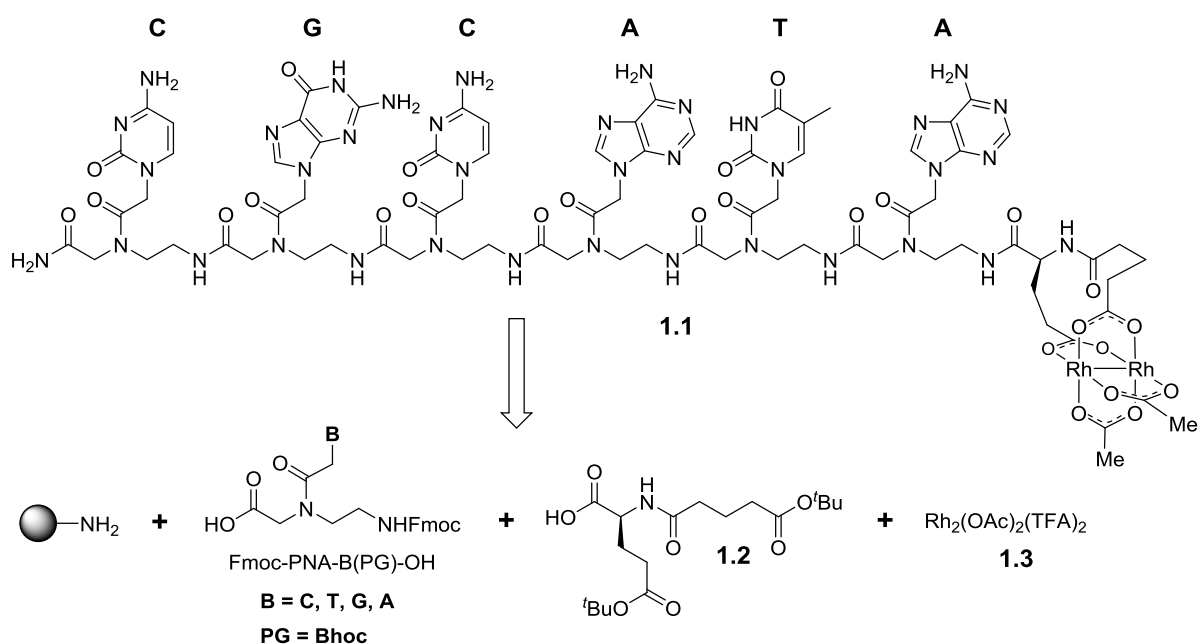
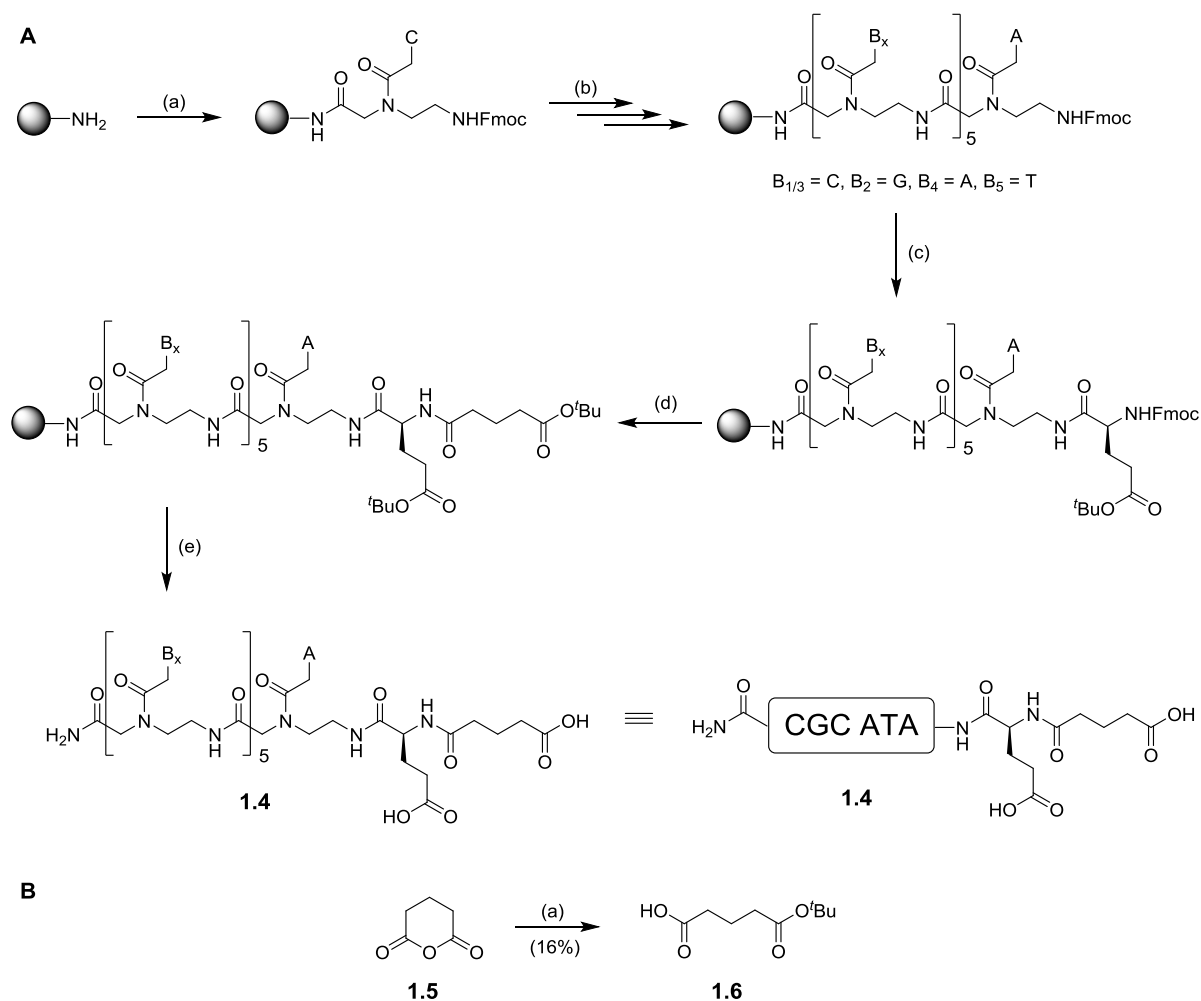


Figure 2.7: Retrosynthetic analysis of hexameric PNA catalyst **1.1**. The Bhoc-protected PNA monomers are assembled on an amino functionalized solid support using SPPS conditions. Synthetic acid **1.2** is attached to the PNA *N*-terminus followed by dicarboxylate ligand exchange with *cis*-Rh₂(OAc)₂(TFA)₂ (**1.3**).

Note: By convention, PNAs are depicted like peptides starting with the *N*-terminus (left) and ending with the *C*-terminus (right).¹⁰⁹ Throughout this thesis the synthesized PNA sequences are noted in the *C* to *N*-terminal form and displayed in a rectangular box for graphical simplicity.

2.3.2 Synthesis of 1st generation PNA and its conjugation to dirhodium

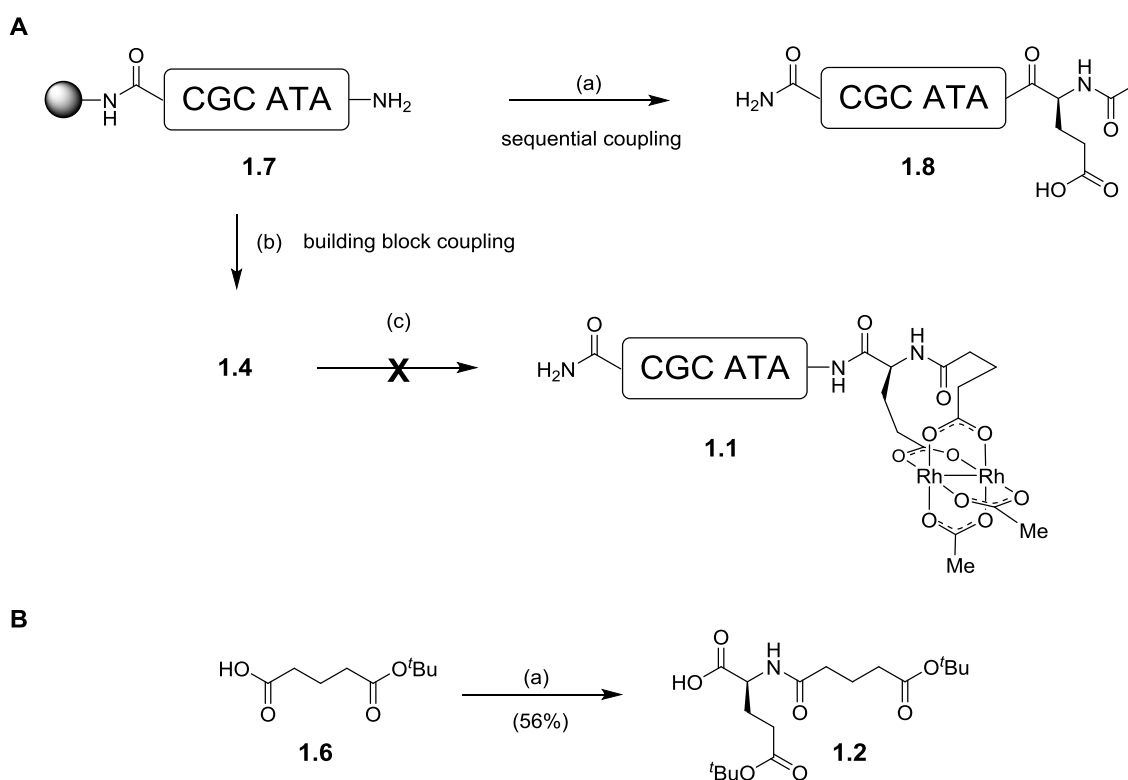
The synthesis of the desired PNA sequence **1.4** was envisioned employing manual SPPS and Fmoc/^tBu strategy on a 4-methylbenzhydrylamine resin (MBHA). A simple procedure was followed using the coupling protocol described by GOODWIN *et al.* for the assembly of PNA monomers or for introduction of amino acids and other carboxylic acid derivatives (**Scheme 2.11**).¹³⁶ In a first synthetic attempt the desired PNA **1.4** couldn't be identified by mass spectrometry (ESI-MS and MALDI-TOF-MS) after semi-preparative HPLC purification. It was not clear at that time why the desired product was not obtained but several factors could have handicapped the synthesis: high initial resin loadings inhibit PNA couplings¹⁶⁷, false positive on bead tests after deprotection/coupling¹⁶⁸ or partial decomposition of the Fmoc deblock solution containing 20% piperidine/DMF.¹⁶⁹



Scheme 2.11: (A) Synthetic sequence for the preparation of pna(CGCG ATA)-diacid **1.4**: (a) Fmoc-PNA-C(Bhoc)-OH, HATU, DIPEA; (b) repetitive cycles of (i) 20% piperidine/DMF, (ii) Fmoc-PNA-B(PG)-OH, HATU, DIPEA - all PNA nucleobases except for T contained Bhoc protection groups - order of PNA nucleobases introduced: GCATA; (c) (i) 20% piperidine/DMF, (ii) Fmoc-Glu(O^tBu)-OH, HCTU, 2,6-lutidine, DIPEA; (d) (i) 20% piperidine/DMF, (ii) **1.6**, HCTU, 2,6-lutidine, DIPEA; (e) TFA/*m*-cresol/thioanisole/TFMSA (6:1:1:2). (B) Synthesis of 5-(*tert*-butoxy)-5-oxopentanoic acid (**1.6**): (a) ^tBuOH, *N*-hydroxysuccinimide, DMAP, NEt₃.

A second attempt using rink amide resin (Novbiochem) containing a lower initial loading proved to be more suitable. A test cleavage of hexameric PNA **1.7** and MALDI-TOF-MS analysis revealed the correct mass for the pna(CGCG ATA) intermediate. After sequential coupling of Fmoc-Glu(O^tBu)-OH and carboxylic acid **1.6** the resulting PNA analysis indicated a mass corresponding to the *N*-acetyl derivative **1.8** which lacked the *N*-terminal carboxylate (**Scheme 2.12**). Although both “peptide” couplings were performed identical, it was obvious from this result that the second one failed completely for unknown reasons and the final capping with Ac₂O prevented further on-resin manipulation. While the PNA assembly seemed to be straightforward, the sequential coupling of the two carboxylic acids caused unexpected problems. It was assumed that a more facile introduction of the acid building block **1.2**, which was obtained in a two-step synthesis from 5-(*tert*-butoxy)-5-oxopentanoic acid (**1.6**), could circumvent this issue. We were pleased to find that this strategy turned

out to be successful delivering the desired PNA diacid **1.4** which was then subjected to several ligand exchange reactions with synthetic *cis*-Rh₂(OAc)₂(TFA)₂ (**1.3**) in pure water at millimolar concentrations. The use of this electron deficient dirhodium catalyst should facilitate double TFA ligand substitution at ambient to slightly elevated temperatures in a few hours as reported by BALL *et al.*^{157,166} Unfortunately none of the ligand exchange attempts were successful and even after days, increased temperature (40°C) and various concentrations unreacted starting materials were detected by HPLC/ESI-MS. It is assumed that higher temperatures could have been beneficial in terms of ligand exchange but inappropriate with respect to the low thermal stability of short PNAs. In retrospect fine tuning of the pH (towards alkaline pH) could have helped too, although both carboxylic acids residues have pK_a values below 5 and should be deprotonated under the conditions employed.



Scheme 2.12: (A) Synthetic pathways for the preparation of hexameric PNA catalyst **1.1**: (a) (i) Fmoc-Glu(O^tBu)-OH, HCTU, 2,6-lutidine, DIPEA; (ii) **1.6**, HCTU, 2,6-lutidine, DIPEA; (iii) 5% Ac₂O, 6% 2,4,6-collidine, NMP; (iv) TFA/TIS/H₂O (95:2.5:2.5); (b) (i) **1.2**, HATU, 2,4,6-collidine, DIPEA; (ii) 5% Ac₂O, 6% 2,4,6-collidine, NMP; (iii) TFA/TIS/H₂O (95:2.5:2.5); (c) *cis*-Rh₂(OAc)₂(TFA)₂ (**1.3**). (B) Synthetic pathway for the preparation of acid building block **1.2**: (a) (i) 4-Nitrophenol, DCC; (ii) H₂N-Glu(O^tBu)-OH, NEt₃.

These results clearly emphasized the need for a different conjugation method since the covalent attachment to a Rh(II) pre-catalyst by simple ligand exchange was found to be the critical step. At this point re-evaluation of the linkage was the next logical step since the PNA synthesis was unproblematic.

2.3.3 Retrosynthesis of 2nd generation PNA catalyst

The strategic change for placing the Rh(II) species to the PNA *N*-terminus directed us towards the principle of bioconjugation. The major criteria which had to be fulfilled was the facile formation of a stable linkage which can be performed in water without generating interfering by-products. It was clear that both components, PNA and Rh(II) pre-catalyst, had to be modified with bioorthogonal FGs that are able to participate in a final bioconjugation reaction to give the desired PNA catalyst. Ideally the chemical modifications should be introduced with little synthetic effort to allow a prompt proof of the envisioned concept. We found that an oxime condensation between a ketone/aldehyde and an *O*-alkylhydroxylamine seemed to be most suitable for the following reasons: 1) high hydrolytic stability of the oxime linkage in aqueous media due to the oxygen α -effect¹⁷⁰ 2) oxime formation is reported for PNA-peptide conjugates¹⁷¹ and peptide dendrimers¹⁷² 3) oxime condensation generates solely water as by-product.

A schematic retrosynthetic analysis of the 2nd generation PNA catalyst is shown in **Figure 2.8**. It is assembled through a peptide coupling of the PNA *N*-terminus with commercial 2-(Boc-aminooxy)-acetic acid (Boc-AOAc-OH, **1.9**) which is then able to form an oxime linkage with a respective dirhodium carbonyl compound after *N*-Boc deprotection.

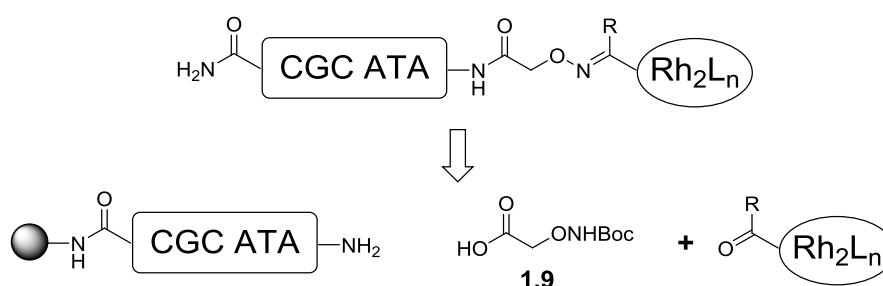


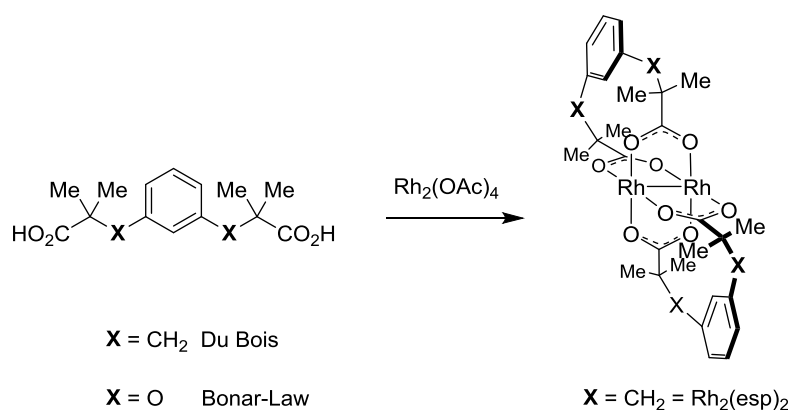
Figure 2.8: Schematic retrosynthesis of oxime-linked PNA catalyst *via* Boc-AOAc-OH **1.9**.

Since the PNA assembly and final peptide coupling were considered unproblematic, focus was laid on the design and synthesis of the desired functionalized dirhodium species. In particular we had to come up with a creative and simple synthetic route for the generation of functionalized and modular ligands which can be installed into the transition metal framework.

2.3.4 Synthesis of modular dicarboxylate ligands and dirhodium catalysts

The results discussed within this section are the cumulative work of the author Pascal Schmidt, Daniel Bachmann, Stefanie Geigle, Wolf-Dietrich Woggon, Antoinette Chougnnet, Dennis Gillingham and have been published in 2015.¹⁷³ The material is used with a personal permission of the publisher John Wiley and Sons and the corresponding license details can be found in the appendix (section 4.3.2).

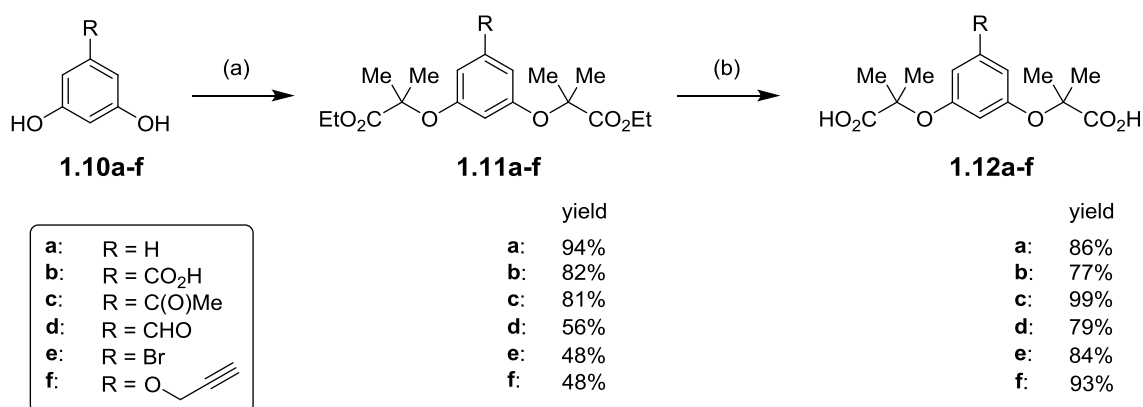
The new Rh(II) pre-catalyst design was inspired by seminal work from DU BOIS and BONAR-LAW.^{174,175} These groups described the synthesis of dicarboxylate ligands which function as a dirhodium tether thus increasing the stability of the respective mono- or bis-chelates (**Scheme 2.13**). In addition these complexes were found to perform outstanding in nitrene and C-H insertions compared to their untethered analogs.



Scheme 2.13: The DU BOIS and BONAR-LAW dicarboxylate ligands and a corresponding tethered dirhodium catalyst: $\text{Rh}_2(\text{esp})_2$ when $\text{X} = \text{CH}_2$. The acronym esp stands for ESPINO, a PhD student of DU BOIS which accomplished the first synthesis of the esp ligand and corresponding dirhodium complex.

We also became interested in such tethered bis-dicarboxylate dirhodium complexes in the context of our recent studies on metal-carbenoid based nucleic acid alkylation.³⁶ To further develop this technology and in order to meet the requirements for the envisioned PNA catalyst (*vide supra*) we needed a set of dirhodium complexes with stable and modular ligands that still performed well in synthetic processes. Most rhodium or metal complexes are highly insoluble in water and not readily amenable to modification.¹⁷⁶⁻¹⁸⁰ We settled on the tethered bis-carboxylate structure because we thought its increased stability¹⁸¹, as well as its potential to intercalate DNA¹⁸², could deliver performance improvements in comparison with simple dirhodium carboxylates (*e.g.*, *cis*- $\text{Rh}_2(\text{OAc})_2(\text{TFA})_2$ or $\text{Rh}_2(\text{OAc})_4$). The ligand introduced by DU BOIS and co-workers¹⁷⁴ was chosen as a starting scaffold but two major problems prompted us to change tack: first, creating a library of ligands proved synthetically cumbersome and second, controlling mono- versus double-substitution in the rhodium carboxylates was unpredictable. Inspired by previous work from BONAR-LAW in creating

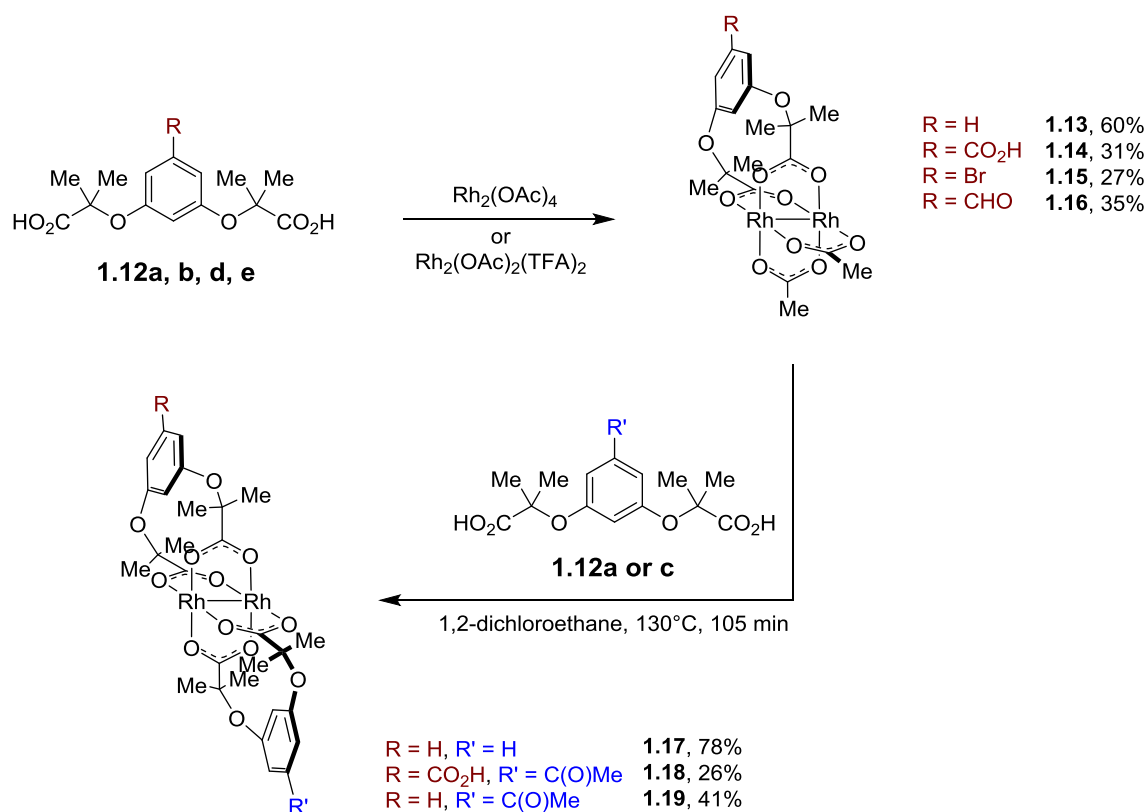
dirhodium-based metal-organic architectures^{175,183-185}, we examined dicarboxylate ligands derived from 1,3-benzenediols. This construct maintains the essential structural features of the ESPINO ligand, but has the advantage of modularity since numerous 1,3-benzenediol derivatives are commercially available. Moreover, since BONAR-LAW used these dicarboxylates to create well-defined supramolecular objects the coordination of each ligand needed to be precisely controlled, providing valuable information for our own studies. Shown in **Scheme 2.14** is the full collection of dicarboxylate ligands **1.12a-f** we have synthesized thus far starting from commercial C5-substituted 1,3-benzenediols **1.10a-f**. Diesters **1.11a-f** were obtained by double *O*-alkylation with ethyl-2-bromoisobutyrate and a mixture of K₂CO₃ and Cs₂CO₃ in yields ranging from 48-94%. Final hydrolysis was accomplished with LiOH to afford the desired dicarboxylate ligands **1.12a-f** in excellent yields, bearing a variety of functional groups poised for further modification such as amide bond formation (triacid **1.12b**), Pd-catalyzed cross coupling (bromide **1.12e**), click chemistry (alkyne **1.12f**) or condensation reactions (ketone **1.12c** or aldehyde **1.12d**).¹⁷³



Scheme 2.14: Synthetic pathway for the preparation of various modular dicarboxylate ligands **1.12a-f**: (a) ethyl-2-bromoisobutyrate, K₂CO₃, Cs₂CO₃; (b) LiOH · H₂O.

Some of these ligands were subjected to ligand exchange reactions with either *cis*-Rh₂(OAc)₂(TFA)₂ or Rh₂(OAc)₄. The syntheses of the various homo- and heteroleptic dirhodium complexes we have prepared are shown in **Scheme 2.15**. Using the conditions developed by BONAR-LAW the monobiscarboxylate complex **1.13** is obtained in 60% yield after three hours in *N,N*-dimethylaniline at 140°C. However, for ligands with electron withdrawing groups at C5 (**12b, d and e**) milder conditions were necessary: *cis*-Rh₂(OAc)₂(TFA)₂ in 1,2-dichloroethane at 60-70°C with small amounts of EtOAc as co-solvent led to acceptable yields (31% for **1.14**, 27% for **1.15**, and 35% for **1.16**). Unfortunately, attempts to perform a second substitution to access the heteroleptic complexes using BONAR-LAW'S conditions led to low yields and mixtures of products. We therefore turned to TABER'S original procedure involving a portion-wise addition of the ligand.¹⁸⁶ Through the combination of these protocols we have been able to synthesize new dirhodium complexes containing a variety of functional

groups (**Scheme 2.15**). In general the isolated yields were rather moderate to low which is a typical feature of dirhodium complex syntheses. However in many cases unreacted starting material could be recovered chromatographically.

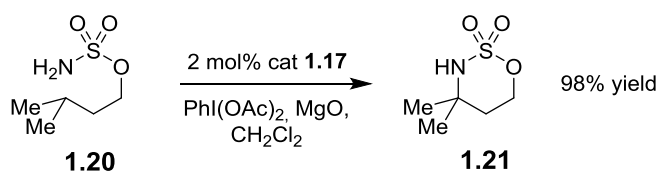


Scheme 2.15: Synthetic pathway for the preparation of various homo- **1.13-1.16** and heteroleptic dirhodium complexes **1.17-1.19**.

2.3.5 Dirhodium catalyzed nitrene-, C-H and O-H insertion

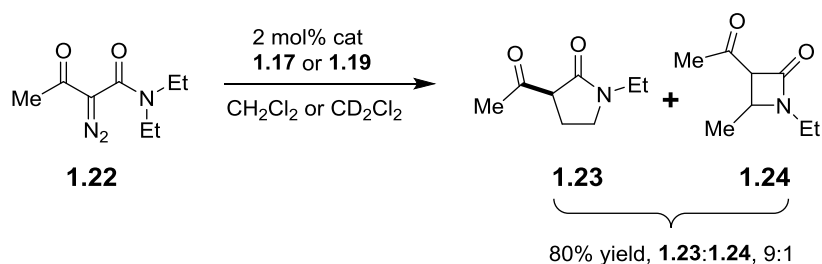
The use of dirhodium catalysts for the bioconjugation to PNA is discussed in section 2.3.6. The present section should give the reader a quick overview of the catalytic potential of newly synthesized dirhodium catalysts we have developed. For a detailed discussion of the following summarized results the reader is referred to our publication.¹⁷³

To probe the impact of the ligand on catalysis dirhodium catalysts **1.17**, **1.18**, and **1.19** were tested in several benchmarking nitrene- and C-H insertion reactions using organic solvents or pure water (**Scheme 2.16**). A typical intramolecular nitrene insertion reaction of sulfamate ester **1.20** with 2 mol% of catalyst **1.17** was found to be as effective as the DU BOIS system $\text{Rh}_2(\text{esp})_2$ delivering oxathiazinane **1.21** in excellent isolated yield.¹⁷⁴



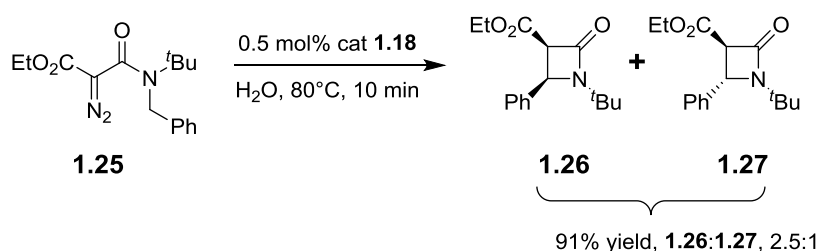
Scheme 2.16: Benchmarking nitrene insertion of sulfamate ester **1.20**.

In a second set of benchmarking experiments catalysts **1.17** and **1.19** were tested in C-H insertion reactions to form γ - **1.23** or β -lactams **1.24** and performed superior compared to $\text{Rh}_2(\text{OAc})_4$ delivering the products in 10 min with a 9:1 ratio in favor of the γ -lactam **1.23** (Scheme 2.17).



Scheme 2.17: Benchmarking C-H insertion for the synthesis of γ - **1.23** and β -lactams **1.24**.

The heteroleptic dirhodium complex **1.18** bearing a ketone functionalized ligand (**1.12c**) and a carboxylate functionalized ligand (**1.12b**) was found to be completely water soluble above the pK_a (~4.2) of the carboxylate. As a proof of concept for the potential of **1.18** in aqueous catalysis we carried out two different types of reactions using pure water as the reaction media. The first was an intramolecular C-H insertion reaction of α -diazoacetamide **1.25** which required lower loading (0.5 vs. 1-2 mol%) and less time (10 min vs. 0.5-24 h) than the previous best catalyst (Scheme 2.18).¹⁸⁷



Scheme 2.18: Intramolecular C-H insertion in water for the formation of diastereomeric β -lactams **1.26** and **1.27**.

Next we tested a simple O-H insertion of α -diazoester **1.28** with water and compared the catalytic activity of **1.18** with $\text{Rh}_2(\text{OAc})_4$ (Figure 2.8). Catalyst **1.18** reaches the first half-life approximately twofold faster than $\text{Rh}_2(\text{OAc})_4$ and converts 90% of the starting material in 100 min whereas the latter required 160 min.

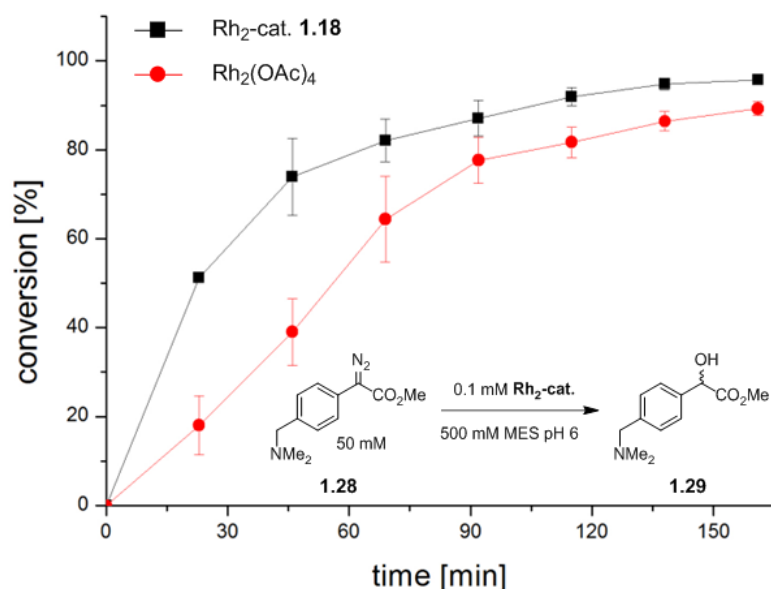
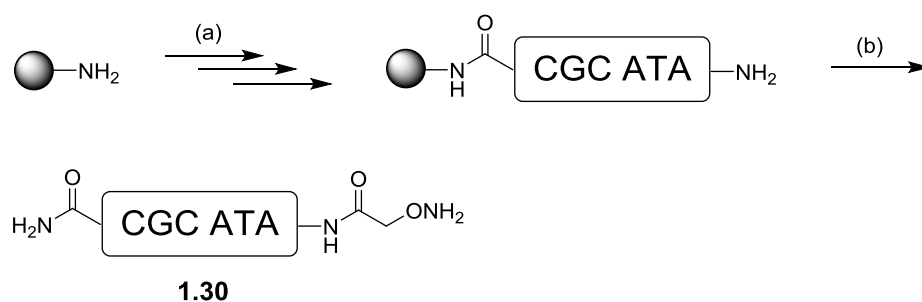


Figure 2.8: Catalytic comparison of dirhodium catalyst **1.18** with $\text{Rh}_2(\text{OAc})_4$ in an O-H insertion reaction performed in water.

2.3.6 Synthesis of 2nd generation PNA and its bioconjugation to dirhodium

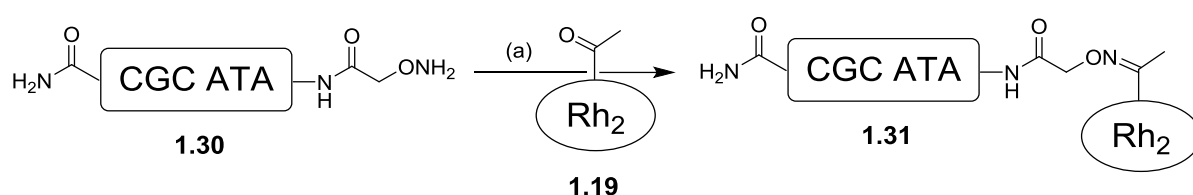
The envisioned hydroxylamine terminated PNA **1.30** was manually synthesized on rink amide resin according to the previously used SPPS protocol for PNA **1.4**. The final peptide coupling was performed for 90 min with five equivalents of Boc-AOAc-OH **1.9** (Bachem) to ensure full conversion (**Scheme 2.19**). To achieve high yields, the respective PNA-hydroxylamine **1.30** cleavage was performed for a prolonged time of 2 h. Subsequent HPLC purification and analysis by mass spectrometry confirmed the PNA-hydroxylamine **1.30**.



Scheme 2.19: Shortened synthetic sequence for the preparation of pna(CGCA ATA)-hydroxylamine **1.30**: (a) (i) Fmoc-PNA-B(Bhoc)-OH, HATU, DIPEA; (ii) repetitive cycles of 20% piperidine/DMF then Fmoc-PNA-B(Bhoc)-OH, HATU, DIPEA with a final Fmoc cleavage; (b) (i) Boc-AOAc-OH **1.9**, HATU, 2,4,6-collidine, DIPEA; (ii) TFA/TIS/H₂O (95:2.5:2.5).

After a test oxime formation with the ketone functionalized dicarboxylate ligand **1.12c** resulted in full conversion of PNA-hydroxylamine **1.30**, as concluded by MALDI-TOF-MS, we tested the aqueous bioconjugation with the ketone functionalized dirhodium catalyst **1.19**. The reaction setup turned out

to be challenging since the hydrophobic dirhodium catalyst **1.19** was found to be only partially soluble even when adding high amounts of organic co-solvents (*e.g.*, CH₂Cl₂ and MeOH) while the PNA-hydroxylamine showed decent water solubility. Nonetheless the system was tested on its ability for bioconjugation and the dirhodium catalyst **1.19** was mixed with the PNA in an approximate 3:1 ratio (**Scheme 2.20**). Upon mixing a color change from light blue to pink was noticed in the heterogeneous reaction which was analyzed over a period of 22 h by MALDI-TOF-MS and LC/MS. While the desired oxime mass of **1.31** could be identified, the PNA conversion didn't exceed ~20%. At that point we decided to reconsider this “heterogenic” system which seemed far from perfect for the envisioned catalysis in water. Obviously the highly hydrophobic nature of catalyst **1.19** had to be replaced with a more soluble variant.



Scheme 2.20: Synthetic pathway for the oxime condensation of PNA-hydroxylamine **1.30** and dirhodium catalyst **1.19**: (a) H₂O/MeOH/CH₂Cl₂ (3:1:0.5).

The next logical step was to test the keto/acid functionalized heteroleptic dirhodium catalyst **1.18** which already performed outstanding under aqueous conditions (*vide supra*) but was not accessible at the time we tested our first bioconjugation to PNA. Once the catalyst **1.18** could be dissolved in a mixture of water/500 mM MES buffer containing a marginal volume of concentrated 1M NaOH it was also tested in an oxime condensation with PNA-hydroxylamine **1.30**. To our disappointment we noticed the immediate precipitation of a pink solid directly after mixing the components which was identified as the PNA-Rh₂ conjugate by ESI-MS but again rendered the system inappropriate for our needs. After having established a perfectly water soluble dirhodium catalyst and a moderately soluble PNA-hydroxylamine we had to fix the solubility of its conjugate in an aqueous environment. It was therefore clear to us that the solubilizing property of the PNA had to be improved which in turn should have a positive impact on the solubility of the oxime. We got inspired by seminal work of the LY research group which reported that (*R*)-diethylene glycol (“miniPEG”, *R*-MP) containing γ -PNAs showed not only superior hybridization properties, but also were highly water soluble (**Figure 2.9**).¹⁸⁸ They demonstrated that the incorporation of a single *R*-MP- γ -PNA monomer into a decameric sequence transforms its randomly folded structure into a highly preorganized right-handed-helix. In addition a hexadecameric PNA sequence containing one *R*-MP- γ -PNA unit enhanced the water solubility by a factor of two as determined by saturation experiments.

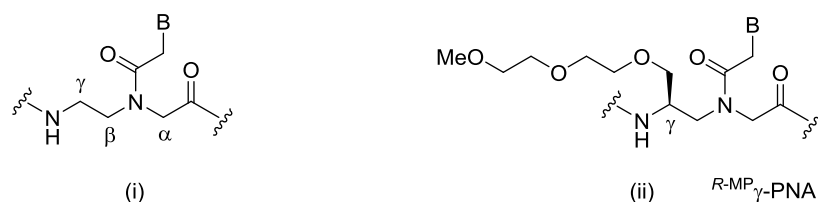
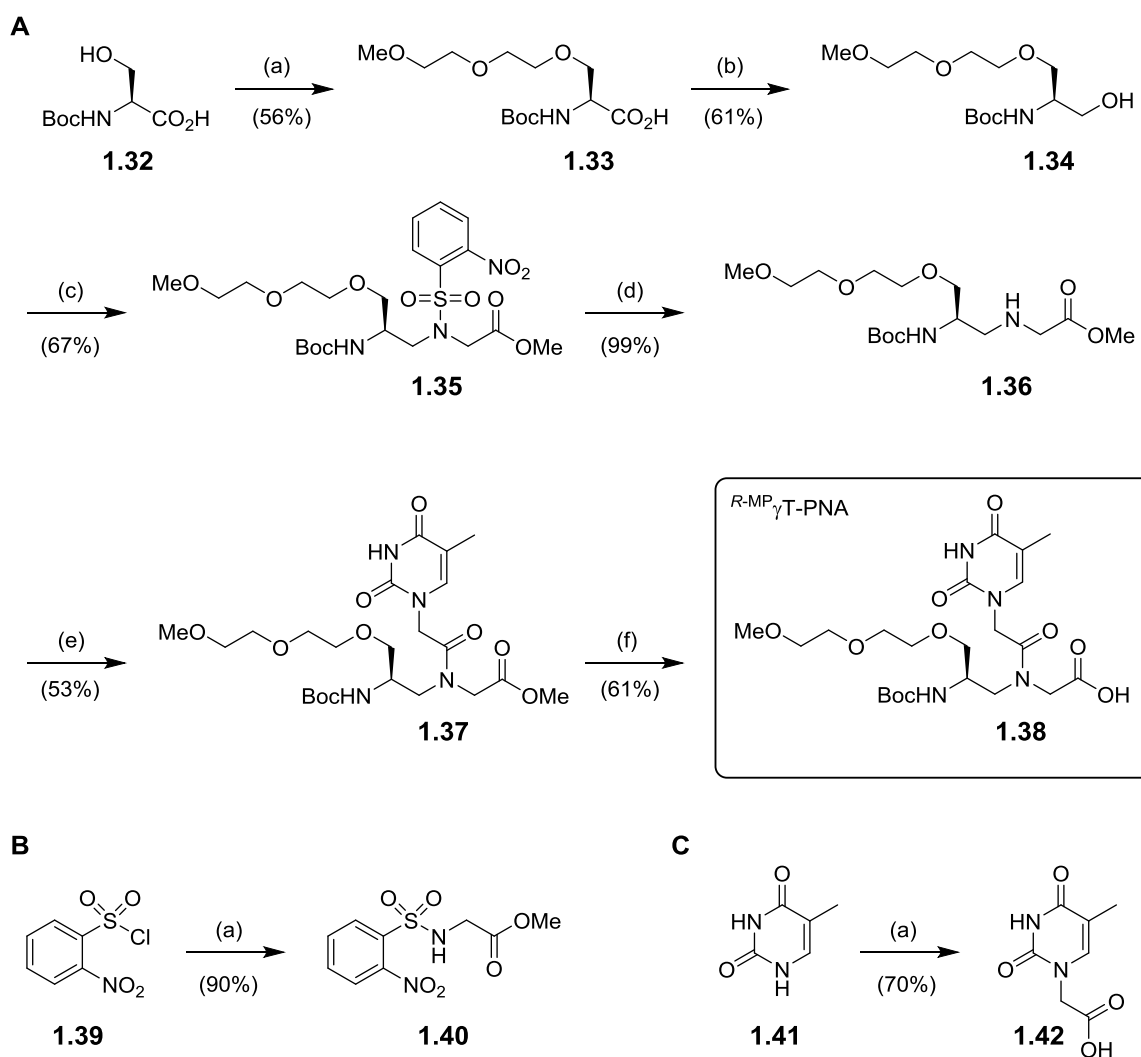


Figure 2.9: (i) Schematic representation of the α -, β - and γ -positions on the PNA backbone available for chemical modifications. (ii) γ -backbone modification with a *R*-MP unit as described by LY *et al.*¹⁸⁸

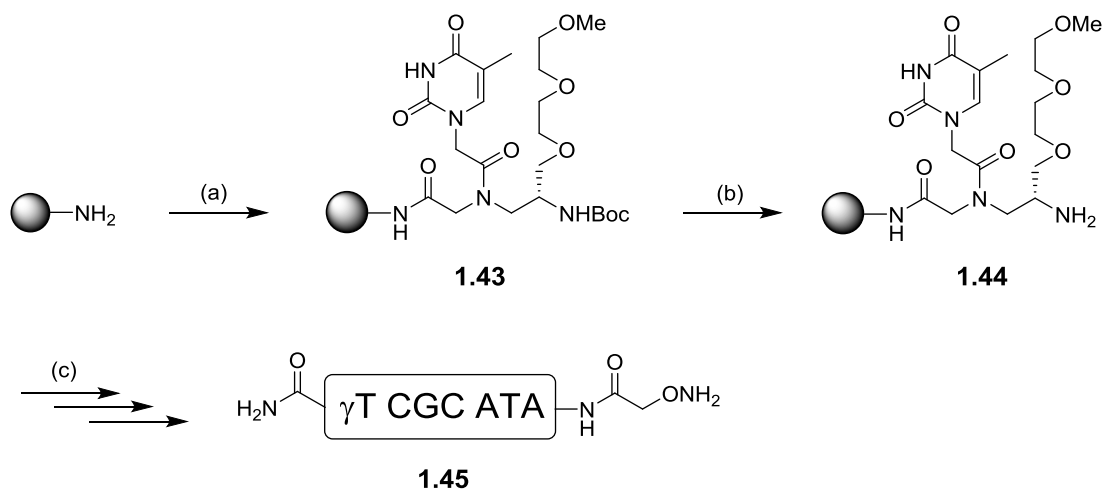
Encouraged by these findings we decided to synthesize such a monomer which we planned to introduce later into the PNA sequence at the C-terminus. For a reason of synthetic simplicity we envisioned the thymine monomer (^{*R*}-MP- γ T-PNA) **1.38** which requires no additional protecting groups thus shortens the synthesis to six linear steps (**Scheme 2.21**, panel A). We adapted the route of LY *et al.* to our needs starting from commercial Boc-Ser-OH (**1.32**) which was *O*-alkylated with the miniPeg-containing 1-Bromo-2-(2-methoxyethoxy)ethane to give methylether **1.33**. Formation of a mixed anhydride with subsequent NaBH₄ reduction afforded the primary alcohol **1.34** in good yield. It was then reacted with separately synthesized nosyl sulfonamide derivative **1.40** in a MITSUNOBU reaction to give the *N*-protected PNA backbone species **1.35**. Quantitative deprotection with thiophenol was followed by PyBrop-mediated coupling with separately synthesized thymine-1-acetic acid (**1.42**) to yield amide **1.37**. After final alkaline ester hydrolysis the desired ^{*R*}-MP- γ T-PNA monomer **1.38** was obtained in an overall yield of 7.3%.



Scheme 2.21: Synthetic pathway for the preparation of $R\text{-MP-}\gamma\text{T-PNA}$ **1.38** and reagents needed throughout this route: (A) Linear six step sequence for the synthesis of $R\text{-MP-}\gamma\text{T-PNA}$ **1.38**; (a) NaH, 1-Bromo-2-(2-methoxyethoxy)ethane; (b) isobutyl chloroformate, NaBH₄; (c) DEAD, PPh₃, **1.40**; (d) thiophenol, KOH (aq); (e) PyBrop, DIPEA, **1.42**; (f) 2M Cs₂CO₃. (B) Synthesis of nosyl sulfonamide derivative **1.40**; (a) H-Gly-OMe · HCl, NEt₃. (C) Synthesis of thymine-1-acetic acid (**1.42**); (a) bromoacetic acid, KOH (aq).

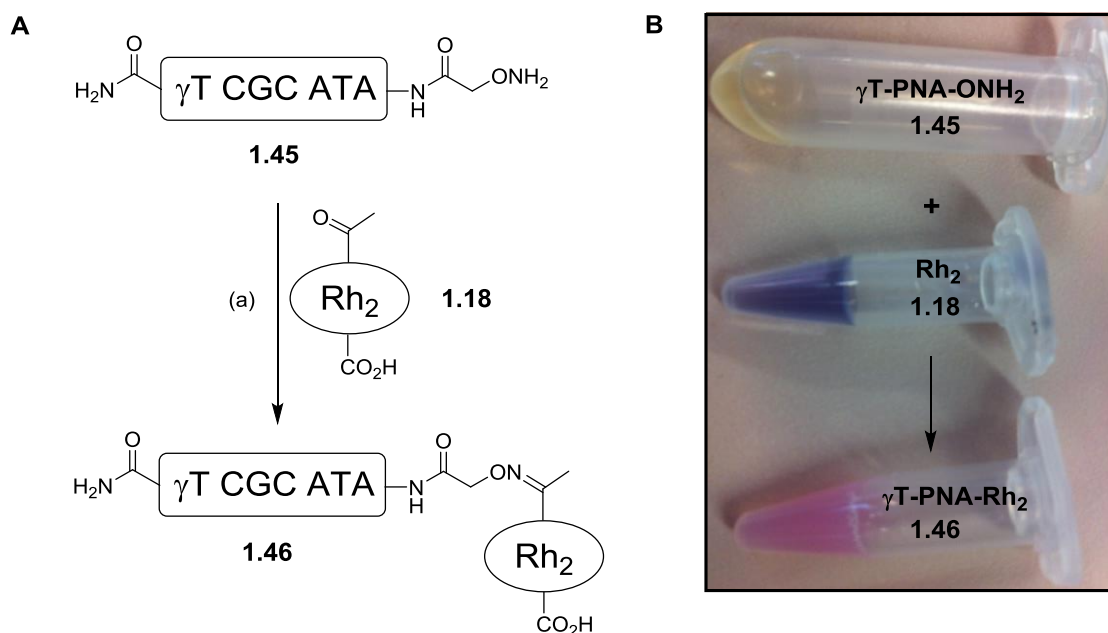
As mentioned before this monomer was envisioned to be introduced as the first unit into the new PNA sequence pna(γ T CGC ATA) to minimize possible interference with the complementary ssDNA strand within our alkylation system (*vide supra*). While the LY group used exclusively Boc protected PNA monomers for their oligomer synthesis we wanted to combine this monomer into our Fmoc/Bhoc strategy for SPPS which seemed challenging using an acid labile solid support. An extensive literature search directed our attention to a tailor-made protocol by ZHANG *et al.* for the selective removal of *N*-Boc protecting groups on acid labile resins.¹⁸⁹ In their studies they used a mixture of TMSOTf/2,6-lutidine in CH₂Cl₂ to remove the *N*-terminal protecting group of peptides on rink amide resin with relative yields up to 93%. This strategy seemed to fit best to our requirement and turned out to be applicable to PNA synthesis. The synthetic multistep sequence of γ T-containing PNA-hydroxylamine **1.45** is outlined in **Scheme 2.22**. First, rink amide resin was loaded with $R\text{-MP-}\gamma\text{T-PNA}$ **1.38** followed by

a mild *N*-Boc deprotection with TMSOTf/2,6-lutidine in CH₂Cl₂ to afford the solid phase bound ^R-MP- γ T-PNA monomer **1.44** which was confirmed by UPLC-MS analysis after a test cleavage. The final PNA sequence **1.45** was assembled with ease using the standard Fmoc/Bhoc SPPS strategy including a final peptide coupling with Boc-AOAc-OH **1.9** followed by TFA cleavage.



Scheme 2.22: Synthetic pathway for the preparation of γ T-containing PNA-hydroxylamine **1.45**: (a) (i) ^R-MP- γ T-PNA **1.38**, HATU, DIPEA, 2,4,6-collidine; (ii) 5% Ac₂O, 6% 2,4,6-collidine, NMP; (b) 1M TMSOTf, 1.5M 2,6-lutidine; (c) repetitive cycles of (i) Fmoc-PNA-B(Bhoc)-OH or Boc-AOAc-OH **1.9**, HATU, DIPEA; (ii) 20% piperidine/DMF and final cleavage (iii) TFA/TIS/H₂O (95:2.5:2.5).

The HPLC purified γ T-containing PNA-hydroxylamine **1.45** was found to be freely soluble in pure water at millimolar concentrations and ready for its oxime bioconjugation to the water soluble dirhodium catalyst **1.18** containing a ketone. A preliminary test reaction indicated that oxime formation was rather slow and PNA conversions at 15 min and 18 h were similar without exceeding ~30%. In a more preparative attempt both components were mixed in water, with the PNA being in a slight excess (1.5:1), whereupon a heterogeneous pink solution formed immediately (**Scheme 2.23**). After centrifugation of the reaction mixture a pink solid separated from the clear supernatant. UPLC-MS analysis of the solution confirmed exclusively unreacted PNA while the pink solid (dissolved in DMSO) contained a mixture of unreacted PNA and dirhodium catalyst along with the desired PNA-Rh₂ oxime **1.46** which could be isolated after semipreparative HPLC. A solubility test with various organic solvents indicated that the oxime conjugate was most soluble in DMSO which is known to be a potential axial ligand in dirhodium complexes.¹⁹⁰⁻¹⁹³ Although these coordinating ligands were found to form a much weaker bond to the reactive rhodium atom than the equatorial ones, they may partially influence the reactivity of the carbenoid catalyst.^{194,195} Nonetheless, after tedious accomplishment of the PNA-dirhodium oxime template **1.46** its catalytic ability was tested in an initial alkylation experiment of ssDNA.



Scheme 2.23: (A) Synthetic pathway for the oxime condensation of γ T-containing PNA-hydroxylamine **1.45** and heteroleptic dirhodium catalyst **1.18**: (a) H_2O ; ratio of PNA:Rh₂ catalyst (1.5:1). (B) Homogenous stock solutions of PNA **1.45** (light yellow) and dirhodium catalyst **1.18** (blue) in water which upon mixing result in a heterogeneous pink solution of the precipitated oxime **1.46**.

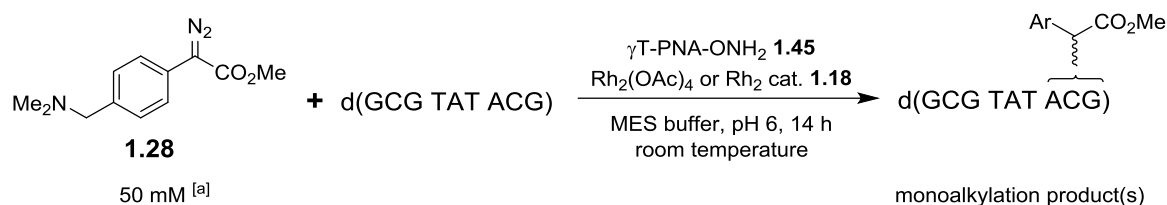
2.3.7 Initial alkylation of ssDNA using template PNA-dirhodium carbenoids

Since the commercial ssDNA sequence d(GCG TAT CCG GCA CGA) was used up at that time in the context of our separate studies on catalytic alkylation of nucleic acids, we synthesized a shorter analog employing oligonucleotide solid-phase synthesis. The new sequence d(GCG TAT ACG) (see section 4.2.1.3 for the full skeletal structure) contained the same hexameric hybridizing region to the PNA complement with an additional **three base overhang** lacking unreactive thymine (see section 1.2.1). We chose a shorter oligonucleotide to limit the possibilities of alkylation sites and for analytical simplicity of potential products.

After successful synthesis of γ T-containing PNA-hydroxylamine **1.45** we began our investigations in a proof of concept experiment series for PNA-dirhodium templated alkylation of d(GCG TAT ACG) using α -diazoester **1.28** in water. First we envisioned the self-assembling of the catalytic system by sequential addition of the guiding PNA sequence, dirhodium catalyst, and substrate to a solution of the target ssDNA. Ideally the oxime bioconjugation of the guiding PNA with the catalyst is followed by duplex formation with the target oligonucleotide and subsequent site-selective alkylation through reaction with the diazo substrate. The results obtained are summarized in **Table 2.1** and show that although oligonucleotide conversions are low using dirhodium catalyst **1.18** (entries 1-5),

monoalkylated species could be detected by MALDI-TOF-MS analysis in most cases (**Figure 2.10**). Throughout these experiments it was noted that upon mixing γ T-containing PNA-hydroxylamine **1.45** with the heteroleptic catalyst a pink solid precipitated inside the reaction vial. It is very likely that the active but insoluble oxime species **1.46** (*vide supra*) inhibits efficient homogeneous catalysis and once omitted, oligonucleotide conversions almost doubles (compare entries 4 and 5). High PNA concentrations though are detrimental and assumed to result in unreactive aggregates (entry 1) while low concentrations couldn't be effectively detected under the HPLC conditions employed (entries 2 and 3). Control reactions with $\text{Rh}_2(\text{OAc})_4$ (entries 6 and 7) indicated higher oligonucleotide conversions up to 70% (at equimolar ratios) but resulted in the same monoalkylated species as concluded from the corresponding HPLC traces.

Table 2.1: Proof of concept experiment for PNA-dirhodium templated alkylation of ssDNA.



Entry	[PNA]	[Rh ₂ cat.]	[oligo]	conv. [%] ^[b]	monoalkylation ^[c]
1	1 mM	1 mM 1.18	5 mM	3	1
2	0.1 mM	0.1 mM 1.18	0.1 mM	n.d.	1
3	0.1 mM	-	0.1 mM	n.d.	0 ^[d]
4	0.5 mM	0.5 mM 1.18	2.5 mM	15	1
5	-	0.5 mM 1.18	2.5 mM	28	1
6	0.5 mM	0.5 mM $\text{Rh}_2(\text{OAc})_4$	0.5 mM	70	1 ^[e]
7	-	0.5 mM $\text{Rh}_2(\text{OAc})_4$	0.5 mM	61	1 ^[e]

Order of addition: 1. γ T-PNA-OH₂ **1.45**, 2. Rh₂ cat., 3. d(GCG TAT ACG), 4. α -diazoester **1.28**. Analyzed by RP-HPLC using 100 mM triethylammonium acetate (pH 7.0)/MeCN. [a] >99% conversion after 14 h. [b] Oligonucleotide conversion - reported after 14 h by integration of the respective HPLC peak area at 254 nm. [c] Identified by collection of the HPLC peak and subsequent MALDI-TOF-MS analysis. [d] No conversion of the diazo substrate was observed after 14 h; upon addition of 1 eq. Rh₂ cat **1.18**, α -diazoester **1.28** was converted by 83% within 3 h but didn't result in an oligonucleotide alkylation. [e] Alkylation product could only be identified through comparison of the respective t_R with previous HPLC traces; MALDI-TOF-MS analysis of the collected peaks were non-informative. n.d. = not determined.

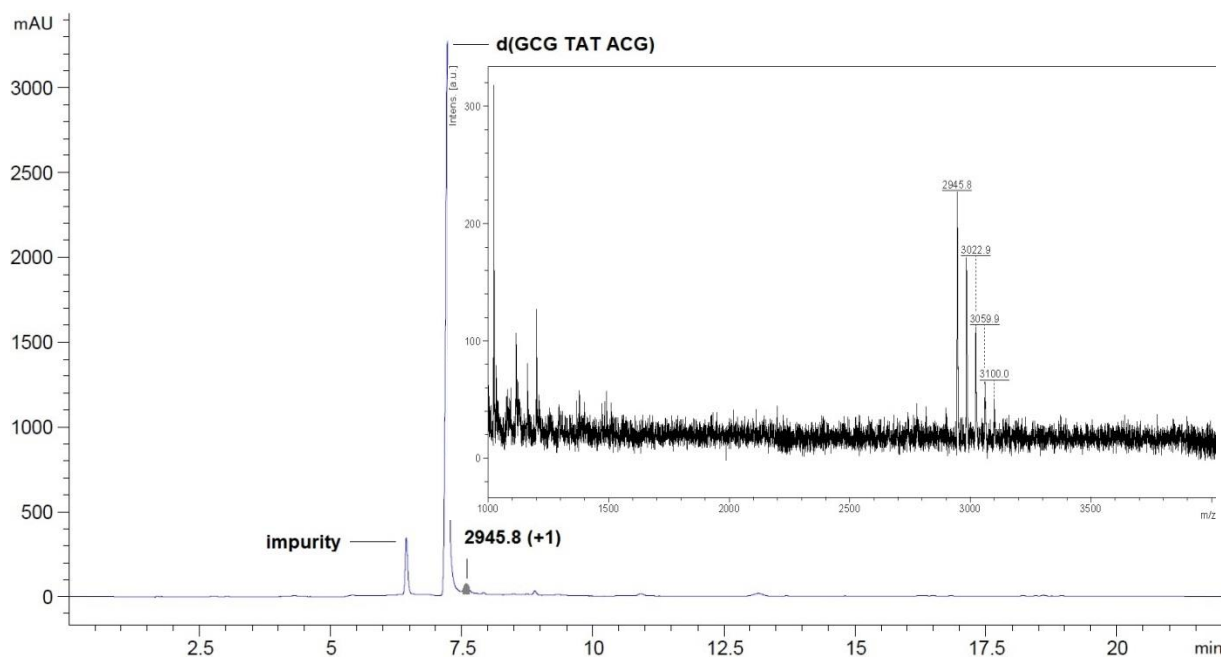
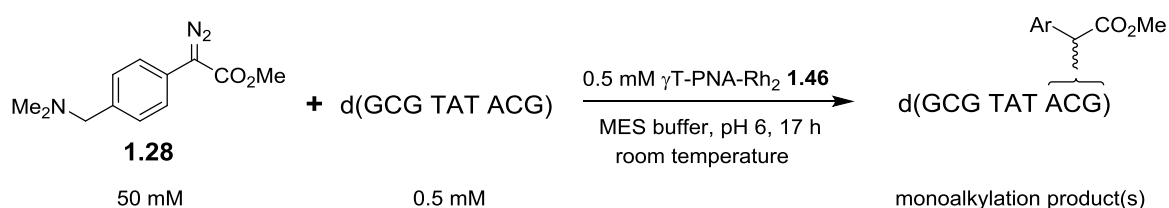


Figure 2.10: Representative HPLC trace after 14 h. The singly modified species ($t_R = 7.64$ min) was characterized by MALDI-TOF-MS (inset).

In summary, these initial results using self-assembling catalysts indicate that although a templating PNA effect was not observed, monoalkylations can be achieved with the novel dirhodium catalyst **1.18** in aqueous media. In addition oligonucleotide conversions are low to moderate using catalyst loadings of 20 mol% while the diazo substrate is completely consumed after 14 h.

Next, we tested the guiding catalyst **1.46** in a direct PNA-dirhodium templated alkylation of d(GCG TAT ACG) using α -diazoester **1.28** in water (**Scheme 2.24**). We chose to use an equimolar ratio of the template and the target strand to achieve higher conversions and force the templating ability of the PNA catalyst.



Scheme 2.24: Attempt for PNA-dirhodium templated alkylation of ssDNA.

Again, upon addition of the aqueous oligonucleotide solution to the oxime in DMSO a pink precipitate was noticed in the reaction vial which was most likely the water-insoluble PNA catalyst **1.46**. HPLC and MALDI-TOF-MS analysis of the reaction mixture after 17 h revealed that <5% of the starting

oligonucleotide has been converted to one singly modified product while α -diazoester **1.28** was completely consumed. From this result, we hypothesized that the PNA-dirhodium catalyst **1.46** is likely to have poor hybridization properties with its ssDNA complement which strongly diminishes catalytic turnovers. This assumption was directly tested by circular dichroism (CD) spectroscopy of the hybrids between d(GCG TAT ACG) and PNA-dirhodium catalyst **1.46** or γ T-containing PNA-hydroxylamine **1.45** (Figure 2.11). The PNAONH₂-DNA duplex was found to have distinct minima at 242 and 271 nm and maxima at 220 and 297 nm, characteristic of a right-handed helix.¹⁸⁸ In contrast the respective PNARh₂oxime-DNA duplex completely lacked spectral transitions suggesting that this randomly organized species is not pre-organized through WATSON-CRICK base-pairing. This finding may explain the marginal oligonucleotide conversion described above when using the templating PNA-dirhodium catalyst **1.46**.

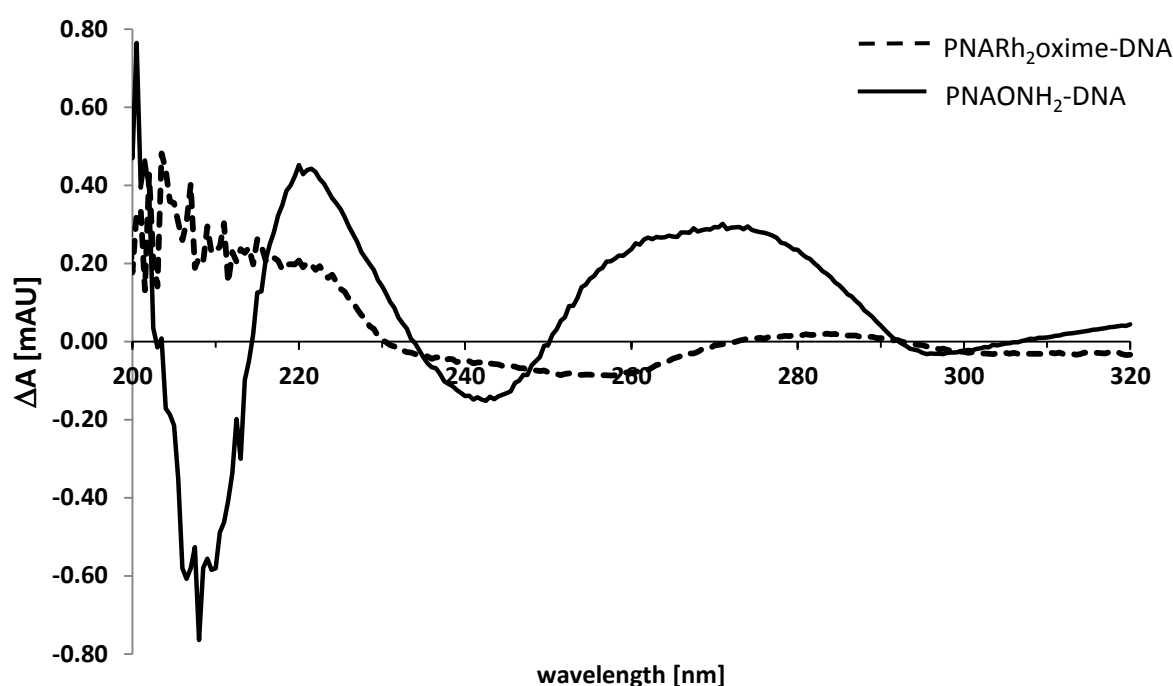
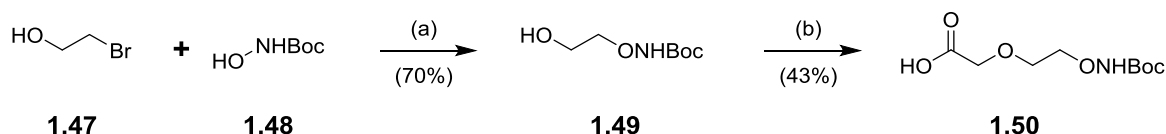


Figure 2.11: CD spectra of the PNA-DNA hybrid duplexes at 8 μ M strand concentrations in 10 mM KP_i buffer pH 7.6 recorded at room temperature. KP_i = potassium phosphate buffer.

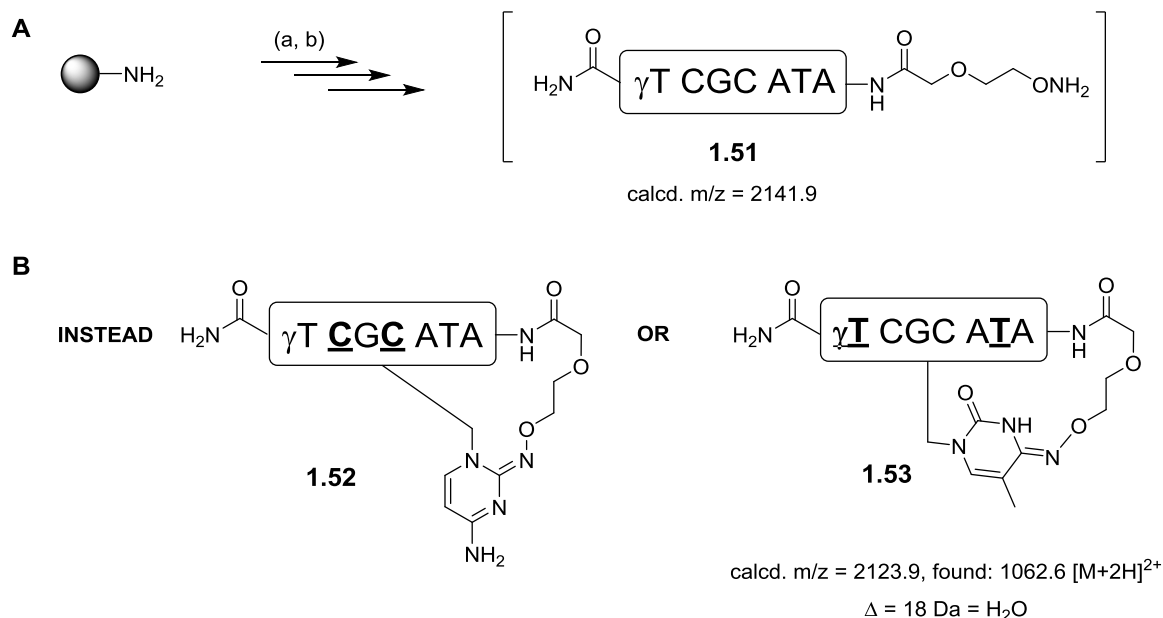
We reasoned that maybe the rigidity of the dirhodium directly attached to the PNA *N*-terminus could be problematic and suppress catalytic activity. Moreover the water solubility of the system was still an issue we had to fix which may allow for homogeneous catalysis. The combination of these particular needs is reflected in the ethylene glycol based linker **1.50** (Scheme 2.25). While its length allows for a more flexible junction to the dirhodium, the additional ethylene glycol unit improves solubility in aqueous media. The linker **1.50** was prepared in a straightforward two-step synthesis with an acceptable overall yield of 30%. Commercial 2-bromoethanol (**1.47**) was first substituted with *tert*-

butyl *N*-hydroxycarbamate (**1.48**) to give the alcohol **1.49** which was then reacted with bromoacetic acid to deliver the desired carboxylic acid **1.50** containing a protected *O*-alkylhydroxylamine.



Scheme 2.25: Synthetic pathway for the preparation of ethylene glycol based linker **1.50**: (a) DBU; (b) NaH, bromoacetic acid.

Once established, linker **1.50** was incorporated into the synthetic cycle of PNA **1.51** which was unproblematic for the assembly of the PNA monomers and an initial test coupling of the *N*-Boc protected *O*-alkylhydroxylamine **1.50** (**Scheme 2.26**, panel A). Unfortunately the attempt to synthesize PNA **1.51** in larger scale failed as indicated by MALDI-TOF-MS and UPLC-MS analysis which both revealed the product mass minus 18 Da after cleavage. This particular mass difference most likely corresponds to the loss of one water molecule thus indicating an intramolecular oxime formation which renders it inappropriate to be further used for the condensation to dirhodium catalyst **1.18**.



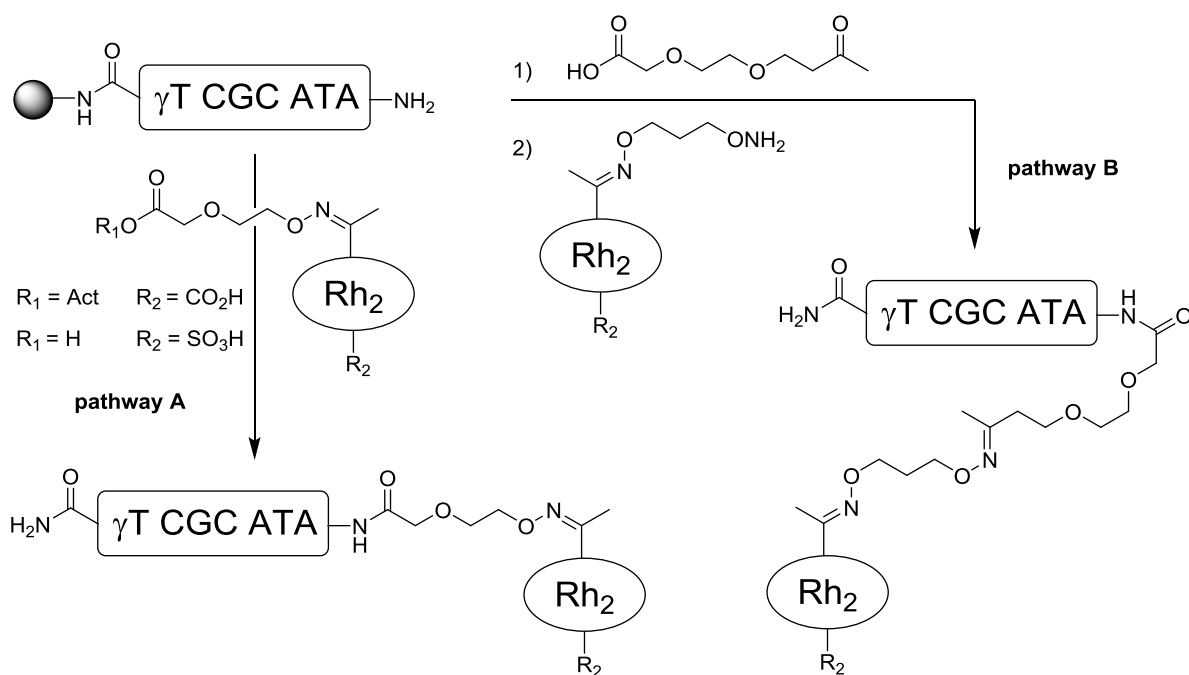
Scheme 2.26: (A) Synthetic attempt for the preparation of ethylene glycol based hydroxylamine PNA **1.51**: (a) $R\text{-MP-}\gamma\text{T}$ -PNA **1.38**, HATU, DIPEA, 2,4,6-collidine; (ii) 5% Ac_2O , 6% 2,4,6-collidine, NMP; (iii) 1M TMSOTf, 1.5M 2,6-lutidine; (b) repetitive cycles of (i) Fmoc-PNA-B(Bhoc)-OH or *O*-alkylhydroxylamine **1.50**, HATU, DIPEA; (ii) 20% piperidine/DMF and final cleavage (iii) TFA/TIS/ H_2O (95:2.5:2.5). (B) Possible cyclic products obtained after full cleavage of the PNA from the solid support. Formation of cytosine oxime **1.52** is less probable compared to thymine oxime **1.53** as suggested by literature examples.¹⁹⁶

It is known that cytosine residues in DNA can react selectively with hydroxylamines in aqueous solutions^{197,198} but also can be transformed to uracil *via* their oxime sulfonates.¹⁹⁹ Although these reaction pathways were found to proceed through modification of the exocyclic amino group in cytosine it could be possible that intramolecular hydroxylamine condensation proceeds at its carbonyl function which to the best of our knowledge has not yet been reported in the literature (**Scheme 2.26**, panel B). A more probable target for condensation is one of the two thymines from the sequence to give cyclic PNA **1.53**. In 2000 the research groups of RODE and KULIKOWSKI showed that a triazole activated deoxythymidine derivative can be modified at O-4 by simple hydroxylamine treatment.¹⁹⁶ While in our case the flexible *N*-terminal hydroxylamine is in a high effective concentration the additional activation of the nucleobase may be irrelevant to achieve successful intramolecular condensation. This however is only a hypothesis based on the obtained results and was not further investigated since the priority of our studies was the final bioconjugation of the PNA to the dirhodium catalyst **1.18**. At that point we decided to examine the rather slow oxime condensation reaction in more detail which is also a key criterion for successful assembly of the catalytic system.

2.3.8 Conclusion and outlook

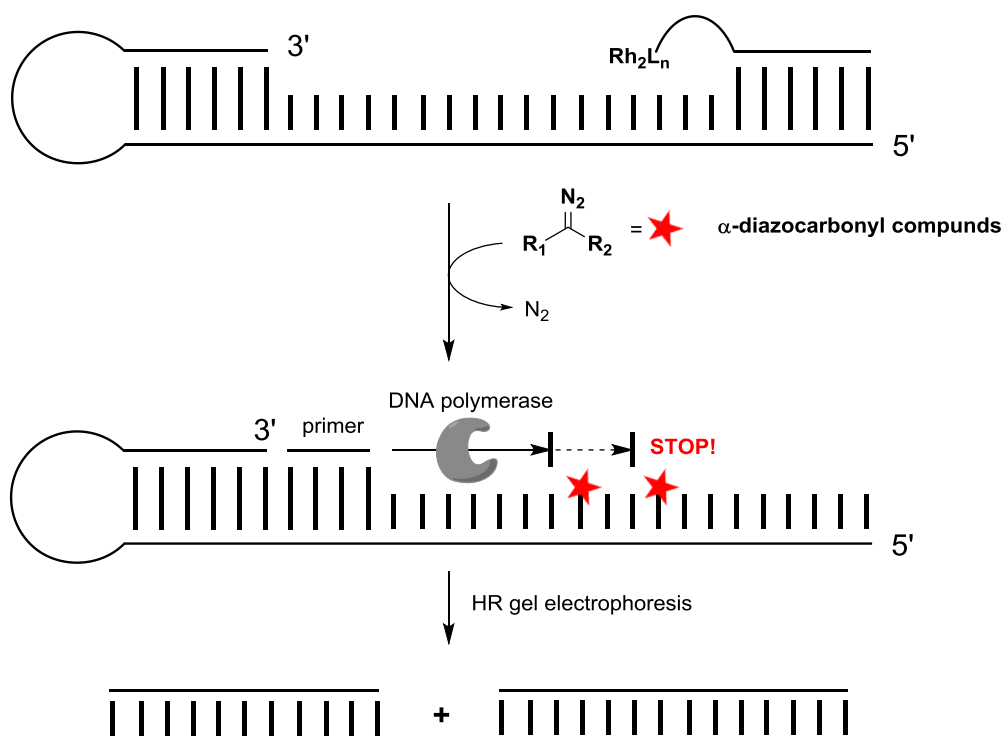
The concept of guided catalysts for the sequence-specific alkylation of ssDNA using Rh(II)-stabilized carbenoids in aqueous media described above was successfully implemented from a synthetic point of view. Although second generation PNA could be connected to a dirhodium catalyst *via* oxime condensation this reaction was found to be slow and water incompatible. A new set of modular ligands for dirhodium complexes gave access to a water soluble candidate which was used for bioconjugation. Even though the separate introduction of a solubilizing γ T monomer gave access to freely soluble PNA the final condensation rate is slow and calls for improvement. The results obtained from initial alkylation studies of ssDNA in water show that the PNA-dirhodium catalyst is active to a certain extent and results in a single modification despite marginal turnovers. Templatation seems to be hindered when dirhodium is covalently attached to PNA as concluded from CD spectroscopy experiments. Attempts to allow for a more soluble and flexible handle on the oxime junction were unsuccessful so far but should be reconsidered in future investigations.

A possible option could be the attachment of the linking unit to the dirhodium precatalyst prior to the connection to the PNA (**Scheme 2.27**). This may be achieved by a simple peptide coupling or an oxime condensation of an *O*-alkylhydroxylamine bearing dirhodium catalyst.



Scheme 2.27: Possible pathways for the preparation of flexible, ethylene glycol based PNA-dirhodium oxime conjugates. **Pathway A:** The linking unit may be attached through an oxime condensation to the dirhodium while a carboxylic acid or an activated derivative is used for the attachment to PNA. **Pathway B:** The free *N*-terminus of the PNA is first reacted with a carboxylic acid containing a terminal ketone which can then form an oxime linkage with the corresponding dirhodium *O*-alkylhydroxylamine to give a highly flexible bisoxime catalyst.

In addition an oligonucleotide target strand with a longer overhang would allow for a higher alkylation probability and needs to be chosen according to the linker length. Computational studies could further help to get more detailed insights on the interaction of the PNA-dirhodium catalyst with the complementary strand in a three-dimensional fashion. Furthermore, it could serve as an early diagnostic tool for locating potential structural incompatibilities and prove beneficial when planning a synthesis. Once a more efficient system is established, in-depth investigations will follow for the sequence-specific alkylation of oligonucleotides. From an analytical point of view these alkylation sites could be determined by primer extension of a DNA hairpin target and subjected to high-resolution gel electrophoresis under denaturing conditions (**Scheme 2.28**). This method will allow the detection of single base-pair size differences and give detailed information on the preferences for nucleobase modification.



Scheme 2.28: Possible pathway for determining the sites of alkylation on a DNA hairpin. Primer extension with subsequent high-resolution gel electrophoresis. Products will give information on the site of modification and have to be compared with reference material.

As mentioned before the rate of oxime bioconjugation in water is of much higher priority and fundamental for a successful assembly of the template catalyst. Future work has therefore to focus primarily on methods which allow for a quick and selective oxime condensation under physiological conditions. Major contributions towards this issue are described in the next chapter of the present thesis and provide a firm basis to promote this interesting project.

3 Novel methods for oxime bioconjugations in chemical biology

3.1 Introduction

Finding new methods for effective bioconjugations in chemical biology is a daunting challenge and of particular interest to the community. Although a broad set of different bioconjugation reactions exist, each individual method exhibits certain limits making them partially useful (*vide supra*). For many applications these reactions have to be chemoselective, perform superior in water at neutral pH and equimolar ratios, and display fast reaction rates even at low concentrations. While searching for completely new bioconjugation reactions is a tedious and expensive endeavor, optimization of current methods is a more direct and quicker way to address a particular research problem.

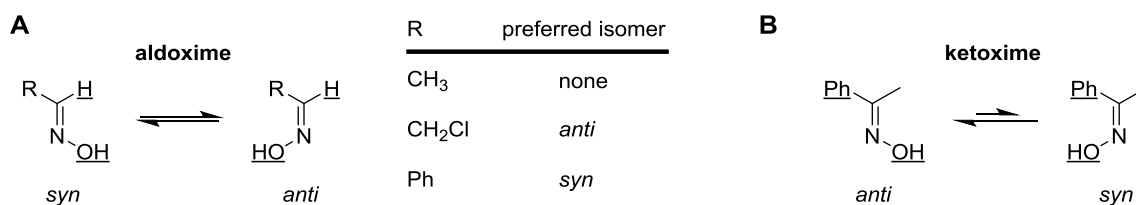
As concluded in the previous chapter, the oxime condensation strategy we used for creating guided catalysts in water was found to exhibit rather slow reaction kinetics. The envisioned self-assembling system (see **Scheme 2.10**) however relies strongly on a rapid bioconjugation to form the catalytically active species used for nucleic acid modification. We therefore became interested in methods for fast oxime condensations which can be performed in water under neutral conditions. The subsequent sections will give the reader an in-depth overview on oxime condensations in general, their challenges and state-of-the-art methods for optimization.

3.2 Characteristics and challenges of oxime condensations

As previously described, oximes (C=N-OR) result from a condensation reaction of an *O*-alkylhydroxylamine with either an aldehyde or a ketone. Since rotation around the final C=N double bond is restricted, oximes exist as two possible stereoisomers: the *syn* and *anti*-isomer. POLITZER and MURRAY investigated the effect of several substituents on the isomerism of oximes and their thermodynamic stabilities using computational models.²⁰⁰ While acetaldoxime was found to exist almost equally in the *syn* and the *anti*-form, a chloromethyl substituent slightly stabilizes the *anti*-isomer whereas benzaldoxime prefers the *syn* conformation (**Scheme 3.1**, panel A). In the case of acetophenone ketoxime the isomer where the phenyl and hydroxyl group are *anti* to each other was found to be lower in energy (**Scheme 3.1**, panel B). Although equilibrium constants may help to make a statement on the isomerization equilibria, their studies in general showed that the magnitudes of the free energy difference (ΔG , see **equation 1**) are very similar and rather small. Therefore the stability of one specific oxime product will be mainly influenced by the interactions with *e.g.*, solvent or other adjacent oxime molecules and cannot be generalized *per se*. Nevertheless, from a bioconjugation point of view both isomers represent a successful linkage of the starting components.

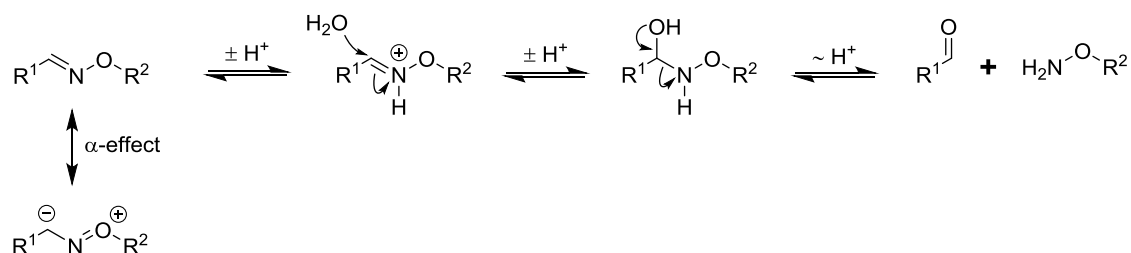
$$K_{\text{eq}} = e^{\frac{-\Delta G}{RT}} \quad (1)$$

Equation 1: Relationship of the equilibrium constant (K_{eq}) and the change in Gibbs free energy (ΔG) where R is the universal gas constant and T is the absolute temperature.



Scheme 3.1: Isomerism in aldoximes and acetophenone ketoxime. The preference for the *syn* or *anti* isomer (corresponding substituents are underlined) was determined by computing the respective free energy change ΔG and equilibrium constant K_{eq} .

Structurally oximes are Schiff bases where the substituent attached to the nitrogen atom is an *O*-alkyl group rather than a simple aryl or alkyl group. In terms of stability the classical Schiff base is prone to rapid hydrolysis in aqueous media whereas oximes are far more hydrolytically stable.¹⁷⁰ This unusual feature is explained by the α -effect of the oxygen atom which participates in electron delocalization and decreases the electrophilicity of the sp^2 carbon atom (**Scheme 3.2**). Nevertheless, their hydrolysis was found to be acid-catalyzed and has an optimum rate at pH 5 which decreases with increasing pH. Once the oxime nitrogen is protonated the electrophilic carbon atom is highly susceptible to attack by water. Subsequent cleavage of the C-N bond results in the formation of the starting aldehyde or ketone and *O*-alkylhydroxylamine.



Scheme 3.2: The α -effect in oximes renders them stable towards hydrolysis which is a reversible process depending on the reaction conditions.

When comparing the hydrolytic stability of an isostructural oxime with hydrazides and an alkylhydrazone as potential linkages for bioconjugation, the RAINES group could further demonstrate that oximes have superior stabilities in water at neutral pH (**Figure 3.1**).¹⁷⁰ They assessed the stability

by kinetic $^1\text{H-NMR}$ quenching experiments plotting the hydrolysis fraction versus the half-life ($t_{1/2}$) of the respective functionality. While the hydrazone and hydrazides were readily hydrolyzed in few hours, the oxime half-life was determined to be 25 days thus making it the ideal candidate for bioconjugations based on C=N linkages. This observation is explained by the higher electronegativity of oxygen ($\chi_{\text{O}} = 3.5$) compared to nitrogen ($\chi_{\text{N}} = 3.0$) which makes protonation of oximes less favorable compared to hydrazones and hydrazides.

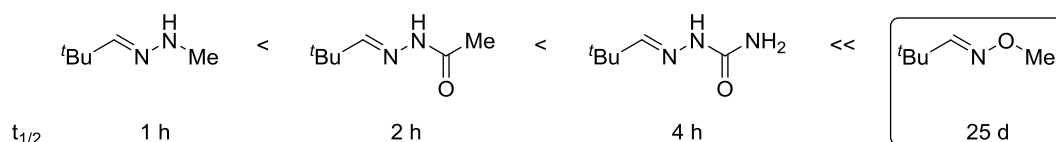
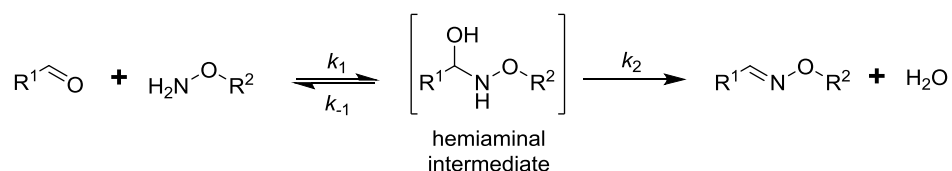


Figure 3.1: Comparison of the hydrolytic stabilities of a hydrazone, two hydrazides and an oxime.

From a synthetic point of view, oximes are readily assembled from the corresponding *O*-alkylhydroxylamines and carbonyl compounds. JENCKS' seminal mechanistic studies in the mid-1960s showed that oxime formation is a two-step process with a tetrahedral intermediate. In a first reversible step the α -nucleophile adds to the electrophilic carbonyl carbon to give a hemiaminal intermediate which then dehydrates to the final oxime product (**Scheme 3.3**).²⁰¹



Scheme 3.3: The JENCKS' two-step mechanism for oxime condensation between a carbonyl compound and an *O*-alkylhydroxylamine.

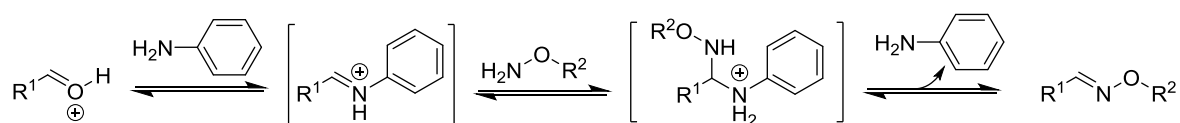
While the addition step typically proceeds through a rapid pre-equilibrium with the tetrahedral hemiaminal intermediate, subsequent elimination of water was found to be rate-limiting. Most strategies for rapid oxime condensations focus therefore on methods which lower the barrier for the dehydration step, *e.g.*, acid catalysis (*vide infra*).

Although the reaction works quite well in organic solvents like DMF¹⁷⁰, methanol²⁰², ethanol²⁰³ or DMSO²⁰⁴ it is rather difficult to obtain a successful oxime ligation in water at pH 7.²⁰⁵ In addition when considered as a potential method for bioconjugation the reaction has to be employed at high dilutions that are often required in biological settings, hence fast reaction rates are essential.

It is therefore of particular importance to optimize the rates of oxime condensations at neutral pH to make them more practical for chemical biologists. The subsequent section will give an overview on present strategies and methods to improve this type of bioconjugation reaction.

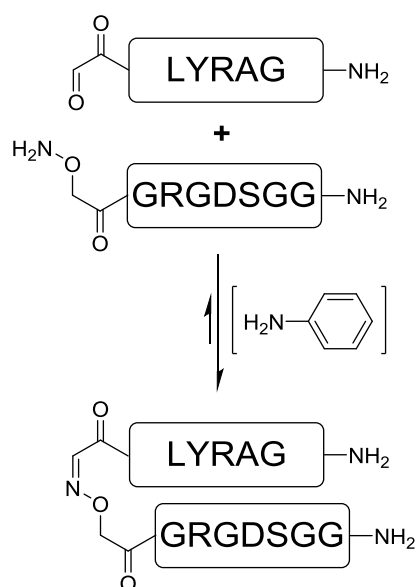
3.3 Present methods for the optimization of oxime condensations

In his early review entitled “*Mechanism and Catalysis of Simple Carbonyl Group Reactions*”, JENCKS describes, amongst other things, the pH dependence of oxime condensations.²⁰¹ His initial studies on the mechanism of oxime formation showed that this reaction exhibits a bell-shaped pH-rate curve with a maximum rate at pH 4.5.²⁰⁶ Acid catalysis therefore represents one way to accelerate oxime condensations and the observed rate enhancement is a result of the protonated hemiaminal which rapidly dehydrates to give the stable conjugate. Nevertheless, once the pH is below this optimum, *O*-alkylhydroxylamine protonation becomes predominant and shuts down the reactivity of the α -effect nucleophile. A more basic pH on the other hand decreases the reaction rate and prevents the intermediate from dehydration. In general these findings provide a good basis for understanding the specific requirements of oxime condensations. Nevertheless, fast reaction rates are still limited by the narrow pH range (pH 4-5) which makes it not applicable for effective bioconjugation under physiological conditions. However, an important advance was JENCKS’ trend-setting finding of nucleophilic aniline catalysis for semicarbazone formation.²⁰⁷ In 2006, DAWSON *et al.* demonstrated that this type of catalysis is a convenient method to accelerate oxime ligations.²⁰⁵ The use of aniline as a catalyst results in a highly populated protonated Schiff base which rapidly undergoes transimination to yield the desired ligated product (**Scheme 3.4**).



Scheme 3.4: Mechanistic pathway for the aniline catalyzed oxime formation *via* transimination.

Compared to the uncatalyzed condensation, the use of *p*-methoxyaniline was found to enhance the second-order rate constant for the ligation of two unprotected peptides by a 40-fold in phosphate buffer at pH 7 (**Scheme 3.5**). A more drastic acceleration up to 400-fold was observed at pH 4.5 where the reaction reaches 50% conversion in only 19 minutes. Although aniline ($pK_a = 4.6$; *p*-methoxyaniline: $pK_a = 5.3$) has a similar pK_a to that of α -effect nitrogens (hydroxylamine: $pK_a \sim 4.6$) the corresponding aniline Schiff base has a higher pK_a than the oxime and is therefore partially protonated under these conditions.



pH	$t_{1/2}$ ^a	k_{obs} [M ⁻¹ s ⁻¹]	catalyst
7.0 ^b	7.6 d	1.5×10^{-3}	no
7.0 ^b	280 min	6.1×10^{-2}	<i>p</i> -methoxyaniline ^c
4.5 ^d	5.7 d	2.0×10^{-3}	no
4.5 ^d	19 min	8.6	aniline ^c

^a Time required to reach 50% conversion. ^b Peptide concentrations: 1 mM. ^c 100 mM. ^d Peptide concentrations: 0.1 mM.

Scheme 3.5: Oxime ligation of two unprotected peptides performed in either the absence or presence of an aniline catalyst at pH 7.0 and 4.5, respectively.

Two years later they extended their concept of nucleophilic aniline catalysis on oxime and hydrazone ligations with aromatic aldehydes in a separate study.²⁰⁸ It was shown that an unprotected peptide and human serum albumin could be efficiently labeled at low μM concentrations with oxime rate constants up to $8.2 \text{ M}^{-1} \text{ s}^{-1}$ under ambient conditions at pH 7.

Recently, the principle of nucleophilic catalysis was further developed by the research group of DISTEFANO which reported the superior water solubility properties of a *m*-phenylenediamine (mPDA) catalyst.⁹³ The use of high concentrations of mPDA up to 900 mM in phosphate buffer at pH 7.3 allows oxime condensations to be performed up to 15-fold faster ($k_{\text{obs}} = 1.1 \text{ M}^{-1} \text{ s}^{-1}$, compared to **Scheme 3.5**) compared to aniline catalysis. Key to these findings is the additional aromatic amino group in mPDA which makes it highly water soluble beyond concentrations of 2 M. On the basis of their studies they could demonstrate that mPDA was an efficient catalyst for the selective capture of aldehyde-functionalized proteins from crude cell lysate *via* hydrazone-oxime exchange.

Another way to overcome the rather slow reaction kinetics of oxime condensations is intramolecular proton assistance. In the context of their studies on water-soluble organocatalysts for hydrazone and oxime formation, the KOOL group reported that anthranilic acid and its derivatives can serve as catalysts superior to aniline under physiological conditions.²⁰⁹ Following up on these findings they separately tested nucleophilic aniline-based catalysts containing *ortho* proton donors for hydrazone formation. It was shown that tuning the pK_a of the proton donor towards the biological buffer pH greatly accelerates the reaction rates up to 8-fold (5-methyl-2-aminobenzenephosphonic acid) compared to aniline (**Figure 3.2**, panel A).²¹⁰

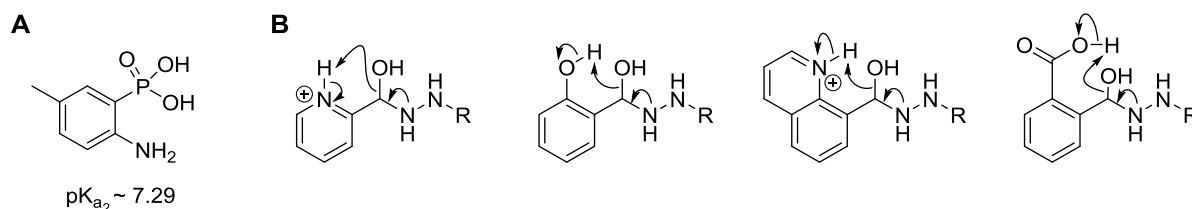


Figure 3.2: (A) Best performing aniline-based catalyst containing an *ortho* proton donor for hydrazone formation. (B) Proposed mechanism for intramolecular proton assistance of various *ortho*-substituted aryl aldehyde/hydrazine conjugates.

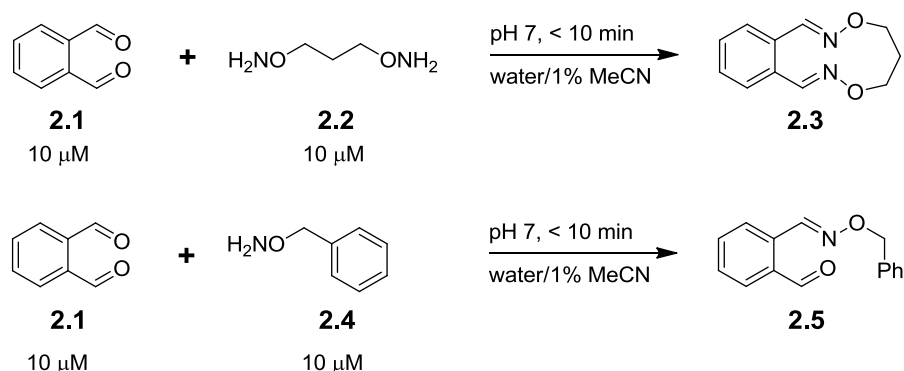
Since the addition of an external catalyst can be undesired in some cases and enhances the complexity of the system, self-catalyzing carbonyl compounds were envisioned as an adequate alternative in a separate study by KOOL *et al.* Several *ortho*-substituted aryl aldehydes were found to speed up the hydrazone ligation rates due to intramolecular protonation of the tetrahedral hemiaminal which aids the dehydration step (**Figure 3.2**, panel B).²¹¹ Although this study was exclusively performed with hydrazines, two analogous *O*-alkylhydroxylamines were also examined recently and successfully connected to 2-formylpyridine with increased reaction rates.²¹²

In summary, the methods developed so far for optimizing oxime condensations under physiological conditions employ nucleophilic catalysis (*e.g.*, aniline and its derivatives) and intramolecular proton donation of either an additional catalyst or a self-catalyzing substrate. Typical second-order reaction rates are found in the range from 10^{-2} - 10^1 $M^{-1} s^{-1}$ and have been applied to a broad spectrum of small molecules as well as peptides and proteins for efficient bioconjugation. Nevertheless additional strategies must be established which give access to reaction rates competitive with *e.g.*, strain-promoted cycloadditions (see **Scheme 1.17**, section 1.3.3). This would significantly broaden the applicability of oxime condensations and render it the method of choice for a variety of challenging bioconjugations in a neutral environment.

3.4 Results and discussion - Rapid oxime condensations using dialdehydes

The results discussed within this section are the cumulative work of the author Pascal Schmidt, Linna Zhou, Kiril Tishinov, Kaspar Zimmermann, Dennis Gillingham and have been published in 2014.²¹³ The material is used with a personal permission of the publisher John Wiley and Sons and the corresponding license details can be found in the appendix (section 4.3.2).

Our initial findings of sluggish oxime condensations for the rapid assembly of guiding catalysts under physiological conditions (see chapter 2, sections 2.3.6 and 2.3.7) have led us to explore this valuable strategy in more detail. An extensive literature search laid our focus finally to the fundamental publications of KOOL *et al.* on fast hydrazone/oxime formations²⁰⁹⁻²¹². Although we became interested in testing various *ortho*-substituted aromatic aldehydes to accelerate oxime condensations we were simultaneously terrified by the possibility of identical studies by the KOOL group. Consistent with their findings, we observed that aldehydes substituted with an acid delivered a substantial rate increase upon reaction with *O*-alkylhydroxylamines, but even this was still too slow at 10 μM of each partner. We reasoned that bisoxime formation might deliver an additional increase in rate and were therefore drawn to the possibility of dialdehyde substrates. Upon mixing commercially available *ortho*-phthalaldehyde (OPA, **2.1**) and 1,3-diaminopropane (**2.2**) in a 1:1 ratio at 10 μM we could only ever detect the bisoxime product **2.3** by HPLC after 10 minutes (**Scheme 3.6**). This surprising observation suggested that the second-order rate constant for this reaction was at least 10^4 higher than a typical uncatalyzed monooxime condensation.²⁰⁸



Scheme 3.6: Unprecedented speed in oxime conjugations: Bisoximes (top) and oximes (bottom) form in minutes without a catalyst at 10 μM in both substrates and water (pH 7) as the reaction medium.

Reaction of *O*-benzylhydroxylamine (**2.4**) with the same dialdehyde **2.1** also led to rapid oxime formation, indicating that the rate acceleration is attributable mainly to the dialdehyde motif and not to bisoxime formation as we initially hypothesized. The major advantage of the bisoxime for bioconjugations will likely be that a potentially reactive aldehyde is not left behind, and the equilibrium constant will overwhelmingly favour the product. To further explore the nature of the acceleration and to establish the reaction scope, we first varied the substrates based on our initial observations.

3.4.1 Substrate synthesis

Inspired by DAWSONS' studies on peptide ligation *via* oxime formation we were particularly interested in peptide substrates bearing an *N*-terminal mono- or bishydroxylamine functional group. We envisioned the LYRAG pentapeptide monohydroxylamine **2.6** and bishydroxylamine **2.7** as more complex test substrates for rapid bioconjugation containing a C-terminal carboxamide. The retrosynthetic analysis of both peptides is outlined in **Figure 3.3**. Peptide **2.6** was imagined to be assembled by conventional SPPS using the Fmoc/*t*Bu strategy, protected amino acids and Boc-AOAc-OH **1.9** in the final coupling step. The bishydroxylamine terminated peptide **2.7** follows the same synthetic route, except that the bishydroxylamine carboxylic acid **2.8** has to be separately synthesized in three linear steps (*O*-alkylation, ozonolysis and reductive amination) from commercial 3-bromo-2-bromomethyl-1-propene (**2.11**).

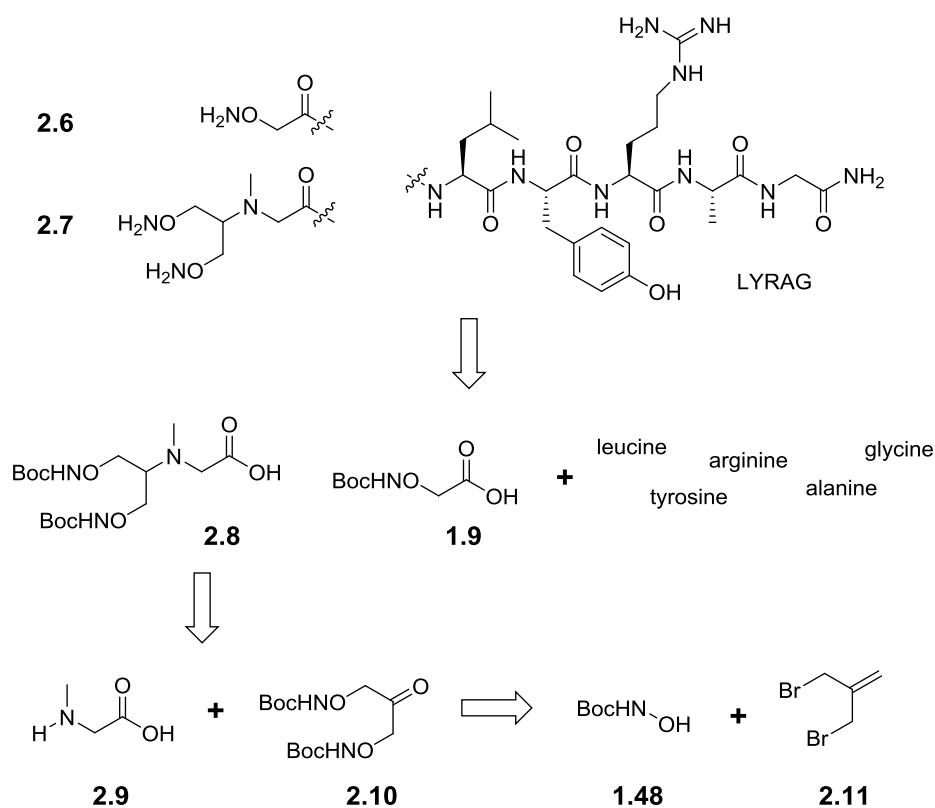
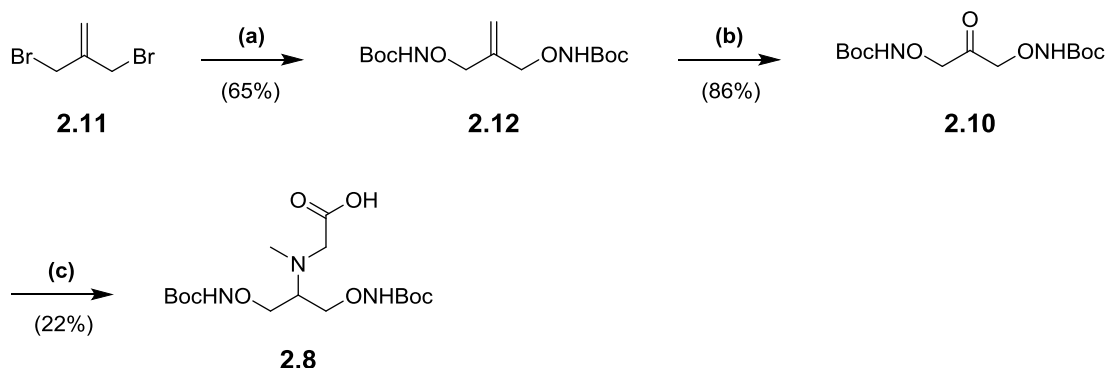


Figure 3.3: Retrosynthetic analysis of two hydroxylamine-containing LYRAG peptides: Peptide **2.6** is synthesized exclusively from commercial compounds whereas the bishydroxylamine building block **2.8** in peptide **2.7** has to be synthesized separately in three linear steps.

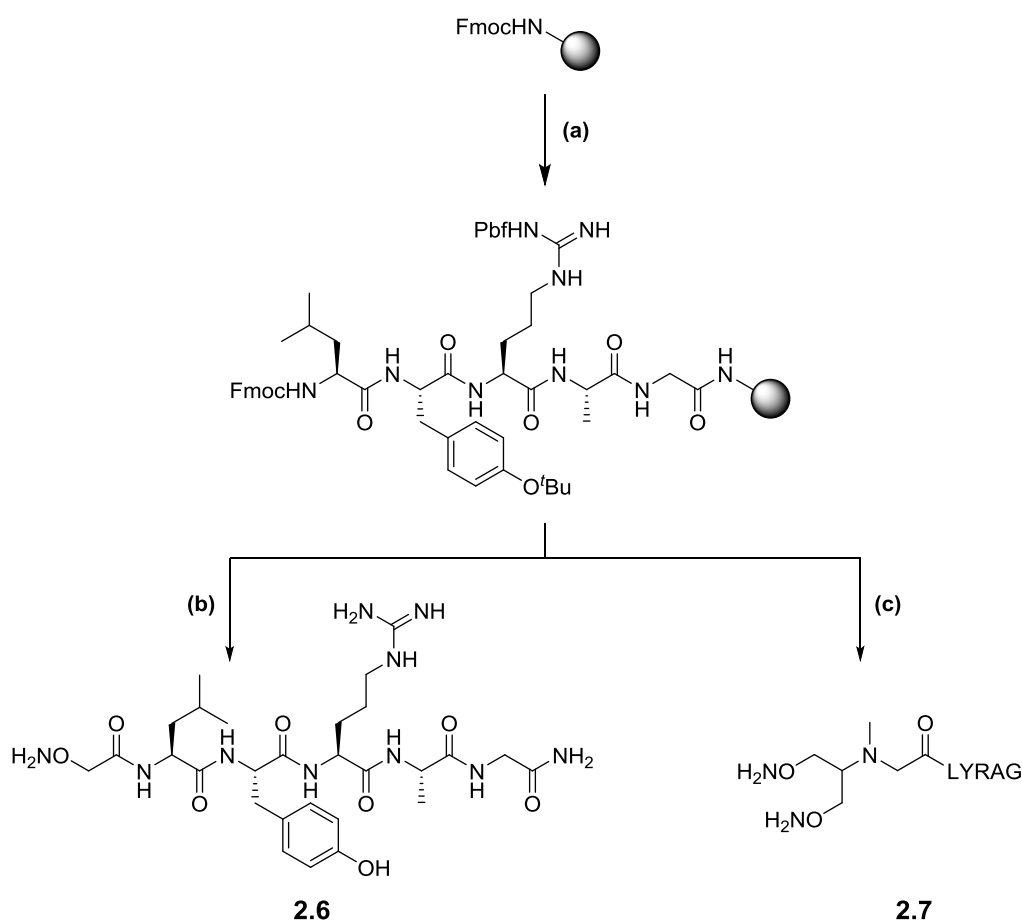
The synthetic route for the preparation of bishydroxylamine carboxylic acid **2.8** started from commercial dibromide **2.11** which was substituted with *tert*-butyl *N*-hydroxycarbamate (**1.48**) under basic conditions to give the Boc-protected bishydroxylamine **2.12**. Ozonolysis of the terminal alkene

with subsequent reductive workup afforded the ketone **2.10** in good yield which was next subjected to reductive amination with sarcosine (**2.9**) and NaBH₃CN to give the final product **2.8** (Scheme 3.7).



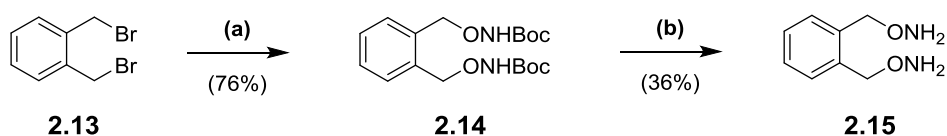
Scheme 3.7: Synthetic sequence for the preparation of bishydroxylamine carboxylic acid **2.8**: (a) *tert*-butyl *N*-hydroxycarbamate (**1.48**), DBU; (b) O₃ then Me₂S; (c) sarcosine (**2.9**), NaBH₃CN.

Next, the two hydroxylamine terminated peptides were synthesized on rink amide resin using an automated peptide synthesizer. The synthetic sequence is depicted in **Scheme 3.8** and starts with initial Fmoc deprotection by repetitive piperidine treatment. After each step several washing cycles were included which used DMF to remove excess reagents. The free amine was then reacted with a mixture of HCTU, DIPEA and the respective Fmoc-AA-OH for 1 h. This was followed by a subsequent capping step with Ac₂O to block unreacted amino groups from chain elongation. Next the deprotection, coupling and capping cycles were repeated with different amino acids until the desired length of the peptide was achieved. In the final coupling steps the solid-phase bound LYRAG peptide was first Fmoc deprotected and then reacted with either commercial Boc-AOAc-OH **1.9** or the separately synthesized bishydroxylamine carboxylic acid **2.8**. Treatment of the resin with high TFA concentrations and a silane-based cation scavenger removed all protecting groups and liberated the crude hydroxylamine equipped peptides **2.6** and **2.7** which were then precipitated from cold ether and purified preparatively employing acidic RP-HPLC. After lyophilizing the pure peptide fractions, aqueous stock solutions were prepared and quantified by UV spectrophotometry at 280 nm using a molar extinction coefficient ϵ_{280} for the amino acid sequence (LYRAG) which was calculated according to the EnCor Biotechnology Inc. webpage.²¹⁴ Both peptide substrates were then tested in mono- and bisoxime condensations with various aromatic aldehydes at different concentrations.



Scheme 3.8: SPPS of hydroxylamine-containing peptides **2.6** and **2.7**: (a) (i) 40% piperidine/DMF, (ii) Fmoc-Gly-OH, HCTU, DIPEA, (iii) 5% Ac₂O, 6% DIPEA, DMF/NMP, (iv) repetitive cycles of (i-iii) using Fmoc-Ala-OH, Fmoc-Arg(Pbf)-OH, Fmoc-Tyr(^tBu)-OH and Fmoc-Leu-OH. (b) (i) 40% piperidine/DMF, (ii) Boc-AOAc-OH **1.9**, HATU, DIPEA, (iii) TFA/TIS/H₂O (95:2.5:2.5). (c) (i) 40% piperidine/DMF, (ii) **2.8**, HATU, DIPEA, (iii) TFA/TIS/H₂O (95:2.5:2.5). LYRAG = leucine-tyrosine-arginine-alanine-glycine containing a C-terminal carboxamide.

In addition to the peptide substrates we also synthesized a simple aromatic bishydroxylamine which served as a candidate for bisoxime formation (**Scheme 3.9**). Commercial α,α' -dibromo-*o*-xylene (**2.13**) was double substituted with *tert*-butyl *N*-hydroxycarbamate (**1.48**) to give intermediate **2.14** which was then deprotected using a TFA/CH₂Cl₂ mixture to afford the aromatic bishydroxylamine **2.15** in moderate yield.

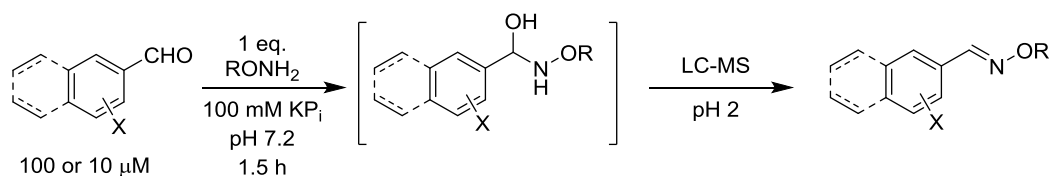


Scheme 3.9: Synthetic sequence for the preparation of aromatic bishydroxylamine **2.15**: (a) *tert*-butyl *N*-hydroxycarbamate (**1.48**), NaH; (b) TFA/CH₂Cl₂ (1:1).

3.4.2 HPLC studies

In a first HPLC assay, we tested various commercial aldehyde/hydroxylamine substrate pairs for efficient and rapid oxime condensations under aqueous and neutral reaction conditions (**Table 3.1**). The reaction mixtures (100 or 10 μM) were analyzed by acidic LC-MS at different time intervals.

Table 3.1: Comparison of oxime ligation reactions with different aromatic aldehydes and mono- or bishydroxylamines.^[a]



Entry	Aldehyde	RONH ₂	Product	conv. [%]
1 ^[b]	<chem>c1ccc(cc1)C=O</chem>	<chem>NCCc1ccccc1</chem>	<chem>c1ccc(cc1)C=NOCc2ccccc2</chem>	< 1 ^[c]
2 ^[b]	<chem>c1ccc(cc1C=O)C(=O)O</chem>	<chem>NCCc1ccccc1</chem>	<chem>c1ccc(cc1C=NOCc2ccccc2)C(=O)O</chem>	< 10
3 ^{[d] [e]}	<chem>c1ccc(cc1)C=O</chem>	<chem>NCCCN</chem>	<chem>c1ccc2c(c1)nc3c2occc3</chem>	> 98
4 ^[d]	<chem>c1ccc(cc1)C=O</chem>	<chem>NCCc1ccccc1</chem>	<chem>c1ccc(cc1C=NOCc2ccccc2)C=O</chem>	> 98
5 ^[d]	<chem>c1ccc(cc1)C=O</chem>	<chem>NCC(O)CCN</chem>	<chem>c1ccc2c(c1)nc3c2occc3</chem>	> 98
6 ^[b]	<chem>c1ccc(cc1)C=O</chem>	<chem>NCCc1ccccc1</chem>	<chem>c1ccc(cc1)C=NOCc2ccccc2</chem>	< 10
7 ^[b]	<chem>c1ccc(cc1)C=O</chem>	<chem>NCCc1ccccc1</chem>	<chem>c1ccc(cc1)C=NOCc2ccccc2</chem>	< 10
8 ^[b]	<chem>CC(=O)c1ccc(cc1)C=O</chem>	<chem>NCCc1ccccc1</chem>	<chem>CC(=O)c1ccc(cc1)C=NOCc2ccccc2</chem>	< 1 ^[c]
9 ^[b]	<chem>c1ccc2cc(C=O)ccc2c1</chem>	<chem>NCCc1ccccc1</chem>	<chem>c1ccc2cc(C=NOCc3ccccc3)ccc2c1</chem>	98

[a] Note that the oxime products are reported as acidic LC-MS detection was employed. Each reaction in **Table 3.1** that employs *ortho*-dialdehydes leads to complete conversion; the 90 min time point is shown for convenient comparison. [b] Substrate concentrations: 100 μM . [c] < 1% means no product was detected by LC-MS. [d] Substrate concentrations: 10 μM . [e] When this reaction is performed at substrate concentrations of $\leq 1 \text{ mM}$ the major product was found to be the tetraoxime **2.3b** consisting of two molecules of each aldehyde and bishydroxylamine (product not shown, see experimental section 4.2.2.1). KP_i = potassium phosphate buffer.

A survey of carbonyl derivatives confirmed the primacy of OPA for rapid oxime condensations: The reactions of benzaldehyde (entry 1), 2-carboxybenzaldehyde (entry 2), diacetylbenzene (entry 8), and dialdehydes with other substitution patterns (entries 6 and 7) were significantly slower delivering only traces of the corresponding products. As shown in entries 3 and 5, bisoximes can also be formed, an approach that may be important when the presence of a residual aldehyde is undesirable. The special reactivity of *ortho*-dialdehydes is not limited to OPA; for example naphthalene dialdehyde was also a highly effective substrate, converting completely into the corresponding oxime within minutes (entry 9).

To demonstrate the broadened scope of oxime formation, we focused next on more complex and precious starting materials which represent “real” targets for bioconjugation applications (**Table 3.2**). Both hydroxylamine terminated peptides **2.6** and **2.7** follow up on the observed trend from the previous table and show good conversions even at low concentrations. As a calibration, the reaction of both peptides with benzaldehyde (see entries 1 and 2) over 1.5 h at 100 μM gave undetectable levels of oxime formation. Recently 2-carboxybenzaldehyde was found to be an exceptionally fast partner for hydrazone condensations²¹⁰; entry 3 suggests that this effect is not as pronounced with hydroxylamines. Some additional important points from **Table 3.2**: (1) Consistent with our results from **Table 3.1**, there is little difference between the rates of mono- and bisoxime formation with dialdehydes (compare entries 4-7); (2) In these more complex substrates the second-order rate constants are smaller, but still amongst the highest ever observed for oximes: judging from the first half-life they are typically around $30 \text{ M}^{-1} \text{ s}^{-1}$, but range between 1 and $50 \text{ M}^{-1} \text{ s}^{-1}$; (3) although the reaction is viable in the presence of 20% (v/v) human serum (approximately 60% conversion: entry 8), there is some concomitant deamination of the hydroxylamine – an observation that sounds a note of caution for employing these reactions *in vivo* or in lysates. The capacity to reduce hydroxylamines and aldoximes has been known for some time, but in humans the enzymology has only recently been characterized.^{215,216} Potential users of hydroxylamine labeling *in vivo* should be aware that knockout of the reductases may be necessary. Background reduction of hydroxylamines is not often discussed in the bioconjugation literature, likely because at high concentrations the capacity of the reducing enzymes is overwhelmed making the effect negligible.

Little is known about bisoxime condensations, and they seem only to have been employed to create macrocyclic ligands for transition metals.²¹⁷⁻²¹⁹ We suspect the reaction has never been studied in detail because it often gives mixtures of linear and cyclic oligomers when run at or above millimolar concentrations. We do not see this as a shortcoming, however, since bioconjugations at concentrations above 100 μM can already be effectively achieved with the existing repertoire of reactions.² At concentrations below 100 μM dialdehyde oxime condensations are typically clean and selective, making these reactions best suited to applications where large second-order rate constants are crucial.

Table 3.2: Comparison of oxime ligation reactions with peptide substrates.^[a]

Entry	Aldehyde	RONH ₂	Product	conv. [%]
1 ^[b]				< 1 ^[c]
2 ^[b]				< 1 ^[c]
3 ^[b]				< 5
4 ^[b]				79
5 ^[b]				58
6 ^[d]				37
7 ^[d]				57
8 ^[e]				~60

[a] Note that the oxime products are reported as acidic LC-MS detection was employed. The 90 min time point is shown for convenient comparison. [b] Substrate concentrations: 100 μ M. [c] < 1% means no product was detected by LC-MS. [d] Substrate concentrations: 10 μ M. [e] Human serum (20% v/v) was added to the reaction mixture; aldehyde concentration in this experiment is 50 μ M; conversion is an estimate since the serum introduces peaks that obscure the starting peptide and product. The serum also leads to some reduction of the hydroxylamine function (loss of NH in the MS). KP_i = potassium phosphate buffer.

3.4.3 Probing the effect of biological interfering additives

For practical applications it is important for a bioconjugation reaction to proceed in complex environments and fulfill the criteria of being bioorthogonal (see **Figure 1.1**). It is particularly important to test the efficacy of oxime ligations in the presence of other nucleophilic amino acid functionalities. We therefore performed reactions between mono hydroxylamine-containing peptide **2.6** and aromatic *ortho*-dialdehydes at a 1:1 ration with an equimolar amount of interfering additives such as unprotected tryptophan or lysozyme (**Table 3.3**). With simple amines, dialdehydes can form a great variety of products depending on the reaction conditions (solvent, stoichiometry, concentration)²²⁰, but are slower than what we observe with *O*-alkylhydroxylamines under aqueous conditions.²²¹ In our case, the oxime formation was equally effective in the presence of equimolar tryptophan (compare entries 1 and 2, entries 4 and 5). In the presence of lysozyme, however, the conversions were lower (see entries 3 and 6), likely as a result of nucleophilic side-chains in the protein trapping some of the *ortho*-dialdehyde. These results suggest that *O*-alkylhydroxylamine additions may be conducted with complex samples, but that a slight excess of the *ortho*-dialdehyde may be necessary for complete conversion.

Table 3.3: Effect of amino acids and proteins on the oxime formation between *ortho*-dialdehydes and mono hydroxylamine peptide **2.6**.^[a]

Entry	Dialdehyde	Additive	Product	conv. [%]
1		—		79
2		tryptophan		67
3		lysozyme		37
4		—		77
5		tryptophan		76
6		lysozyme		57

[a] Note that the oxime products are reported as acidic LC-MS detection was employed. The 90 min time point is shown for convenient comparison.

3.4.4 ¹H-NMR studies – a mechanistic and kinetic insight

While trying to obtain an authentic sample of oxime **2.5** for full NMR characterization we were surprised to detect a stable intermediate which formed within seconds of mixing OPA **2.1** with *O*-benzylhydroxylamine (**2.4**) in a 1:1 ratio at 100 μM and neutral pH (**Figure 3.4**, panel A). A complete NMR characterization confirmed the structure of the cyclic isoindole bis(hemiaminal) (IBHA, **2.16**) intermediate which slowly dehydrated to give the expected oxime **2.5** over a time scale of hours.

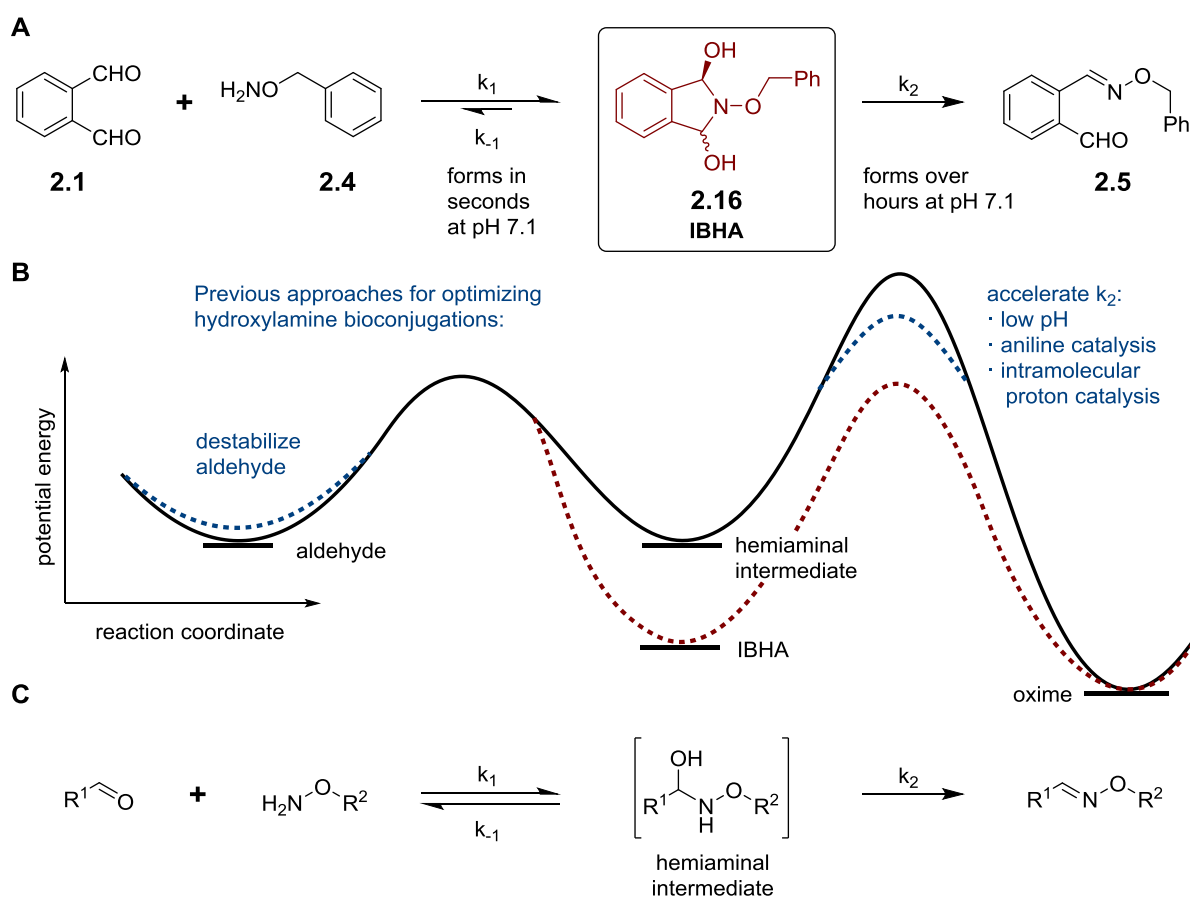
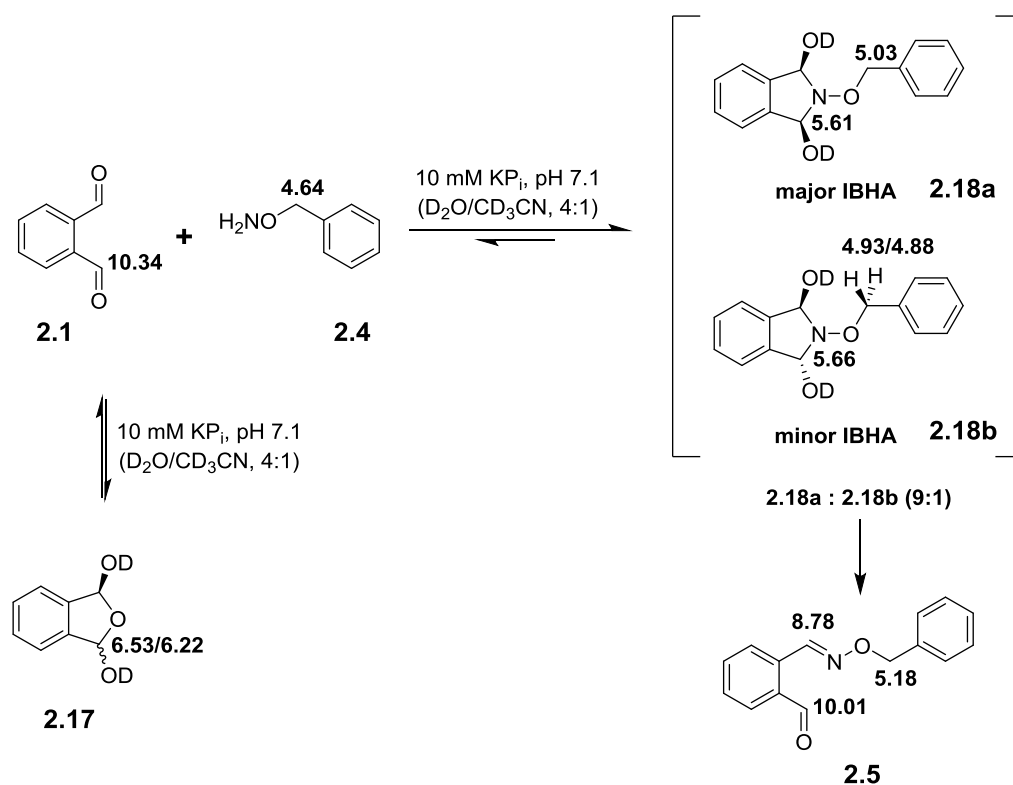


Figure 3.4: (A) The approach outlined here is given in brown: *ortho*-phthalaldehyde (OPA, **2.1**) reacts with *O*-benzylhydroxylamine (**2.4**) to give a stable isoindole bis(hemiaminal) (IBHA, **2.16**) within seconds at neutral pH values (conditions: 10 mM KP_i , pH 7.1, 20% MeCN). Please note that the reaction coordinate diagram is qualitative; smooth curves are drawn between kinetically relevant steps although proton transfer steps and intermediate addition products are likely to be involved. (B) Known approaches for accelerating the reaction are shown in blue on the reaction coordinate diagram. (C) The JENCKS' mechanism for condensations with *O*-alkylhydroxylamines.

As described in section 3.2, JENCKS' seminal work showed that oxime condensations typically proceed through a rapid pre-equilibrium with a tetrahedral hemiaminal intermediate followed by a rate-limiting dehydration (**Figure 3.4**, panel C). Most attempts to optimize oxime condensations have therefore focused on lowering the barrier of the dehydration step or destabilizing the starting aldehyde (**Figure 3.4**, panel B) (*vide supra*). The exciting observation of a cyclic IBHA intermediate motivated us to lay our focus on this particular reaction and elucidate its mechanistic pathway as well as collect

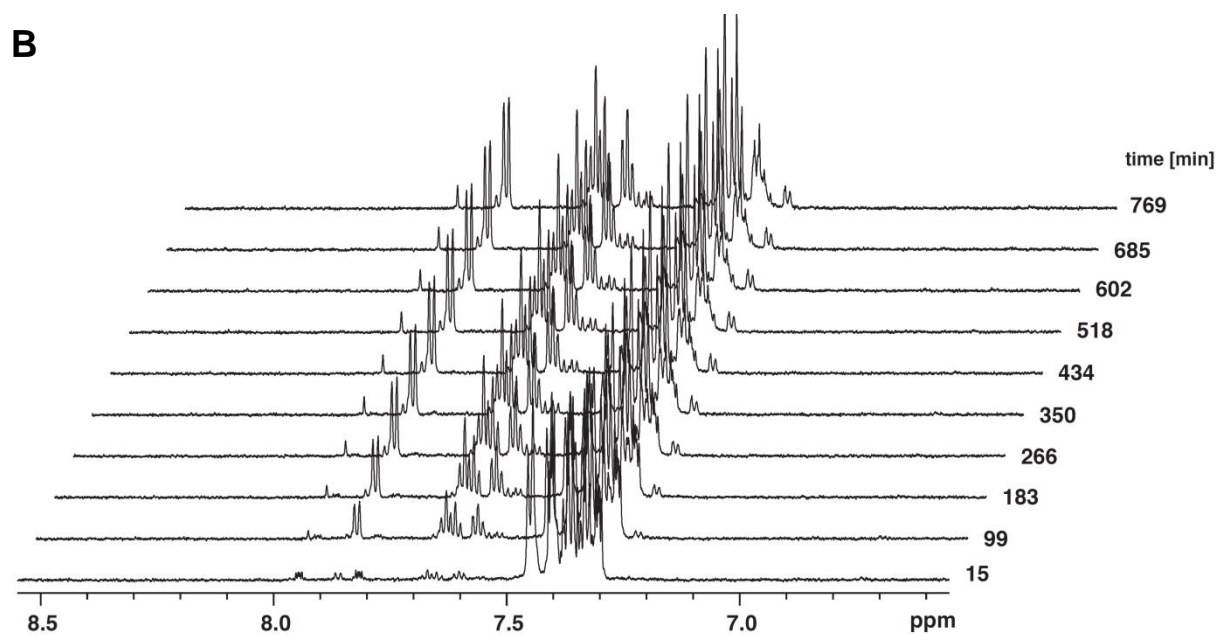
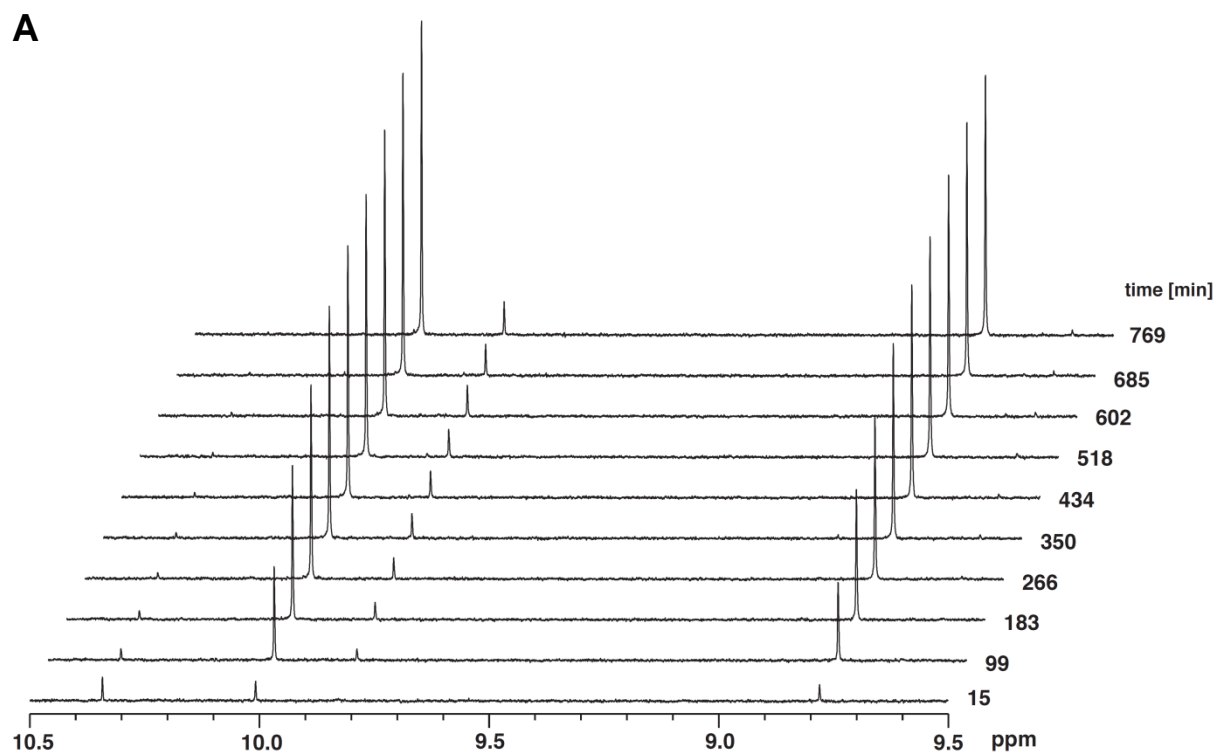
kinetic information on the slow dehydration step by performing a series of time course $^1\text{H-NMR}$ studies (see **Scheme 3.10** and **Figure 3.5**, A-C).



Scheme 3.10: Mechanistic pathway of oxime condensation between OPA **2.1** and *O*-benzylhydroxylamine (**2.4**) with competing hydrate formation in aqueous media and the two possible IBHA intermediates **2.18a/b**. The numbers represent the chemical shifts in ppm for the corresponding protons.

OPA **2.1** is known to form a cyclic hydrate **2.17** in the presence of water.²²² This hydration process was also observed while performing $^1\text{H-NMR}$ measurements and the corresponding shifts for the acetal protons of the OPA hydrate **2.17** (*meso* form and its diastereomer) were found to be at 6.53 ppm and 6.22 ppm, respectively (**Figure 3.5**, C). The aldehyde peak of OPA **2.1** at 10.34 ppm is almost completely consumed after 15 minutes and vanishes over time to be indistinguishable from noise (**Figure 3.5**, A). At the same time the aldehyde peak of **2.5** at 10.01 ppm along with the oxime proton peak at 8.78 ppm are increasing. In the aromatic region (**Figure 3.5**, B) new peaks appear between 7.50 ppm and 8.00 ppm over time which are also product related. A detailed assignment of all aromatic peaks during the reaction was not pursued since there is extensive overlap of all species. A full characterization of oxime **2.5** is described in the experimental part, sections 4.2.2.1 and 4.2.2.4. The two possible IBHA stereoisomers **2.18a** and **2.18b** were found to be a 9:1 mixture favouring the *meso*-IBHA **2.18a** over its *C*₂-symmetric diastereomer **2.18b**. The corresponding shifts for the acetal protons were determined to be 5.61 ppm and 5.66 ppm, respectively. The benzylic protons of the major IBHA resonate as a singlet at 5.03 ppm (*meso*-isomer **2.18a**) whereas the two diastereotopic benzylic protons of the minor IBHA **2.18b** appear as a set of two doublets at 4.93 ppm and 4.88 ppm along with a roof effect. The peak at 5.37 ppm is unconfirmed but seems to come from an impurity

since its ratio doesn't change over time. Preliminary exchange spectroscopy (EXSY) measurements strongly suggest cross peaks for the peaks at 10.01 ppm and 9.83 ppm (aldehyde proton) as well as for the peaks at 5.18 ppm and 5.04 ppm (benzylic protons) – an observation which most likely comes from a *cis/trans* isomerization of the final oxime **2.5**.



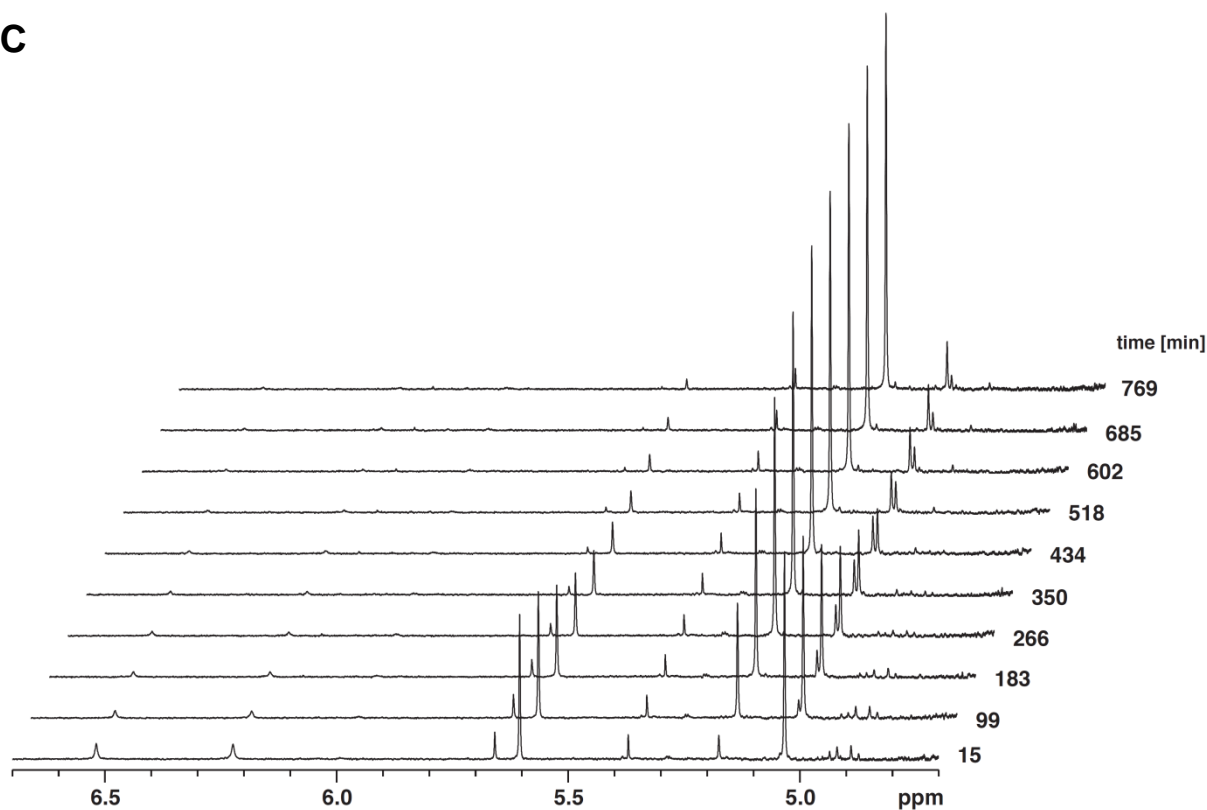
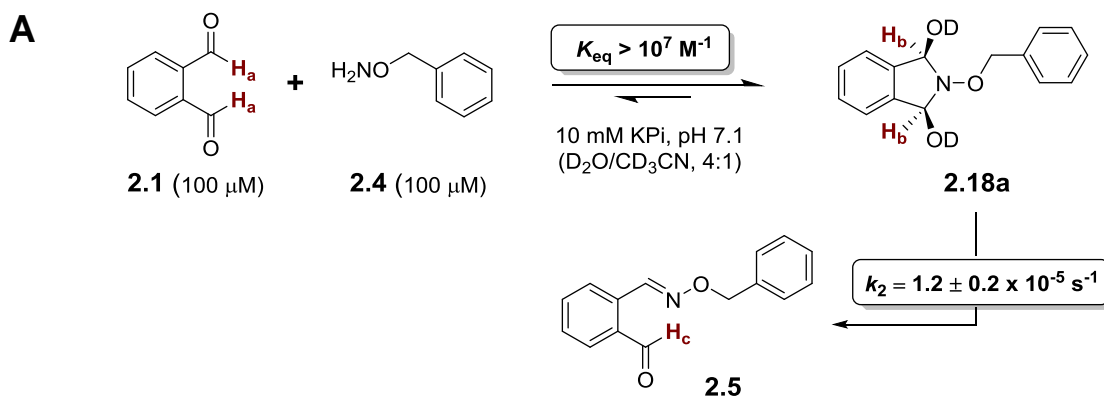
C

Figure 3.5: Time dependent $^1\text{H-NMR}$ analysis: (A) Aldehyde and oxime region. (B) Aromatic region. (C) Benzylic and acetal/bis-hemiaminal region of IBHA **2.18a/b** and oxime **2.5**.

In addition to this mechanistic insight on rapid oxime condensations using dialdehydes, time course $^1\text{H-NMR}$ analysis also provided a value for k_2 and a lower bound for K_{eq} (**Figure 3.6**, panel A). As the dehydration is effectively irreversible over the time scales we monitored,²²³ the appearance of oxime could be taken as a direct measure of k_2 (see the **H_c** proton signal in **Figure 3.6**, panel B).



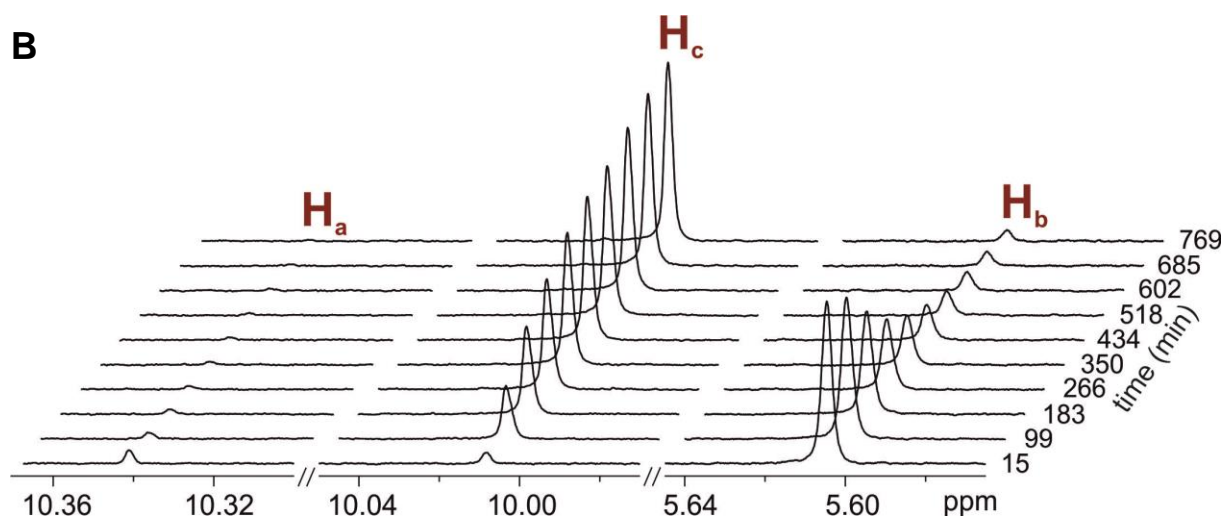


Figure 3.6: Kinetic analysis: (A) NMR tube reaction at 100 μM substrate concentrations; characteristic proton signals $\text{H}_{\text{a-c}}$ are highlighted in brown. Note: Minor species **2.18b** was also formed but not of importance for this analysis. (B) ^1H -NMR analysis indicating the peaks that were monitored with time to determine the value of k_2 . Kinetic parameters are an average of two experiments.

The value obtained, $1.2 \pm 0.2 \times 10^{-5} \text{ s}^{-1}$, is two to three orders of magnitude smaller than those of typical oxime condensations at pH 7,²⁰⁵ consistent with the intermediate IBHA sitting in a deep energy minimum. No equilibrium for the initial addition was measurable over the observed time scale (20 h), a point independently confirmed in a separate experiment: When the IBHA **2.16** was dissolved in phosphate buffer, and the reaction mixture monitored by ^1H -NMR spectroscopy, the formation of OPA **2.1** was not observed; instead, the substrate was gradually converted into the oxime. The IBHA **2.16** could be preparatively isolated as a mixture with the oxime product **2.5** by performing the reaction in pure MeCN at room temperature in less than a minute (**Figure 3.7**, panel A). Leaving the neat mixture at room temperature or when redissolved in MeCN it converted completely to the oxime product over hours whereas treatment with DCl vapor resulted immediately in the exclusive formation of lactam derivative **2.19** which was confirmed by X-ray analysis (**Figure 3.7**, panel B).

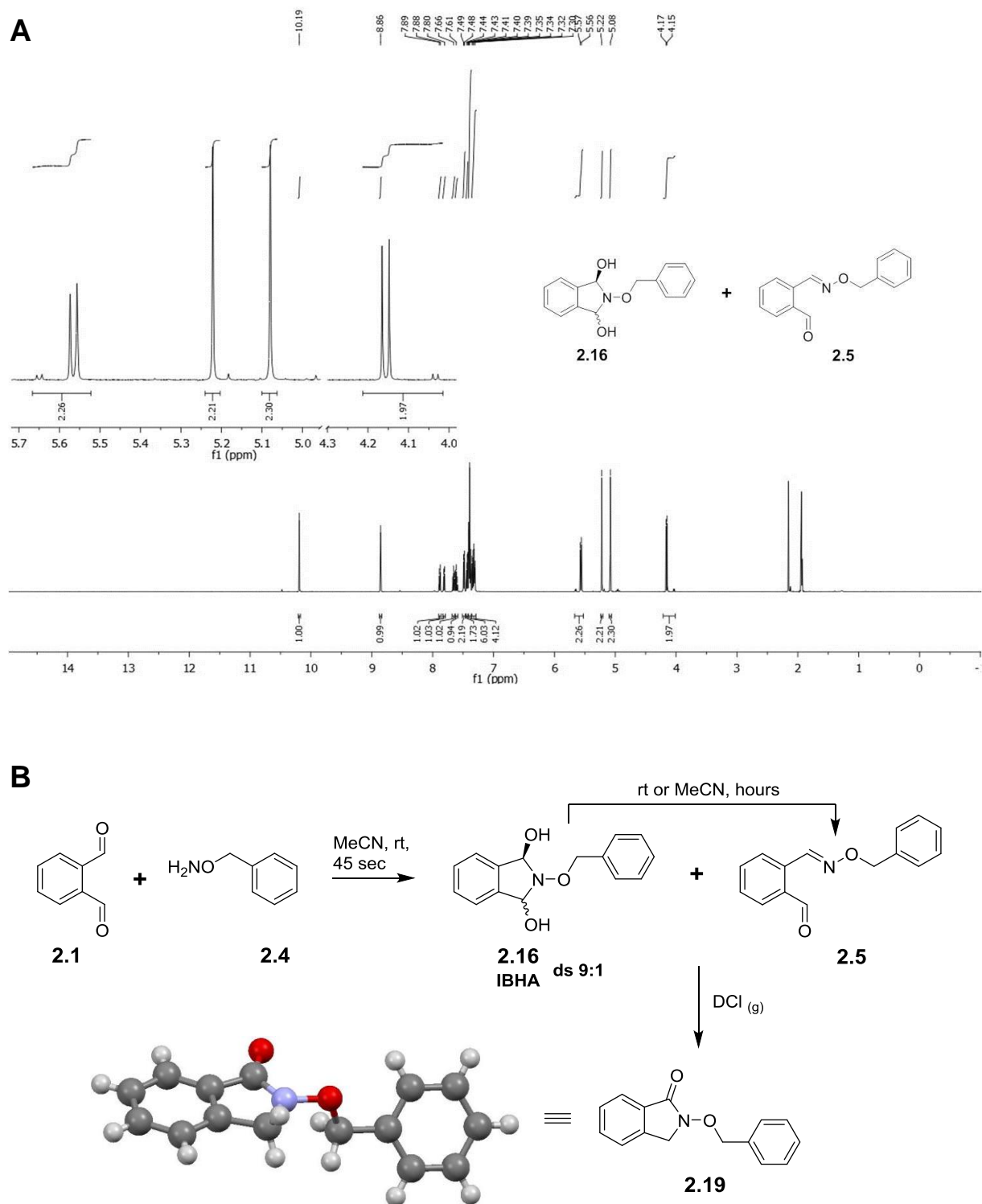


Figure 3.7: (A) $^1\text{H-NMR}$ spectrum of the IBHA **2.16** and oxime **2.5** mixtures recorded in CD_3CN . (B) Reaction conditions: 0.4 M OPA **2.1** and *O*-benzylhydroxylamine (**2.4**) result in a 1:1.5 mixture of oxime **2.5** and IBHA **2.16**. Treatment of the mixture with DCl vapor gives lactam derivative **2.19**.

Although an accurate K_{eq} value could not be determined, a lower bound of approximately 10^7 M^{-1} may be assumed since low micromolar concentrations of the aldehyde would be well above the detection limit of the 700 MHz NMR spectrometer. In terms of the reaction coordinate diagram (see **Figure**

3.4), the fact that the IBHA led to oxime formation but not to formation of OPA **2.1** suggests that dehydration is faster than retro-IBHA formation (*e.g.*, $k_2 > k_1$). This was corroborated in a separate $^1\text{H-NMR}$ experiment which also suggests that the first step is not in equilibrium: When a sample containing the IBHA of naphthalene dialdehyde **2.20** was treated with a large excess of OPA **2.1**, no scrambling to the OPA-derived IBHA **2.16** was observed (**Figure 3.8**). This suggests that once the IBHA is formed, the *O*-alkylhydroxylamine is never released again.

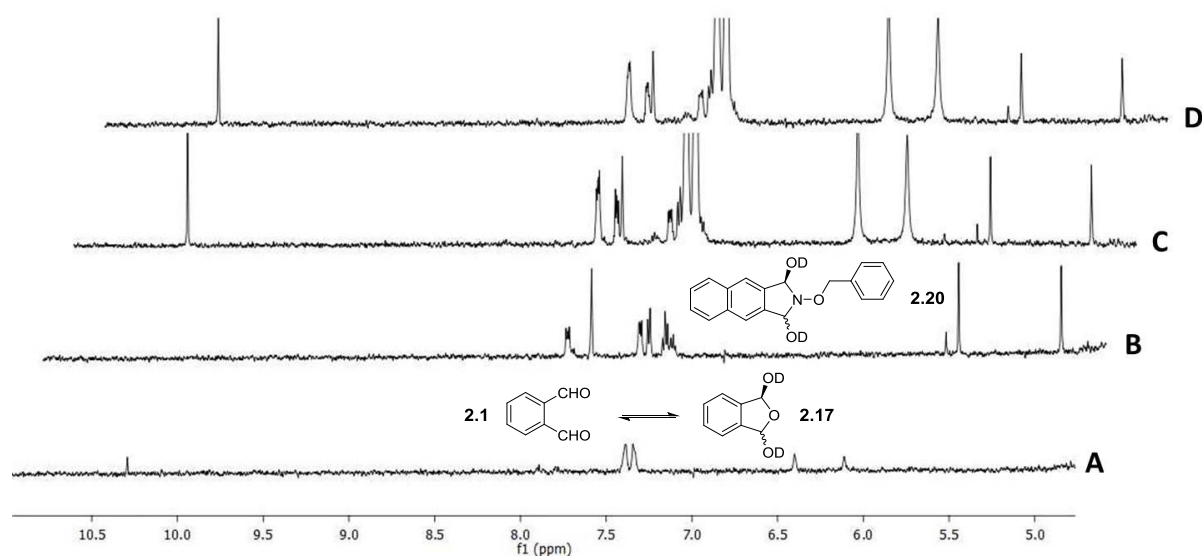


Figure 3.8: Time dependent $^1\text{H-NMR}$ analysis to determine the reversibility of IBHA formation: (A) 100 μM OPA **2.1**. (B) 100 μM naphthalene IBHA **2.20**. (C) 100 μM naphthalene IBHA **2.20** + 10 eq. OPA **2.1** after 3 min. (D) 100 μM naphthalene IBHA **2.20** + 10 eq. OPA **2.1** after 75 min. Conditions: 10 mM KP_i ($\text{D}_2\text{O}/\text{DMSO-}d_6$, 1:1), pH 7.1.

Overall, the mechanism of oxime formation that we observe with dialdehydes parallels JENCKS' proposal for simple oximes (see **Scheme 3.3** - above), with the key distinction that the equilibrium constant for the formation of the intermediate overwhelmingly favors addition. The formation of the IBHA was so rapid that even at a concentration of 100 μM , $^1\text{H-NMR}$ analysis lacked the time resolution to measure the initial bimolecular rate constant k_1 . However, a value for k_1 is important in the planning of experiments because it forecasts the required concentrations and stoichiometries.

3.4.5 Fluorescence quench assay – determining k_1

To access the initial rate of addition we developed a fluorescence quenching assay which is a common method for the determination of reaction kinetics.^{224,225} Fluorogenic probes equipped with reporter (fluorophore) and quencher dyes use a change in fluorescence upon association which allows monitoring of (bio)chemical events.²²⁶ Usually the reporter absorbs light (excitation) at a characteristic wavelength and emits light (fluorescence) of lower energy (longer wavelength). Depending on the nature of the quencher, the energy transferred by the fluorophore can either be re-emitted as light to a

certain extent or as heat through a non-radiative pathway, a characteristic of so-called dark quenchers. Two possible mechanisms for quenching fluorescence through non-radiative energy transfer are shown in **Figure 3.9** and highlight the important differences. FÖRSTER resonance energy transfer (FRET) is a dynamic quenching mechanism based on dipole-dipole interactions of the reporter and quencher during excitation. It was found that FRET is highly dependent on the distance (r) between the reporter-quencher pair with $r_{\text{max}} \sim 100 \text{ \AA}$ and decreases at a rate of $1/r^6$ (**Figure 3.9**, panel A). Contact or static quenching occurs when the reporter and quencher bind together and result in a ground state complex with unique properties. As a result of this newly formed intramolecular dimer the fluorescent properties of the individual components can be lost completely depending on the reporter-quencher pair (**Figure 3.9**, panel B).²²⁶

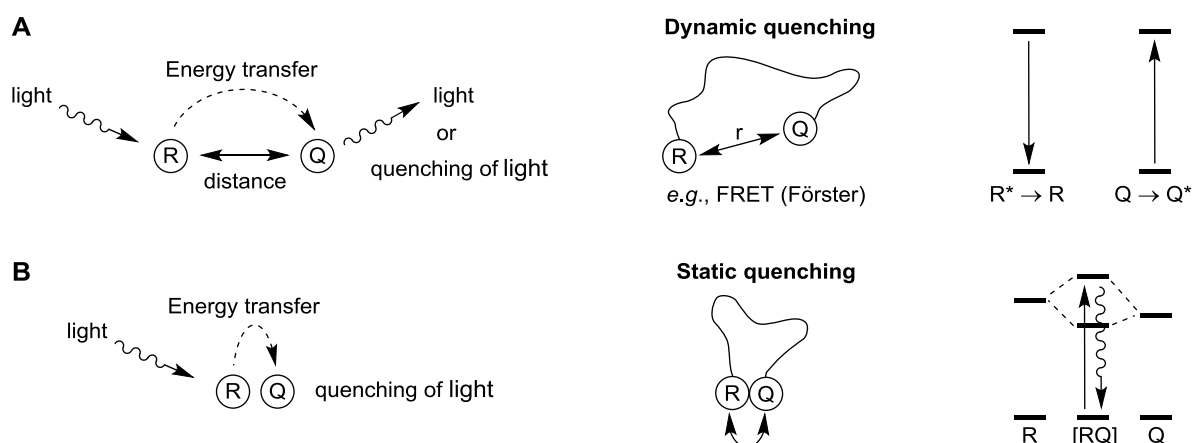
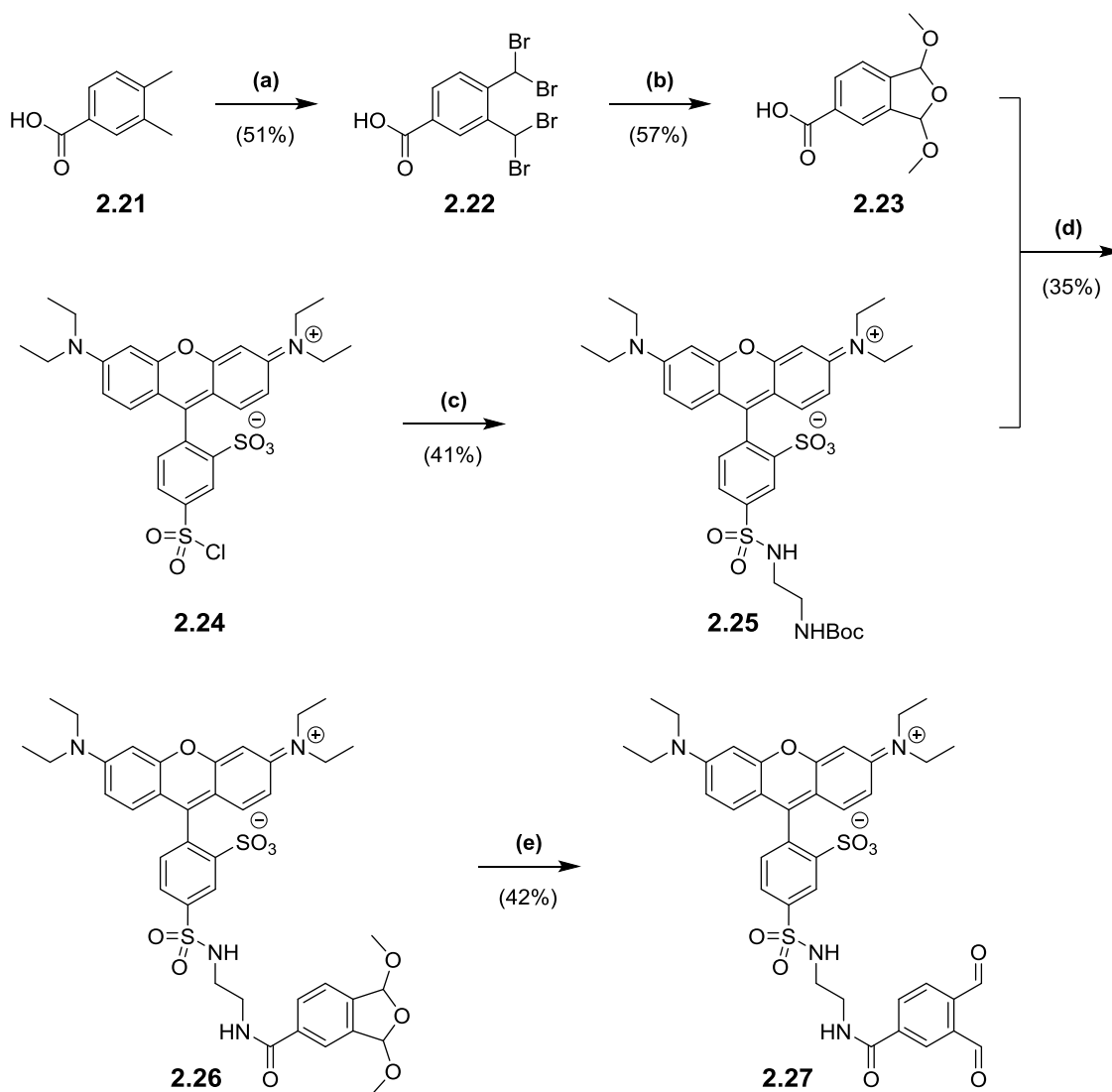


Figure 3.9: Comparison of fluorescence quenching pathways: (A) Dynamic quenching mechanism with energy transfer occurring during excitation of the reporter dye. (B) Static quenching mechanism in a ground state complex [RQ] proceeding through a non-radiative pathway.

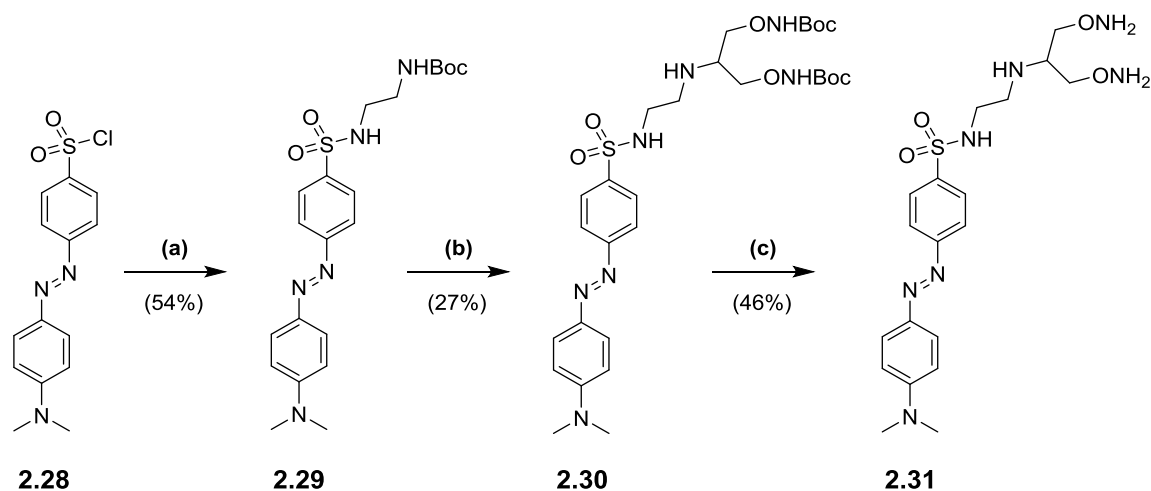
It seemed reasonable to us that a dynamic fluorescence quenching assay would be best suited to determine k_1 for the oxime condensation between *ortho*-dialdehydes and *O*-alkylhydroxylamines. Therefore we synthesized a lissamine-tagged version of OPA **2.27** (**Scheme 3.11**) and a dabsyl derivative bearing a bishydroxylamine **2.31** (**Scheme 3.12**). Lissamine was chosen as a fluorophore because its excitation wavelength of around 568 nm does not interfere with biological autofluorescent molecules (e.g., NADH, tyrosine, flavins, porphyrins) and may be selectively monitored if considered for *in vivo* applications.²²⁷ Dabsyl, a dark quencher, was used since it is a typical, non-fluorescent quencher frequently used in FRET applications and may be easily attached to the target molecule.²²⁸

The synthetic route for the lissamine fluorophore **2.27** commenced with a radical tetrabromination of 3,4-dimethyl-benzoic acid (**2.21**) followed by lewis acid-catalyzed acetalization to give acid **2.23** (**Scheme 3.11**). In a separate step, lissamine rhodamine B sulfonyl chloride (**2.24**) was substituted with *N*-Boc-ethylenediamine to give protected lissamine **2.25**. *N*-Boc deprotection was followed by a DCC-mediated peptide coupling with acid **2.23** to give lissamine bisacetal **2.26** which after final acidic cleavage provided the desired lissamine-tagged OPA derivative **2.27**.



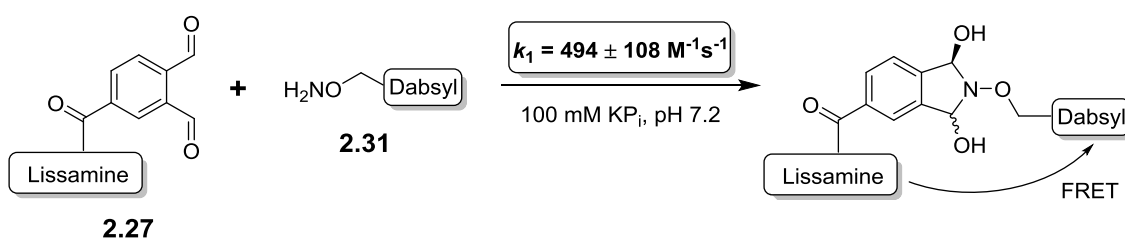
Scheme 3.11: Synthetic sequences for the preparation of lissamine-tagged OPA **2.27**: (a) NBS, benzoyl peroxide; (b) (i) 10% Na_2CO_3 (aq.); (ii) $\text{Sc}(\text{OTf})_3$, MeOH; (c) *N*-Boc-ethylenediamine, NEt_3 ; (d) (i) 4M HCl in 1,4-dioxane/MeOH (1:1); (ii) NEt_3 , DCC; (e) TFA/ H_2O (1:1).

The second synthetic route shown in **Scheme 3.12** started with a simple $\text{S}_{\text{N}}2$ reaction of dabsyl chloride **2.28** with *N*-Boc-ethylenediamine to give sulfonamide **2.29**. A two-step deprotection/reductive amination sequence using synthetic ketone **2.10** (see **Scheme 3.7**) gave access to the bis-protected dabsyl derivative **2.30**. High TFA concentrations afforded finally the dabsyl quencher **2.31** ready to be tested in a fluorescence quenching assay.



Scheme 3.12: Synthetic sequences for the preparation of dabsyl quencher **2.31**: (a) *N*-Boc-ethylenediamine, NEt_3 ; (b) (i) 4M HCl in 1,4-dioxane/MeOH (1:1); (ii) **2.10**, NaBH_3CN ; (c) TFA/TIS/ H_2O (95:2.5:2.5).

With the target molecules in hand we next determined the kinetic parameters at concentrations of 5 μM and 2 μM for each substrate (100 mM KP_i , pH 7.2). The resulting data fit best to a second-order rate equation and gave an average over the two concentrations of $k_1 = 494 \pm 108 \text{ M}^{-1} \text{ s}^{-1}$ (see **Scheme 3.13**). Although the fluorescence quenching assay was run with different substrates (the tags necessary for the readout), the magnitude of k_1 is qualitatively consistent with the rapid formation of the intermediate that was observed by $^1\text{H-NMR}$ spectroscopy. Using these numbers (*vide supra*) we can now annotate the major elementary steps for oxime formation with dialdehydes: (1) a large equilibrium constant ($K_{\text{eq}} > 10^7 \text{ M}^{-1}$); (2) a fast reaction rate for the initial addition step ($k_1 = 494 \text{ M}^{-1} \text{ s}^{-1}$) and (3) a slow rate for the dehydration ($k_2 = 1.2 \times 10^{-5} \text{ s}^{-1}$). The most rapid extant small molecule bioconjugation is the tetrazine-strained olefin Diels–Alder reaction, which typically has second-order rate constants between 1 and $10^3 \text{ M}^{-1} \text{ s}^{-1}$,^{86,88,91} and in the best cases up to $10^6 \text{ M}^{-1} \text{ s}^{-1}$.^{229,230} Despite these impressive rate constants, the widespread adoption of the tetrazine-strained Diels–Alder reaction has been hindered by challenging substrate syntheses and the instability of the tetrazines. In comparison, IBHA formation has rate constants that compete with the fastest cycloaddition reactions,²²⁹ but employs far simpler substrates.



Scheme 3.13: A fluorescence quenching assay was used to establish the rate of the initial bimolecular addition. k_1 is the combined average of six repeats at two different concentrations (see **Figure E3** in section 4.2.2.5 for the kinetic plots).

3.4.6 Bioconjugation with a complex DNA substrate

To further demonstrate the practical potential of the dialdehyde method we examined a bioconjugation with a complex DNA substrate. We synthesized a 5'-*O*-alkylhydroxylamine terminated DNA 41-mer **2.32** and tested it with various concentrations of fluorescent lissamine-tagged OPA derivative **2.27** (**Figure 3.10**, left). As the gel data illustrate, under neutral conditions, even down to 5 μM of DNA, almost complete conversion into the labeled product **2.33** was observed after one hour (compare lanes 3–7), whereas the control lanes using either a monoaldehyde (lane 8) or a native DNA (lane 9) showed no labeling (**Figure 3.10**, right). Given the proclivity of nucleic acids to depurinate at the low pH values needed for most oxime condensations, the neutral conditions employed here provide a mild alternative for DNA and RNA bioconjugations.

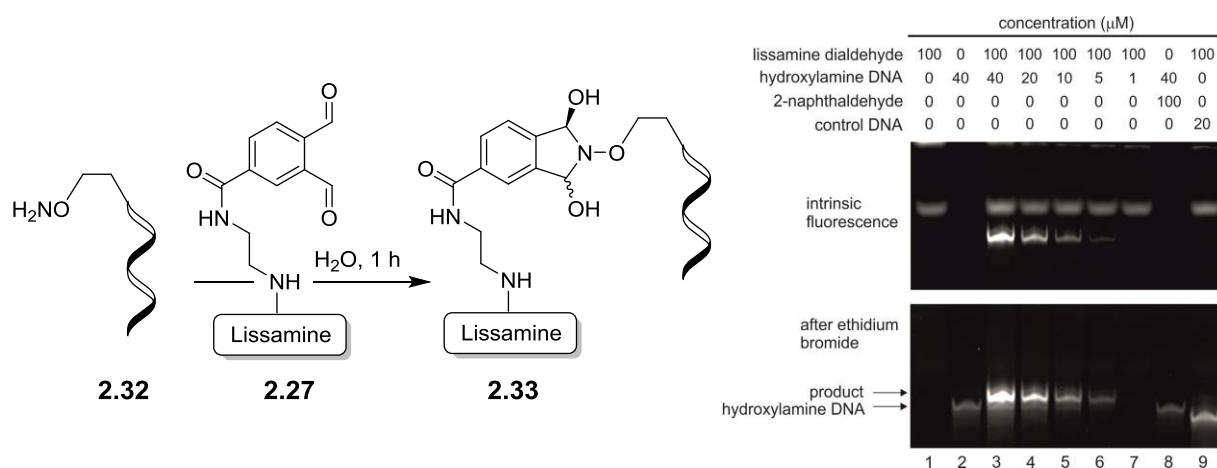


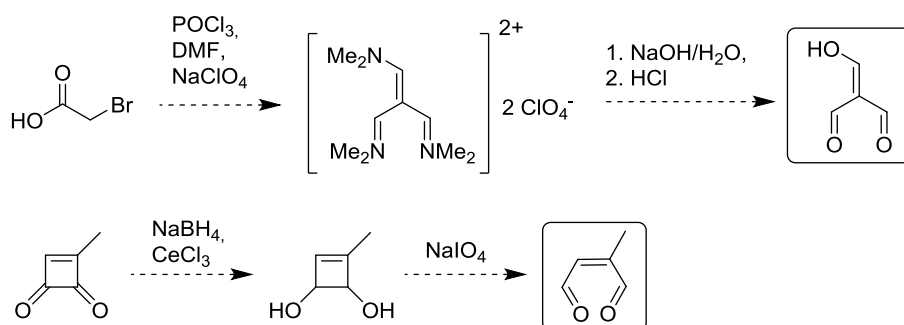
Figure 3.10: Left: DNA was efficiently labeled under mild conditions (pH 7). Please note that for simplicity, the IBHA **2.33** is drawn, but the conjugation products were likely to be a mixture of IBHA and oxime. Gel: Lane 1: lissamine dialdehyde **2.27**. Lane 2: 41-mer 5'-*O*-alkylhydroxylamine DNA **2.32**. Lanes 3–7: IBHA conjugations at various DNA concentrations. Lane 8: control reaction of 5'-*O*-alkylhydroxylamine DNA **2.32** with the fluorescent monoaldehyde 2-naphthaldehyde. Lane 9: control reaction confirming that the lissamine dialdehyde **2.27** does not react with a native DNA oligomer (39-mer). Note that the reactions were run in unbuffered water; the pH value measured at the end of the reaction was 7.

Most effort in optimizing oxime and hydrazone condensations has been devoted to accelerating the final dehydration step as it has the highest activation barrier (see **Figure 3.4**). However, at sufficiently low concentrations, bimolecular elementary steps will begin to dominate the rate equation of any reaction irrespective of barrier heights. Further development of *O*-alkylhydroxylamine bioconjugations at low concentrations will therefore require an increased focus on the initial bimolecular addition step. The propensity of OPA **2.1** to form a stable IBHA is one such example, but additional possibilities could be imagined: Other dicarbonyl compounds that lead to stable IBHAs or *O*-alkylhydroxylamines that also deliver stable intermediates present new targets for future studies.

3.4.7 Conclusion and outlook

The work presented within this section should find broad applicability in the labeling of biomolecules at high dilutions and provide a framework for engineering further variants of *O*-alkylhydroxylamine addition reactions. Dialdehyde conjugations present a novel method for rapid oxime formation under physiological conditions with unusually high reaction rates of $500 \text{ M}^{-1} \text{ s}^{-1}$ as determined by a kinetic fluorescence quenching assay. Mechanistic studies revealed that dialdehydes provide an internal trap to stabilize hemiaminals as IBHAs, leading to an enormous shift in the equilibrium position. The K_{eq} is so large that the initial addition step becomes effectively irreversible; this simplifies hydroxylamine-based bioconjugations because the timing of the typically slow dehydration reaction is rendered immaterial: Both IBHAs and oximes represent successful conjugations at low μM concentrations. In addition $^1\text{H-NMR}$ analysis revealed that the low energy IBHA intermediate is not in a measurable equilibrium with the starting materials. Instead it dehydrates at unprecedented low rates of 10^{-5} s^{-1} when compared to normal oxime condensations under similar conditions. All tested substrates bearing the *ortho*-dialdehyde motif resulted in a fast formation of the corresponding oxime conjugates, even with complex hydroxylamine peptides, oligonucleotides or fluorescence quenchers. Varying the aldehyde substitution pattern (*meta* or *para*) was found to be detrimental to the reaction and confirmed the primacy of the OPA scaffold. The reaction tolerates other nucleophilic amino acid functionalities and can be performed in the presence of human serum (20% v/v). Bishydroxylamines were found to be as effective as simple *O*-alkylhydroxylamines with the difference that the formed bisoxime lacks the reactive aldehyde moiety present in a simple oxime. To the best of our knowledge IBHAs have never been observed with *O*-alkylhydroxylamines or simple amines under aqueous conditions.²²¹ In retrospect our strategy may be considered an innovation for rapid oxime-based bioconjugations at neutral pH and provides a basis for further developments in this particular research field.

Future work should focus on the exploration of other substrate pairs which may exhibit improved accelerating abilities. In particular it would be interesting to test aliphatic dialdehydes which might react with a totally different second-order rate constant than we observed for OPA 2.1 (Scheme 3.14).



Scheme 3.14: Proposed synthetic sequences for the preparation of aliphatic dialdehydes separated by one^{231,232} or two carbon atoms²³³.

When reconsidering aromatic aldehydes it would be worth to test some species which were not included in our studies and could give additional information on the influence of further or different substituents. Although diketones were found to be unsuitable (see **Table 3.1**) the reactivity of aldehydes containing an *ortho*-keto group is unknown to us so far. In dependence on the work of the KOOL group²¹¹ additional functional groups (*e.g.*, -NO₂, -OMe, -OH, -CO₂H and -CO₂R) on the aromatic ring of OPA could give access to candidates with superior reaction rates (**Figure 3.11**, left). Likewise we would be keen to know if there is a way to connect two *O*-alkylhydroxylamines through an OPA-derived linker containing several formyl groups and if commercial triformylmethane is also a suitable candidate for oxime condensations (**Figure 3.11**, right).

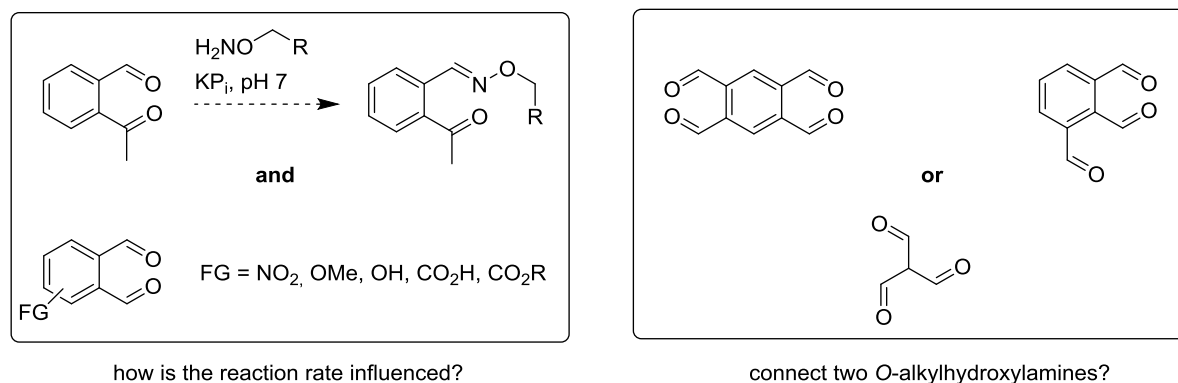
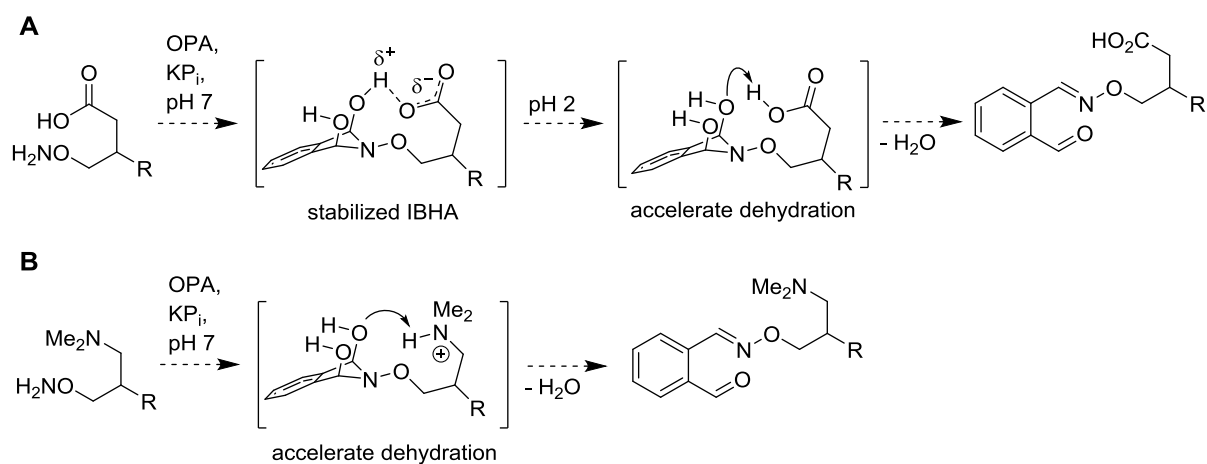


Figure 3.11: Left: 2-Acetylbenzaldehyde (top) and various substituted OPA derivatives (bottom) which could be employed to extend the scope of the reaction. Right: Possible candidates for multiple oxime condensations.

Probably one of the most interesting questions to answer would be to know if *O*-alkylhydroxylamines can be varied structurally to either accelerate the dehydration or stabilize the IBHA intermediate. Inspired by previous work on intramolecular proton assistance (*vide supra*) two possible structures are presented in **Scheme 3.15**. A carboxylic acid group, deprotonated under the reaction conditions, is imagined to participate in hydrogen bonding of the IBHA intermediate which after lowering the pH (*e.g.*, acidic LC analysis) becomes a proton donor facilitating the dehydration step (**Scheme 3.15**, panel A). In analogy a tertiary amine ($pK_a \sim 10$ for Me_3N^+H)²³⁴ in close proximity to the hydroxyl group of the IBHA intermediate could provide a proton thus lowering the barrier for the rate-limiting step (**Scheme 3.15**, panel B).



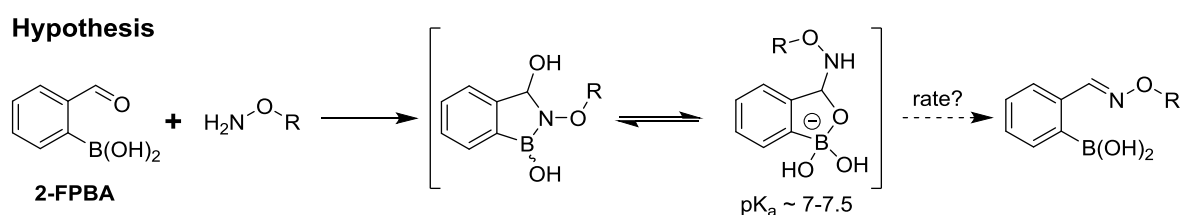
Scheme 3.15: Proposed *O*-alkylhydroxylamines equipped with functional groups for intramolecular proton assistance: (A) Carboxylic acids as tunable groups to stabilize or accelerate oxime formations depending on the pH chosen. (B) Tertiary amines as promoters for the usually slow dehydration step.

Although the method we reported within this section represents a very successful improvement of oxime-based bioconjugations, optimizing and fine tuning of substrate pairs and reaction conditions is a never-ending story on the way of finding the perfect method. The next chapter is directly related to this work and represents an advancement of the present method based on boronic acids facilitating rapid oxime condensations.

3.5 Results and discussion - Rapid oxime condensations using boronic acids

The results discussed within this section are the cumulative work of the author Pascal Schmidt, Cedric Stress, Dennis Gillingham and have been published in 2015.²³⁵ Figures, schemes and paragraphs described in this thesis are partially reproduced from reference #235 with permission from the Royal Society of Chemistry.

Our fundamental findings of rapid oxime formation using dialdehydes at neutral pH were accompanied by the drawback of *in vivo* incompatibility since the OPA motif is well known to react with amines and thiols in a three-component reaction to give fluorescent isoindoles.^{236,237} In addition the left over formyl group in the oxime product is susceptible to other nucleophiles and may deliver by-products over time. While this particular method is only applicable for *in vitro* applications we were keen to probe other proximal functional groups able to form a stable and rapid oxime linkage. From that point on, it was clear to us that the second aldehyde group has to be replaced with a more tolerable functionality suitable for later *in vitro* studies. Based on this requirement and the insights of our previous study we hypothesized that the Lewis acidity of boron²³⁸ coupled with its ability to modulate alcohol pK_as through coordination (Scheme 3.16),^{239,240} might facilitate rapid oxime formation. Moreover, boron is a chemically versatile element and its presence in oxime products would open the door to many applications in chemical biology. For example boron compounds have found uses in medicinal chemistry,^{241,242} cross-coupling reactions,^{243,244} carbohydrate detection,^{245,246} promoting endocytosis,²⁴⁷ and reactivity-based peroxide sensing.^{248,249} Boron's rich coordination chemistry is pivotal for many of its applications. For example the N → B dative interaction has been proposed to stabilize otherwise labile Schiff bases, and these iminoboronates have been used in supramolecular chemistry,^{250,251} enantiomer analysis by NMR,^{252,253} and protein labeling.^{254,255}



Scheme 3.16: The unique abilities of boron led to the hypothesis that proximal boron substituents would have an impact on oxime condensations.

We selected the 2-formylphenylboronic acid (2-FPBA, **2.34**) scaffold as a model system to explore boron's influence on oxime condensations. 2-FPBA has previously been shown to modify lysine residues or *N*-termini in proteins in a process controlled by rapid equilibria.²⁵⁵ Little is known, however, about the analogous condensation with α -effect nucleophiles. We have found two cases of

alkoxyiminoboronates (AIBs),^{253,256} two cases of *O*-alkylAIBs^{257,258} and two cases of the related hydrazinoiminoboronates,^{256,259} but in each of those studies the coupling itself was not of central importance and therefore not examined in detail.

3.5.1 ¹H-NMR studies – initial findings

We began our studies on boron-assisted oxime ligations with the reaction of 2-FPBA **2.34** and *O*-benzylhydroxylamine (**2.4**) monitoring its progress by ¹H-NMR under neutral (pH 7.2), aqueous conditions (10 mM KP_i in D₂O) as shown in **Figure 3.12**. Initial experiments at equimolar substrate concentrations of 100 μM at room temperature clearly indicated a fast reaction rate. Oxime **2.35** was the exclusive product present after the first measurement (~5 min) and its structure was additionally confirmed by a separate X-ray analysis (see top of **Figure 3.12**).

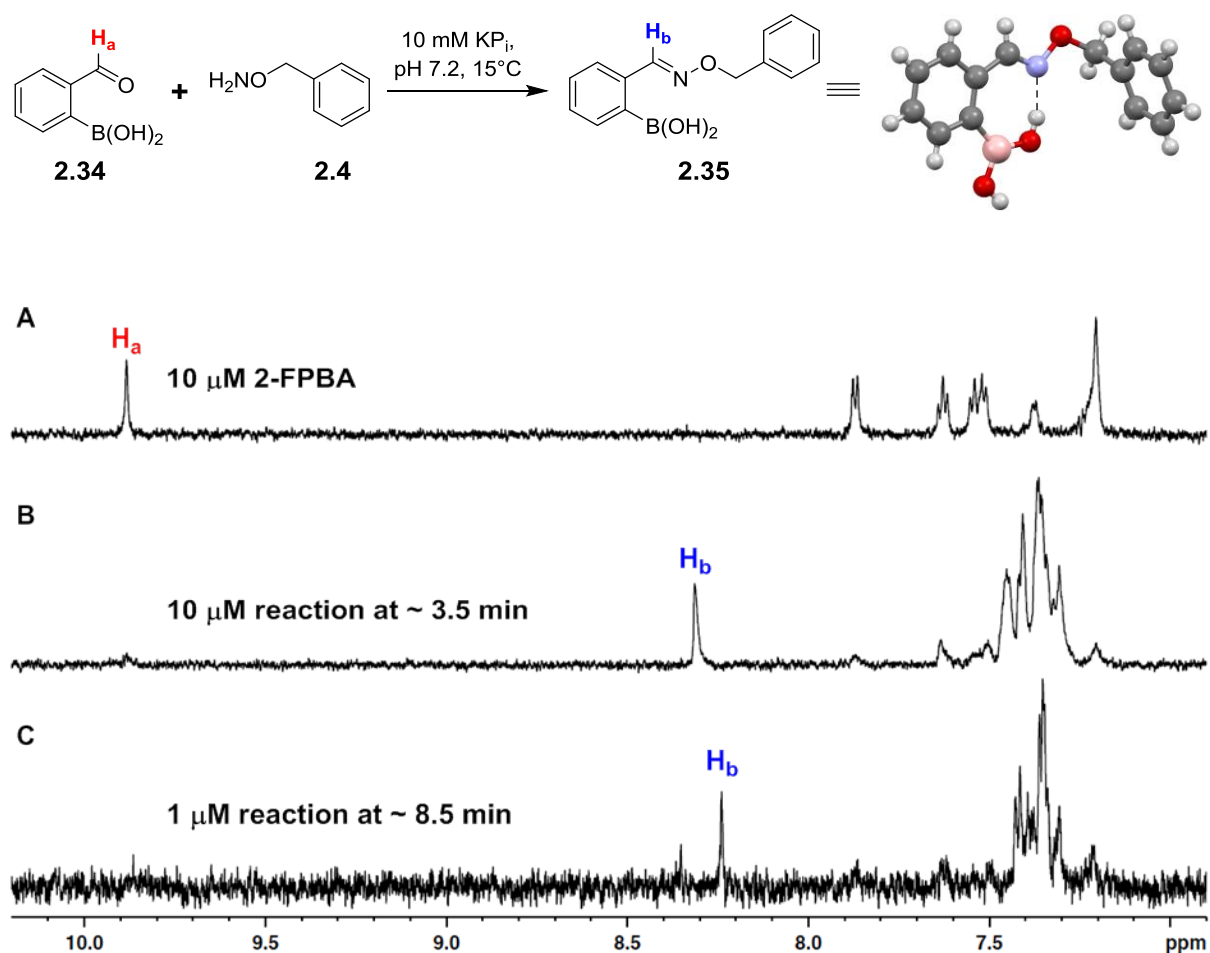


Figure 3.12: All spectra were recorded at 15°C. (A) 10 μM 2-FPBA **2.34** (9.88 ppm, H_a) reference spectrum in 4:1 (10 mM KP_i in D₂O/CD₃CN). (B) 10 μM reaction (8.31 ppm, H_b) spectrum in 4:1 (10 mM KP_i in D₂O/CD₃CN) after ~3.5 min. (C) 1 μM reaction (8.24 ppm, H_b) spectrum in 54:1 (10 mM KP_i in D₂O/CD₃CN) after ~8.5 min – the difference in the chemical shift is attributed to the solvent ratio.

To be able to observe a potential intermediate species the reaction was repeated at substrate concentrations as low as 10 μM and 1 μM , respectively. In addition the cryoprobe was cooled down to 15°C to retard the process of oxime formation, increasing the chance of detecting an intermediate. Both reactions were identical in their final outcome – after the earliest possible $^1\text{H-NMR}$ measurement (10 μM ~3.5 min; 1 μM ~8.5 min) the reactions were nearly complete (>90% conversion) showing exclusively the product signals. Limited by the nature of the solvent system and the S/N ratio neither the temperature nor the concentration could be further tuned to get a more detailed insight into the reaction kinetics and potential intermediate species. These findings confirmed the potential of boron to accelerate oxime formation in aqueous media at neutral pH with high reaction rates.

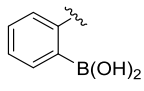
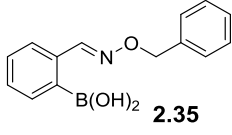
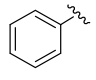
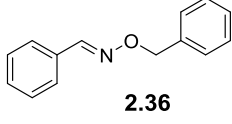
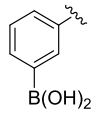
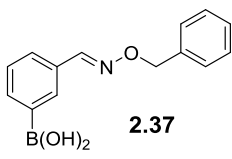
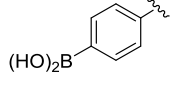
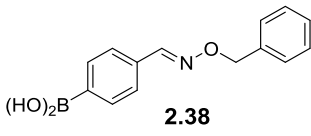
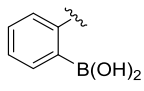
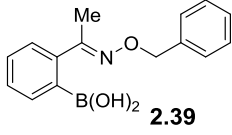
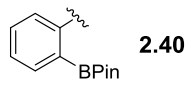
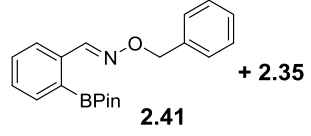
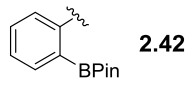
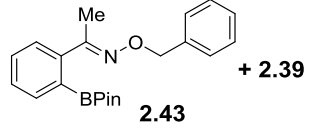
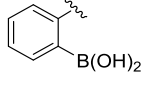
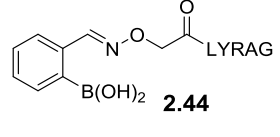
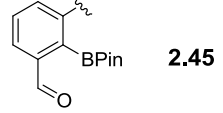
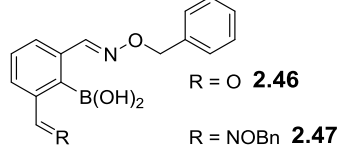
3.5.2 HPLC studies

The potential of this particular oxime formation as a powerful and fast method for effective bioconjugation was further explored by HPLC employing neutral elution conditions (acidic conditions led to some reversibility).

The reaction of 2-FPBA **2.34** with *O*-benzylhydroxylamine (**2.4**) at near-equimolar concentrations of 100 μM and 10 μM in 100 mM KPi , pH 7.2 was found to deliver the desired product after the first HPLC injection (~1 min) with >98% conversion (**Table 3.4**, entry 1). The control experiment using benzaldehyde as substrate was found to be inappropriate as previously mentioned in section 3.4.2 (**Table 3.1** and **Table 3.2**). The corresponding *meta*- and *para*-substituted structural isomers of FPBA behaved similar, delivering nearly undetectable levels of oxime even after 90 min (entries 3 and 4). These results emphasize the importance of boronic acid positioning which facilitates rapid oxime formation under the reported conditions. Next, the necessity for the aldehyde and boronic acid motif were explored by replacing the respective functional groups with closely related ones. In general, aldehydes are substantially more reactive than ketones which cause greater steric interaction as the hybridization changes from trigonal to tetrahedral.²⁶⁰ Therefore the aldehyde moiety was substituted for a simple ketone and the boronic acid function was replaced by its boronic acid pinacol ester (BPin) analogue. All three possible combinations were investigated separately and proved to be highly reactive substrates. Condensation with 2-acetylphenylboronic acid gave a marginal lower conversion (94%) after the first measurement compared to the 2-FPBA **2.34** (entry 5), but it is still faster than normal ketoxime formations.²⁶¹ The BPin-containing aldehyde **2.40** and ketone **2.42** derivatives were equally efficient and gave complete conversion after one minute but the hydrolyzed boronic acid **2.35** was the main product with only 10% BPin oxime **2.41** observed; after ninety minutes only **2.35** was present (entry 6). These findings are supported by ACHILLI describing fast BPin hydrolysis at physiological pH in buffered aqueous media.²⁶² The ketoxime pinacol product **2.43** (entry 7), on the other hand, was more stable and comprised ~97% of the product after the first injection (the remainder

being **2.39**); after thirty minutes **2.43** had also completely hydrolyzed to **2.39**. The increased hydrolytic stability of pinacol ester **2.43** could also be attributed to the extended steric hindrance of the ketoxime and BPin moiety which hinder nucleophilic attack of water. The ability to use boronic acid pinacol esters is additionally valuable since these are readily obtained from Pd-catalyzed routes to boronic esters, and their deprotections in organic solvents are often tricky and require additional reagents.²⁶³⁻²⁶⁶ More complex hydroxylamines, such as the pentapeptide shown in entry 8, were also excellent substrates, delivering complete conversion after the first injection. We also tested 2,5-diformylphenylboronic acid pinacol ester (**2.45**) containing two reactive sites for hydroxylamine condensations (entry 9). Contrary to our assumption that this type of bifunctional molecule may improve the rate of oxime formation initial conversions were significantly lower and didn't exceed 93% even after almost a day. A series of additional experiments indicated the bisoxime **2.47** to be the kinetic product forming after the first injection as the major product and equilibrating over time to the thermodynamically favored monooxime **2.46**. When two equivalents of *O*-benzylhydroxylamine (**2.4**) were added a mixture of mono- and bisoxime was observed which after adding another two equivalents of **2.4** completely converted to the C₂-symmetric product **2.47**. These results clearly show that unfortunately the strategy to rapidly connect two different *O*-alkylhydroxylamines through this linker-type boronic ester **2.45** is unsuitable and needs further investigations.

Table 3.4: Probing the importance of boron positioning and substitution on oxime condensations.

Entry	Ar	X	Product	conv. [%] ^[b]
$\text{Ar}-\overset{\text{X}}{\text{C}}=\text{O} \xrightarrow[100 \text{ mM KP}_{11}, \text{ pH } 7.2, \sim 1 \text{ min}^{[a]}]{\text{H}_2\text{NO}-\text{CH}_2-\text{R} \text{ 1.1 eq.}} \text{Ar}-\overset{\text{X}}{\text{C}}=\text{N}-\text{O}-\text{CH}_2-\text{R}$ <p style="text-align: right;">R = Ph, LYRAG pentapeptide X = H, Me</p>				
1 ^[c]		H	 2.35	> 98
2		H	 2.36	< 5 ^[d]
3		H	 2.37	< 5 ^[d]
4		H	 2.38	< 5 ^[d]
5		Me	 2.39	94
6	 2.40	H	 2.41 + 2.35	> 98 ^[e]
7	 2.42	Me	 2.43 + 2.39	> 98
8		H	 2.44	> 98
9	 2.45	H	 2.46 (R = O) 2.47 (R = NOBn)	61 ^[f]

[a] Time is approximate since samples are injected directly after mixing. [b] Conversions are based on the peak disappearance of 2-FPBA **2.34** after ~1 min at 254 nm. [c] Reaction was also performed at 10 μM giving the same conversion number after the first injection. [d] Injections after 90 minutes still show < 5% conversion. [e] At the first injection approximately 10% of the boronic acid pinacol ester oxime **2.40** is observed, but only the hydrolyzed product **2.35** is detected after 1.5 h. [f] Concentrations were 100 μM for both substrates; 73% conversion after 90 minutes and 93% after 21 h with bisoxime **2.46** being the kinetic (t ~1 min) and monooxime **2.47** the thermodynamic product (t = 21 h).

The results obtained from NMR and HPLC studies makes it clear that boronic acids facilitate rapid oxime condensations at neutral pH, in most respect the reaction turned out to be superior to the dialdehyde method. The reaction is very fast and displays second order kinetics. With a generously assumed half-life of around 30 seconds (HPLC) or 120 seconds (¹H-NMR) these observations imply a rate upwards of 10³ M⁻¹ s⁻¹ and represent only a lower bound for the rate constant (**Equation 2**).

$$t_{\frac{1}{2}} = \frac{1}{k [A_0]} \quad (2)$$

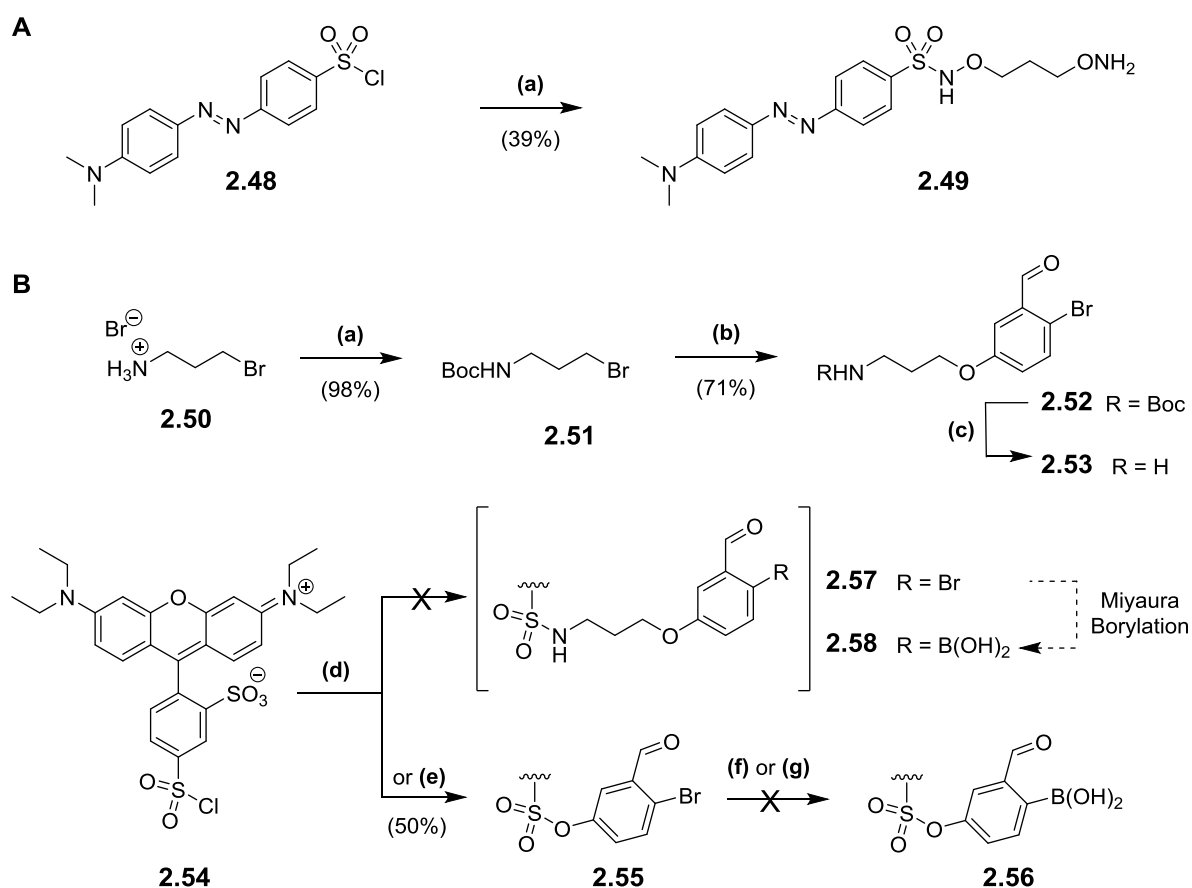
Equation 2: $t_{1/2}$ = half life [s], k = rate constant [M⁻¹ s⁻¹], $[A_0]$ = initial concentration of the starting material [M].

3.5.3 Fluorescence quench assay: determining k_1

Since reactions with half-lives smaller than several seconds to minutes are hard to follow and monitor with standard methods (*e.g.*, NMR, HPLC, GC or UV-spectroscopy), special techniques have to be considered which are more sensitive and allow for an extended time resolution. In addition a good S/N ratio will also allow substrate ratios near unity at low concentrations (*e.g.*, μM -nM regime) which are among the key criteria in the field of bioconjugation.⁷ A more quantitative assessment of the rate constant was obtained using fluorescence quenching which is a very sensitive technique to study chemical and biological interactions (*vide supra*).²⁶⁷

3.5.3.1 Synthesis

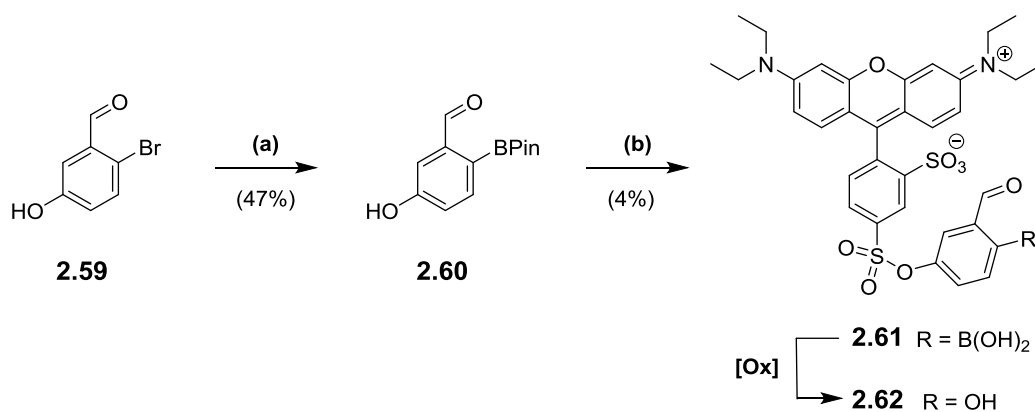
The initial design of the target molecules used in the assay comprised a dabsyl quencher bearing a terminal hydroxylamine **2.49** (Scheme 3.17, panel A) and a 2-FPBA connected to a lissamine fluorophore **2.58** (Scheme 3.17, panel B) as a proof of principle.



Scheme 3.17: (A) Preparation of dabsyl quencher **2.49**: (a) *O,O'*-1,3-propanediylbishydroxylamine dihydrochloride, NEt₃. (B) Synthetic attempt for the preparation of lissamine fluorophore **2.58**: (a) Boc₂O, NEt₃; (b) 2-bromo-5-hydroxybenzaldehyde, K₂CO₃; (c) CH₂Cl₂/TFA (1:1); (d) **2.53**, NEt₃, DMAP; (e) 2-bromo-5-hydroxybenzaldehyde, NEt₃, DMAP; (f) *bis*-(pinacolato)diboron, NaOAc, Pd(dppf)Cl₂; (g) pinacolborane, NEt₃, Pd(P^{*t*}Bu)₃)₂.

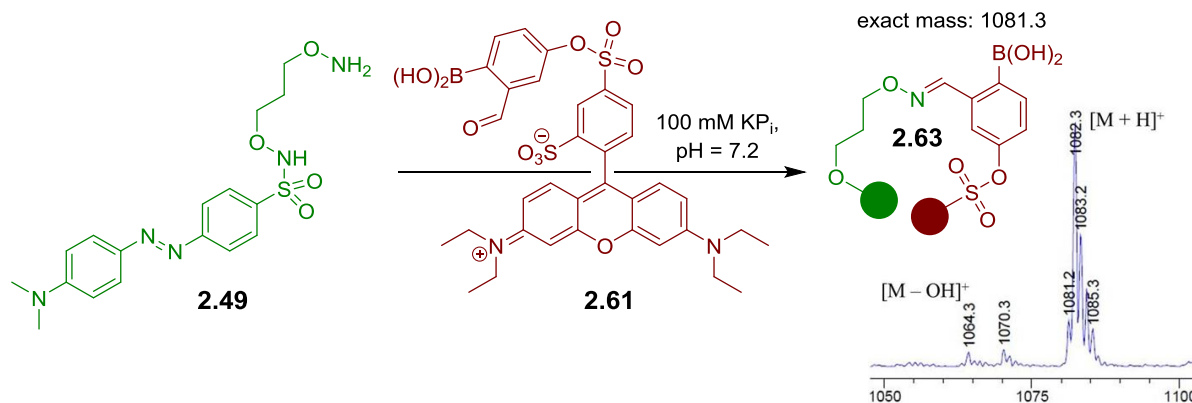
The synthetic effort to isolate the desired components however turned out to be more challenging and time consuming as previously expected. While the dabysl hydroxylamine **2.49** was isolated in a one-step S_N2 process²⁶⁸ from commercial dabysl chloride **2.48** and *O,O'*-1,3-propanediylbishydroxylamine dihydrochloride in moderate yield the fluorophore synthesis failed at its second last step. The primary amine **2.53** was synthesized in a three step synthesis from commercial 3-bromopropylamine hydrobromide (**2.50**). *N*-Boc protection was straightforward yielding almost quantitative amounts of **2.51**. Subsequent aromatic *O*-alkylation with 2-bromo-5-hydroxybenzaldehyde didn't give full conversion after 21 h but yielded the aromatic *N*-Boc derivative **2.52** in 71% yield after two chromatographic purification cycles. Unfortunately the starting 2-bromo-5-hydroxybenzaldehyde co-eluted with the desired product and decreased its purity by 10%. Although *N*-Boc deprotection of **2.52** proceeded quickly with full conversion the isolated crude amine **2.53** showed a higher mass balance than expected. It is very likely that the TFA salt of **2.53** was isolated although the ¹³C-NMR spectrum lacked both TFA anion signals. Nonetheless the obtained product was further reacted with lissamineTM rhodamine B sulfonylchloride (**2.54**) employing DMAP-accelerated nucleophilic catalysis²⁶⁹ under basic conditions. Reaction controls by UPLC-MS indicated primarily hydrolyzed lissamine derivative along with unreacted starting amine **2.53** and the undesired side product **2.55** which is probably the thermodynamically favored species comparing the S-N (464 kJ/mol) and S-O (522 kJ/mol) bond energies.²⁷⁰ The addition of more equivalents of **2.53**, NEt₃ as well as increasing the reaction time (overnight) didn't help formation of the envisioned product **2.57**. Although the undesired sulfonate ester **2.55** could be prepared selectively in 50% yield it was attractive enough to serve as a test substrate for the final palladium-catalyzed MIYAJIMA borylation using *bis*-(pinacolato)diboron.²⁷¹ Unfortunately the reaction failed twice, even when elevated temperatures, extended reaction times (19 h) and up to 50 mol% of Pd(dppf)Cl₂ were used no conversion of the starting bromide **2.55** was observed. In a third attempt the borylation protocol developed by CHRISTOPHERSEN *et al.* using pinacolborane and Pd(P(^tBu)₃)₂ was applied.²⁷² Reaction controls after several time intervals by UPLC-MS indicated a mixture of unreacted starting material, reduced aldehyde of **2.55** and the proto-dehalogenated side product as the major species without any evidence for the desired boronic acid **2.56**. These results showed that although oxidative addition is achieved the transmetalation of the boron derivative is unfavored and the increase in reaction time leads to the observed protidepalladation which is most affected for aldehyde substrates.²⁷³

Since the final cross-coupling reaction turned out to be rather difficult with the deactivated sulfonate ester substrate **2.55** a more convenient approach was envisioned (**Scheme 3.18**).



Scheme 3.18: Synthetic sequence for the preparation of the fluorophore analogue **2.61**: (a) *bis*-(pinacolato)diboron, KOAc, Pd(dppf)Cl₂; (b) **2.54**, NEt₃.

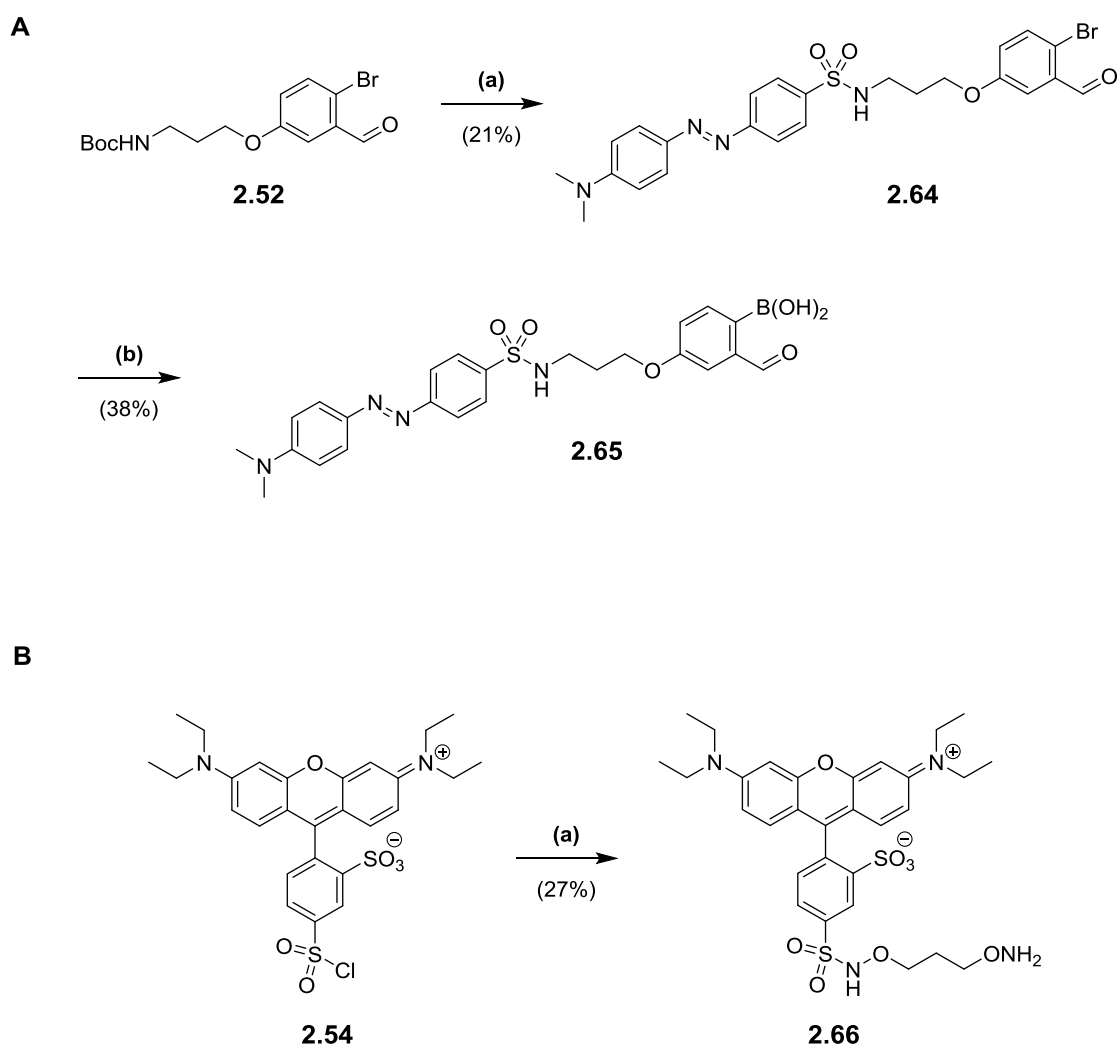
Lissamine boronic acid **2.61** was synthesized in very low yield starting from commercial 2-bromo-5-hydroxybenzaldehyde (**2.59**) by a MIYAURO borylation and subsequent aromatic *O*-alkylation. The electron deficient boronic acid product was found to be prone to autoxidation resulting in the phenol **2.62** after a few days. The concept of oxime formation between the quencher **2.49** and the fluorophore analogue **2.61** was tested in a UPLC-MS assay under neutral reaction conditions (**Scheme 3.19**).



Scheme 3.19: UPLC-MS assay of the oxime condensation using 2-FPBA tagged fluorophore **2.61** and the hydroxylamine quencher **2.49**. Reaction conditions: 100 μ M final concentration in both substrates in 100 mM KP_i at pH = 7.2. The reaction was monitored at 254 nm by UPLC-MS tracing the disappearance of starting materials and formation of the oxime conjugate **2.63**. The inset shows the extracted ESI-MS spectra for the successful formation of **2.63** after 10 min.

Mixing the two starting materials at equimolar concentrations of 100 μ M in 100 mM KP_i and neutral pH afforded the desired oxime **2.63** in 10 minutes along with its oxidized oxime analogue (see **Figure E11** in section 4.2.3.4). This result corroborated the suitability of this particular reaction in a kinetic fluorescence quench assay but indicated also the need for a more stable, synthetically accessible fluorophore at the same time. Therefore the 2-FPBA motif was envisioned to be installed into the dabsyl quencher containing a C₃ linking unit *via* electron rich sulfonamide formation preventing the

boronic acid moiety from autoxidation. The hydroxylamine was considered to be easily introduced into the lissamine fluorophore counterpart in a single chemical transformation from commercial starting materials (**Scheme 3.20**).



Scheme 3.20: (A) Synthetic sequences for the preparation of the 2-FPBA connected dabsyl quencher **2.65**: (a) (a) (i) $\text{CH}_2\text{Cl}_2/\text{TFA}$ (4:1); (ii) **2.48**, NEt_3 ; (b) *bis*-(pinacolato)diboron, NaOAc , $\text{Pd}(\text{PPh}_3)_2\text{Cl}_2$. (B) Preparation of hydroxylamine-containing lissamine fluorophore **2.66**: (a) *O,O'*-1,3-propanediylbishydroxylamine dihydrochloride, NEt_3 .

The target 2-FPBA equipped quencher **2.65** was synthesized in two steps. Initial *N*-Boc deprotection of carbamate **2.52** and subsequent sulfonamide formation afforded dabsyl precursor **2.64** in low yield. Palladium-catalyzed MIYAUORA borylation followed by acidic preparative HPLC purification resulted finally in the free boronic acid-containing quencher **2.65** in moderate yield. We were delighted to discover that the product was air stable and didn't decompose according to HPLC injections of aliquots over several days. Hydroxylamine-containing fluorophore **2.66** was obtained in a single chemical step by reacting lissamine™ rhodamine B sulfonylchloride (**2.54**) with *O,O'*-1,3-propanediylbishydroxylamine dihydrochloride under basic conditions in 27% isolated yield.

3.5.3.2 Kinetic assay

Recent work by us²¹³ and others²²⁵ have shown that fluorescence quenching can be used as an indirect but quantitative technique for the determination of rate constants. The two promising substrates for oxime condensation **2.65** and **2.66** shown in **Figure 3.13**, panel A were tested using a fluorescence plate reader device. The decrease of the fluorescence signal was monitored at the maximum absorption of lissamine derivative **2.66** (566 nm) in 100 mM KP_i at pH 7.2 after adding equimolar amounts of 2-FPBA tagged dabsyl quencher **2.65**. Initial experiments at 5 μM , 2 μM and 500 nM clearly indicated second order behavior of the reaction within the first 105 seconds as determined by inverse concentration plots (**Figure 3.13**, panel B).

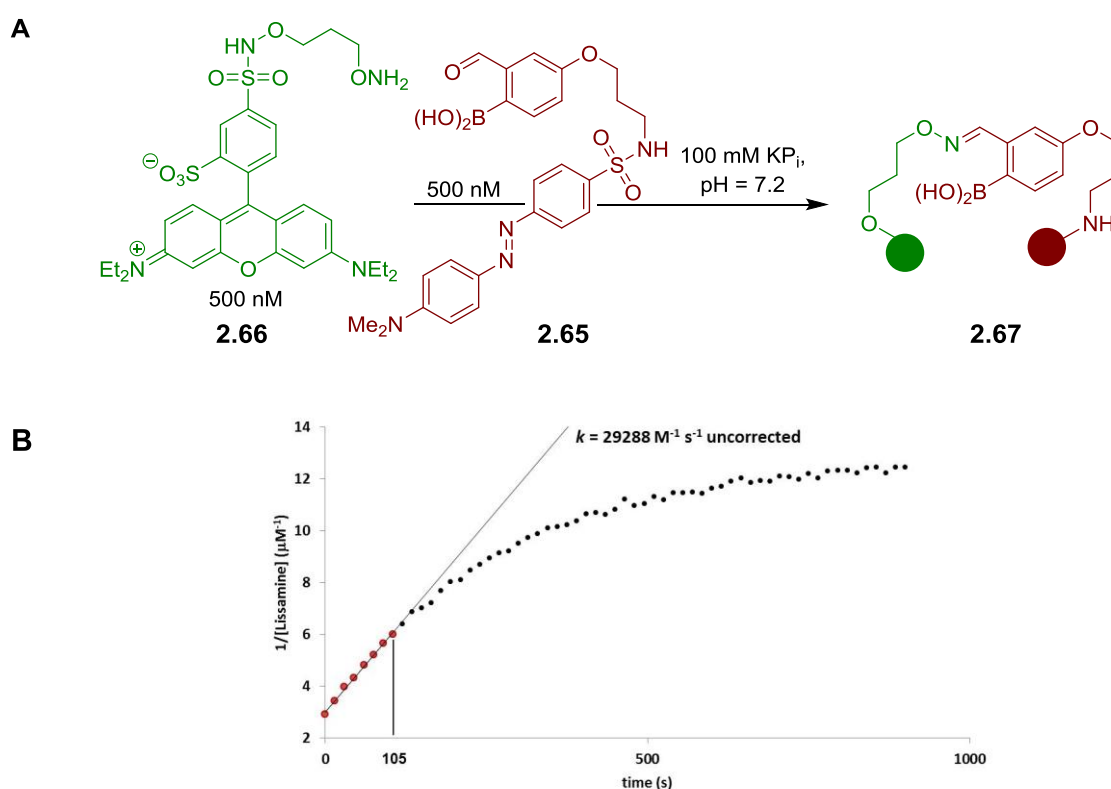


Figure 3.13: (A) General reaction scheme of the oxime condensation between lissamine fluorophore **2.66** and dabsyl quencher **2.65**. (B) Fluorescence quench assay at 500 nM in 100 mM KP_i at pH 7.2 and 26°C. • Data points recorded over 15 min; • Data points within the linear region of the first 105 seconds fitted by an extrapolated trend line. Second order rate constant k was directly determined from the trend line slope and was uncorrected for the time and photobleaching.

An extrapolated trend line of the initial linear region indicated a second order rate constant of $3 \times 10^4 \text{ M}^{-1} \text{ s}^{-1}$ which was considered vague according to the marginal collection of data points. This result suggested that monitoring at 100 nm would be required to obtain sufficient data at early reaction conversion. Additionally the crude set of data was uncorrected for the time between mixing the samples, recording of the first measurement (~ 30 sec) as well as for photobleaching (**Figure 3.14**,

panel A). The latter, being a dynamic and irreversible decomposition of the fluorescent molecule in its excited state, is due to interactions with molecular oxygen or surrounding molecules prior to emission. This often results in chemical damage or covalent modification and reduces the effective concentration of the fluorophore over time.²⁷⁴ To account for this photochemical alteration we performed a control reaction to determine fluorescence correction values caused by dabsyl-induced and lissamine photobleaching and to assure the validity of the respective fluorescence quench assay (**Figure 3.14**, panel B).

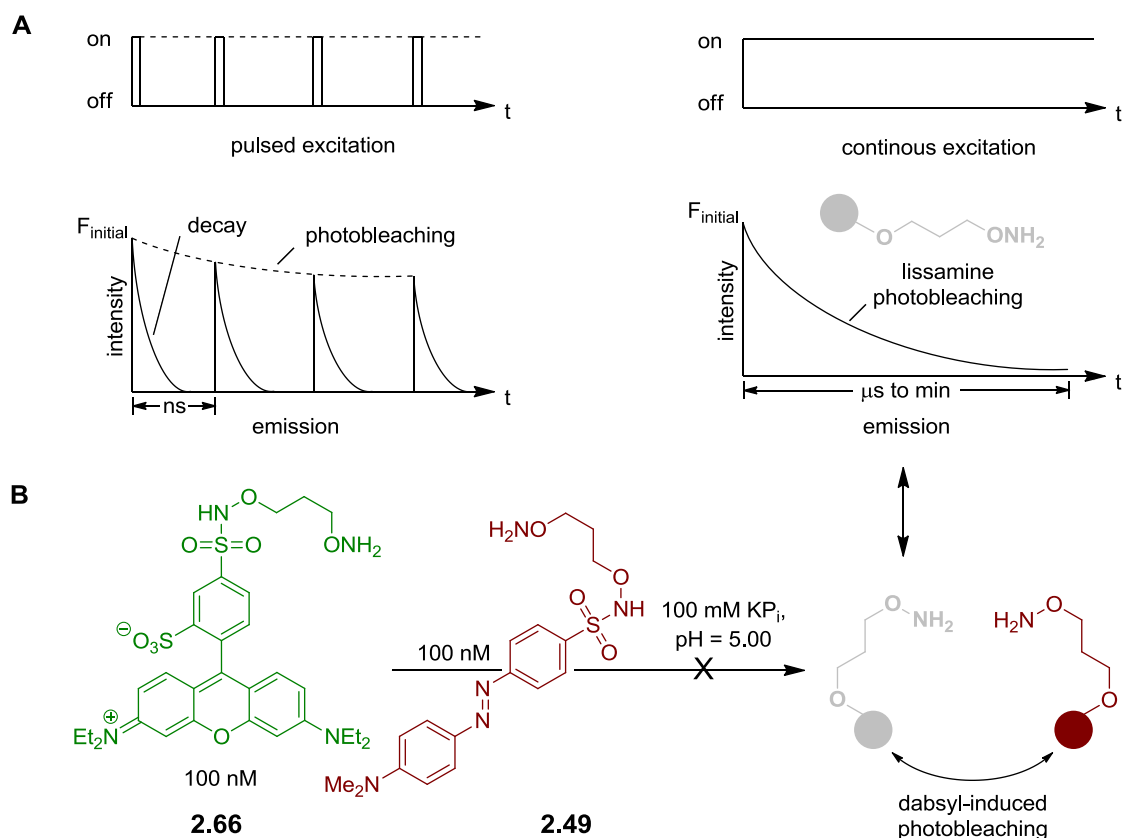


Figure 3.14: (A) Schematic diagrams depicting the differences between the decay (left) and photobleaching process (right). After each pulsed excitation the intensity of the fluorescence emission rapidly decreases through a decay process which can be resolved on the time scale of nanoseconds. At continuous excitation of *e.g.* hydroxylamine substituted lissamine **2.66** a constant photobleaching effect can be observed on the time scale of microseconds to minutes. The photobleached lissamine fluorophore is highlighted in grey. (B) Reaction scheme of a control experiment using hydroxylamine substituted lissamine **2.66** and hydroxylamine substituted dabsyl derivative **2.49** at 100 nM in 100 mM KP_i at pH 5.00 and 26°C to determine the effect of dabsyl-induced photobleaching.

Having established correction values for the photobleaching process we next set up a series of rate measurements by fluorescence quenching of the oxime conjugate **2.67** varying the pH (**Figure 3.15**). Triplicate rate measurements at 100 nM showed excellent linearity in inverse concentration plots (see **Figure 3.15**, **Figure E12** and **Figure E13**) with a rate constant of $\sim 11,000 \text{ M}^{-1} \text{ s}^{-1}$ – several orders of magnitude faster than the fastest neutral pH oxime condensations.²⁰⁸

Although fluorescence quenching is an indirect measurement technique, HPLC injections of aliquots from the assay mixture showed only product and starting materials (indicating a clean reaction) and gave conversions qualitatively in agreement with the fluorescence measurements. In addition, the fact that 10 and 1 μM reactions monitored by $^1\text{H-NMR}$ showed $>90\%$ conversion at the earliest possible measurements (**Figure 3.12**) provides independent verification of a rate constant $>10^4 \text{ M}^{-1} \text{ s}^{-1}$ since the first half-life would have to be less than 90 seconds. The general pH dependence, with a maximum in the range of 4.5–5, is consistent with normal oxime formation²⁰¹ except there is a distortion in the sigmoidal shape at higher pH (*e.g.* 7.2 & 8.1). The asymmetry in the pH dependence curve is inverted in comparison to a typical oxime condensation (acetone with hydroxylamine),²⁰¹ which shows a more pronounced drop-off in rate at higher pH than at lower pH. Based on the build-up of a tetrahedral intermediate at higher pH, JENCKS attributed this pH dependence to the need for a proton in the dehydration step.²⁰¹ Although we have thus far not been able to detect intermediates, we speculate that the near neutral pK_a of amine-substituted aqueous boronates^{240,275} provides the ideal environment for acceleration of the normally rate-limiting dehydration.

Fluorescence quench assay

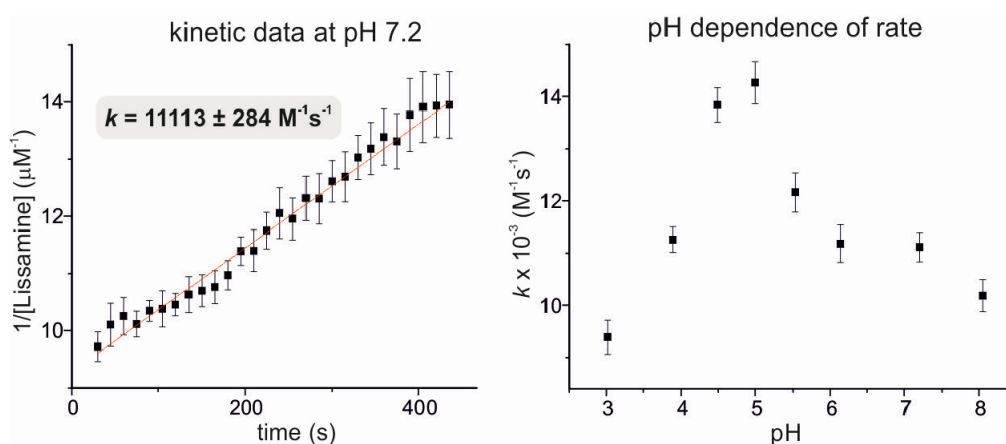
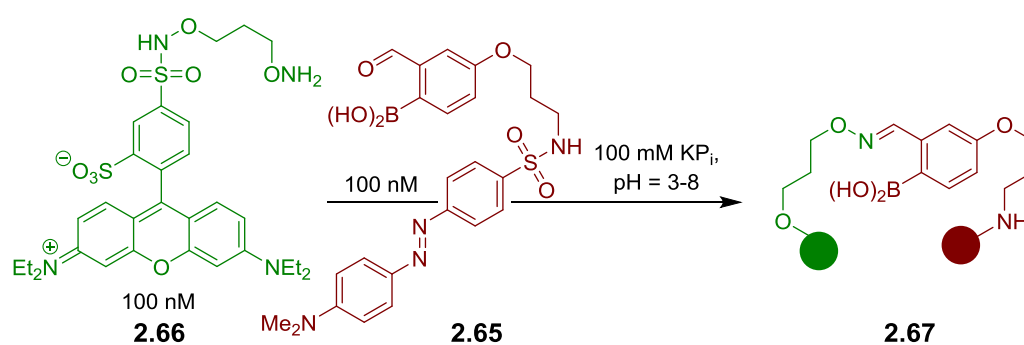
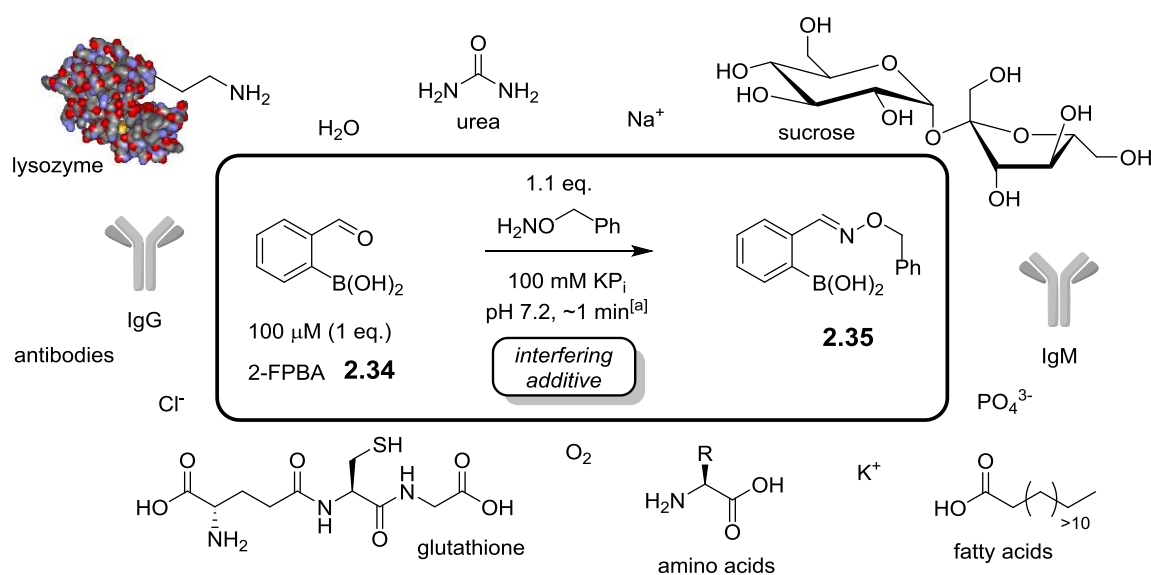


Figure 3.15: Fluorescence quenching assay at 100 nm and 26°C to determine rate constants and pH dependence. All measurements were done in triplicate and are corrected by subtracting a control measurement where everything was identical except that the dabcyI moiety lacked a 2-FPBA function.

3.5.4 Probing the effect of biological interfering additives

In a subsequent set of experiments we explored the efficacy of the boron-assisted oxime ligation in the presence of common interfering additives (sugars, biothiols, proteins and human serum). As mentioned before it is important for a bioconjugation to proceed in complex environment when considered for practical applications or *in vivo* studies. The additives led to no detectable reduction in reaction efficiency with the exception of human serum (see **Table 3.5**).

Table 3.5 Tolerance of the boron-assisted oxime condensation to biological interfering agents.



Entry	Additive (conc.)	Normalized 2.35 integral ^[b] (%)	Significance
1	-	100	-
2	Glutathione (5 mM)	98	Biothiols do not interfere
3	Sucrose (100 μM & 5 mM)	106/92 ^[c]	Boron chelators do not interfere
4	Lysozyme (100 μM)	105	Amino acid side-chains cannot compete with <i>O</i> -alkylhydroxylamine for 2-FPBA
5	Human serum (20% v/v)	80 ^[d]	Reaction is compatible with complex media

[a] Time is approximate since samples are injected directly after mixing. [b] Determined by reverse phase HPLC analysis under neutral conditions. [c] This reaction was also performed by pre-mixing the boronic acid with the sucrose, with no measurable change in conjugation efficiency. [d] Human serum leads to oxidation of the boronic acid to a phenol probably through a Baeyer–Villiger type reaction.²⁶⁴ The 80% number represents only the measurement of **2.35**, when the phenol is included nearly complete mass balance was observed. KP_i = potassium phosphate buffer.

Interestingly in human serum the boronic acid in **2.35** partially oxidized to a phenol, leading to an apparent loss of material: after the first injection 80% of **2.35** were present while after 18 h only 20% remained (see **Figure E8** in section 4.2.3.3). Even in the oxidized product, however, the oxime was still intact and if both components are added together the mass balance was nearly complete. Furthermore, lysozyme, which has previously been shown to react with 2-FPBA **2.34**,²⁵⁵ showed no modification according to LC-MS, indicating that the *O*-alkylhydroxylamine entirely outcompetes nucleophilic amino acid functionalities for 2-FPBA **2.34** (see **Figure E10** in section 4.2.3.3).

3.5.5 Stability and reversibility tests

As mentioned before a bioconjugation reaction ideally forms stable conjugates which do not decompose or hydrolyze under the conditions they are generated. To make a statement on the stability of the respective oxime bond under neutral conditions we performed continuous recordings of ¹H-NMR spectra of oxime **2.35** integrating and comparing its characteristic proton signals over time (**Figure 3.16**). A water soluble internal standard (IS = TMSP-d₄) was used as reference and served for accurate integral comparisons. The NMR data collected over the course of three days led to little change in concentration (< 5%) as indicated by the respective oxime (blue), benzyl (red) and IS (pink) protons and corroborates the fact that this oxime conjugate is stable under the present conditions.

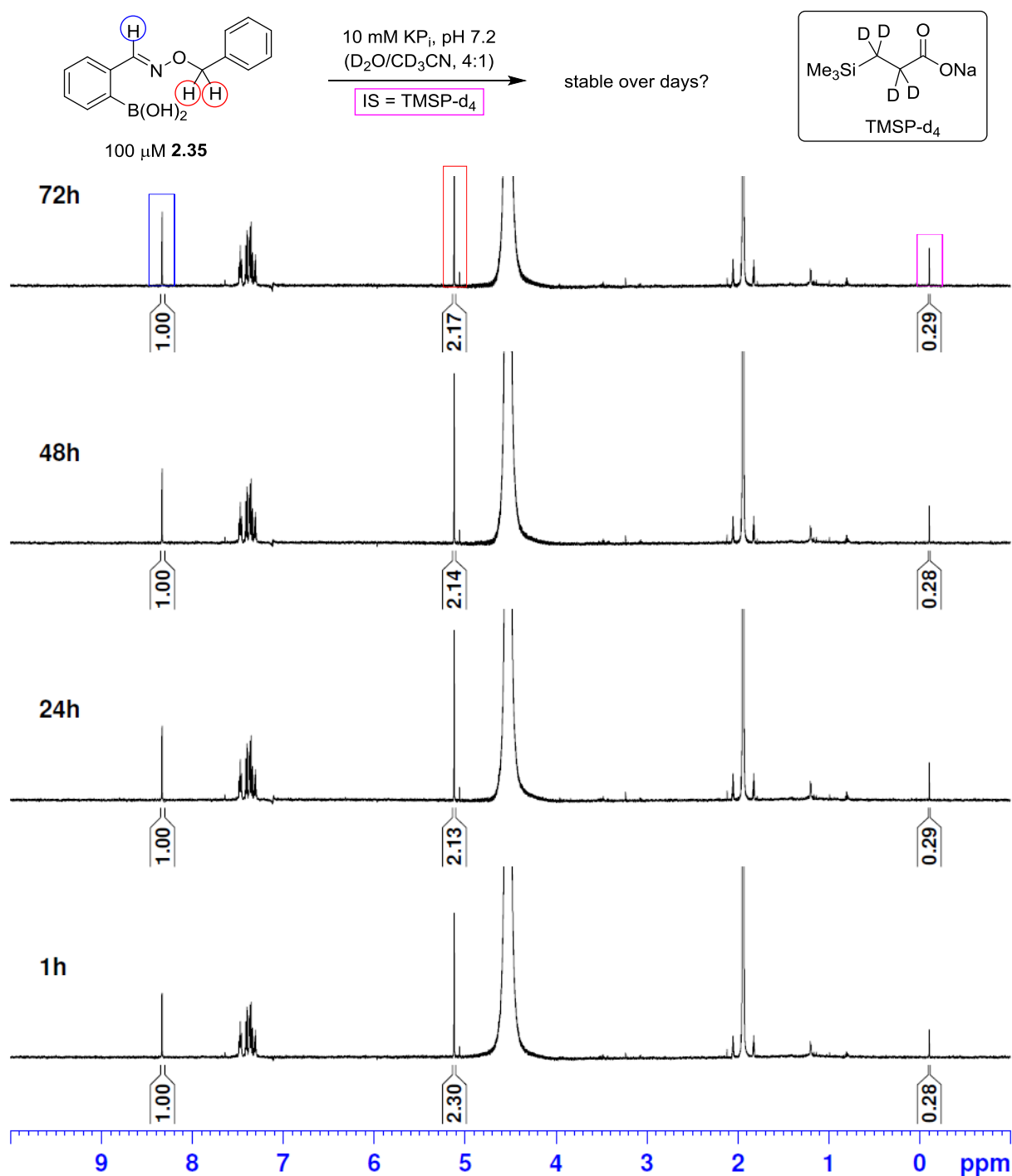


Figure 3.16: ¹H-NMR stability test of a 100 μM oxime **2.35** solution over the course of 72 h at pH 7.2. The change in concentration over the course of time was determined to be < 5% which lies within the accuracy of integration at 100 μM.

Next we were keen to get insights into the equilibrium process between oxime **2.35** and its starting materials. Therefore we added a five-fold excess of *O*-methylhydroxylamine to an NMR sample of oxime **2.35** and recorded continuous ¹H-NMR spectra (**Figure 3.17**, panel A). As shown in panel B of **Figure 3.17**, *O*-methylhydroxylamine leads to a new oxime product **2.68**, with equilibrium being established after 10–15 hours at 100 μM in pH 7.2 phosphate buffer. Although the equilibrium

constant is too large to allow a static equilibrium measurement, k_{-1} can be calculated directly from the exchange rate between oximes **2.35** and **2.68** ($4.2 \pm 0.4 \times 10^{-5} \text{ s}^{-1}$). From this value and the k_1 value obtained from fluorescence quenching (**Figure 3.15**) an equilibrium constant of $2.6 \pm 0.3 \times 10^8 \text{ M}^{-1}$ can be estimated. The reversibility assay shown in panel A of **Figure 3.17** would not be able to distinguish between hydrolysis and direct *O*-methylhydroxylamine attack; therefore we also ran the experiment by adding a different boronic acid to **2.35** instead of *O*-methylhydroxylamine (**Figure 3.18**, panel A). A stack of selected $^1\text{H-NMR}$ spectra is presented in panel B of **Figure 3.18** and shows the process of oxime interconversion from **2.35** to **2.69** over 24 h. Within experimental error, the data clearly indicates the exchange of reaction partner which is only possible through initial oxime hydrolysis of **2.35**. The liberated *O*-benzylhydroxylamine (**2.4**) is then able to undergo another oxime condensation with **2.60** to give oxime **2.69** as the major species after 24 h. This reaction pathway shows that the oxime equilibration takes place by oxime hydrolysis and subsequent condensation rather than a direct addition of the *O*-alkylhydroxylamine to the oxime.

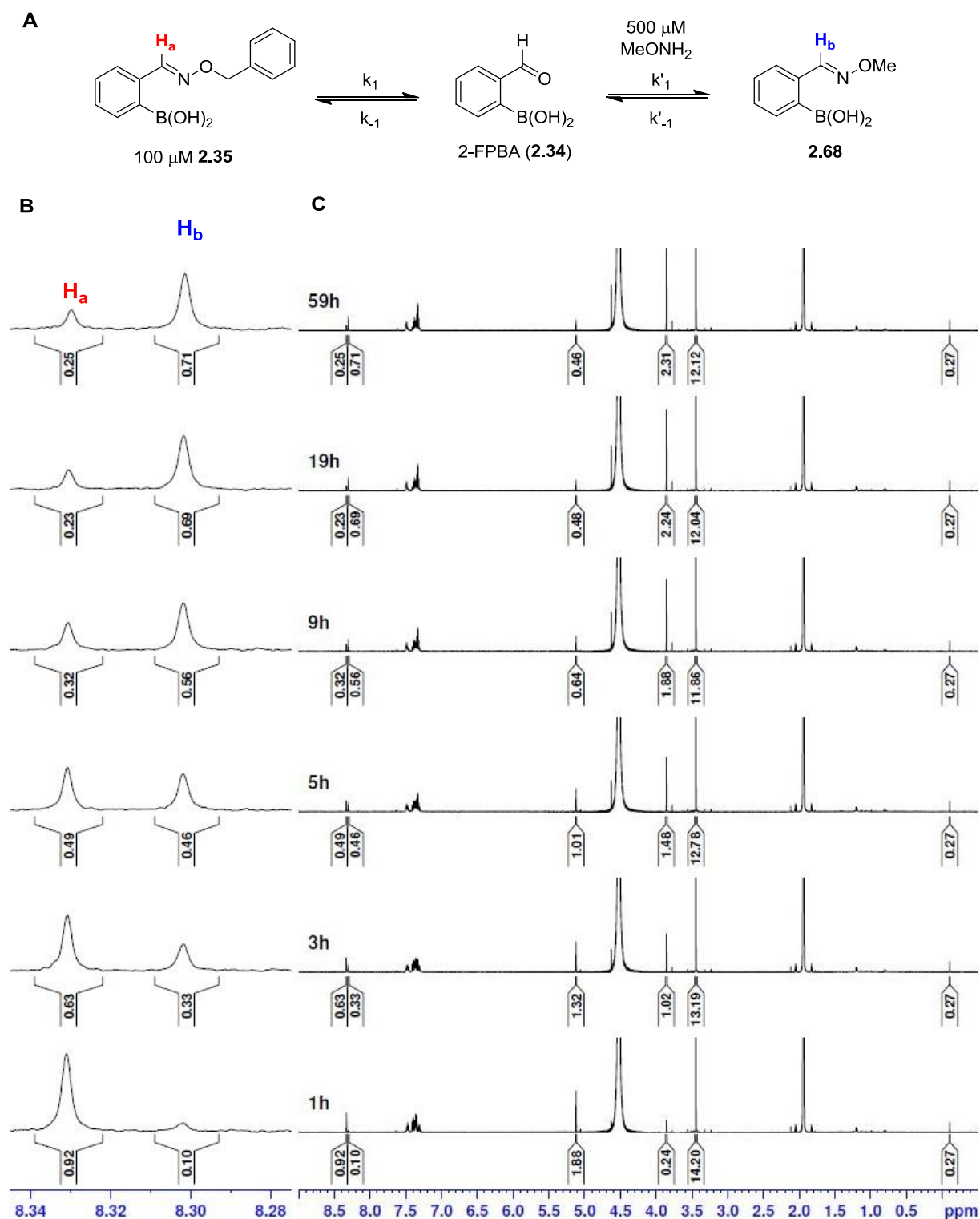


Figure 3.17: (A) Qualitative reversibility scheme of oxime **2.35** which is treated with a five-fold excess of *O*-methylhydroxylamine. The respective oxime protons **H_a** and **H_b** are highlighted for clearer differentiation. Conditions: 10 mM KP_i, pH 7.2 (D₂O/CD₃CN, 4:1), IS = TMSP-d₄. (B) Quantitative reversibility test of oxime **2.35** and *O*-methylhydroxylamine. Only six selected ¹H-NMR time points are shown from a total of 30 measurements: zoomed region (8.28 - 8.34 ppm) of the oxime protons **H_a** and **H_b**. (C) full ¹H-NMR spectrum of the reaction mixture at different time points containing integration values (up- to downfield) for the internal standard, methyl group of methoxyamine, methyl group of the newly formed oxime **2.68**, benzyl protons of **2.35** and the two different oxime protons **H_a** and **H_b**.

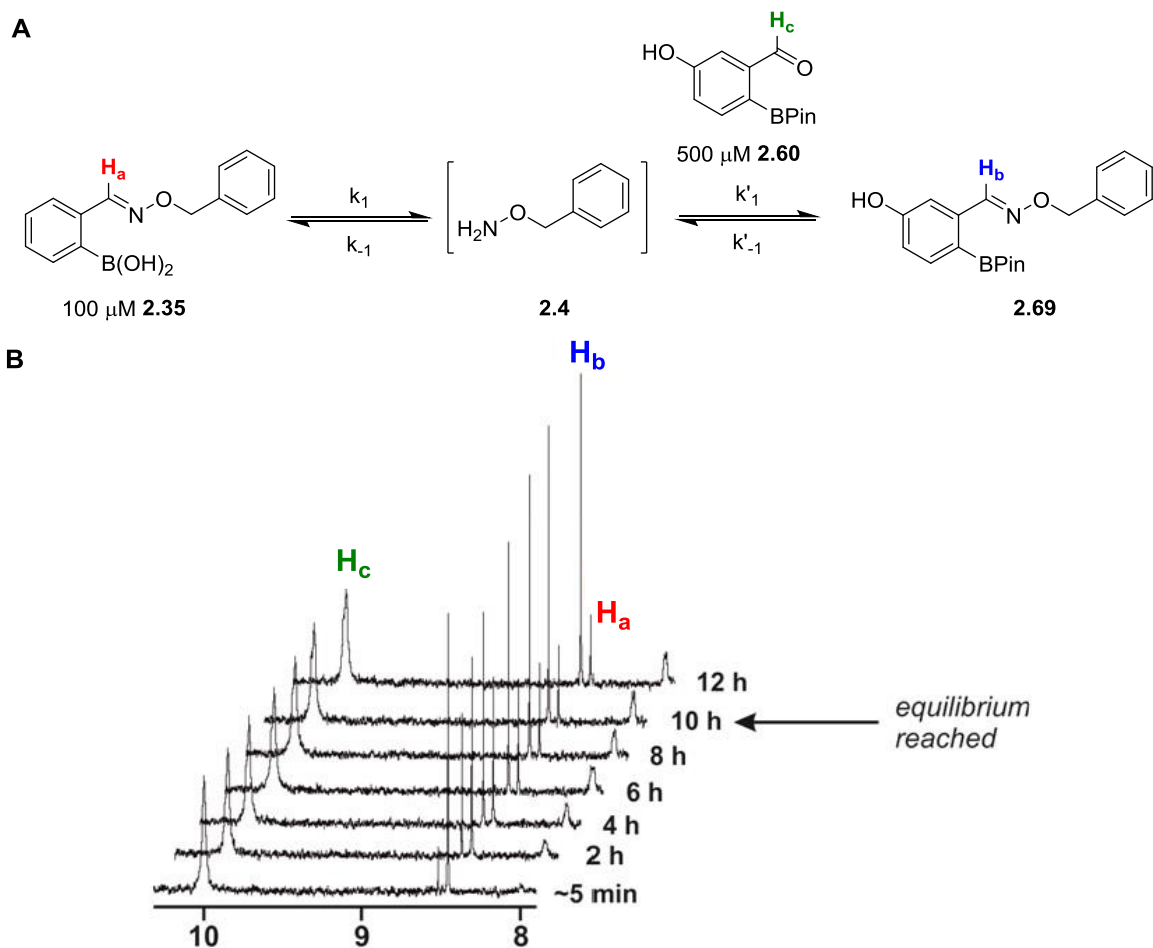


Figure 3.18: (A) Qualitative reversibility scheme of oxime **2.35** which was treated with a five-fold excess of aldehyde **2.60**. The respective oxime protons **H_a**, **H_b** and aldehyde proton **H_c** are highlighted for clear differentiation. Conditions: 10 mM KP_i, pH 7.2 (D₂O/CD₃CN, 4:1), IS = TMSP-d₄. (B) Time dependent ¹H-NMR interconversion of oxime **2.35** to oxime **2.69**. The ¹H-NMR spectrum shows only the zoomed regions (7.8 - 10.3 ppm) of the relevant protons **H_a**, **H_b** and **H_c**. The equilibrium is reached after 10 h where the final ratio of **2.69** to **2.35** is 10:1.

3.5.6 Conclusions and outlook

Herein we described that *O*-alkyliminoboronates form with remarkable speed and selectivity in neutral aqueous buffer at low substrate concentrations. The reaction is unaffected by proteins, carbohydrates, biothiols, human serum and has an equilibrium constant of $>10^8 \text{ M}^{-1}$. A great advantage of the present method over many coupling reactions is the simplicity and ready availability of the starting materials. There are commercial libraries of phenylboronic acid and boronic ester compounds, many of which contain an aldehyde or can be trivially elaborated to incorporate one. Furthermore, the widespread use of oxime conjugations for connective processes at high concentration means that a variety of *O*-alkylhydroxylamines are also available. A shortcoming of the present method in comparison to the classical oxime condensation is the size of required 2-FPBA motif. Although for most applications this should present no difficulties, examples where the compactness of the oxime is critical (such as, for example, as a functional isostere of peptide bonds)²⁷⁶ would not be possible. The ability to run conjugations at 1:1 ratios of partners at biological pH means that either or both components can be complex, precious materials. Although we have focused on oxime condensation for proof of concept the coordinating properties of boron in aqueous media could potentially be exploited to accelerate other important reactions whose rates are limited by the kinetics of Schiff base formation.²⁷⁷

A potential application of this method could be its use in the field of imaging or labeling as a “turn-on” fluorescence probe. A non-fluorescent molecule equipped with a hydroxylamine and a boron chelator could be reacted with 2-FPBA (**2.34**) which after rapid oxime formation results in a fluorescent conjugate. This method would allow visualizing a target within seconds under neutral and aqueous conditions as shown in **Figure 3.19**.

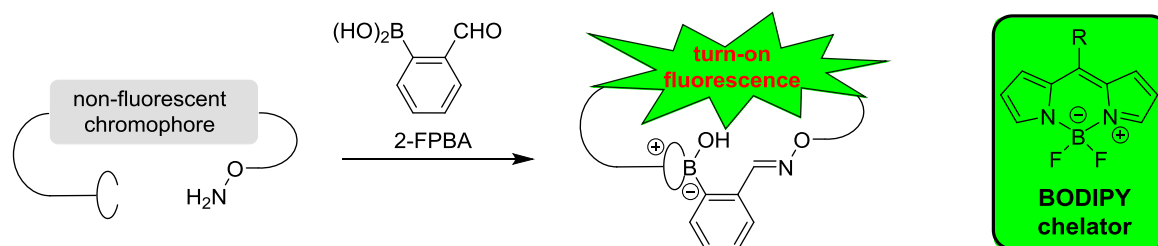


Figure 3.19: Schematic principle for a potential application of boron-assisted oxime formation based on a “turn on” fluorogenic probe.

BODIPY-based chelators are well known for the fluorescence imaging of biomolecules in living cells and represent a promising scaffold to test this hypothesis.²⁷⁸ These dyes, consisting of a difluoroboron-dipyrromethane core, have outstanding properties *e.g.*, high quantum yields contributing to the overall brightness, sharp excitation and emission bands as well as a reasonable stability to physiological conditions.^{279,280} Introducing new substituents on the BODIPY scaffold offers the possibility to build a

molecular structure capable to incorporate 2-FPBA (**2.34**) via oxime condensation and subsequent boron complexation to give a fluorescent dye (**Scheme 3.21**).

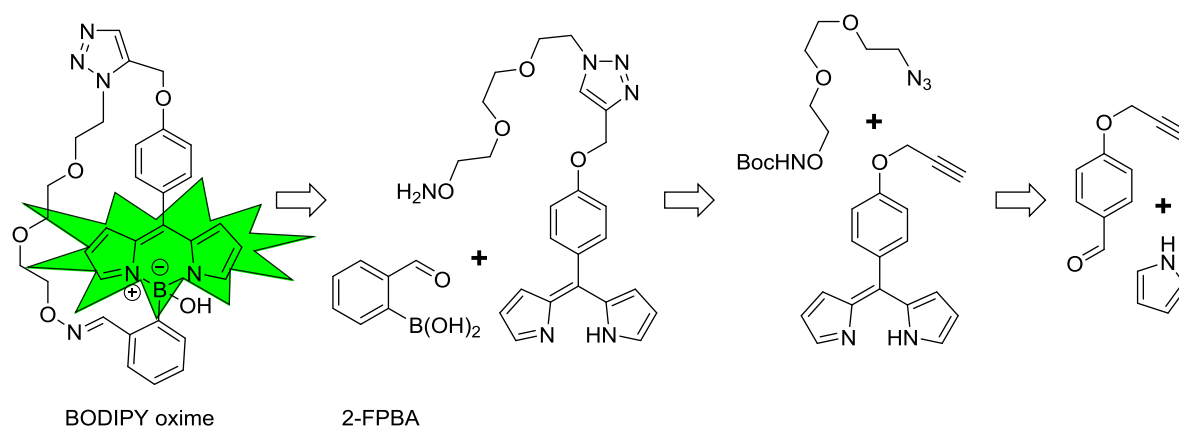


Figure 3.21: Retrosynthetic analysis of a possible “turn-on” fluorescent BODIPY oxime target. The non-fluorescent dipyrromethene core can be prepared by a functionalized aldehyde and pyrrole. The reaction with a water soluble and azide equipped hydroxylamine gives access to the “clicked” triazole ready for rapid oxime condensation with 2-FPBA followed by an intramolecularly favoured boron complexation resulting in a fluorescent BODIPY dye.

So far we were able to isolate the alkyne-containing dipyrromethane shown in **Figure 3.21** but preliminary boron complexations in water led unfortunately to no fluorogenesis. In due course this project will be investigated in more detail and the need for the intramolecular hydroxylamine handle will provide valuable information on our hypothesis of a “turn-on” fluorescent BODIPY oxime.

If we reconsider the oximes formed in the course of our studies, the boronic acid/ester group which is left behind could be used as a potential reactive group for subsequent Suzuki-Miyaura cross-coupling. DAVIS *et al.* demonstrated the ability to cross-couple boronic acid-containing molecules with proteins under aqueous, neutral conditions with excellent conversions in only 30 min.²⁴³ Despite the huge excess of boronic acid they used, further functional group manipulation would be very useful and informative with regards to other potential applications.

4 Experimental

4.1 General Information

All commercial reagents and solvents used were of analytical grade unless otherwise mentioned in the respective synthetic procedure and purchased from ABCR, Acros, Alfa Aesar, Apollo Scientific, Bachem, Fischer Chemicals, Fluorochem, Iris, Novabiochem, Sigma Aldrich or Strem. 1,4-dioxane was freshly distilled from sodium benzophenone ketyl under dry nitrogen prior to use. Buffers and HPLC eluents were prepared with Milli-Q water (electrical resistivity of 18.2 MΩcm) which was filtered through a Quantum® TEX polishing cartridge from Merck Millipore. Analytical TLC was performed on Silica gel 60 F₂₅₄ pre-coated aluminium sheets (Merck) or glass plates (Merck) and visualized by fluorescence quenching under UV light at 254 nm or by staining with potassium permanganate and heating. Flash chromatography was performed on SilicaFlash® gel P60 40-63 μm (230-400 mesh) (SiliCycle, Quebec). Concentration under reduced pressure was performed by rotatory evaporation of solvents at 40°C (unless otherwise specified). Manual PNA synthesis was performed using Fmoc-protected rink amide AM resin (100-200 mesh) from NovaBiochem with an initial loading of 0.61 mmol/g. Couplings were performed using 2 mL polyethylene syringe (BD Discardit™ II) reactors equipped with a fritted disc and closed with a luer stopper (both parts from MultiSynTech GmbH, Witten, Germany). PNA monomers (Fmoc-A(Bhoc)-OH, Fmoc-C(Bhoc)-OH, Fmoc-G(Bhoc)-OH and Fmoc-T-OH) were purchased from Panagene. Automated solid-phase oligonucleotide synthesis was carried out on an Expedite 8909 nucleic acid synthesizer (PerCepTiveBiosystems, Framingham, Ma, USA). Phosphoramidites for DNA synthesis (A^{Bz}, G^{dmf}, C^{Ac}, T) were purchased from Proligo Reagents, SAFC. SynBase 500/110 AllFit pre-modified oligonucleotide synthesis columns, MeCN anhydrous wash, BTT activator, CapA, CapB and oxidizer for the Expedite device were purchased from Link Technologies. Automated solid-phase peptide synthesis (SPPS) was performed on a Syro I Peptide synthesizer (MultiSynTech GmbH, Witten, Germany) using the software SyroXP Peptide. ¹H, ¹³C, ³¹P, ¹⁹F, ¹¹B and 2D-NMR spectra were acquired on a BrukerAvance (250, 400, 500, 600 or 700 MHz proton frequency) spectrometer at 298.15 K unless otherwise mentioned. Chemical shifts (δ values) relative to TMS are referenced to the solvent's residual peak and reported in ppm. Multiplicities are reported as follows: s = singlet, s_{br} = broad singlet, d = doublet, t = triplet, q = quartet, quint. = quintet, m = multiplet or unresolved and coupling constant *J* in Hz. Low resolution ESI-MS spectra were recorded on a Bruker Esquire3000+ spectrometer by direct injection in positive or negative polarity of the ion trap detector. High resolution mass spectra (HRMS) were recorded by the mass spectrometric service of the University of Basel (**Dr. Heinz Nadig**) on a Bruker maXis 4G QTOF ESI mass spectrometer. The crystal structures of selected compounds were solved by the X-ray crystallographic service of the University of Basel on a Bruker Kappa Apex2 diffractometer at 123 K. Preparative flash column chromatography was performed either using an Isolera Four device (Biotage, Uppsala, Sweden) equipped with pre-loaded

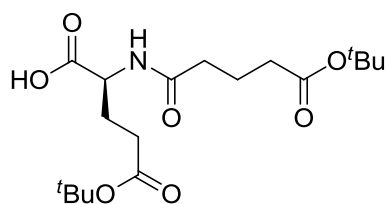
silica gel cartridges and monitoring elution at 254/280 nm or by manual column chromatography using nitrogen pressure. The crude compound mixtures were either dry loaded by adsorption onto silica gel or directly applied as liquids using the eluent mixture. Analytical and micro-preparative RP-HPLC was carried out at room temperature on a Hewlett Packard 1100 Liquid Chromatograph or a Shimadzu Prominence UFLC Liquid Chromatograph system using a C18 column (Eclipse XDB, 5 μ m, 4.6 x 150 mm) from Agilent with a flow rate of 1 mL/min monitoring and collecting the products at 254 nm or 280 nm if not otherwise specified. Semi-preparative RP-HPLC was carried out on a Shimadzu VP Liquid Chromatograph using a C18 column (LiChroCART[®], 5 μ m, 10 x 250 mm) from Merck with a flow rate of 5 mL/min monitoring and collecting the products at 254 nm or 280 nm if not otherwise specified. Detection was done by monitoring the absorbance of the column effluent at 254 nm. Preparative RP-HPLC was carried out at room temperature on a Shimadzu Prominence UFLC Preparative Liquid Chromatograph using a C18 column (Gemini NX5u, 110Å, AXIA, 250 x 21.2 mm) from Phenomenex with a flow rate of 20 mL/min monitoring and collecting the products at 254 nm if not otherwise specified. The crude compound mixtures were injected as DMSO solutions. UPLC-MS was carried out on an Agilent 1290 Infinity system equipped with an Agilent 6130 Quadrupole LC/MS using a C18 column (ZORBAX Eclipse Plus RRHD, 1.8 μ m, 2.1 x 50 mm) from Agilent with a flow rate of 0.45 mL/min or 0.60 mL/min at 40°C. Elution was done with 0.1% (v/v) formic acid in H₂O /10% (v/v) MeCN (A) and 0.1% (v/v) formic acid in MeCN/10% (v/v) H₂O (B) using the following gradient: 5-90% (B) in 3.5 min, 90% (B) in 1 min, detection at 254/280 nm, ESI-MS in positive ion mode of the ion trap. MALDI-TOF-MS analyses were carried out on a Bruker Microflex or PerSeptive Biosystems Voyager mass spectrometer in linear positive or negative mode using 3-hydroxypicolinic acid/ammonium citrate buffer, pH 6.0 as the matrix. A Chirascan Plus device (Applied Photophysics Ltd, Leatherhead, UK) was used for CD measurements. The solutions were measured in a quartz cell with a path length of 10 mm (Hellma 110-QS).

4.2 Chemical synthesis

4.2.1 Guided catalysts studies

4.2.1.1 Synthesis of small molecules and dirhodium catalysts

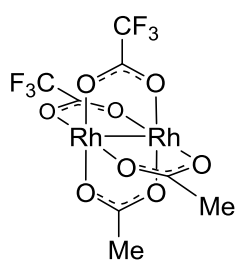
Compound **1.2** was prepared in analogy to a literature procedure by GAGNON *et al.*²⁸¹



Acid **1.5** (266 mg, 1.41 mmol, 1.00 eq.) and *p*-Nitrophenol (196 mg, 1.41 mmol, 1.00 eq.) were dissolved in 6 mL of EtOAc. A DCC solution in EtOAc (323 mg, 1.57 mmol, 1.11 eq. in 4 mL) was added to the mixture at room temperature. The mixture was stirred for 4 h, filtered through Celite and the cake was washed with

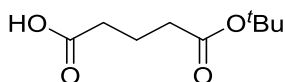
15 mL of EtOAc. The solvent was removed under reduced pressure to give 740 mg of a colorless solid. Upon re-dissolving the solid in 2 mL of EtOAc, dicyclohexylurea precipitated which was filtered off followed by solvent removal under reduced pressure to give 528 mg of a yellow oil which was 90% pure as determined by ¹H-NMR. The crude was used without further purification for the subsequent peptide coupling.

H₂N-Glu(O^tBu)-OH (431 mg, 2.12 mmol, 1.50 eq.) and NEt₃ (290 μL, 2.12 mmol, 1.50 eq.) were dissolved in 10 mL of H₂O using sonication and added to a solution of the *p*-Nitrophenyl ester (437 mg, 1.41 mmol, 1.00 eq.) in MeCN (10 mL). The mixture turned immediately yellow and was stirred at room temperature for 24 h. Then the MeCN was removed under reduced pressure and the remaining aqueous solution was cooled to 0°C and acidified with 1M HCl until pH 2 was reached. The mixture was extracted with CH₂Cl₂ (4 x 10 mL) and the combined organics were washed once with brine (10 mL) and H₂O (10 mL). The organics were dried over MgSO₄, filtered and the solvent removed under reduced pressure to give 825 mg of a slightly yellow oil. The crude was purified by flash chromatography (40:1 → 10:1 CH₂Cl₂/MeOH, ninhydrin stain) to afford acid **1.2** (299 mg, 801 μmol, 56%) as white crystalline solid. ¹H-NMR (500 MHz, CDCl₃) δ/ppm: 9.89 (s_{br}, 1H), 6.84 (d, *J* = 7.1 Hz, 1H), 4.56-4.50 (m, 1H), 2.50-2.39 (m, 1H), 2.38-2.33 (m, 1H), 2.33-2.26 (m, 4H), 2.21-2.12 (m, 1H), 2.05-1.96 (m, 1H), 1.95-1.87 (m, 2H), 1.44 (s, 9H), 1.43 (s, 9H). ¹³C-NMR (126 MHz, CDCl₃) δ/ppm: 174.36, 173.66, 173.18, 172.92, 81.45, 80.80, 52.30, 35.36, 34.65, 31.84, 28.23, 28.17, 26.86, 21.09. HRMS (ESI): C₁₈H₃₁NNaO₇⁺ *calcd.*: 396.1993, *found*: 396.1995 [M+Na]⁺.



cis-Rh₂(OAc)₂(TFA)₂ **1.3**: Compound **1.3** was synthesized in analogy to a literature procedure by LOU *et al.*²⁸²

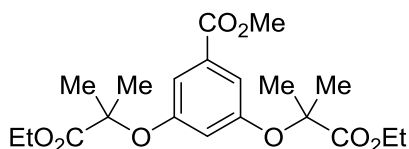
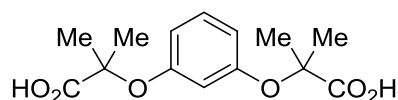
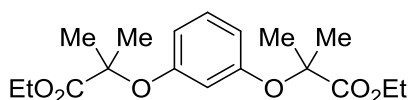
¹H-NMR (400 MHz, CDCl₃) δ/ppm: 2.54 (s, 3H), 1.98 (s, 3H). ¹⁹F-NMR (400 MHz, CDCl₃) δ/ppm: -74.42. (This compound was synthesized and characterized by Prof. Dr. Dennis Gillingham).



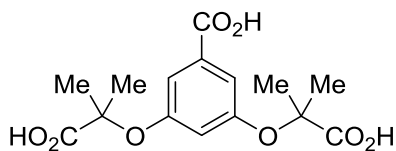
Compound **1.6** was prepared according to a literature procedure by LELAIS *et al.*²⁸³ The analytical data are in agreement with the values reported by BITAN *et al.*²⁸⁴

¹H-NMR (500 MHz, CDCl₃) δ/ppm: 2.42 (t, *J* = 7.5 Hz, 2H), 2.30 (t, *J* = 7.5 Hz, 2H), 1.92 (quint., *J* = 7.4 Hz, 2H), 1.45 (s, 9H). ¹³C-NMR (126 MHz, CDCl₃) δ/ppm: 179.11, 172.40, 80.68, 34.58, 33.14, 28.24, 20.14. HRMS (ESI): C₉H₁₆NaO₄⁺ *calcd.*: 211.0941, *found*: 211.0941 [M+Na]⁺.

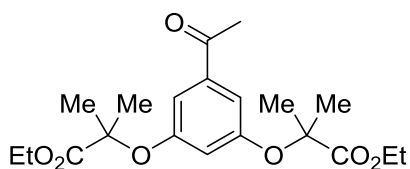
The synthesis and spectroscopic characterization of diester **1.11a** and diacid **1.12a** has been described by BONAR-LAW *et al.*¹⁷⁵



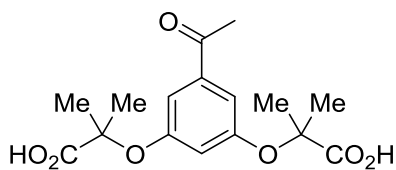
Triester **1.11b**: A round bottom flask was charged with methyl 3,5-dihydroxybenzoate (840 mg, 5.00 mmol, 1.00 eq.) and dissolved in 12 mL DMF. Then K₂CO₃ (2.76 g, 20.0 mmol, 4.00 eq.), Cs₂CO₃ (1.63 g, 5.00 mmol, 1.00 eq.) and Ethyl 2-bromoisobutyrate (3.72 mL, 25.0 mmol, 5.00 eq.) were added. The mixture was stirred at 80°C for 24 h and allowed to cool down to room temperature. The mixture was poured into 50 mL H₂O and extracted with Et₂O (3 x 20 mL). The combined organics were consecutively washed with a 1M aqueous HCl solution (portions of 10 mL), H₂O (20 mL), dried over Na₂SO₄, filtered and evaporated under reduced pressure. In order to remove the excess of Ethyl 2-bromoisobutyrate the obtained oil was heated to 50°C under high vacuum for 2 h to afford **1.11b** (1.63 g, 4.10 mmol, 82%) as a pale yellow oil. ¹H-NMR (400 MHz, CDCl₃) δ/ppm: 7.17 (d, *J* = 2.3 Hz, 2H), 6.59 (t, *J* = 2.3 Hz, 1H), 4.25 (q, *J* = 7.1 Hz, 4H), 3.86 (s, 3H), 1.58 (s, 12H), 1.26 (t, *J* = 7.1 Hz, 6H). ¹³C-NMR (101 MHz, CDCl₃) δ/ppm: 173.9, 166.5, 156.3, 131.5, 115.4, 114.3, 79.8, 61.7, 52.4, 25.5, 14.2. HRMS (ESI): C₂₀H₂₈NaO₈⁺ *calcd.*: 419.1677, *found*: 419.1676 [M+Na]⁺.



Triacid **1.12b**: A round bottom flask was charged with **1.11b** (300 mg, 757 μmol , 1.00 eq.) and dissolved in 5 mL THF. Then 5 mL H_2O were added which resulted in a milky suspension. $\text{LiOH} \cdot \text{H}_2\text{O}$ (953 mg, 230 mmol, 30.0 eq.) was added in one scoop and the mixture was heated to 60°C for 20 h. After cooling to room temperature 13 mL of a 2M aqueous HCl solution were added slowly and the mixture extracted with EtOAc (3 x 20 mL). The combined organics were dried over MgSO_4 , filtered and concentrated under reduced pressure to give a yellow oil. The crude product was then applied as a solution in DMSO (3 mL) on a 50g C-18 reverse phase column and eluted using a Biotage Isolera Four device (MeCN in H_2O , 5-40% over 11 CV, eluted after 9 CV). The product fractions were lyophilized to afford **1.12b** (190 mg, 583 μmol , 77%) as a white semi solid. $^1\text{H-NMR}$ (400 MHz, MeOD) δ/ppm : 7.20 (d, $J = 2.3$ Hz, 2H), 6.67 (s, 1H), 1.58 (s, 12H). $^{13}\text{C-NMR}$ (101 MHz, MeOD) δ/ppm : 177.3, 157.6, 133.3, 115.8, 115.0, 80.6, 25.7 (one carbon missing). HRMS (ESI): $\text{C}_{15}\text{H}_{18}\text{NaO}_8^+$ *calcd.*: 349.0895, *found*: 349.0894 $[\text{M}+\text{Na}]^+$.

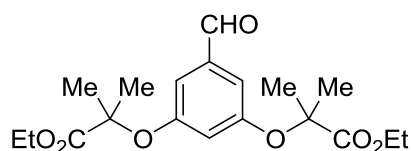


Ketone **1.11c**: A round bottom flask was charged with 3,5-dihydroxyacetophenone (380 mg, 2.50 mmol, 1.00 eq.) and dissolved in 6 mL DMF. Then K_2CO_3 (1.38 g, 10.0 mmol, 4.00 eq.), Cs_2CO_3 (800 mg, 2.50 mmol, 1.00 eq.) and Ethyl 2-bromoisobutyrate (1.86 mL, 12.0 mmol, 5.00 eq.) were added. The mixture was stirred at 80°C overnight and allowed to cool down to room temperature. The mixture was poured into 50 mL H_2O and extracted with Et_2O (3 x 20 mL). The organic phase was consecutively washed with H_2O (portions of 20 mL), dried over Na_2SO_4 , filtered and evaporated under reduced pressure. The resulting brown oil was purified by flash chromatography (hexane/EtOAc 6:1) to afford **1.11c** (775 mg, 2.04 mmol, 81%) as a colorless oil. $^1\text{H-NMR}$ (500 MHz, CDCl_3) δ/ppm : 7.08 (d, $J = 2.2$ Hz, 2H), 6.55 (t, $J = 2.2$ Hz, 1H), 4.25 (q, $J = 7.1$ Hz, 4H), 2.51 (s, 3H), 1.59 (s, 12H), 1.26 (t, $J = 7.2$ Hz, 6H). $^{13}\text{C-NMR}$ (126 MHz, CDCl_3) δ/ppm : 197.2, 173.9, 156.5, 138.6, 114.7, 113.0, 79.7, 61.8, 26.8, 25.5, 14.2. HRMS (ESI): $\text{C}_{20}\text{H}_{28}\text{NaO}_7^+$ *calcd.*: 403.1728, *found*: 403.1727 $[\text{M}+\text{Na}]^+$.

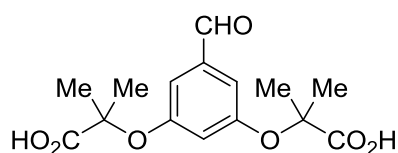


Diacid **1.12c**: A round bottom flask was charged with ketone **1.11c** (330 mg, 860 μmol , 1.00 eq.) and dissolved in 4 mL MeOH. Then, 2 mL of a solution containing $\text{LiOH} \cdot \text{H}_2\text{O}$ (300 mg, 12.5 mmol, 15.0 eq., in 2 mL H_2O) was added. After heating the mixture for 3 h at 60°C it was allowed to cool to room temperature and the reaction mixture was poured into 20 mL of a 1M aqueous HCl solution and extracted with EtOAc (3 x 20 mL). The combined organics were washed with H_2O (20 mL), dried over Na_2SO_4 , filtered and evaporated under reduced pressure to give

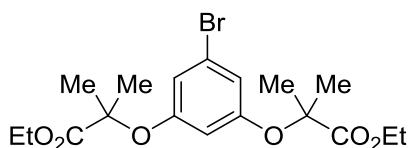
1.12c (280 mg, 860 μmol , 99%) colourless crystals. $^1\text{H-NMR}$ (500 MHz, $\text{DMSO-}d_6$) δ/ppm : 13.21 (s, 2H), 7.01 (d, $J = 2.3$ Hz, 2H), 6.50 (t, $J = 2.2$ Hz, 1H), 2.49 (s, 3H), 1.52 (s, 12H). $^{13}\text{C-NMR}$ (126 MHz, $\text{DMSO-}d_6$) δ/ppm : 174.7, 156.2, 122.4, 111.0, 99.5, 97.4, 78.9, 26.7, 25.0. HRMS (ESI): $\text{C}_{16}\text{H}_{20}\text{NaO}_7^+$ *calcd.*: 347.1102, *found*: 347.1101 $[\text{M}+\text{Na}]^+$.



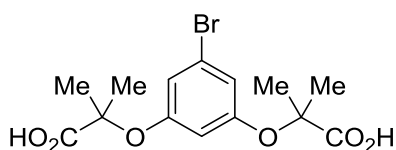
Aldehyde **1.11d**: A round bottom flask was charged with 3,5-dihydroxybenzaldehyde (345 mg, 2.50 mmol, 1.00 eq.) and dissolved in 6 mL DMF. Then K_2CO_3 (1.38 g, 10.0 mmol, 4.00 eq.), Cs_2CO_3 (800 mg, 2.50 mmol, 1.00 eq.) and Ethyl 2-bromoisobutyrate (1.86 mL, 12.0 mmol, 5.00 eq.) were added. The mixture was stirred at 80°C overnight and allowed to cool down to room temperature. The mixture was poured into 50 mL H_2O and extracted with Et_2O (3 x 20 mL). The combined organics were consecutively washed with a 1M aqueous HCl solution (portions of 10 mL), H_2O (portions of 20 mL), dried over Na_2SO_4 , filtered and evaporated under reduced pressure. The resulting brown oil was purified by flash chromatography (hexane/ EtOAc 6:1) to afford **1.11d** (525 mg, 1.4 mmol, 56%) as a colorless oil. $^1\text{H-NMR}$ (400 MHz, CDCl_3) δ/ppm : 9.83 (s, 1H), 6.97 (d, $J = 2.3$ Hz, 2H), 6.64 (t, $J = 2.3$ Hz, 1H), 4.25 (q, $J = 7.1$ Hz, 4H), 1.60 (s, 12H), 1.25 (t, $J = 7.1$ Hz, 6H). $^{13}\text{C-NMR}$ (101 MHz, CDCl_3) δ/ppm : 191.4, 173.8, 157.0, 138.0, 116.3, 113.7, 79.9, 61.8, 25.5, 14.2. HRMS (ESI): $\text{C}_{19}\text{H}_{26}\text{NaO}_7^+$ *calcd.*: 389.1576, *found*: 389.1571 $[\text{M}+\text{Na}]^+$.



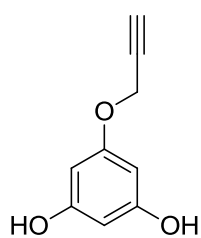
Diacid **1.12d**: A round bottom flask was charged with **1.11d** (525 mg, 1.40 mmol, 1.00 eq.) and dissolved in 4 mL MeOH. Then, 2 mL of a solution containing $\text{LiOH} \cdot \text{H}_2\text{O}$ (300 mg, 12.5 mmol, 9.00 eq., in 2 mL H_2O) was added. After heating the mixture for 3 h at 60°C a TLC control (5% MeOH/ EtOAc) indicated full conversion of the diester **1.11d**. The reaction mixture was poured into 20 mL of a 1M aqueous HCl solution and extracted with EtOAc (3 x 20 mL). The combined organics were washed with H_2O (20 mL), dried over Na_2SO_4 , filtered and evaporated under reduced pressure to afford **1.12d** (345 mg, 1.10 mmol, 79%) as a yellow oil. $^1\text{H-NMR}$ (400 MHz, CD_2Cl_2) δ/ppm : 9.85 (s, 1H), 7.08 (d, $J = 2.2$ Hz, 2H), 6.59 (t, $J = 2.2$ Hz, 1H), 1.61 (s, 12H). $^{13}\text{C-NMR}$ (101 MHz, CD_2Cl_2) δ/ppm : 191.8, 178.4, 156.9, 139.0, 115.4, 114.6, 80.1, 25.6. HRMS (ESI): $\text{C}_{15}\text{H}_{18}\text{NaO}_7^+$ *calcd.*: 333.0950, *found*: 333.0945 $[\text{M}+\text{Na}]^+$.



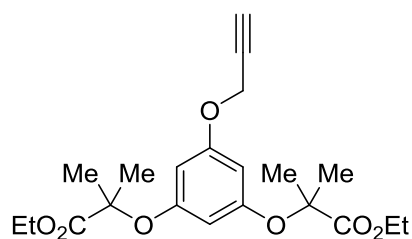
Bromide **1.11e**: A flame dried round bottom flask under N_2 atmosphere was charged with 3-Bromoresorcinol (200 mg, 1.06 mmol, 1.00 eq.), Ethyl 2-bromoisobutyrate (780 μ L, 5.29 mmol, 5.00 eq.) and dissolved in 3 mL dry DMF. Then K_2CO_3 (585 mg, 4.23 mmol, 4.00 eq.) and Cs_2CO_3 (345 mg, 1.06 mmol, 1.00 eq.) were added. The slurry was subsequently immersed into a preheated oil bath at $80^\circ C$ and stirred vigorously for 22 h. After cooling down to room temperature the mixture was poured into H_2O (25 mL) and extracted with Et_2O (3 x 20 mL). The combined organics were then washed once with a 1M aqueous HCl solution (10 mL), H_2O (20 mL), dried over $MgSO_4$, filtered and concentrated under reduced pressure. The yellow oil was purified by flash chromatography (cyclohexane/ $EtOAc$ 9:1) to afford **1.11e** (211 mg, 510 μ mol, 48%) as a colourless oil. 1H -NMR (400 MHz, $CDCl_3$) δ /ppm: 6.66 (d, $J = 2.2$ Hz, 2H), 6.28 (t, $J = 2.2$ Hz, 1H), 4.24 (q, $J = 7.1$ Hz, 4H), 1.56 (s, 12H), 1.26 (t, $J = 7.1$ Hz, 6H). ^{13}C -NMR (101 MHz, $CDCl_3$) δ /ppm: 173.81, 156.82, 122.05, 116.56, 109.16, 79.83, 61.75, 25.48, 14.18. HRMS (ESI): $C_{18}H_{25}BrNaO_8^+$ *calcd.*: 439.0727, *found*: 439.0726 $[M+Na]^+$. (This compound was synthesized and characterized by Daniel Bachmann).



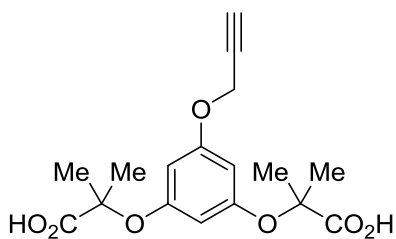
Diacid **1.12e**: A round bottom flask was charged with **1.11e** (103 mg, 247 μ mol, 1.00 eq.) and dissolved in 3 mL THF/ H_2O (1:1) resulting in a milky suspension. $LiOH \cdot H_2O$ (207 mg, 4.94 μ mol, 20.0 eq.) was added in one scoop and the mixture was heated to $60^\circ C$ for 13 h. After cooling to room temperature 3 mL of a 2M aqueous HCl solution were added slowly and the mixture transferred into a separation funnel. Extraction was performed with $EtOAc$ (3 x 10 mL) and the combined organics were dried over $MgSO_4$, filtered and concentrated under reduced pressure to give a yellow oil. The crude product was then applied as a solution in DMSO (3 mL) on a 50g C-18 reverse phase column and eluted using a Biotage Isolera Four device (MeCN in H_2O , gradient 5-40% over 8 CV, elutes after 3 CV). The product fractions were lyophilized to afford **1.12e** (89 mg, 207 μ mol, 84%) as a colorless oil. 1H -NMR (400 MHz, MeOD) δ /ppm: 6.70 (d, $J = 2.1$ Hz, 2H), 6.39 (t, $J = 2.2$ Hz, 1H), 1.56 (s, 12H). ^{13}C -NMR (101 MHz, MeOD) δ /ppm: 177.1, 158.3, 122.8, 117.2, 110.0, 80.8, 25.7. HRMS (ESI): $C_{14}H_{17}BrNaO_6^+$ *calcd.*: 383.0101, *found*: 383.0104 $[M+Na]^+$. (This compound was synthesized and characterized by Daniel Bachmann).



Alkyne **1.10f**: A round bottom flask equipped with a stir bar was charged with propargyl bromide (80% in toluene, 600 μ L, 5.42 mmol, 1.08 eq.), K_2CO_3 (760 mg, 5.50 mmol, 1.10 eq.) and dissolved in 2.2 mL DMF. Then phloroglucinol (637 mg, 5.05 mmol, 1.00 eq.) dissolved in 3.6 mL DMF was added dropwise to the yellow suspension during 10 min. After heating the mixture to 60°C for 24 h a TLC control (cyclohexane/EtOAc 1:1) indicated full conversion of the phloroglucinol. The solid was filtered off, washed with DMF and the solvent was evaporated under reduced pressure. The remaining red brown oil was diluted with CH_2Cl_2 (15 mL) and a 1M aqueous HCl solution (10 mL) was added. The organic layer was separated and the aqueous layer was washed again with CH_2Cl_2 (2 x 10 mL). The combined organics were dried over $MgSO_4$ filtered and concentrated under reduced pressure. The crude dark red oil was purified by flash chromatography (cyclohexane/EtOAc 3:1) to afford **1.10f** (155 mg, 651 μ mol, 13%, 69% purity) as a slightly orange oil and as a mixture of mono- and di-alkylated species. A pure analytical sample for characterization was obtained after preparative RP-HPLC purification as a white sticky semi solid. 1H -NMR (500 MHz, $DMSO-d_6$) δ /ppm: 9.25 (s, 2H), 5.86 (t, $J = 2.1$ Hz, 1H), 5.83 (d, $J = 2.1$ Hz, 2H), 4.63 (d, $J = 2.4$ Hz, 2H), 3.54 (t, $J = 2.4$ Hz, 1H). ^{13}C -NMR (126 MHz, $DMSO-d_6$) δ /ppm: 159.1, 159.0, 96.1, 93.4, 79.6, 78.0, 55.2. HRMS (ESI): $C_9H_8NaO_3^+$ *calcd.*: 165.0546, *found*: 165.0546 $[M+Na]^+$.

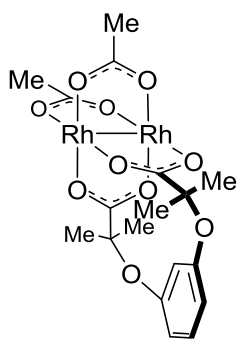


Diester **1.11f**: A round bottom flask equipped with a stir bar was charged with alkyne **1.10f** (155 mg, 651 μ mol, 69% purity, 1.00 eq.) and Ethyl 2-bromoisobutyrate (690 μ L, 4.70 mmol, 7.22 eq.) in dry MeCN. While stirring K_2CO_3 (522 mg, 3.78 mmol, 5.80 eq.) and Cs_2CO_3 (308 mg, 945 μ mol, 1.45 eq.) were added. The mixture was stirred at 80°C for 24 h. Then it was poured into a 2M aqueous HCl solution (5 mL) and EtOAc (5 mL) was added. The organic layer was separated and the aqueous layer extracted with EtOAc (3 x 5 mL). The combined organics were washed with H_2O (5 mL), dried over $MgSO_4$ filtered and concentrated under reduced pressure. The crude brown oil was purified by flash chromatography (cyclohexane/EtOAc 9:1) to afford diester **1.11f** (122 mg, 311 μ mol, 48%). 1H -NMR (500 MHz, $CDCl_3$) δ /ppm: 6.16 (d, $J = 2.1$ Hz, 2H), 5.99 (t, $J = 2.2$ Hz, 1H), 4.24 (q, $J = 7.0$ Hz, 4H), 2.51 (t, $J = 2.5$ Hz, 1H), 1.56 (s, 12H), 1.25 (t, $J = 7.1$ Hz, 6H). ^{13}C -NMR (126 MHz, $CDCl_3$) δ /ppm: 174.2, 158.8, 156.9, 103.8, 102.8, 100.6, 79.5, 75.7, 61.6, 56.0, 25.5, 14.2. HRMS (ESI): $C_{21}H_{28}NaO_7^+$ *calcd.*: 415.1727, *found*: 415.1726 $[M+Na]^+$.

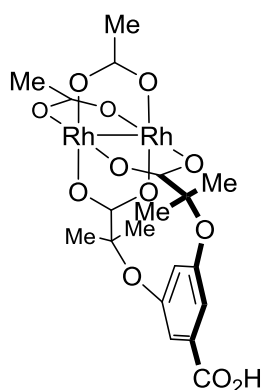


Diacid **1.12f**: A round bottom flask equipped with a stir bar was charged with diester **1.11f** (116 mg, 296 μmol , 1.00 eq.) and dissolved in 4 mL MeOH. A solution of LiOH \cdot H₂O (333 mg, 7.94 mmol, 26.0 eq.) in H₂O (2 mL) was added. After heating the mixture for 3 h at 60°C a TLC control (cyclohexane/EtOAc 3:1) indicated the full conversion of the diester. The reaction mixture was poured into a 1M aqueous HCl solution (5 mL) and extracted with EtOAc (3 x 5 mL). The combined organic phases were washed with H₂O (5 mL) dried over MgSO₄ and evaporated under reduced pressure. The product **1.12f** (96.0 mg, 285 μmol , 93%) was isolated as a colourless oil. ¹H-NMR (500 MHz, DMSO-*d*₆) δ : 13.07 (s, 2H), 6.06 (d, *J* = 2.1 Hz, 2H), 5.89 (t, *J* = 2.3 Hz, 1H), 4.69 (d, *J* = 2.7 Hz, 2H), 3.58 (t, *J* = 2.5 Hz, 1H), 1.49 (s, 12H). ¹³C-NMR (126 MHz, DMSO-*d*₆) δ : 174.8, 158.3, 156.6, 78.6, 78.4, 55.5, 25.1 (three carbon signals missing). HRMS (ESI): C₁₇H₂₀NaO₇⁺ *calcd.*: 359.1102 *found*: 359.1101 [M+Na]⁺.

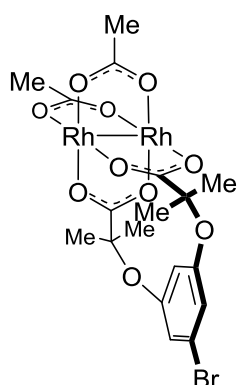
The synthesis and spectroscopic characterization of dirhodium dicarboxylate (**1.13**) has been described by BONAR-LAW *et al.*¹⁸⁴



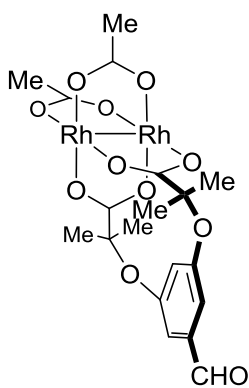
Rhodium complex **1.13**: A dry round bottom flask under a N₂ atmosphere was charged with Rh₂(OAc)₄ (156 mg, 348 μmol , 1.00 eq.), **1.12a** (98.2 mg, 348 μmol , 1.00 eq.) and dissolved in 15.6 mL *N,N*-dimethylaniline. The mixture was stirred at 140°C for 3 h and allowed to cool down to room temperature. Then the mixture was extracted first with CH₂Cl₂ (50 mL) followed by MeCN (3 mL). In order to remove excess of *N,N*-dimethylaniline, the organic phase was extracted with a 2M aqueous HCl solution (3 x 90 mL) and washed with H₂O (2 x 100 mL). The combined organics were dried over Na₂SO₄, filtered and concentrated under reduced pressure to give a blue oil. The crude was purified by flash chromatography on 17 g of silica gel to elute first the bis-adduct (CH₂Cl₂/EtOAc: 95:5) **1.17** (23.0 mg, 30.0 μmol , 10%) followed by **1.13** after changing the gradient (CH₂Cl₂/EtOAc: 90:10). The product fractions were combined to afford **1.13** (125 mg, 210 μmol , 60%) as a green solid.



Rhodium complex **1.14**: A dry round bottom flask under a N₂ atmosphere was charged with *cis*-Rh₂(OAc)₂(TFA)₂²⁸² (30.0 mg, 54.6 μmol, 1.00 eq.) and subsequently dissolved in 3 mL 1,2-dichloroethane. Then triacid **1.12b** (18.0 mg, 54.6 μmol, 1.00 eq.) was added followed by a dropwise addition of 0.6 mL dry EtOAc to dissolve the ligand upon sonication. The green/blue solution was then immersed into a preheated oil bath at 60°C and stirred for 16 h. After cooling down to room temperature all volatiles were removed under reduced pressure. The crude solid was then applied as a solution in DMSO (1 mL) to preparative RP-HPLC (MeCN/0.1% TFA in H₂O, 2% to 50% over 28 min, t_R = 26 min, 254 nm). The product eluted as a purple liquid. The corresponding product fractions were lyophilized to afford **1.14** (11.0 mg, 17.0 μmol, 31%) as a green solid. ¹H-NMR (400 MHz, 5% v/v MeOD in CD₂Cl₂) δ/ppm: 7.16 (d, *J* = 2.3 Hz, 2H), 6.20 (t, *J* = 2.3 Hz, 1H), 1.87 (s, 6H), 1.37 (s, 12H). ¹³C-NMR (101 MHz, 5% v/v MeOD in CD₂Cl₂) δ/ppm: 192.9, 192.0, 168.4, 156.4, 132.4, 116.9, 114.1, 81.4, 25.1, 23.7. HRMS (ESI): C₁₉H₂₂NaO₁₂Rh₂⁺ *calcd.*: 670.9119, *found*: 670.9112 [M+Na]⁺.

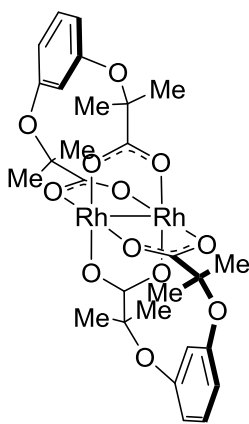


Rhodium complex **1.15**: A dry round bottom flask under a N₂ atmosphere was charged with diacid **1.12e** (20.0 mg, 55.5 μmol, 1.00 eq.) as a solution in EtOAc and all volatiles were subsequently removed under reduced pressure. Then 2 mL of 1,2-dichloroethane were added followed by *cis*-Rh₂(OAc)₂(TFA)₂²⁸² (30 mg, 54.7 μmol, 1.00 eq.). The green solution was immersed into a preheated oil bath at 60°C and stirred for 7 h. At this time most of the ligand was consumed and the amount of side products was lowest compared to the desired complex **1.15**. After cooling to room temperature all volatiles were removed under reduced pressure. The crude green solid was then applied as a solution in DMSO (1 mL) to preparative RP-HPLC (MeCN/0.1% TFA in H₂O, 2% to 70% over 28 min, t_R = 27 min, 254 nm). The product eluted as a purple liquid. The corresponding product fractions were lyophilized to afford **1.15** (10.0 mg, 14.7 μmol, 27%) as a green solid. Excess *cis*-Rh₂(OAc)₂(TFA)₂ (3 mg, t_R = 26 min) could be re-isolated. ¹H-NMR (500 MHz, 5% v/v MeOD in CDCl₃) δ/ppm: 6.67 (d, *J* = 2.1 Hz, 2H), 5.93 (t, *J* = 2.1 Hz, 1H), 1.89 (s, 6H), 1.36 (s, 12H). ¹³C-NMR (126 MHz, 5% v/v MeOD in CDCl₃) δ/ppm: 192.5, 191.7, 156.4, 121.8, 118.1, 107.7, 81.1, 25.0, 23.6. HRMS (ESI): C₁₈H₂₁BrNaO₁₀Rh₂⁺ *calcd.*: 704.8320, *found*: 704.8311 [M+Na]⁺.



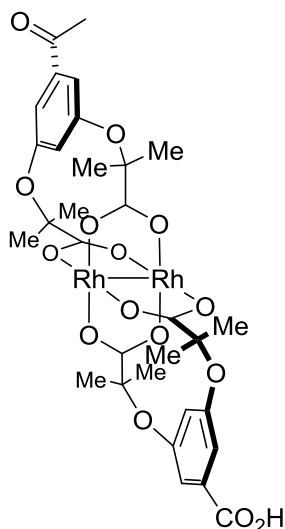
Rhodium complex **1.16**: A dry round bottom flask under a N_2 atmosphere was charged with **1.12d** (23.0 mg, 73.0 μmol , 1.00 eq.) as a solution in EtOAc and all volatiles were subsequently removed under reduced pressure. Then 12 mL of 1,2-dichloroethane were added followed by *cis*- $\text{Rh}_2(\text{OAc})_2(\text{TFA})_2^{282}$ (80.0 mg, 150 μmol , 2.00 eq.). The green-blue solution was immersed into a preheated oil bath at 70°C and stirred for 2 h. A $^1\text{H-NMR}$ aliquot suggested full conversion of the ligand. Thus, all volatiles were removed under reduced pressure to give a green solid. The crude product was then applied as a solution in DMSO (2 mL) to preparative RP-HPLC (MeCN/0.1% TFA in H_2O , 2% to 70% over 25 min, $t_R = 23$ min, 254 nm). The product eluted as a purple liquid. The corresponding product fractions were lyophilized to afford **1.16** (16.0 mg, 25.3 μmol , 35%) as a green solid. Excess *cis*- $\text{Rh}_2(\text{OAc})_2(\text{TFA})_2$ (27 mg, $t_R = 26$ min) could be re-isolated. $^1\text{H-NMR}$ (400 MHz, 5% v/v MeOD in CD_2Cl_2) δ/ppm : 9.83 (s, 1H), 7.00 (d, $J = 2.2$ Hz, 2H), 6.22 (t, $J = 2.2$ Hz, 1H), 1.87 (s, 6H), 1.39 (s, 12H). $^{13}\text{C-NMR}$ (101 MHz, 5% v/v MeOD in CD_2Cl_2) δ/ppm : 192.8, 192.2, 192.0, 157.1, 138.5, 116.2, 115.1, 81.6, 25.2, 23.7. HRMS (ESI): $\text{C}_{19}\text{H}_{22}\text{NaO}_{11}\text{Rh}_2^+$ *calcd.*: 654.9164, *found*: 654.9163 $[\text{M}+\text{Na}]^+$.

Dirhodium tetracarboxylate **1.17** was prepared according to the synthesis protocol of ESPINO *et al.*¹⁷⁴



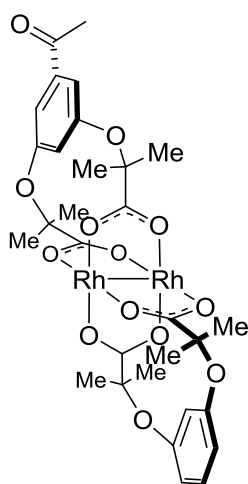
The chelate was synthesized by reacting $\text{Rh}_2(\text{TFA})_4$ (50.0 mg, 77.2 μmol , 1.00 eq.) with six equivalent portions of diacid **1.12a** (43.0 mg, 152 μmol in total, 2.00 eq.) in 1.5 mL 1,2-dichloroethane at 130°C for a total of 3 h. A TLC control (cyclohexane/EtOAc 1:1) indicated full conversion of the $\text{Rh}_2(\text{TFA})_4$. The solvent was removed under reduced pressure to give a green solid (80.0 mg) which was purified by flash chromatography (cyclohexane/EtOAc 9:1). First the mono-substituted complex **1.13** (12.0 mg, 19.9 μmol , 26%) was isolated as a green solid followed by dirhodium tetracarboxylate **1.17** (46.0 mg, 60.0 μmol , 78%) as a green solid. $^1\text{H-NMR}$ (400 MHz, CD_2Cl_2) δ/ppm : 7.11 (t, $J = 8.2$ Hz, 2H), 6.52 (dd, $J = 8.2, 2.1$ Hz, 4H), 5.91 (t, $J = 2.3$ Hz, 2H), 1.39 (s, 24H). $^{13}\text{C-NMR}$ (101 MHz, CD_2Cl_2) δ/ppm : 194.4, 156.4, 130.0, 115.2, 108.8, 81.2, 25.3. HRMS (ESI): $\text{C}_{28}\text{H}_{32}\text{NaO}_{12}\text{Rh}_2^+$ *calcd.*: 788.9923, *found*: 788.9896 $[\text{M}+\text{Na}]^+$.

Dirhodium tetracarboxylate **1.18** was prepared according to the synthesis protocol of dirhodium tetracarboxylate **1.19**.



The chelate was synthesized by reacting dirhodium carboxylate **1.14** (35.0 mg, 54.0 μmol , 1.00 eq.) with three equivalent portions of diacid **1.12c** (19.0 mg, 58.6 μmol in total, 3.00 eq.) in 1,2-dichloroethane (1.5 mL) at 130°C for a total of 105 min. A TLC control (cyclohexane/EtOAc 1:1) indicated full conversion of the dirhodium carboxylate **1.14**. Upon cooling down the mixture to room temperature a green solid precipitated (26.0 mg). The supernatant was collected and the solvent was evaporated under reduced pressure to give 30 mg of a green solid. ESI-MS analysis indicated unreacted diacid **1.12c** as well as $\text{Rh}_2(\text{OAc})_4(\text{N,N-dimethylaniline})_2$. ESI-MS analysis of the remaining green precipitate indicated the desired product mass along with some impurities. The crude was purified by flash chromatography (cyclohexane/EtOAc 4:1 to 1:2) to afford dirhodium tetracarboxylate **1.18** (12.0 mg, 14.0 μmol , 26%) as a pale blue solid. $^1\text{H-NMR}$ (600 MHz, 5% v/v MeOD in CD_2Cl_2) δ /ppm: 7.17 (d, $J = 2.3$ Hz, 2H), 7.07 (d, $J = 2.2$ Hz, 2H), 6.15 (t, $J = 2.3$ Hz, 1H), 6.12 (t, $J = 2.2$ Hz, 1H), 2.50 (s, 3H), 1.37 (s, 12H), 1.37 (s, 12H). $^{13}\text{C-NMR}$ (151 MHz, 5% v/v MeOD in CD_2Cl_2) δ /ppm: 197.7, 193.6, 167.8, 156.6, 156.4, 139.3, 132.1, 116.8, 115.0, 113.8, 113.3, 81.4, 81.4, 30.3, 27.1, 25.2, 25.2. HRMS (ESI): $\text{C}_{31}\text{H}_{34}\text{NaO}_{15}\text{Rh}_2^+$ *calcd.*: 874.9922, *found*: 874.9900 $[\text{M}+\text{Na}]^+$.

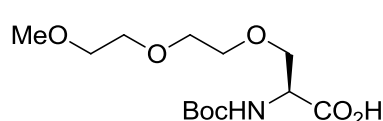
Dirhodium tetracarboxylate **1.19** was prepared according to a slightly modified procedure described by DU BOIS *et al.*¹⁷⁴



A 4 mL microwave vial equipped with a stirring bar was charged with dirhodium complex **1.13** (72.0 mg, 119 μmol , 1.00 eq.) and dissolved in 1.5 mL 1,2-dichloroethane. To this solution was added diacid **1.12c** (16.0 mg, 49.1 μmol , 0.34 eq.) and the vial was sealed with the corresponding cap and heated to 130°C in an oil bath. After 35 min the vial was removed from the oil bath and cooled down to room temperature in a H_2O bath. Another portion of diacid **1.12c** (14.0 mg, 42.9 μmol , 0.31 eq) was added before resealing the vial. The mixture was heated to 130°C for another 35 min, cooled down to room temperature and charged with the third portion of diacid **1.12c** (15.0 mg, 46.0 μmol , 0.33 eq), sealed and heating was resumed at 130°C for another 35 min. After the mixture was allowed to cool down to room temperature the solvent was evaporated under reduced pressure to give a dark green solid which was purified by flash chromatography (cyclohexane/EtOAc 4:1 to 2:3). A light green solid was isolated (76 mg) which was purified again by flash chromatography (cyclohexane/EtOAc 9:1 to 1:1). Three green bands were isolated where the

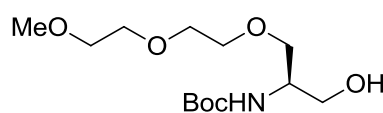
second one was identified as the desired product. Dirhodium tetracarboxylate **1.19** (39.0 mg, 48.3 μmol , 41%). $^1\text{H-NMR}$ (400 MHz, $\text{DMSO-}d_6$) δ/ppm : 7.10 (t, $J = 8.0$ Hz, 1H), 7.05 (d, $J = 2.2$ Hz, 2H), 6.49 (dd, $J = 8.1, 2.3$ Hz, 2H), 6.03 (t, $J = 2.2$ Hz, 1H), 5.83 (t, $J = 2.3$ Hz, 1H), 2.51 (s, 3H), 1.31 (s, 12H), 1.28 (s, 12H). $^{13}\text{C-NMR}$ (101 MHz, DMSO) δ/ppm : 197.2, 193.1, 192.6, 155.6, 155.4, 138.6, 129.4, 114.8, 114.4, 112.5, 108.5, 80.6, 80.1, 26.9, 24.5, 24.4 (one carbon missing). HRMS (ESI): $\text{C}_{30}\text{H}_{34}\text{NaO}_{13}\text{Rh}_2^+$ *calcd.*: 831.0024, *found*: 831.0002. *calcd.*: 788.9923, *found*: 788.9896 $[\text{M}+\text{Na}]^+$.

Serine methylether **1.33** was prepared according to LY *et al.*¹⁸⁸ Spectroscopic data was in agreement with their published data.



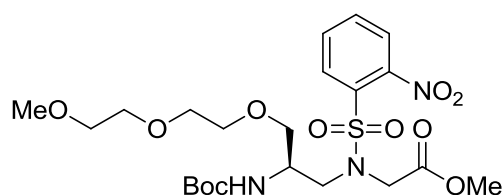
It is noteworthy to mention that the crude product was purified by flash chromatography using 2.5-10% MeOH in CH_2Cl_2 . $^1\text{H-NMR}$ (400 MHz, CDCl_3) δ/ppm : 5.59 (d, $J = 6.8$ Hz, 1H), 4.46-4.37 (m, 1H), 3.98-3.89 (m, 1H), 3.78-3.69 (m, 2H), 3.67-3.56 (m, 7H), 3.41 (s, 3H), 1.45 (s, 9H). LRMS (FAB): $\text{C}_{13}\text{H}_{25}\text{NNaO}_7^+$ *calcd.*: 330.1, *found*: 330.1 $[\text{M}+\text{Na}]^+$, $\text{C}_{13}\text{H}_{26}\text{NO}_7^+$ *calcd.*: 308.2, *found*: 308.1 $[\text{M}+\text{H}]^+$.

Primary alcohol **1.34** was prepared according to LY *et al.*¹⁸⁸ Spectroscopic data was in agreement with their published data.



It is noteworthy to mention that the crude product was purified by flash chromatography using 2:1 EtOAc/cyclohexane and later 5% MeOH in EtOAc. $^1\text{H-NMR}$ (400 MHz, CDCl_3) δ/ppm : 5.26 (s_{br}, 1H), 3.85-3.71 (m, 2H), 3.70-3.61 (m, 9H), 3.57-3.53 (m, 2H), 3.39 (s, 3H), 1.45 (s, 9H). LRMS (FAB): $\text{C}_{13}\text{H}_{28}\text{NO}_6^+$ *calcd.*: 294.2, *found*: 294.2 $[\text{M}+\text{H}]^+$, $\text{C}_8\text{H}_{20}\text{NO}_4^+$ *calcd.*: 194.1, *found*: 194.1 $[\text{M}-\text{C}_5\text{H}_8\text{O}_2]^+$.

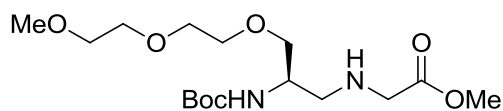
Nosyl sulfonamide **1.35** was prepared in analogy to LY *et al.*¹⁸⁸



To a stirred, cold solution of **1.40** (1.12 g, 4.09 mmol, 1.00 eq.), triphenylphosphine (1.07 g, 4.91 mmol, 1.00 eq.), and compound **1.34** (1.20 g, 4.09 mmol, 1.00 eq.) in dry THF (8 mL) under an inert atmosphere was added DEAD (1.86 mL, 4.09 mmol, 1.00 eq., 40% in toluene) dropwise over a period of 30 min at 0°C . The reaction mixture was allowed to warm to room temperature and then stirred for 14 h. The solvent was evaporated, and the oily residue was purified by

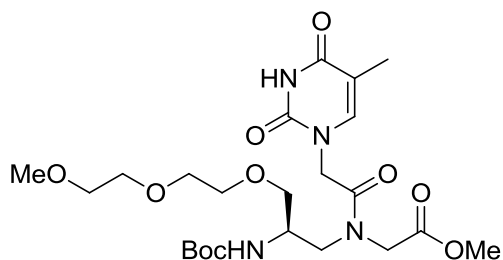
flash chromatography (1:1 EtOAc/cyclohexane) to give **1.35** (1.51 g, 2.75 mmol, 67%) as a yellow oil. ¹H-NMR (400 MHz, CDCl₃) δ/ppm: 8.12-8.03 (m, 1H), 7.72-7.66 (m, 2H), 7.61-7.57 (m, 1H), 5.15 (d, *J* = 8.4 Hz, 1H), 4.45-4.34 (m, 1H), 4.26-4.17 (m, 1H), 3.95-3.85 (m, 1H), 3.71-3.46 (m, 15H), 3.39 (s, 3H), 1.45 and 1.42 (2 x s, 9H, rotamers). Mass spectrometry was unsuccessful although electron impact (EI) and FAB ionization were used.

Methyl ester **1.36** was prepared in analogy to FUKUYAMA *et al.*²⁸⁵



An oven dried 4 mL vial, equipped with a magnetic stirring bar and a rubber septum was charged with thiophenol (345 μL, 3.38 mmol, 2.50 eq.) and dissolved in MeCN (1 mL) under an N₂ atmosphere. While cooling with an ice bath, a solution of KOH_(aq) (10.9 M, 2.50 eq.) was added at once and the mixture allowed to warm up to room temperature. Then a solution of **1.35** (743 mg, 1.35 mmol, 1.00 eq.) dissolved in MeCN (1 mL) was added dropwise over 2 min. The reaction was heated to 50°C for 1 h (TLC, 10% MeOH/CH₂Cl₂ indicated full conversion), cooled to room temperature, diluted with 5 mL of H₂O and extracted with CH₂Cl₂ (3 x 10 mL). The combined organics were washed with 5 mL brine, dried over MgSO₄ and concentrated under reduced pressure to give 1.06 g of a yellow malodorous oil. The crude was purified by flash chromatography (1% MeOH/CH₂Cl₂ to 10% MeOH/CH₂Cl₂) to give **1.36** (518 mg, 1.42 mmol, 105%, containing approximately 6% of PPh₃=O) as a light yellow oil. Therefore the yield can be given as 99%. ¹H-NMR (400 MHz, CDCl₃) δ/ppm: 5.16 (s_{br}, 1H), 3.84-3.39 (m, 15H), 3.38 (2 x s, 3H, rotamers), 2.82 and 2.72 (2 x dd, *J* = 6.0 Hz, 2H, rotamers), 1.75 (s_{br}, 2H), 1.44 (2 x s, 9H, rotamers). LRMS (FAB): C₁₆H₃₂N₂NaO₇⁺ *calcd.*: 387.2, *found*: 387.2 [M+Na]⁺, C₁₆H₃₃N₂O₇⁺ *calcd.*: 365.2, *found*: 365.2 [M+H]⁺, C₁₁H₂₅N₂O₅⁺ *calcd.*: 265.2, *found*: 265.2 [M-C₅H₈O₂]⁺.

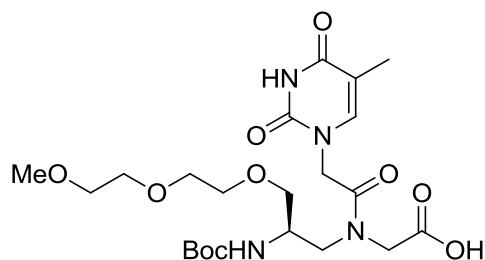
Amide **1.37** was prepared in analogy to BIALY *et al.*²⁸⁶



To a solution of **1.42** (230 mg, 1.25 mmol, 1.10 eq.) and **1.36** (415 mg, 1.14, 1.00 eq.) in 4 mL of dry DMF at 0°C was added PyBrop (559 mg, 1.14 mmol, 1.00 eq.) and DIPEA (395 μL, 2.28 mmol, 2.00 eq.). The ice bath was removed and the reaction was stirred at room temperature for 4.5 h (TLC, 10% MeOH/CH₂Cl₂ indicated full conversion of the amine). The solvent was evaporated under reduced pressure and dried under high vacuum over night. The next day the crude turbid residual oil was dissolved in 15 mL CH₂Cl₂ and extracted with 1 M KHSO₄ (15 mL), 10% NaHCO₃ (15 mL) and brine (15 mL). The combined organics were re-extracted with H₂O (5 mL), dried over MgSO₄ and concentrated to give 1.02 g of a yellow oil. The crude product was then applied on a 50g C-18 reverse phase column and eluted using a

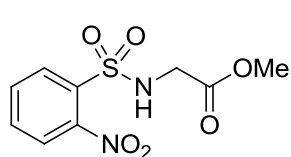
Biotage Isolera Four device (MeCN in H₂O, 0-40% over 13 CV). The product fractions were lyophilized to afford **1.37** (321 mg, 605 μmol, 53%) as a white solid. ¹H-NMR (400 MHz, DMSO-*d*₆) δ/ppm: 11.29 (s, 1H), 7.31-7.21 (m, 1H), 6.91-6.57 (2 x d, *J* = 8.4 Hz, 1H), 4.75-4.39 (2 x q, *J* = 16.7 Hz, 2H), 4.34 (s, 1H), 4.14-4.05 (m, 1H), 4.04-3.95 (m, 1H), 3.89-3.78 (m, 1H), 3.72 (s, 1H), 3.62 (s, 2H), 3.59-3.45 (m, 8H), 3.44-3.35 (m, 3H), 3.35-3.25 (m, 3H), 3.23 and 3.22 (2 x s, 3H, rotamers), 1.75 (s, 3H), 1.38 and 1.37 (2 x s, 9H, rotamers). Please note that there are too many proton signals (41 instead of 38) and it was not clear to us which signals don't belong to the product. It is assumed that the signal at 3.33 ppm where residual H₂O would resonate in DMSO-*d*₆ has a bigger integral and potentially contributes to the additional protons since it overlaps with product signals. UPLC-MS (ESI): *t*_R = 2.714 min, C₂₃H₃₈N₄NaO₁₀⁺ *calcd.*: 553.2, *found*: 553.3 [M+Na]⁺, C₁₈H₃₁N₄O₈⁺ *calcd.*: 431.2, *found*: 431.2 [M-C₅H₈O₂]⁺.

Carboxylic acid **1.38** was prepared in analogy to BIALY *et al.*²⁸⁶



Amide **1.37** (334 mg, 630 μmol, 1.00 eq.) was dissolved in 3.5 mL of MeOH followed by the addition of 3.5 mL of a 2M Cs₂CO₃ solution at room temperature. The reaction mixture was then stirred for 2 h (TLC, 5% MeOH/CH₂Cl₂ indicated full conversion). After the MeOH was evaporated under reduced pressure 5 mL of H₂O were added. The mixture was then extracted with EtOAc (3 x 10 mL). The combined aqueous layers were acidified at 0°C with 5% HCl to pH ~1-2 and then extracted with EtOAc (4 x 15 mL), dried over MgSO₄, filtered and concentrated under reduced pressure to give 200 mg of a white solid after extensive drying under high vacuum over night. ¹H-NMR and UPLC-MS analysis indicated the desired product **1.38** (200 mg, 387 μmol, 61%) which was clean enough for further usage. ¹H-NMR (400 MHz, DMSO-*d*₆) δ/ppm: 12.58 (s_{br}, 1H), 11.29 (s, 1H), 7.28 and 7.25 (2 x s, 1H, rotamers), 6.87 and 6.67 (2 x d, *J* = 8.6 Hz, 1H, rotamers), 4.66 (q, *J* = 16.4 Hz, 2H), 4.50-4.42 (m, 1H), 4.22 (s, 1H), 4.02-3.88 (m, 1H), 3.87-3.70 (m, 1H), 3.58-3.45 (m, 7H), 3.44-3.34 (m, 3H), 3.31-3.25 (m, 1H), 3.23 and 3.22 (2 x s, 3H, rotamers), 1.91 (s, 1H), 1.75 (s, 3H), 1.37 (s, 9H). LRMS (ESI): C₂₂H₃₅N₄O₁₀⁻ *calcd.*: 515.2, *found*: 515.3 [M-H]⁻. UPLC-MS (ESI): *t*_R = 2.279 min, C₂₂H₃₆N₄NaO₁₀⁺ *calcd.*: 539.2, *found*: 553.3 [M+Na]⁺, C₁₇H₂₉N₄O₈⁺ *calcd.*: 417.2, *found*: 417.2 [M-C₅H₈O₂]⁺.

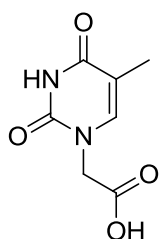
Nosyl sulfonamide **1.40** was prepared according to FUKUYAMA *et al.*²⁸⁷ Spectroscopic data was in agreement with their published data.



¹H-NMR (500 MHz, CDCl₃) δ/ppm: 8.12-8.07 (m, 1H), 7.97-7.91 (m, 1H), 7.78-7.71 (m, 2H), 6.04 (t, *J* = 5.5 Hz, 1H), 4.03 (d, *J* = 5.9 Hz, 2H), 3.61 (s, 3H). ¹³C-NMR (126 MHz, CDCl₃) δ/ppm: 169.1, 134.1, 133.8, 133.1, 130.7, 125.8, 52.7, 44.9. LRMS (FAB): C₉H₁₁N₂O₆S⁺ *calcd.*: 275.0, *found*:

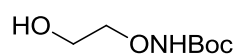
275.0 [M+H]⁺.

Thymine-1-acetic acid **1.42** was prepared according to KATRITZKY *et al.*¹³³ Spectroscopic data was in agreement with their published data.



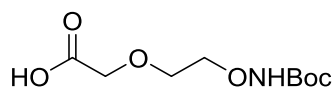
¹H-NMR (500 MHz, CDCl₃) δ/ppm: 13.13 (s_{br}, 1H), 11.34 (s, 1H), 7.49 (s, 1H), 4.36 (s, 1H), 1.75 (s, 3H). LRMS (ESI): C₇H₈N₂NaO₄⁺ *calcd.*: 207.0, *found*: 206.9 [M+Na]⁺, C₇H₉N₂O₄⁺ *calcd.*: 185.0, *found*: 184.9 [M+H]⁺.

Compound **1.49** was prepared in analogy to a literature procedure by MAYNAR *et al.*²⁸⁸



In a flame dried flask under N₂ atmosphere, 2-bromoethanol (**1.47**) (300 μL, 4.11 mmol, 1.00 eq.) and *tert*-butyl *N*-hydroxycarbamate (**1.48**) (1.15 g, 8.21 mmol, 2.00 eq.) were dissolved in 10 mL of dry CH₂Cl₂. Then DBU (614 μL, 4.11 mmol, 1.00 eq., filtered over neutral aluminum oxide) was added dropwise and the mixture stirred for 72 h at room temperature. Next, it was diluted with another 10 mL of CH₂Cl₂ and extracted with H₂O (3 x 10 mL). The combined organics were dried over MgSO₄, filtered and concentrated under reduced pressure to give 323 mg of a slight yellow oil. Since the mass balance was too low, the aqueous phase was concentrated (50°C, 23 mbar) and the organic residue combined with the first portion to give 2.64 g of a slight yellow oil. The crude was purified by flash chromatography (cyclohexane/EtOAc 4:1 to 1:1) to afford **1.49** (511 mg, 2.88 mmol, 70%) as a colorless oil. TLC (cyclohexane/EtOAc, 2:1, KMnO₄) R_f = 0.14. ¹H-NMR (500 MHz, CDCl₃) δ/ppm: 7.22 (s_{br}, 1H), 3.92-3.89 (m, 2H), 3.75-3.72 (m, 2H), 1.49 (s, 9H). ¹³C-NMR (126 MHz, CDCl₃) δ/ppm: 158.72, 82.87, 78.42, 59.57, 28.27. HRMS (ESI): C₇H₁₅NNaO₄⁺ *calcd.*: 200.0893, *found*: 200.0894 [M+Na]⁺.

Compound **1.50** was prepared in analogy to a literature procedure by YEUNG *et. al.*²⁸⁹

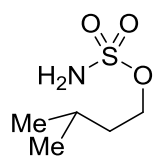


To an ice-cold, stirred suspension of NaH (24.0 mg, 600 μmol , 3.54 eq., 60% in mineral oil) in dry THF (300 μL) was added a solution of alcohol **1.49** (30.0 mg, 169 μmol , 1.00 eq.) in dry THF (100 μL) dropwise. After 10 min a solution of bromoacetic acid (24.0 mg, 171 μmol , 1.01 eq.) in dry THF (100 μL) was added dropwise and the reaction mixture stirred at 70°C. The progress of the reaction was monitored by UPLC-MS at 195 nm and after 2.5 h the reaction mixture was diluted with H₂O (3 mL) and washed with Et₂O (2 x 3 mL). The aqueous phase was then acidified with cold 1M HCl to pH 1 and quickly extracted with Et₂O (3 x 3 mL). The combined organics were washed with brine (5 mL), dried over MgSO₄, filtered and concentrated under reduced pressure to give the desired acid (**1.50**) (19.0 mg, 80.8 μmol , 43%) as a clear semisolid. ¹H-NMR indicated a purity of 91% with some residual starting alcohol **1.49**. The batch was pure enough to be used for a peptide coupling reaction and was used without further purification. ¹H-NMR (400 MHz, CDCl₃) δ /ppm: 8.09 (s_{br}, 1H), 7.77 (s, 1H), 4.18 (s, 2H), 4.06-4.01 (m, 2H), 3.80-3.76 (m, 2H), 1.47 (s, 9H). ¹³C-NMR (101 MHz, CDCl₃) δ /ppm: 173.59, 157.47, 82.48, 75.39, 69.60, 68.34, 28.32. HRMS (ESI): C₉H₁₇NNaO₆⁺ *calcd.*: 258.0948, *found*: 258.0950 [M+Na]⁺.

4.2.1.2 Substrate synthesis and experimental details for dirhodium catalyzed nitrene, C-H and O-H insertion

Nitrene insertion

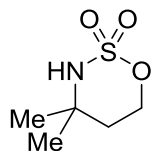
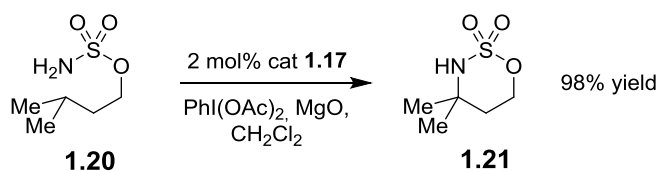
Sulfamate ester **1.20** was prepared according to a published procedure by FRUIT *et al.*²⁹⁰ The analytical



data is in agreement with the values reported by DILLON *et al.*²⁹¹

¹H-NMR (500 MHz, CDCl₃) δ/ppm: 4.97 (s_{br}, 2H), 4.24 (t, *J* = 6.8 Hz, 2H), 1.81-1.70 (m, 1H), 1.63 (q, *J* = 6.8 Hz, 2H), 0.94 (d, *J* = 6.6 Hz, 6H).

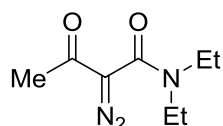
The intramolecular nitrene insertion was performed on a 646 μmol scale according to and compared with the results of BRODSKY *et al.*²⁹²



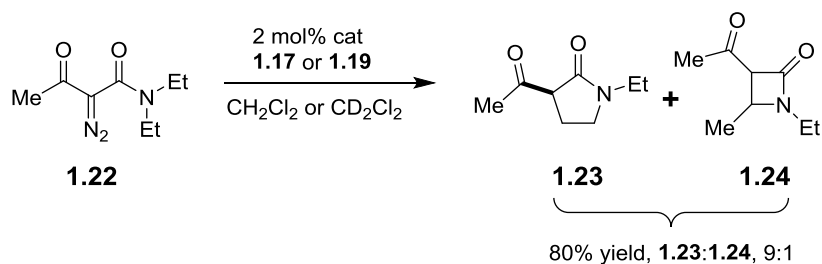
The oxathiazinane **1.21** was isolated as a white, crystalline solid (105 mg, 636 μmol, 98%). ¹H-NMR (400 MHz, CDCl₃) δ/ppm: 4.70-4.65 (m, 2 H), 4.15 (s_{br}, 1 H), 1.79-1.73 (m, 2H), 1.42 (s, 6H). ¹³C-NMR (101 MHz, CDCl₃) δ/ppm: 69.30, 56.56, 35.61, 28.36.

C-H insertion

α-diazoacetamide **1.22** was prepared in two steps according to HOFFMAN *et al.*²⁹³ and ROBBACH *et al.*²⁹⁴

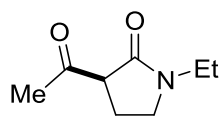


¹H-NMR (500 MHz, CDCl₃) δ/ppm: 3.39 (q, *J* = 7.1 Hz, 4H), 2.34 (s, 3H), 1.20 (t, *J* = 7.2 Hz, 6H).



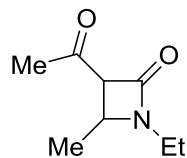
To a solution of α -diazoacetamide **1.22** (43.3 mg, 236 μmol , 1.00 eq.) in CH_2Cl_2 (1.18 mL), a stock solution of dirhodium catalyst **1.17** (1.18 mL, 4 mM in CH_2Cl_2 , 2 mol%) was added and the reaction mixture was stirred at room temperature. Analysis of the mixture by $^1\text{H-NMR}$ spectroscopy after 10 min indicated full conversion of the starting material to the C-H insertion products in a ratio of 9:1 (**1.23**:**1.24**). The solvent was removed under reduced pressure and the residue was purified by flash chromatography (EtOAc/cyclohexane 3:1) to afford γ -lactam **1.23** (5.20 mg, 33.5 μmol , 14%) and β -lactam **1.24** (24.1 mg, 155 μmol , 66%) as colorless oils. (This synthesis was performed by Stefanie Geigle)

γ -lactam **1.23**:



$^1\text{H-NMR}$ (250 MHz, CDCl_3) δ/ppm : 3.54 (dd, $J = 9.2, 6.0$ Hz, 1H), 3.42 – 3.30 (m, 2H), 3.27 (q, $J = 7.3$ Hz, 2H), 2.49 (ddt, $J = 12.8, 8.5, 5.7$ Hz, 1H), 2.38 (s, 3H), 1.99 (dtd, $J = 13.1, 8.9, 5.5$ Hz, 1H), 1.07 (t, $J = 7.2$ Hz, 3H). $^{13}\text{C-NMR}$ (101 MHz, CDCl_3) δ/ppm : 204.00, 169.35, 55.99, 44.87, 37.66, 30.05, 19.59, 12.44.

β -lactam **1.24**:



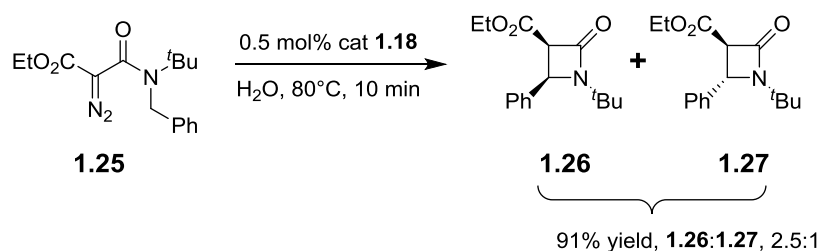
$^1\text{H-NMR}$ (250 MHz, CDCl_3) δ/ppm : 4.08 (qd, $J = 6.3, 2.1$ Hz, 1H), 3.71 (d, $J = 2.1$ Hz, 1H), 3.43-3.27 (m, 1H), 3.07 (dtd, $J = 14.6, 7.4, 6.6$ Hz, 1H), 2.30 (s, 3H), 1.34 (d, $J = 6.2$ Hz, 3H), 1.17 (t, $J = 7.3$ Hz, 3H). $^{13}\text{C-NMR}$ (101 MHz, CDCl_3) δ/ppm : 200.80, 162.40, 69.51, 48.56, 35.38, 29.97, 17.82, 13.34.

For comparison the dirhodium catalyst **1.19** was tested in a $^1\text{H-NMR}$ reaction. A stock solution of **1.19** (810 μg , 1.00 μmol , 2 mol%) in CD_2Cl_2 (250 μL , Cambridge Isotope Laboratories, Inc.) was prepared adding one drop of $\text{MeOD-}d_4$ for complete catalyst dissolution. A second stock solution of the α -diazoacetamide **1.22** (9.20 mg, 50.2 μmol , 1.00 eq.) in CD_2Cl_2 (250 μL) was prepared.

¹H-NMR reaction setup

250 μL of the α -diazooacetamide **1.22** stock solution was transferred into a NMR tube (throw away quality) and mixed with 250 μL of the dirhodium catalyst **1.19** stock solution. Time was taken after catalyst addition and the NMR tube was shaken on a Vortex Genie2. After 10 min the first measurement indicated $\geq 95\%$ conversion with a product ratio of 9:1 (**1.23**:**1.24**). (These experiments were performed by Stefanie Geigle and Daniel Bachmann)

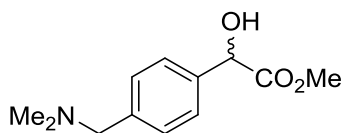
α -diazooacetamide **1.25** was prepared in two steps according to QI *et al.*²⁹⁵ and CHOI *et al.*²⁹⁶ Spectroscopic data was in agreement with their published data. (This synthetic sequence was performed by Stefanie Geigle)



To a suspension of α -diazooacetamide **1.25** (21.5 mg, 70.6 μmol , 1.00 eq.) in H_2O (671 μL) a stock solution of dirhodium catalyst **1.18** (71.7 μL , 4.93 mM in H_2O /500 mM MES, pH = 7.6, few drops 1M NaOH for solubility, 0.5 mol%) were added and the reaction mixture was stirred at 80°C . Analysis of the mixture by ¹H-NMR spectroscopy after 10 min indicated full conversion of the starting material to the target C-H insertion products. The obtained white solid was filtered off and washed with H_2O to afford the β -lactams **1.26** and **1.27** (17.6 mg, 63.9 μmol , 91%) as a white solid. (This synthesis was performed by Stefanie Geigle)

O-H insertion

The synthesis and spectroscopic characterization of α -diazoester **1.28**, as well as its catalytic decomposition to **1.29** has been previously described by our group.³⁶



O-H insertion product **1.29**: A stock solution of **1.28** (125 mM in MES pH 6, ca. 0.7 mL) was treated with $\text{Rh}_2(\text{OAc})_4$ (4.00 mg, 89.0 μmol , 10 mol%) and the mixture stirred under ambient conditions. The progress of the reaction was monitored by UPLC-MS (254 nm) and after stirring for two days the creamy pink solution was lyophilized. The grayish solid was dissolved in CH_2Cl_2 and the precipitate (MES) was filtered off through a plug of cotton followed by removal of the solvent under reduced pressure. The crude sample was purified by flash chromatography on a Biotage Isolera Four device (20% MeOH/ CH_2Cl_2). The product eluted after two column volumes and the purity of the fractions was analyzed by TLC (20% MeOH/ CH_2Cl_2 , KMnO_4). The pure fractions were combined and concentrated under reduced pressure to give **1.29** (8.40 mg, 37.6 μmol , 43%) as colorless oil which crystallized upon standing. TLC (20% MeOH/ CH_2Cl_2 , KMnO_4) $R_f = 0.26$. $^1\text{H-NMR}$ (400 MHz, CDCl_3) δ/ppm : 7.39-7.35 (m, 2H), 7.33-7.29 (m, 2H), 5.17 (s, 1H), 3.76 (s, 3H), 3.43 (s, 2H), 2.23 (s, 6H). $^{13}\text{C-NMR}$ (126 MHz, CDCl_3) δ/ppm : 174.25, 138.72, 137.42, 129.64, 126.74, 72.86, 63.85, 53.16, 45.22. HRMS (ESI): $\text{C}_{12}\text{H}_{18}\text{NO}_3^+$ *calcd.*: 224.1287, *found*: 224.1284 $[\text{M}+\text{H}]^+$.

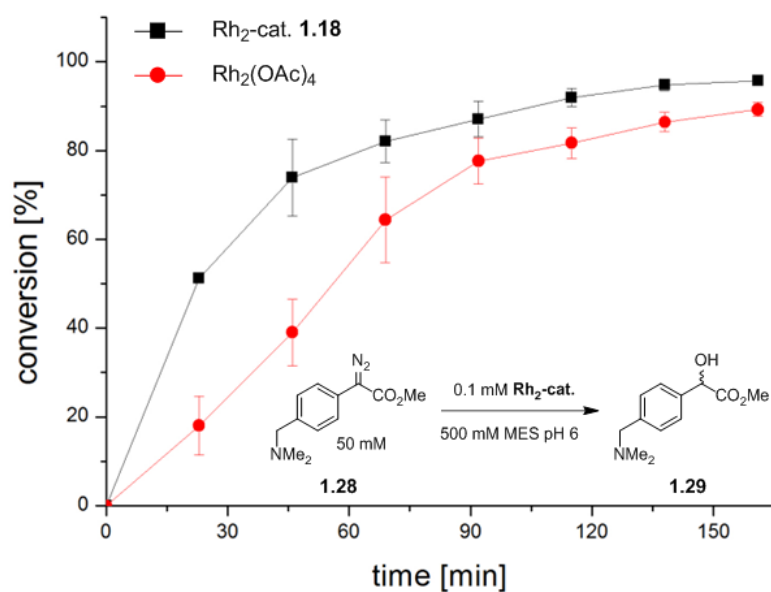
The catalytic comparison of dirhodium catalyst **1.18** with $\text{Rh}_2(\text{OAc})_4$ in an O-H insertion reaction by water was performed using HPLC on an Agilent 1100 LC system equipped with a Chromolith Performance RP18e 4.6×100 mm column from Merck with a flow rate of 1 mL/min. Elution was performed using the following gradient: 0-80% MeCN in $\text{H}_2\text{O}/0.1\%$ TFA in 16 min, then 80% in 2 min.

The following stock solutions were used for this experiment:

α -diazoester **1.28** (250 mM in 500 mM MES, pH 6), $\text{Rh}_2(\text{OAc})_4$ (1 mM in H_2O) and dirhodium catalyst **1.18** (4.90 mM in $\text{H}_2\text{O}/500$ mM MES, pH = 7.6, few drops 1M NaOH for solubility).

Reaction setup

Typically 20 μL reaction mixtures containing 0.1 mM $\text{Rh}_2\text{-cat}$, 50 mM α -diazooester **1.28** and H_2O in a HPLC vial (Agilent) were kept at room temperature and analyzed by injecting 2 μL of the reaction mixture every 23 min for a total of 160 min. Conversions (%) were determined by integrating the peak area of starting α -diazooester **1.28** at 254 nm and plotted against the time (min). For both catalysts triplicate measurements were done and the data points in the plotted graph below represent the mean values including their experimental error.



4.2.1.3 Synthesis of PNA, PNA-Rh₂ catalysts and oligonucleotides

Manual solid-phase PNA synthesis according to the Fmoc-strategy

For manual PNA synthesis, the rink amide AM resin (100-200 mesh, attached to aminomethylpolystyrene, 0.61 mmol/g, from Novabiochem) was weighed and added to a 2 mL polyethylene syringe equipped with a plunger and a fritted disc. This resin contains a linker which yields a C-terminal amide upon TFA cleavage of the final PNA. Syntheses were routinely carried out on a 10-20 μ mol scale based upon the stated loading capacity of the resin. The dry resin was swollen with *N*-methylpyrrolidinone (NMP, peptide grade from IRIS) for 1 h at room temperature, reacted with two successive portions of 20 or 40% piperidine (Alfa or Sigma) in NMP for 10 min (Fmoc removal), then washed three times with NMP/CH₂Cl₂ 1:1 for 1 min. PNA coupling was achieved at room temperature through careful shaking of the reactor fixed on top of a vortex-genie 2 (Scientific Industries) by treating the resin for 20-30 min with a fourfold excess of PNA monomer (Panagene or **1.38**) in NMP (0.1 M) containing four equivalents each of HATU (Fluorochem), DIPEA (Sigma) and 2,4,6-collidine (Acros).¹³⁶ Couplings were repeated for each Fmoc-PNA-G(Bhoc)-OH monomer using a freshly prepared coupling solution. When amino acid couplings were performed (PNA **1.4**, **1.8** and **1.30**), the resin was treated for 30 min with a fivefold excess of amino acid (Bachem) in DMF (0.5 M, peptide grade from IRIS) containing five equivalents of HCTU (Novabiochem), 13.5 eq. of DIPEA (Sigma) and 11.5 eq. of 2,6-lutidine (Sigma) according to a published procedure.²⁹⁷ For commercial amino acids this coupling was repeated once to ensure completion. Unreacted amino groups were “capped” with 5% Ac₂O and 6% 2,4,6-collidine in NMP for 5-10 min. Capping was usually done prior to cleavage after coupling of PNA monomer **1.38** and in general after double couplings. After coupling or capping, the resin was washed three times with NMP/CH₂Cl₂ 1:1 for 1 min, then the appropriate number of iterations of the deprotection/coupling cycle was performed as described above. When a coupling was performed the next day, the Fmoc-protected resin was washed first with three portions of NMP/CH₂Cl₂ 1:1 for 1 min followed by a triple wash with CH₂Cl₂ for 1 min, dried under high vacuum for at least 10 min and stored at -20°C after the previous coupling. The same procedure was performed when the resin-bound and fully protected PNA had to be stored after its final assembly.

Resin cleavage and PNA isolation

For cleavage, the dry resin was weighed and transferred to a fresh 1 or 2 mL polyethylene syringe equipped with a plunger and a fritted disc. A mixture of TFA/*m*-cresol/thioanisole/TFMSA (6:1:1:2)¹³⁶ for PNA **1.4** or TFA/TIS/H₂O (95:2.5:2.5)²⁹⁸ for PNA **1.4**, **1.8**, **1.30**, **1.45** and **1.51/1.53**. (1-2 mL) was added. The reactor was closed with a luer stopper and the mixture was gently shaken on top of a vortexer at room temperature for 2 h. The PNA-containing cleavage cocktail was transferred into a 2 mL Eppendorf plastic vial and carefully concentrated (30 mbar, 40-45°C) under reduced pressure to 0.1-0.2 mL. To the residual oil was added ice-cold Et₂O (1-1.5 mL) to precipitate the PNA. The Eppendorf tube was closed, vortexed and centrifuged at room temperature (2500 rpm, 3 min). The

supernatant was carefully discarded using a pipette and the beige PNA pellet was diluted with fresh ice-cold Et₂O, vortexed and centrifuged. This process was done for a total of three times and the final crude PNA was then air dried.

Purification and analysis

The crude PNA pellet was dissolved in 100-500 µL of Milli-Q water and purified by preparative RP-HPLC at 254 nm with a flow rate of 5 mL/min using MeCN and H₂O containing 0.1% TFA as eluents. All product fractions were re-analyzed by LC-MS prior to lyophilization. The corresponding gradients used for the purification of each individual compound as well as the UPLC-MS or MALDI-TOF-MS analysis data are given on the next page(s).

Stock solutions

The purified and re-analyzed white PNA powder (5-25 mg) was dissolved in Milli-Q water (20-100 µL) and the concentration of the stock solutions determined using a NanoDrop 2000 spectrophotometer from Thermo Scientific with a path length of 1 mm. For each individual PNA the extinction coefficient (ϵ) was calculated according to the guidelines provided by Panagene Inc.¹⁴⁰ Triplicate measurements of various dilutions were performed and the final concentration was calculated according to **equation 3** as the average of all concentrations.

$$c = \frac{A_{260} d_f}{d \epsilon} \quad (3)$$

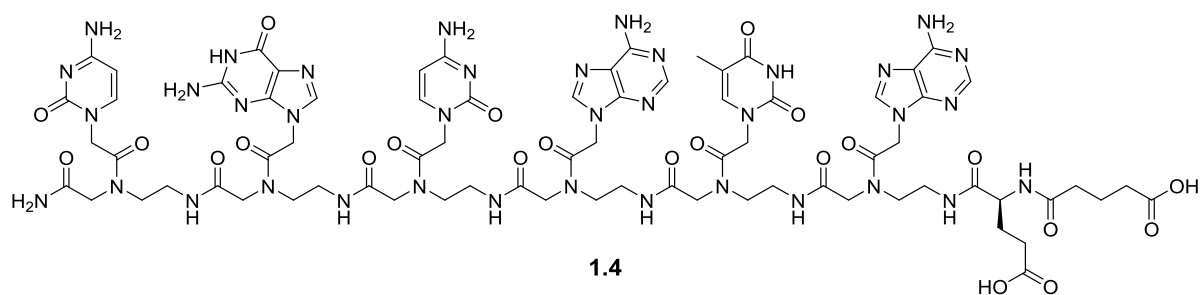
Equation 3: c = concentration [mol/L], A₂₆₀ = absorption at 260 nm (< 1), d_f = dilution factor, d = path length [cm], ϵ = extinction coefficient [L/mol cm].

All stock solutions were stored at -20°C if not used. For reactions the corresponding PNA stock solution was thawed up, vortexed and the appropriate amount added to the respective reaction vial with a Gilson pipette. When a stock solution was used after more than 4-6 months, the concentration was determined again as described above.

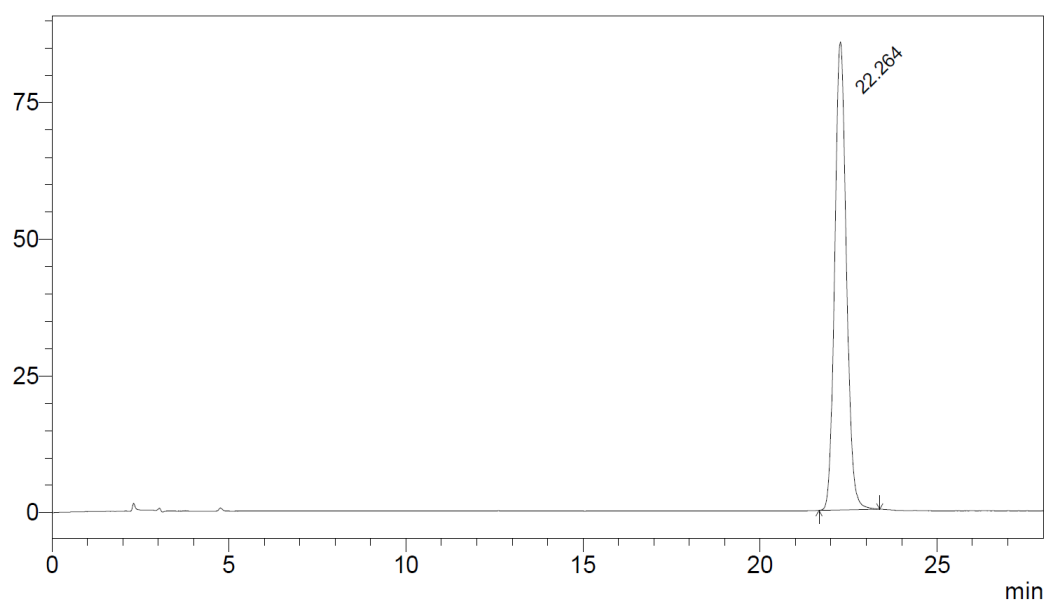
Qualitative chloranil test¹⁶⁸

A few beads (2-4 mg) were placed in a petri dish and treated with three drops of 2% acetaldehyde in DMF and three drops of 2% chloranil in DMF and left at room temperature for 5 min. The beads were then inspected under a microscope. Blue beads indicated free amines (positive) whereas colorless beads were indicative for protected amino groups (negative).

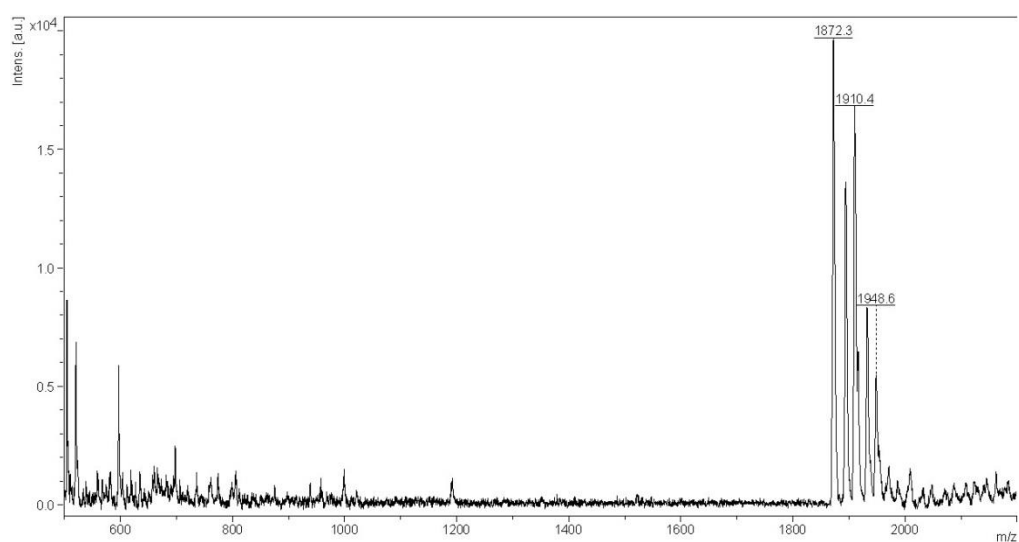
PNA-diacid 1.4:



Chemical Formula: $C_{74}H_{95}N_{37}O_{23}$; Exact Mass: 1869.7402 ; Molecular Weight: 1870.8100

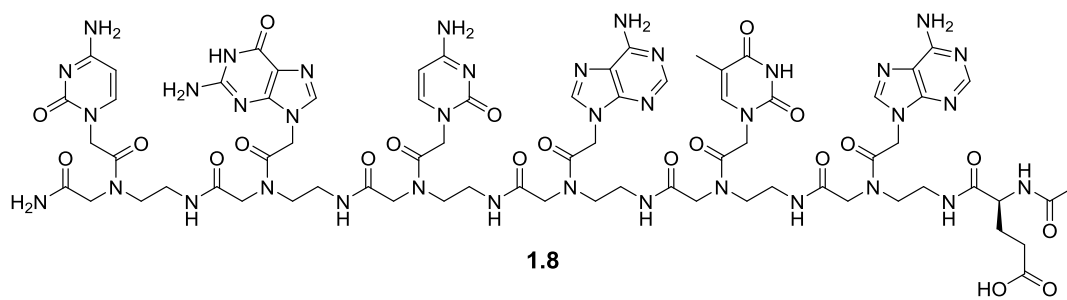


RP-HPLC: 5-10% MeCN in H_2O , 0.1% TFA in 25 min, 1 mL/min, $t_R = 22.264$ min.

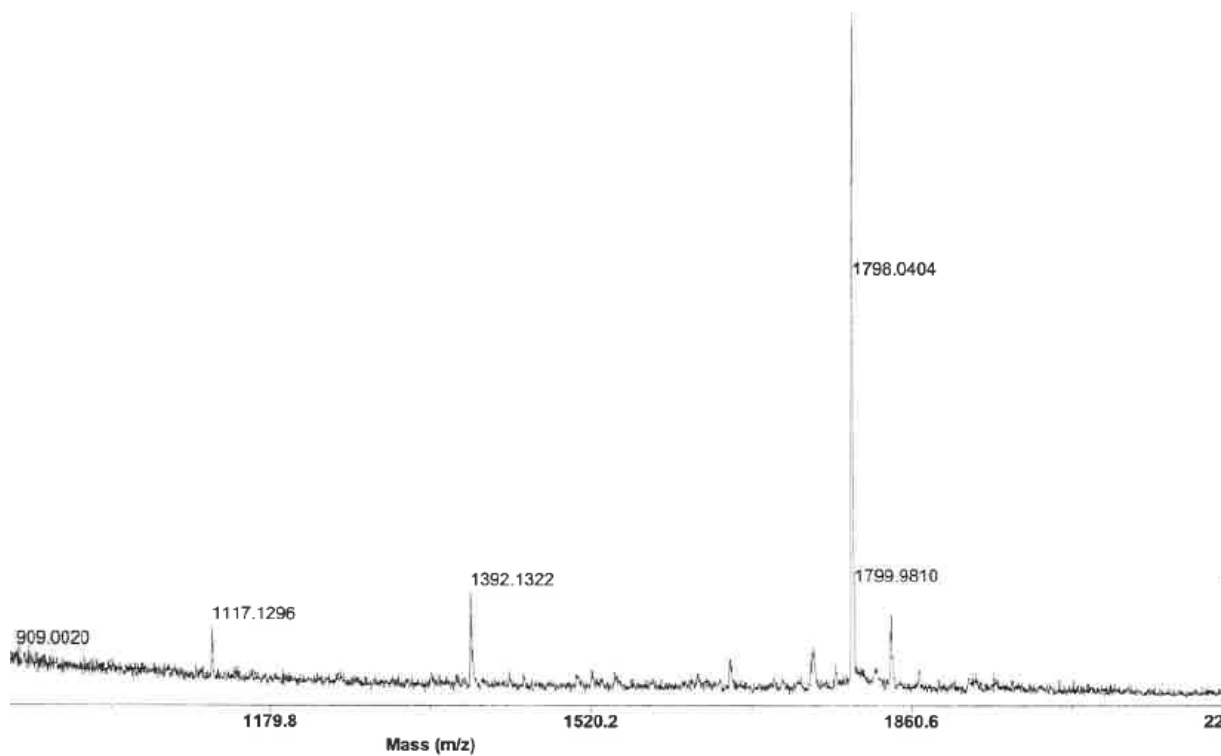


MALDI-TOF-MS: 1872.3 $[M+H]^+$, 1894.4 $[M+Na]^+$, 1910.4 $[M+K]^+$, 1932.7 $[M-H+Na+K]^+$, 1948.6 $[M-H+2K]^+$.

N-acetyly PNA 1.8:

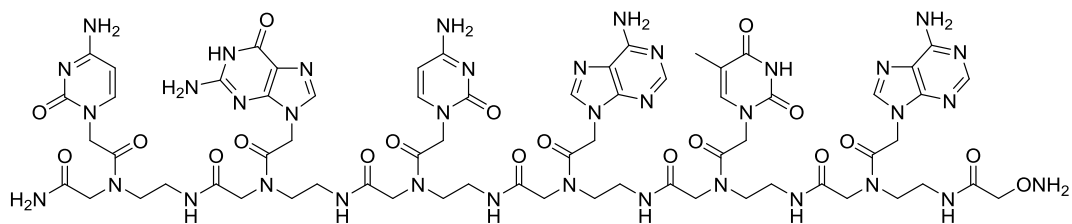


Chemical Formula: C₇₁H₉₁N₃₇O₂₁ ; Exact Mass: 1797.7190 ; Molecular Weight: 1798.7470



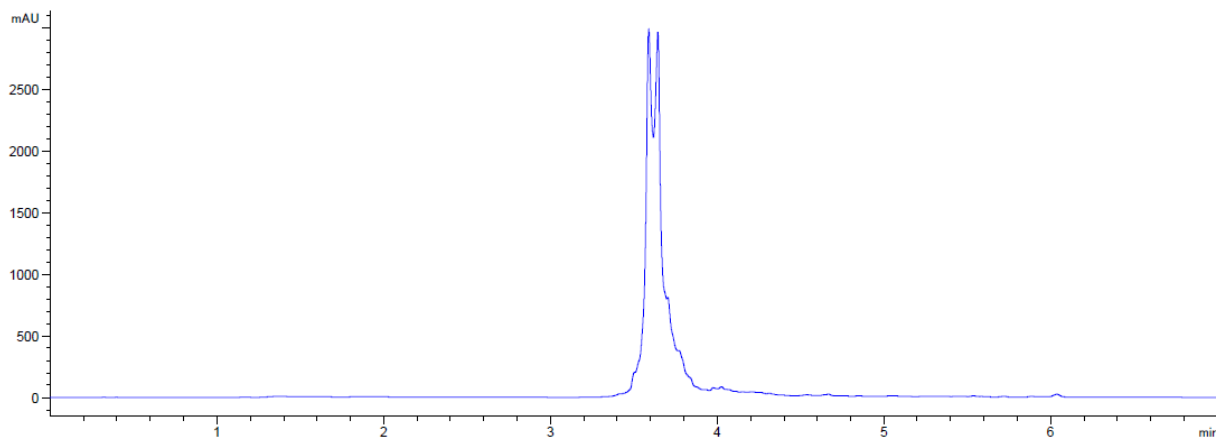
MALDI-TOF-MS: 1798.0 [M+H]⁺.

PNA-OH₂ 1.30:



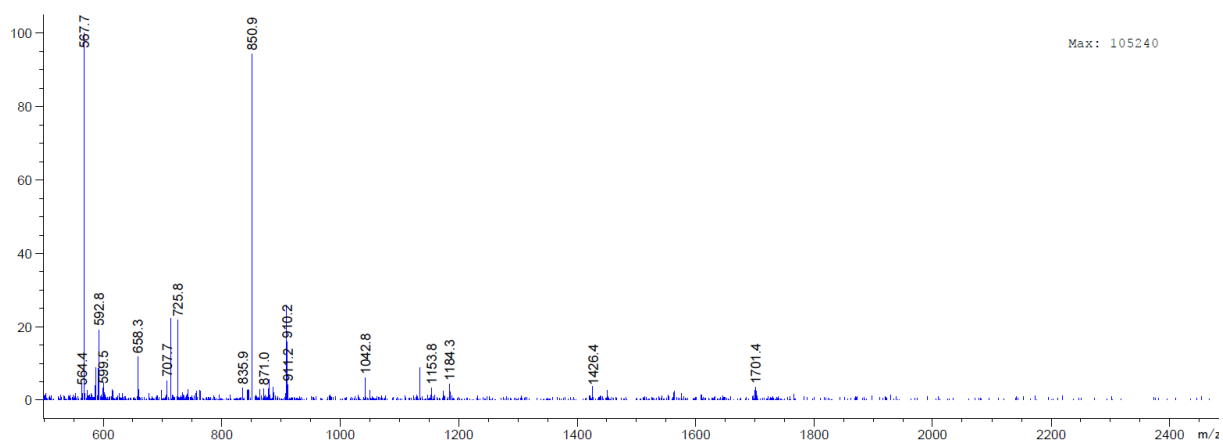
1.30

Chemical Formula: C₆₆H₈₅N₃₇O₁₉ ; Exact Mass: 1699.6822 ; Molecular Weight: 1700.6460



At that time double peaks were observed for each compound as a result of column aging.

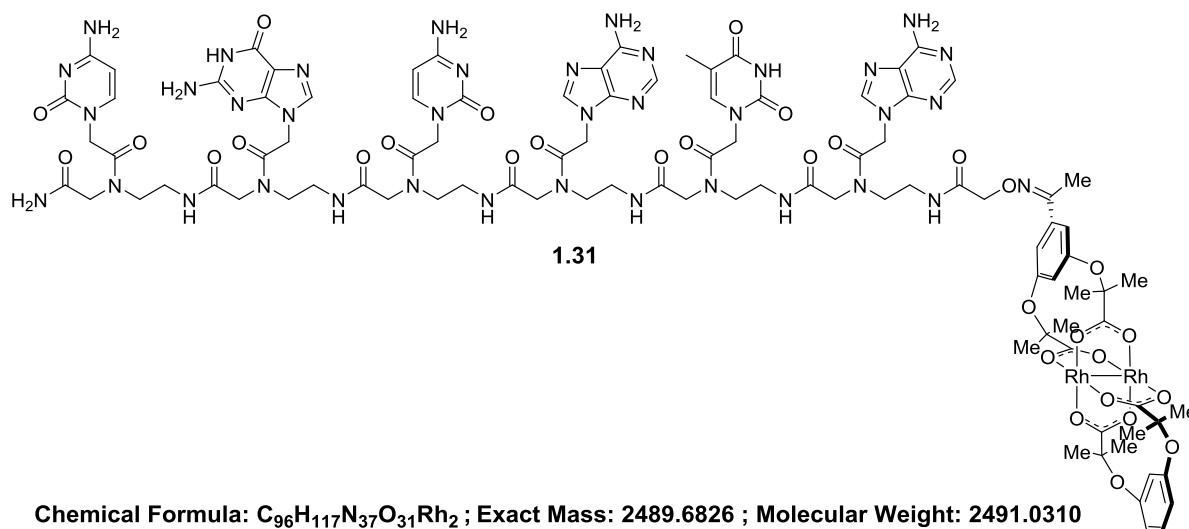
Gradient: 5-100% MeCN in H₂O, 0.1% TFA in 5 min, 0.5 mL/min.



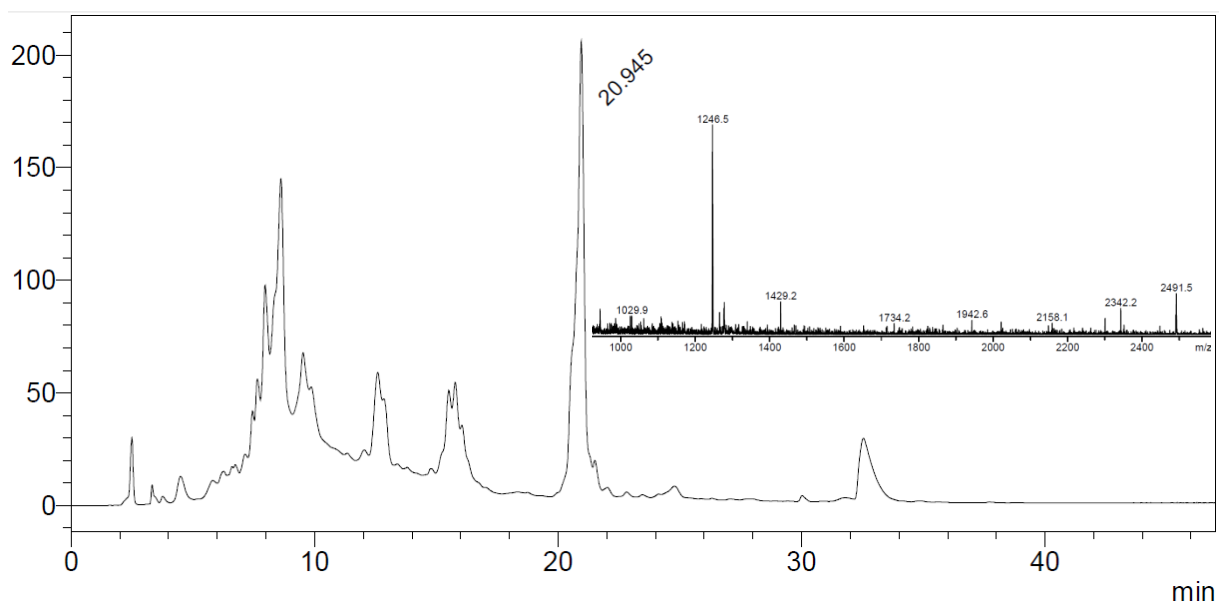
UPLC-MS (ESI): $t_R = 3.616$ min, 1700.4 [M+H]⁺, 850.9 [M+2H]²⁺, 567.7 [M+3H]³⁺.

PNA-Rh₂ 1.31:

To the hydroxylamine terminated PNA **1.30** (4.25 mg, 2.50 μmol , 1.00 eq.) was added 330 μL ($\sim 3:1:0.5$ H₂O/MeOH/CH₂Cl₂) of a 10 mM stock solution of ketone functionalized dirhodium catalyst **1.19** (2.67 mg, 3.30 μmol , 1.32 eq.) and left at room temperature with occasional mixing. The heterogenous mixture turned immediately pink and LC/MS analysis over a total of 22 h indicated a sluggish reaction although the desired product could be identified.



LC/MS after 22 h:

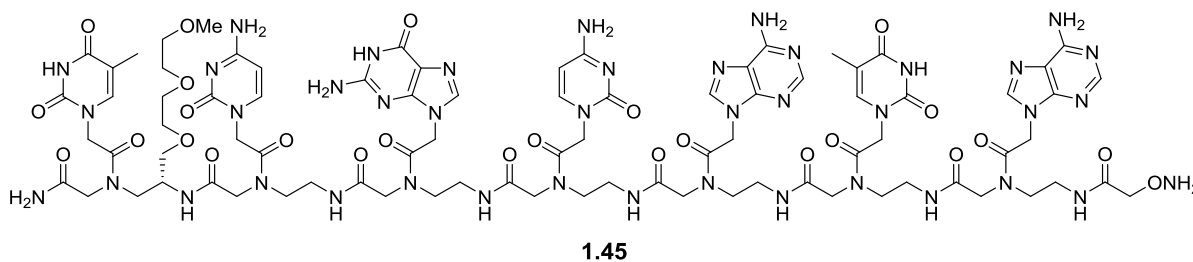


LRMS (ESI): 2491.5 [M+H]⁺, 1246.5 [M+2H]²⁺.

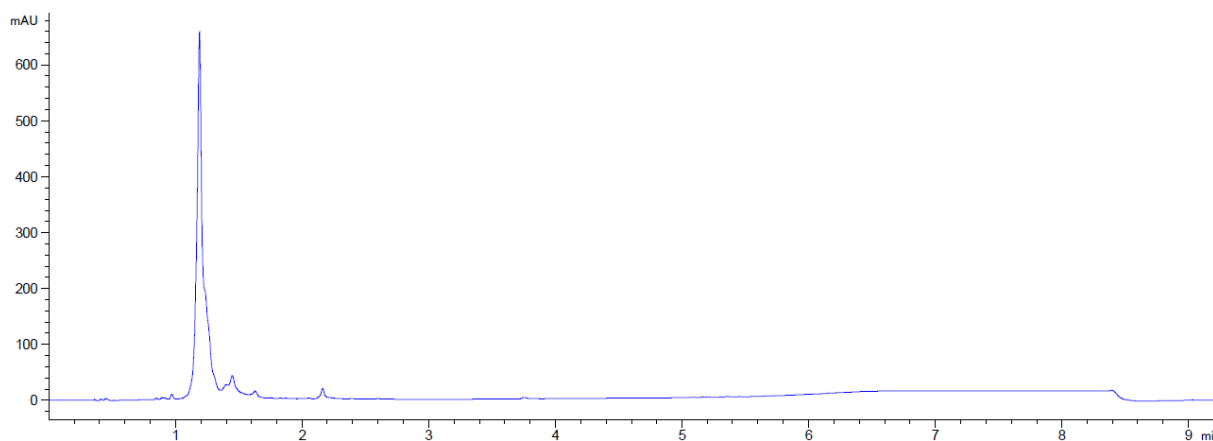
RP-HPLC: 5-100% MeCN in H₂O, 0.1% TFA in 40 min, 1 mL/min, t_R = 20.945 min.

γ T-PNA 1.45:

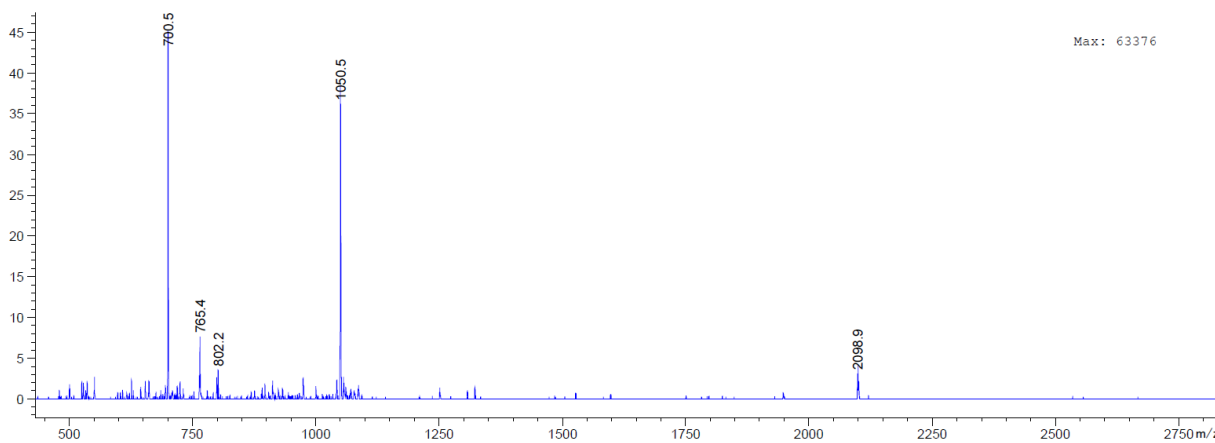
γ T-PNA **1.45** was synthesized according to the above described protocol for manual solid-phase PNA synthesis except for the selective on-bead *N*-Boc removal after coupling of thymine monomer (^{R-MP} γ T-PNA) **1.38**. This was achieved using the protocol published by ZHANG *et al.*¹⁸⁹ To the resin was added a solution containing 1M TMSOTf, 1.5M 2,6-lutidine in CH₂Cl₂ (1.5 mL) and shaken at room temperature for 1 h. The resin was then washed as described above and a qualitative chloranil test¹⁶⁸ was found to be positive.



Chemical Formula: C₈₃H₁₁₁N₄₁O₂₆ ; Exact Mass: 2097.8624 ; Molecular Weight: 2099.0620



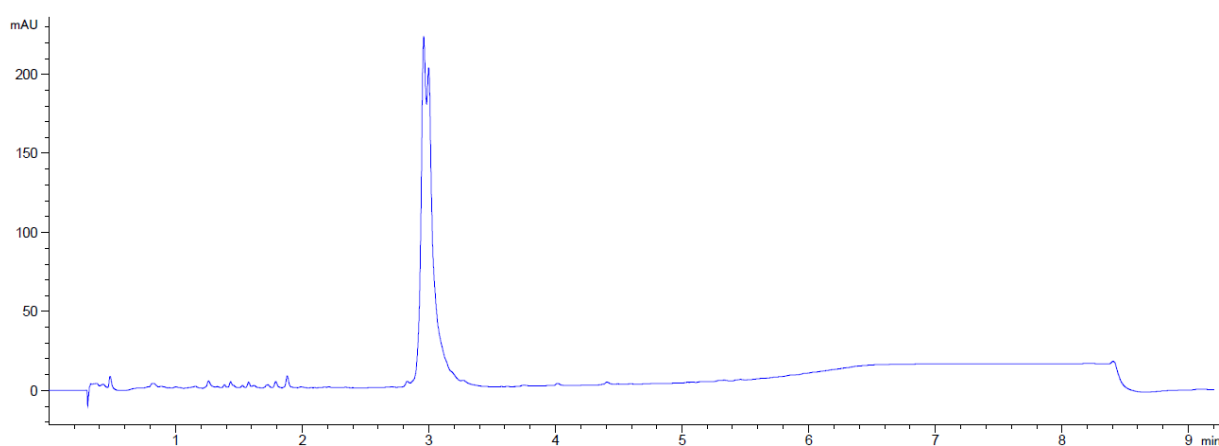
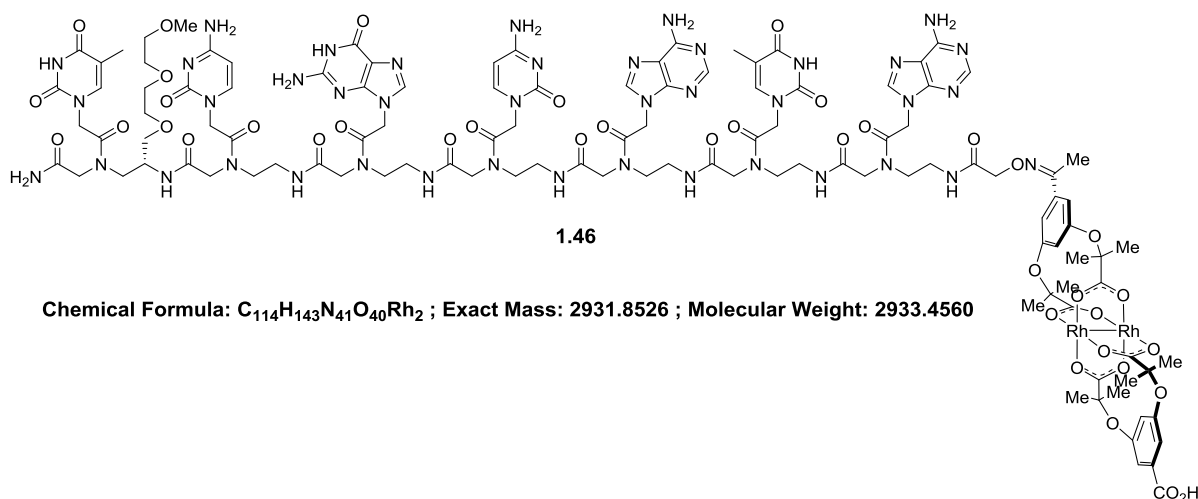
Gradient: 5-70% MeCN in H₂O, 0.1% TFA in 5 min, 0.4 mL/min.



UPLC-MS (ESI): $t_R = 1.189$ min, 2098.9 [M+H]⁺, 1050.5 [M+2H]²⁺, 700.5 [M+3H]³⁺.

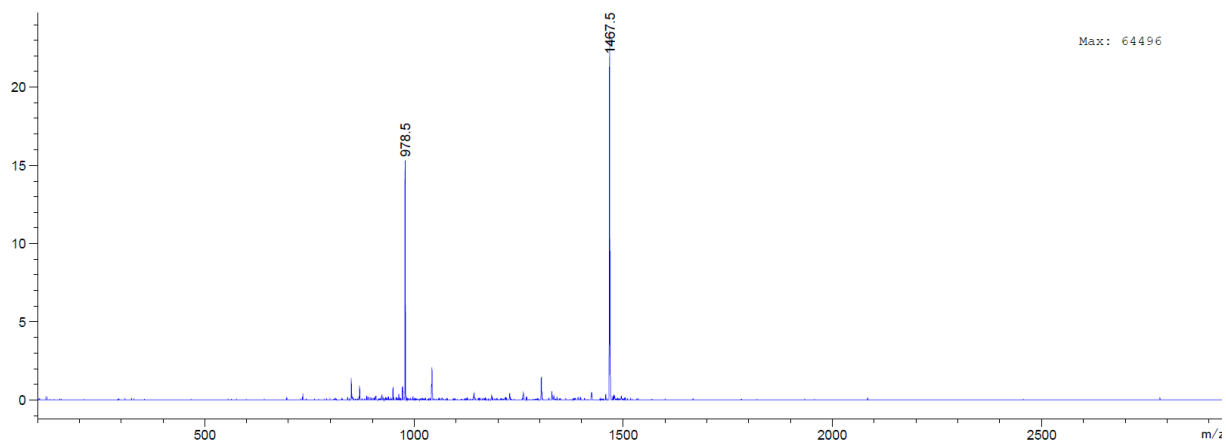
PNA-Rh₂ 1.46:

A stock solution of γ T-PNA **1.45** (81.8 μ L, 7.4 mM) was mixed with a stock solution of dirhodium catalyst **1.18** (81.8 μ L, 4.93 mM in Milli-Q water + 1 drop of conc. NaOH for solubility) in a 0.5 mL Eppendorf tube. Excess of γ T-PNA **1.45** was used to assure full conversion of the dirhodium catalyst **1.18**. Upon mixing the solution turned immediately pink (see **Scheme 2.23** in section 2.3.6) and after centrifuging the sample a pink solid settled. UPLC-MS indicated exclusively unreacted γ T-PNA **1.45** in the supernatant whereas the analysis of the pink solid (dissolved in DMSO) indicated a mixture of starting materials and PNA-Rh₂ **1.46** product. The crude solid was dissolved in 100 μ L of DMSO and purified by semi-preparative HPLC (5-80% MeCN in H₂O, 0.1% TFA in 30 min, 5 mL/min). A pink fluffy solid was obtained and a stock solution in DMSO (2.56 mM, determined spectrophotometrically) was prepared and stored at -20°C.



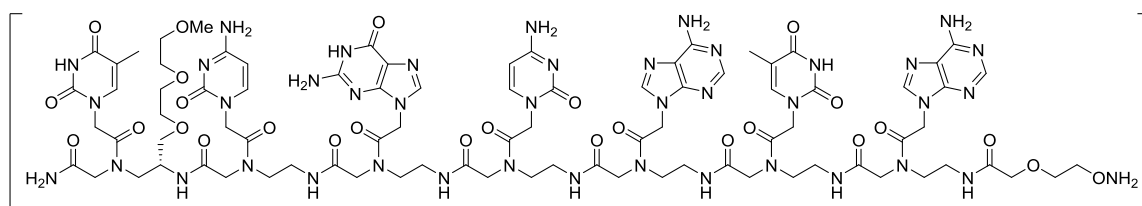
At that time double peaks were observed for each compound as a result of column aging.

Gradient: 5-100% MeCN in H₂O, 0.1% TFA in 5 min, 0.5 mL/min.



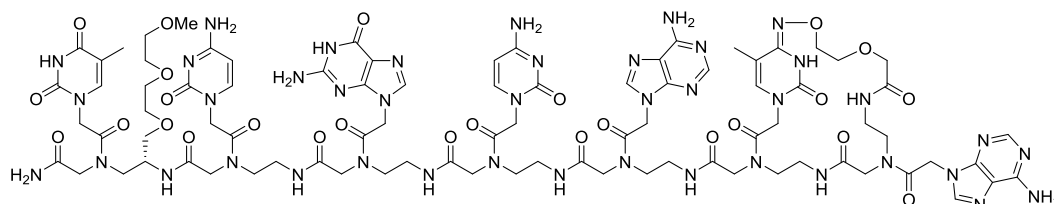
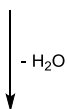
UPLC-MS (ESI): $t_R = 2.985$ min, 1467.5 $[M+2H]^{2+}$, 978.5 $[M+3H]^{3+}$.

PNA 1.51/1.53:



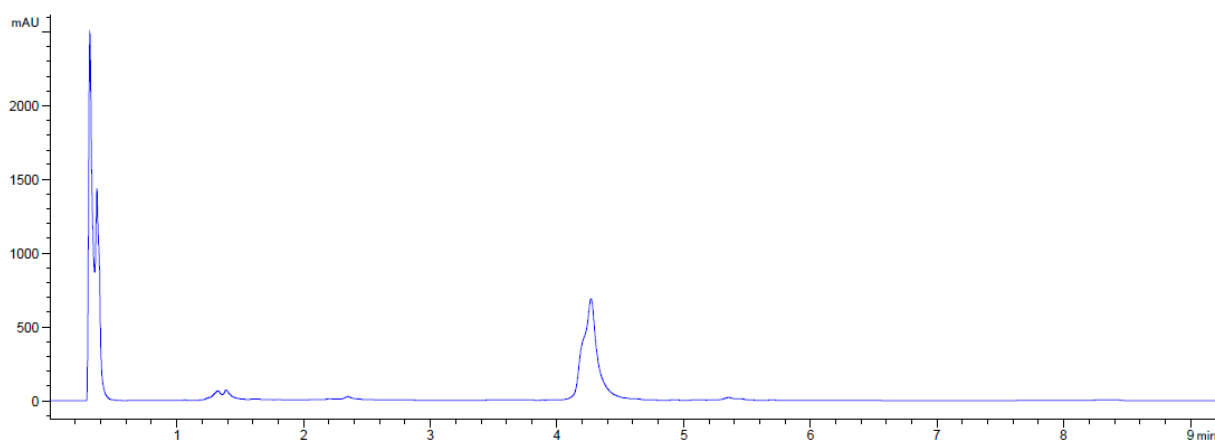
1.51

Chemical Formula: $C_{85}H_{115}N_{41}O_{27}$; Exact Mass: 2141.8886 ; Molecular Weight: 2143.1150



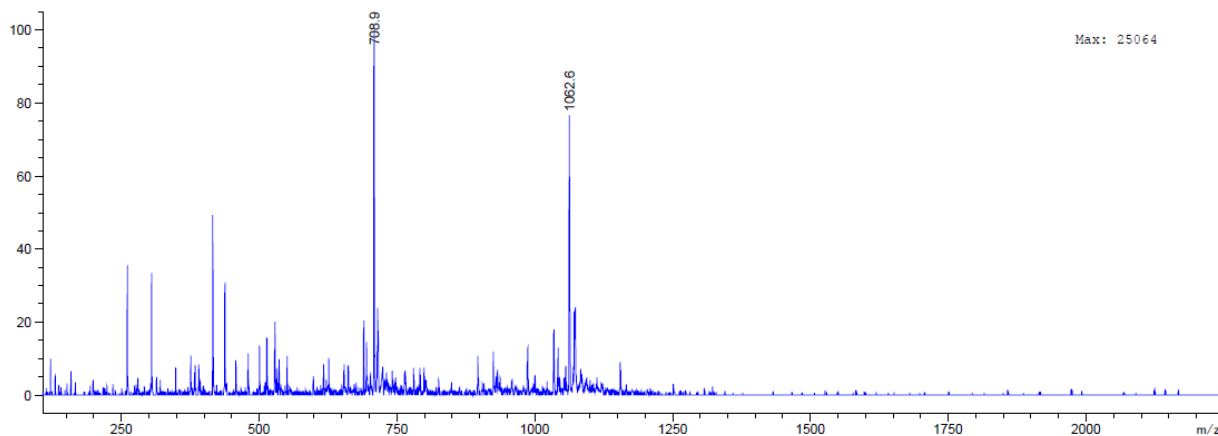
proposed structure 1.53

Chemical Formula: $C_{85}H_{113}N_{41}O_{26}$; Exact Mass: 2123.8780 ; Molecular Weight: 2125.1000



Peak at 4.25 min was unrelated to PNA.

Gradient: 5-70% MeCN in H₂O, 0.1% TFA in 5 min, 0.4 mL/min.

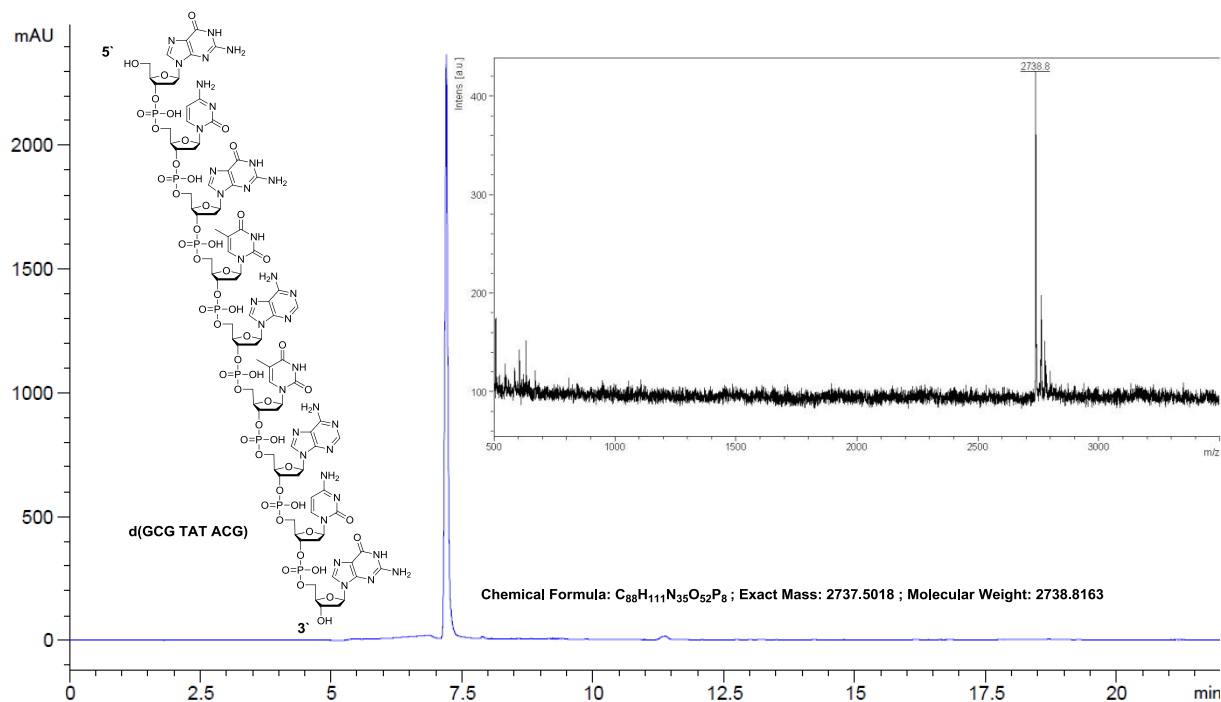


UPLC-MS (ESI): $t_R = 0.364$ min, 1062.6 $[M+2H]^{2+}$, 708.9 $[M+3H]^{3+}$.

Oligonucleotide synthesis and purification

Solid-phase oligonucleotide synthesis was carried out on four 1- μ mol CPG columns (pre-loaded with G) using standard phosphoramidite chemistry with 0.3 M 5-benzylthio-1-H-tetrazole as activator. The DNA oligonucleotides were cleaved from the support with 32% (v/v) aqueous ammonia for 2 h at room temperature and deprotected for 18 h at 55°C, then freeze-dried and purified by semi-preparative HPLC. Purification was done using the following gradient: 0-18% MeCN in 100 mM triethylammonium acetate (pH 7.0) in 15 min, 18-80% in 5 min. The DNA concentration was determined using a NanoDrop 2000 spectrophotometer from Thermo Scientific at 260 nm with a path length of 1 mm and $\epsilon_{(\text{GCG TAT ACG})} = 89900 \text{ M}^{-1} \text{ cm}^{-1}$. A stock solution (14.6 mM) in Milli-Q water containing 160 mM MgCl_2 was prepared and stored at -20°C.

d(GCG TAT ACG):



RP-HPLC: 0-80% MeCN in 100 mM triethylammonium acetate (pH 7.0) in 16 min, 1 mL/min, $t_R = 7.192$ min.

MALDI-TOF-MS: 2738.8 $[\text{M}+\text{H}]^+$.

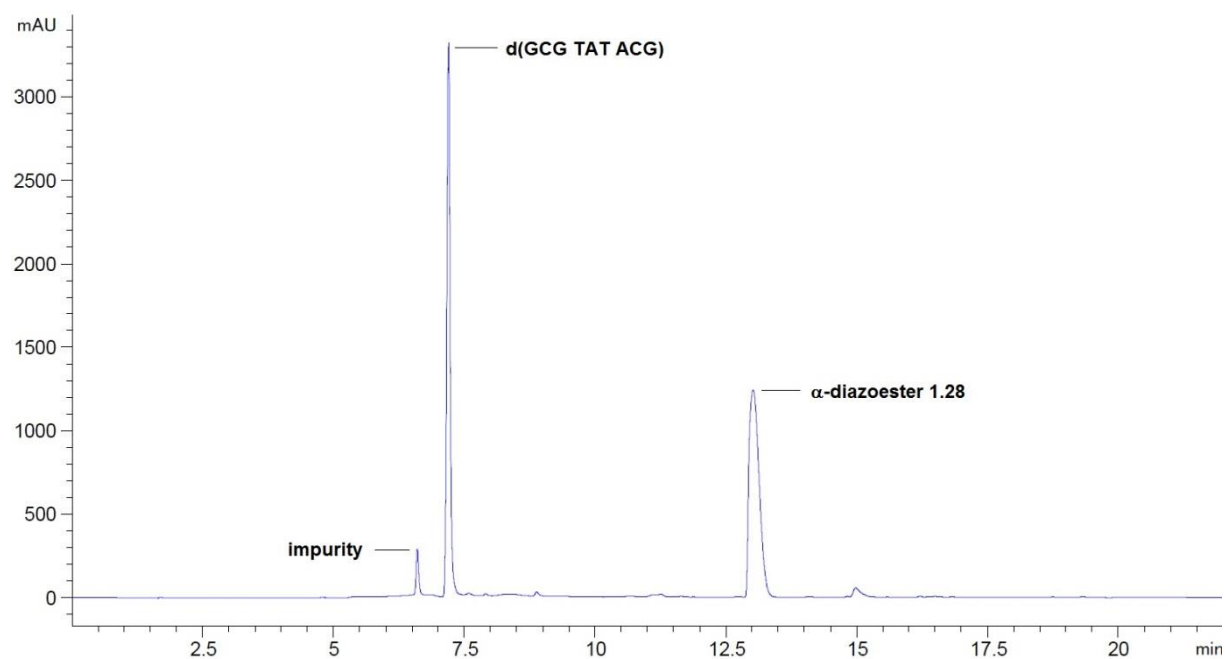
4.2.1.4 Alkylation studies using PNA-dirhodium carbenoids

Procedure used for entries 1-7 in table 2.1

Typically 20 μL reaction mixtures containing 0.1-1 mM $\gamma\text{T-PNA-hydroxylamine}$ **1.45**, 0.1-1 mM dirhodium catalyst, 0.1-5 mM oligonucleotide and 50 mM $\alpha\text{-diazocarbonyl}$ compound **1.28** in 100 mM MES buffer, pH 6.0 were sequentially mixed at room temperature. The reaction was analyzed every 2 h (2 μL injections) for a total of 14 h and the remaining sample (6 μL) purified by micro-preparative HPLC-separation. The collected peak fractions were analyzed by MALDI-TOF-MS.

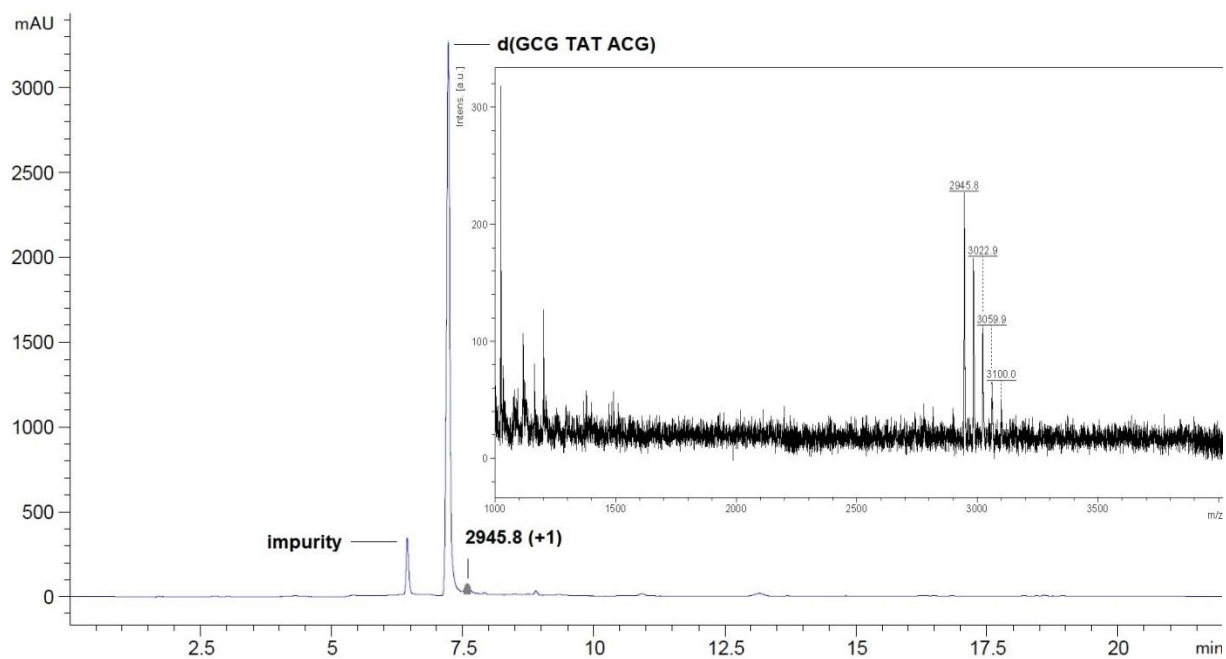
Analytical data

Representative HPLC trace at $t = 0$ h for entry 1 in **table 2.1**. $\alpha\text{-diazocarbonyl}$ compound **1.28** contained a small impurity which did not interfere during the course of the reaction as stated by integration values.



RP-HPLC: 0-80% MeCN in 100 mM triethylammonium acetate (pH 7.0) in 16 min, 1 mL/min, $t_{\text{R (oligo)}}$ = 7.192 min.

Representative HPLC trace at $t = 14$ h for entry 1 in table 2.1 (identical to entries 2 and 4-7). The conversions were determined to be 3% for the oligonucleotide and $> 99\%$ for the $\alpha\text{-diazocarbonyl}$ compound **1.28**. The new peak at 7.583 min was confirmed as a (+1) modified oligonucleotide species.

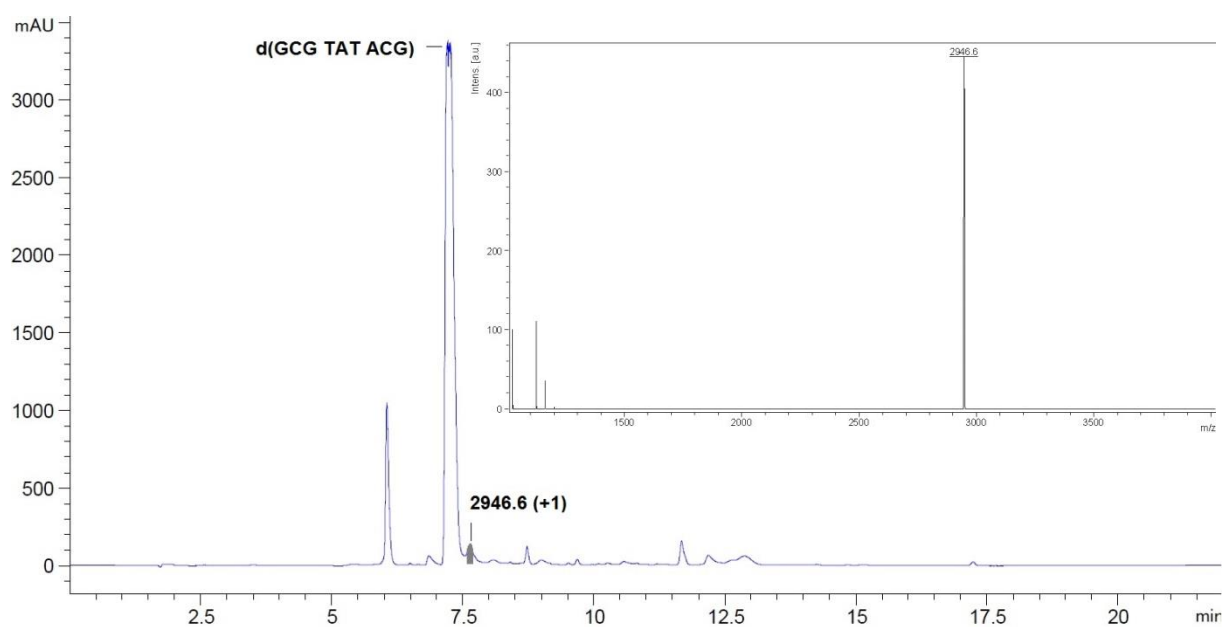
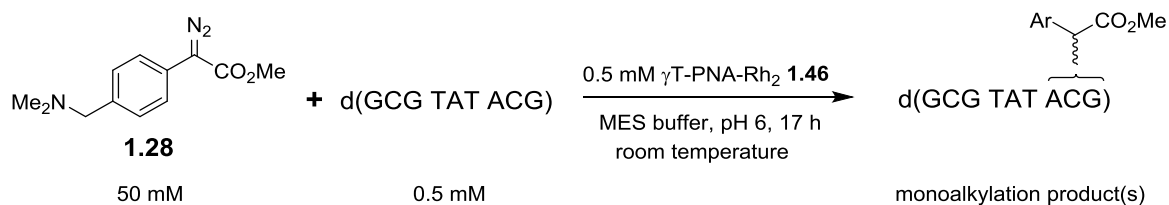


RP-HPLC: 0-80% MeCN in 100 mM triethylammonium acetate (pH 7.0) in 16 min, 1 mL/min, t_R (modified oligo) = 7.583 min.

MALDI-TOF-MS: 2945.8 $[M+H]^+$, 2983.9 $[M+K]^+$, 3022.9 $[M-H+2K]^+$, 3059.9 $[M-2H+3K]^+$, 3100.0 $[M-3H+4K]^+$.

Procedure for the alkylation using PNA-Rh₂ oxime **1.46**

A 20 μ L reaction mixture containing 0.5 mM γ T-PNA-Rh₂ oxime **1.46**, 0.5 mM oligonucleotide and 50 mM α -diazocarbonyl compound **1.28** in 100 mM MES buffer, pH 6.0 were sequentially mixed at room temperature. The reaction was analyzed every 2 h (2 μ L injections) for a total of 14 h and the remaining sample (6 μ L) purified by micro-preparative HPLC-separation after 17 h. The collected peak fractions were analyzed by MALDI-TOF-MS.



RP-HPLC: 0-80% MeCN in 100 mM triethylammonium acetate (pH 7.0) in 18 min, 1 mL/min, t_R (modified oligo) = 7.638 min.

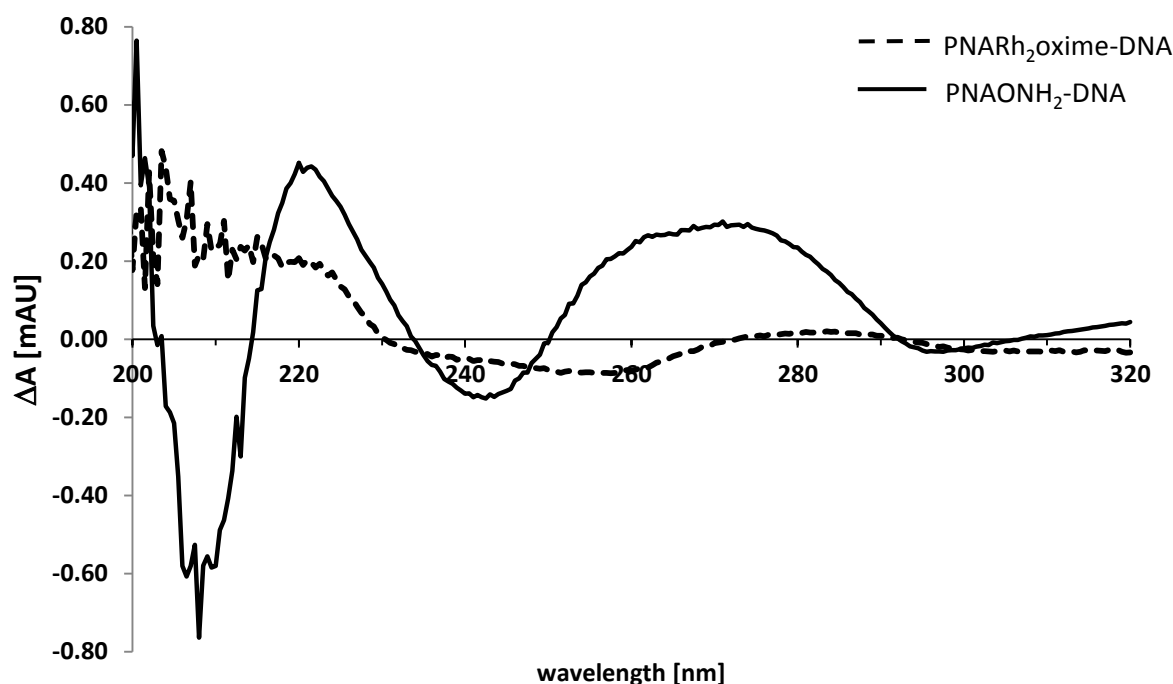
MALDI-TOF-MS: 2946.6 $[M+H]^+$.

4.2.1.5 Circular dichroism studies

Circular Dichroism (CD)

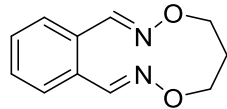
All CD data were recorded at room temperature from 190-320 nm at the rate of 100 nm/min using a spectral bandwidth of 1 nm with a time constant of 5 s and a step resolution of 0.5 nm. A 10 mm path length cuvette was used and the temperature was maintained at 22°C. The resulting CD signal, obtained as ellipticity θ in mdeg, was converted into a difference in absorption ΔA and is reported in mAU.

Stock solutions of the γ T-containing PNA-hydroxylamine **1.45** (12.1 mM), d(GCG TAT ACG) (14.6 mM containing 160 mM MgCl_2) and PNA-Rh₂oxime **1.46** (2.56 mM in DMSO) were used. The stock solutions were mixed and diluted in KP_i buffer (10 mM in Milli-Q water, pH 7.6) to a final hybridizing concentration of 8.1 μM . All solutions were equilibrated at room temperature for 5-10 min before the measurements.

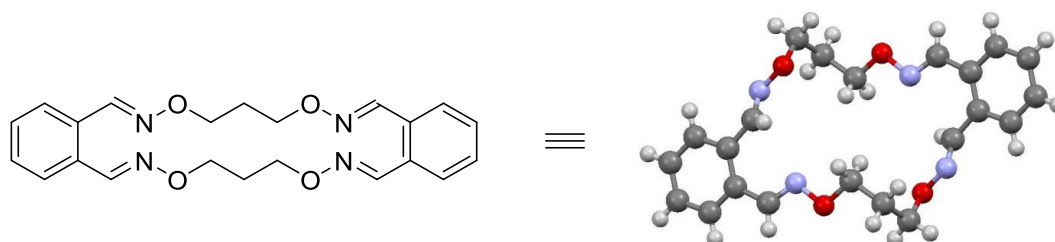


4.2.2 Dialdehyde studies

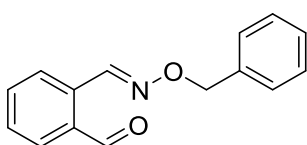
4.2.2.1 Synthesis of small molecules and dirhodium catalysts



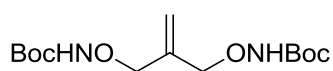
Bisoxime **2.3a**: The reaction of OPA **2.1** and 1,3-diaminohydroxypropane (**2.2**) was conducted at 10 μM (at a 1:1 ratio) in $\text{H}_2\text{O}/1\%$ MeCN. After 10 min an aliquot was analyzed by UPLC-MS indicating full conversion of OPA **2.1** showing bisoxime **2.3a** as the single product. HRMS (ESI): $\text{C}_{11}\text{H}_{13}\text{N}_2\text{O}_2^+$ *calcd.*: 205.0972, *found*: 205.0974 $[\text{M}+\text{H}]^+$. NMR characterization was impossible since at high substrate concentrations (>1 mM) the tetraoxime **2.3b** was the exclusive product.



Tetraoxime **2.3b**: ^1H NMR (400 MHz, CDCl_3) δ/ppm : 8.56 (s, 4 H), 7.59-7.55 (m, 4 H), 7.40-7.36 (m, 4 H), 4.36 (t, $J = 6.3$ Hz, 8 H), 2.17-2.11 (m, 4 H). LRMS (ESI): $\text{C}_{22}\text{H}_{25}\text{N}_4\text{O}_4^+$ *calcd.*: 409.2, *found*: 409.2 $[\text{M}+\text{H}]^+$. (These compounds were synthesized and characterized by Dr. Linna Zhou).

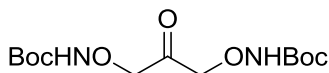


Oxime **2.5**: The reaction of OPA **2.1** and *O*-benzylhydroxylamine (**2.4**) was conducted at 10 mM (at a 1:1 ratio) in MeCN. The crude was purified by preparative RP-HPLC to give oxime **2.5** as colorless oil. ^1H -NMR (500 MHz, CDCl_3) δ/ppm : 10.26 (s, 1 H), 8.92 (s, 1 H), 7.86 (t, $J = 8.7$ Hz, 2 H), 7.61 (t, $J = 7.5$ Hz, 1 H), 7.55 (t, $J = 7.5$ Hz, 1 H), 7.47-7.34 (m, 5 H), 5.28 (s, 2 H). ^{13}C -NMR (101 MHz, CDCl_3) δ/ppm : 192.46, 146.97, 137.26, 133.90, 133.53, 133.02, 132.08, 129.72, 128.50, 128.48, 128.32, 128.10, 76.78. HRMS (ESI): $\text{C}_{15}\text{H}_{14}\text{NO}_2^+$ *calcd.*: 240.1019, *found*: 240.1019 $[\text{M}+\text{H}]^+$.

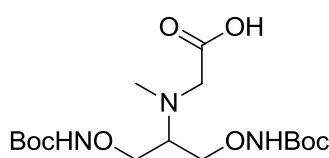


Bis(carbamate) **2.12**: 3-Bromo-2-bromomethyl-1-propene **2.11** (704 mg, 3.19 mmol, 1.00 eq.) was dissolved in dry CH_2Cl_2 (8.0 mL) under nitrogen. While stirring *tert*-butyl *N*-hydroxycarbamate (**1.48**) (868 mg, 6.39 mmol, 2.00 eq.) was added and the resulting mixture cooled to 0°C . DBU (1.43 mL, 9.58 mmol, 3.00 eq.) was added dropwise and the mixture allowed to warm up to room temperature. The reaction was monitored by TLC (cyclohexane/EtOAc, 3:1, KMnO_4) and full conversion was observed after 3 h. The solvent was removed under reduced pressure and the residue was purified by flash chromatography (cyclohexane/EtOAc 3:1) to afford the target product **2.12** as an off-white solid (662 mg, 2.08 mmol, 65%). TLC (cyclohexane/EtOAc, 3:1, KMnO_4) $R_f = 0.23$. ^1H -NMR (400 MHz,

CDCl₃) δ /ppm: 7.55 (s, 2H), 5.34 (s, 2H), 4.41 (s, 4H), 1.47 (s, 18H). ¹³C-NMR (101 MHz, CDCl₃) δ /ppm: 156.88, 139.29, 120.96, 81.85, 77.59, 28.36. HRMS (ESI): C₁₄H₂₆N₂NaO₆⁺ *calcd.*: 341.1684, *found*: 341.1683 [M+Na]⁺.

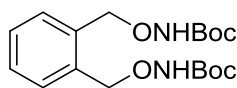


Ketone 2.10: A 25 mL two-necked flask equipped with a stir bar, containing a gas inlet (pasteur pipet and quick fit) and a connected tygon tube filled with blue silica gel was charged with olefin **2.12** (207 mg, 0.65 mmol, 1.00 eq.) dissolved in dry MeOH/CH₂Cl₂ (4 mL, 1:3). The mixture was cooled to -78°C and O₃ gas was gently bubbled through the stirred solution. After 5 min the solution was saturated with O₃ and turned blue. The gas supply was ceased and air was bubbled through the solution until all excess of O₃ was removed as indicated by the disappearance of the blue color. The reaction mixture was allowed to warm up to room temperature and Me₂S (480 μ L, 6.57 mmol, 10.1 eq.) was added. The solvent was removed under reduced pressure to give 238 mg of a colorless oil which had a purity of 83% as determined by ¹H-NMR. A 102 mg sample was passed through a short plug of silica with cyclohexane/EtOAc 1.5:1. The target ketone was dried extensively over night at 40°C under high vacuum to give the title compound **2.10** as a colorless oil (78 mg, 0.24 mmol, 86%, yield is based on the molar percentage of the total sample taken in the aliquot). TLC (cyclohexane/EtOAc, 1:1, KMnO₄) R_f = 0.37. ¹H-NMR (500 MHz, CDCl₃) δ /ppm: 7.65 (s, 2H), 4.63 (s, 4H), 1.48 (s, 18H). ¹³C-NMR (126 MHz, CDCl₃) δ /ppm: 204.07, 156.56, 82.59, 78.95, 28.29. HRMS (ESI): C₁₃H₂₄N₂NaO₇⁺ *calcd.*: 343.1476, *found*: 343.1475 [M+Na]⁺.

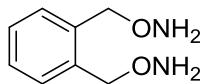


Carboxylic acid 2.8: To a nitrogen flushed 2.5 mL screw cap vial equipped with a stir bar containing ketone **2.10** (51.0 mg, 80.7 μ mol, 50% purity, different batch than described above) was added dry MeOH (0.50 mL), followed by sarcosine (22.0 mg, 0.24 mmol, 3.04 eq.) and finely crushed and flame dried 4Å molecular sieve. Then 1.25 M HCl in MeOH (130 μ L, 163 μ mol, 2.02 eq.) was added and the mixture stirred for 10 min at room temperature. It was cooled with an ice bath to 0°C and NaBH₃CN (6.00 mg, 95.5 μ mol, 1.14 eq.) was added. The ice bath was removed and the reaction stirred at room temperature for 18 h. UPLC-MS confirmed the desired product mass of m/z = 394 [M+H]⁺ along with an unknown mass of m/z = 424 Da. The reaction mixture was filtered over Celite and washed with MeOH. The solvent was removed under reduced pressure to give 65 mg of a viscous turbid oil which was purified by reverse phase flash chromatography (dry loaded) on a Biotage Isolera Four device using RP-C18 silica gel and H₂O/MeCN (0-70% MeCN over 24 min). The non UV-active fractions were analyzed by direct injection into an ESI-MS device using positive and negative ion polarity mode. The fractions containing the product mass (33-35% MeCN) were additionally analyzed by UPLC-MS, combined and lyophilized to give the desired product **2.8** as a

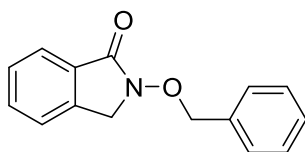
white fluffy powder (7.0 mg, 17.8 μmol , 22%, estimated purity from $^1\text{H-NMR}$ is $\sim 95\%$). No further purification was necessary for the subsequent SPPS. $^1\text{H-NMR}$ (400 MHz, $\text{DMSO-}d_6$) δ/ppm : 10.05 (s, 1H), 4.75 (s, 1H), 4.01-3.72 (m, 4H), 3.36 (s, 2H), 3.12-3.04 (m, 1H), 2.36 (s, 3H), 1.41 (s, 18H); the signals at 3.36, 2.36 and 1.41 ppm were sets of two overlapping singlets from the corresponding rotamers and were integrated together. Additionally one of the acidic protons seems not to be observable under the conditions we ran the $^1\text{H-NMR}$. Even with 2-D spectra it was not possible to clearly assign the signals at 10.05 and 4.75 ppm. $^{13}\text{C-NMR}$ (126 MHz, $\text{DMSO-}d_6$) δ/ppm : 172.28, 156.11/154.65 (rotamer), 80.85/79.74 (rotamer), 73.78/72.88/71.50 (rotamer), 59.24, 56.03, 38.48/38.30 (rotamer), 27.89. HRMS (ESI): $\text{C}_{16}\text{H}_{32}\text{N}_3\text{O}_8^+$ *calcd.*: 394.2184, *found*: 394.2191 $[\text{M}+\text{H}]^+$.



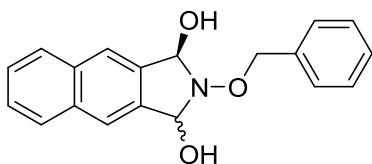
Bis(carbamate) **2.14**: NaH (110 mg, 2.80 mmol, 2.54 eq., 60% in mineral oil) was suspended in dry THF (9 mL) under nitrogen. *tert*-butyl *N*-hydroxycarbamate (**1.48**) (330 mg, 2.48 mmol, 2.25 eq. as a solution in 1 mL dry THF) was carefully added dropwise to the stirring suspension. After gas evolution had ceased, α,α' -dibromo-*o*-xylene (**2.13**) (300 mg, 1.10 mmol, 1.00 eq.) was added and the mixture was stirred for 2 h at room temperature. The mixture was concentrated under reduced pressure and the residue was partitioned between EtOAc and H_2O . The aqueous phase was extracted once more with EtOAc, the combined organic layers were washed with brine, dried over Na_2SO_4 and evaporated. The residue was purified by flash chromatography (cyclohexane/EtOAc and $\text{CH}_2\text{Cl}_2/\text{MeOH}$) to yield the desired product **2.14** as a colorless oil (310 mg, 842 μmol , 76%). $^1\text{H-NMR}$ (500 MHz, CD_3CN) δ/ppm : 8.27-8.14 (s_{br} , 2H), 7.40-7.36 (m, 4H), 4.94 (s, 4H), 1.42 (s, 18 H). $^{13}\text{C-NMR}$ (126 MHz, CD_3CN) δ/ppm : 157.50, 136.31, 131.83, 129.57, 81.50, 76.29, 28.36. HRMS (ESI): $\text{C}_{18}\text{H}_{28}\text{N}_2\text{NaO}_6^+$ *calcd.*: 391.1840, *found*: 391.1843 $[\text{M}+\text{Na}]^+$. (This compound was synthesized and characterized by Dr. Linna Zhou).



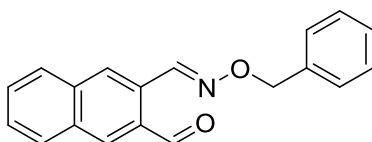
bishydroxylamine **2.15**: Bis(carbamate) **2.14** (120 mg, 326 μmol , 1.00 eq.) was dissolved in 1 mL dry CH_2Cl_2 under nitrogen and concentrated TFA (1 mL) was added with continuous stirring at room temperature. After 4 h the reaction was concentrated under reduced pressure and the residue was partitioned between a saturated sodium carbonate solution and CH_2Cl_2 . The aqueous phase was extracted twice with CH_2Cl_2 , the combined organic layers were washed with brine, dried over Na_2SO_4 , filtered and concentrated under reduced pressure. The residue was purified by flash chromatography ($\text{CH}_2\text{Cl}_2/\text{MeOH}$) to yield the target product **2.15** as a colorless oil (20.0 mg, 119 μmol , 36%). $^1\text{H-NMR}$ (500 MHz, CD_3CN) δ/ppm : 7.37-7.36 (m, 2H), 7.32-7.30 (m, 2H), 5.57 (s_{br} , 4H), 4.71 (s, 4H). $^{13}\text{C-NMR}$ (126 MHz, CD_3CN) δ/ppm : 137.55, 130.17, 128.65, 75.82. HRMS (ESI): $\text{C}_8\text{H}_{13}\text{N}_2\text{O}_2^+$ *calcd.*: 169.0972, *found*: 169.0972 $[\text{M}+\text{H}]^+$. (This compound was synthesized and characterized by Dr. Linna Zhou).



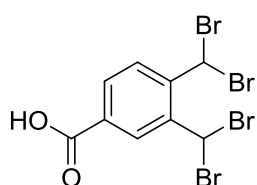
Lactam **2.19**: A NMR sample containing a mixture of IBHA **2.16** (ds 9:1) and oxime **2.5** in CD₃CN was treated with DCI gas (pipetting the vapor phase of a DCI bottle into the NMR tube). The tube was sealed and homogenized through gentle shaking. Subsequent NMR analysis indicated the exclusive formation of lactam derivative **2.19**. The crystal structure of **2.19** is shown in **Figure 3.7**. ¹H-NMR (400 MHz, CD₃CN) δ/ppm: 7.76 (d, *J* = 7.5 Hz, 1H), 7.62 (t, *J* = 7.5 Hz, 1H), 7.56-7.35 (m, 7H), 5.13 (s, 2H), 4.47 (s, 2H). ¹³C-NMR (101 MHz, CD₃CN) δ/ppm: 165.88, 140.04, 136.57, 133.07, 131.37, 130.49, 129.80, 129.54, 129.19, 124.37, 124.03, 78.46, 51.27.



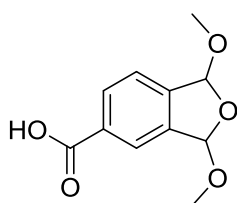
IBHA of naphthalene dialdehyde **2.20**: A 2.5 mL screw-cap vial equipped with a stir bar was charged with 2,3-naphthalenedicarboxaldehyde (15.0 mg, 81.5 μmol, 1.02 eq.) dissolved in 0.5 mL dry MeCN. A solution of *O*-benzylhydroxylamine (**2.4**) (10.0 mg, 80.1 mmol, 1.00 eq.) in dry MeCN (0.20 mL) was added to the stirring solution at room temperature. The reaction was stopped when a white solid precipitated (45 sec) which prevented efficient stirring. The stir bar was removed, washed with dry MeCN and the solvent evaporated under reduced pressure. The sample was extensively dried under high vacuum to give 23 mg of a white fluffy solid which turned out to be a 9:1 mixture naphthalene IBHA **2.20** (as a 24:1 mixture of diastereomers) and its oxime **2.20a** (see below). Due to this ratio the ¹³C-NMR in DMSO-*d*₆ of the mixture only indicated the signals for **2.20**. ¹H NMR (400 MHz, DMSO-*d*₆) δ/ppm: 8.02-7.95 (m, 2H), 7.81 (s, 2H), 7.54-7.48 (m, 4H), 7.41-7.35 (m, 2H), 7.35-7.30 (m, 1H), 6.63 (*d*, *J* = 8.3 Hz, 2H), 5.62 (dd, *J* = 8.4 Hz, *J* = 1.0 Hz, 2H), 5.12 (s, 2H). ¹³C NMR (101 MHz, DMSO-*d*₆) δ/ppm: 137.66, 137.00, 133.38, 128.41, 128.27, 128.08, 127.64, 125.84, 121.47, 88.42, 77.67. HRMS (ESI): C₁₉H₁₇NNaO₃⁺ *calcd.*: 330.1101, *found*: 330.1103 [M+Na]⁺.



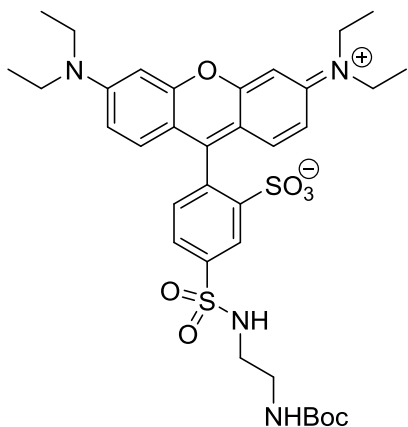
Oxime **2.20a**: The above mixture was heated in the NMR tube at 80°C for 5 h whereupon all the intermediate was converted to oxime **2.20a**. ¹H NMR (600 MHz, DMSO-*d*₆) δ/ppm: 10.28 (s, 1H), 9.02 (s, 1 H), 8.59 (s, 1H), 8.33 (s, 1H), 8.17 (d, *J* = 8.2 Hz, 1H), 8.12 (d, *J* = 8.2 Hz, 1H), 7.77-7.72 (m, 1H), 7.72-7.67 (m, 1H), 7.49-7.43 (m, 2H), 7.43-7.38 (m, 2H), 7.36-7.30 (m, 1H), 5.25 (s, 2H). ¹³C NMR (151 MHz, DMSO-*d*₆) δ/ppm: 193.50, 148.04, 137.47, 135.85, 134.47, 132.28, 131.67, 129.89, 129.38, 128.44, 128.41, 128.29, 128.22, 128.04, 127.92, 127.55, 75.69. HRMS (ESI): C₁₉H₁₅NNaO₂⁺ *calcd.*: 312.0995, *found*: 312.0997 [M+Na]⁺.



Tetrabromide 2.22: Compound **2.22** was synthesized in analogy to literature procedures by HARIS *et al.*²⁹⁹ and SHOKAT *et al.*²³⁷ 3,4-dibromobenzoic acid **2.21** (6.00 g, 39.9 mmol, 1.00 eq.) was dissolved in warm carbon tetrachloride (40 mL). *N*-bromosuccinimide (28.9 g, 162 mmol, 4.06 eq.) and benzoyl peroxide (810 mg, 3.35 mmol, 0.08 eq.) were added slowly and the reaction mixture was refluxed overnight. After cooling down, the white precipitate was filtered off and washed twice with toluene (60 mL) and Et₂O (80 mL). The filtrate was concentrated and the residue was recrystallized from MeCN to give the desired tetrabromide **2.22** (9.54 g, 20.5 mmol, 51%) as a white solid. ¹H-NMR (400 MHz, DMSO-*d*₆) δ/ppm: 13.53 (s, 1H), 8.34 (s, 1H), 7.99 (d, *J* = 7.8 Hz, 1 H), 7.95 (s, 1H), 7.78 (s, 1H), 7.77 (d, *J* = 7.8 Hz, 1 H). LRMS (ESI): C₉H₃Br₄O₂⁻ *calcd.*: 464.7, *found*: 464.7 [M-H]⁻. (This compound was synthesized and characterized by Dr. Linna Zhou).

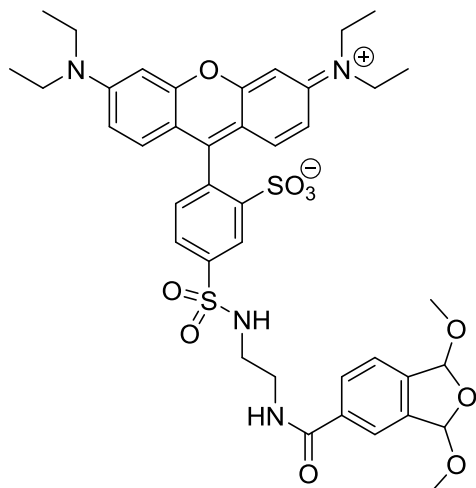


Acid 2.23: Compound **2.23** was synthesized in analogy to literature procedures by HARIS *et al.*²⁹⁹ and SHOKAT *et al.*²³⁷ Tetrabromide **2.22** (2.00 g, 4.29 mmol, 1.00 eq.) was dissolved in 10% Na₂CO₃ (20 mL). The reaction mixture was heated to 70°C and stirred for 4 h. After cooling down, the reaction mixture was acidified carefully with concentrated HCl to pH 1, followed by extraction with EtOAc (3 x 20 mL). The combined organics were washed with brine (30 mL), dried over Na₂SO₄, filtered and concentrated under reduced pressure. The light yellow solid was then dissolved in dry MeOH (20 mL) and Sc(OTf)₃ (100 mg, 203 μmol, 0.05 eq.) was added. The reaction mixture was stirred at room temperature overnight. The solvent was removed under reduced pressure and the residue purified by flash chromatography (CH₂Cl₂/MeOH) to afford the target product **2.23** (550 mg, 2.45 mmol, 57%) as a white solid. ¹H-NMR (400 MHz, DMSO-*d*₆) δ/ppm: 13.21 (s_{br}, 1H), 8.05 (d, *J* = 7.6 Hz, 1 H), 7.93 (s, 1H), 7.55 (d, *J* = 7.6 Hz, 1 H), 6.36 (s, 1H), 6.11 (s, 1H), 3.37-3.32 (m, 6H). LRMS (ESI): C₁₁H₁₁O₅⁻ *calcd.*: 223.1, *found*: 223.2 [M-H]⁻. (This compound was synthesized and characterized by Dr. Linna Zhou).



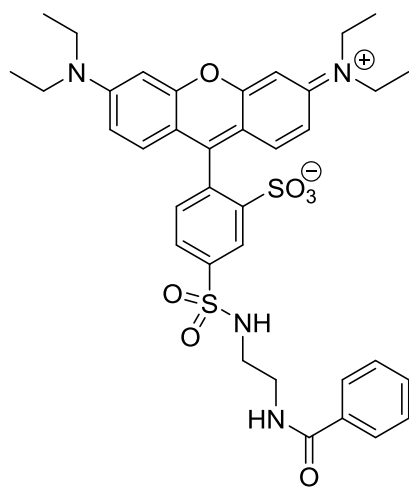
***N*-Boc protected lissamine 2.25:** Lissamine™ rhodamine B sulfonyl chloride **2.24** (200 mg, 347 μmol, 1.00 eq.) and *N*-Boc-ethylenediamine (110 μL, 694 μmol 2.00 eq.) were dissolved in EtOH (30 mL). NEt₃ (97.0 μL, 694 μmol, 2.00 eq.) was added dropwise and the reaction mixture was stirred at room temperature under N₂ atmosphere. The solvent was removed under reduced pressure and the residue purified by flash chromatography (CH₂Cl₂/MeOH) to afford the target product **2.25** (85.0 mg, 142 μmol, 41%) as a dark purple solid. ¹H-NMR

(500 MHz, DMSO- d_6) δ /ppm: 8.42 (d, $J = 1.8$ Hz, 1 H), 8.04 (t, $J = 6.0$ Hz, 1 H), 7.93 (dd, $J = 8.0$ Hz, $J = 1.8$ Hz, 1 H), 7.49 (d, $J = 8.0$ Hz, 1 H), 7.05-6.94 (m, 6H), 6.89 (t, $J = 5.6$ Hz, 1 H), 3.68-3.60 (m, 8H), 3.04-3.00 (m, 2H), 2.90-2.86 (m, 2H), 1.38 (s, 9H), 1.19 (t, $J = 7.0$ Hz, 12 H). ^{13}C -NMR (101 MHz, DMSO- d_6) δ /ppm: 157.43, 157.08, 155.47, 154.97, 148.02, 141.40, 133.04, 132.67, 130.65, 126.48, 125.63, 113.59, 113.44, 95.35, 77.79, 45.23, 42.19, 40.42, 28.18, 12.44. HRMS (ESI): $\text{C}_{34}\text{H}_{45}\text{N}_4\text{O}_8\text{S}_2^+$ *calcd.*: 701.2673, *found*: 701.2674 $[\text{M}+\text{H}]^+$. (This compound was synthesized and characterized by Dr. Linna Zhou).

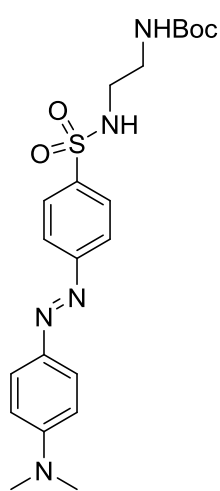


Lissamine bisacetal **2.26**: Lissamine derivative **2.25** (85.0 mg, 142 μmol , 1.00 eq.) was dissolved in methanol (10 mL) and 4M HCl in 1,4-dioxane (10 mL). The reaction mixture was stirred at room temperature for 4 h. The solvent was removed under reduced pressure and the residue was further treated with NEt_3 (193 μL , 139 μmol , 0.98 eq.), acid **2.23** (48.0 mg, 213 μmol , 1.50 eq.) and DCC (44.0 mg, 213 μmol , 1.50 eq.) in dry MeCN. The reaction mixture was stirred at room temperature overnight and the solvent was removed under reduced

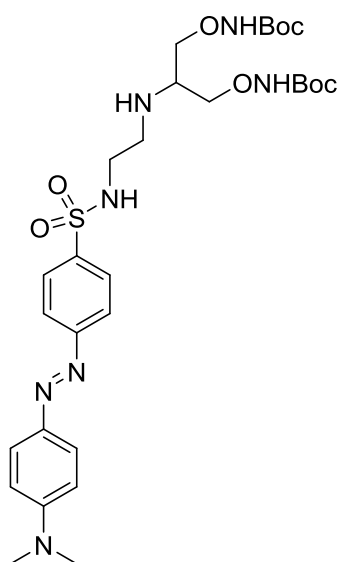
pressure. The residue was purified by flash chromatography ($\text{CH}_2\text{Cl}_2/\text{MeOH}$) to afford the target product **2.26** (40 mg, 49.6 μmol , 35%) as a dark purple solid. ^1H -NMR (500 MHz, DMSO- d_6) δ /ppm: 8.71 (t, $J = 5.4$ Hz, 1 H), 8.44 (d, $J = 1.8$ Hz, 1 H), 8.16 (t, $J = 5.8$ Hz, 1 H), 7.95 (dd, $J = 8.0$ Hz, $J = 1.8$ Hz, 1 H), 7.89 (s, 1 H), 7.50-7.44 (m, 2H), 7.04-6.93 (m, 7H), 6.33 (s, 1 H), 6.08 (s, 1 H), 3.67-3.59 (m, 8H), 3.35-3.24 (m, 8H), 3.08-3.03 (m, 2H), 1.20 (t, $J = 7.0$ Hz, 12 H). ^{13}C -NMR (126 MHz, DMSO- d_6) δ /ppm: 165.67, 157.38, 157.06, 154.97, 148.02, 141.42, 140.85, 138.45, 135.75, 133.06, 132.68, 130.67, 128.90, 126.50, 125.68, 122.99, 121.94, 113.60, 113.42, 105.57, 104.57, 95.33, 54.02, 53.90, 47.47, 45.22, 41.76, 12.43. HRMS (ESI): $\text{C}_{40}\text{H}_{47}\text{N}_4\text{O}_{10}\text{S}_2^+$ *calcd.*: 807.2728, *found*: 807.2732 $[\text{M}+\text{H}]^+$. (This compound was synthesized and characterized by Dr. Linna Zhou).



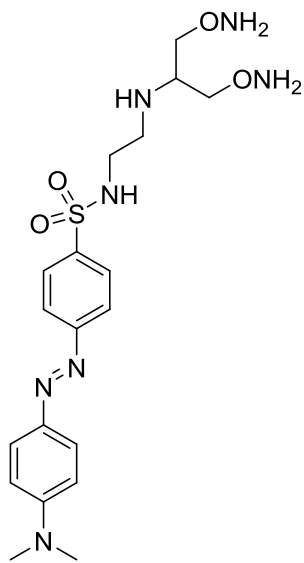
Lysamine-tagged OPA derivative **2.27**: Compound **2.26** (20.0 mg, 24.8 μmol , 1.00 eq.) was treated with TFA (2 mL) and H_2O (2 mL) at room temperature for 2 h. TLC ($\text{CH}_2\text{Cl}_2/\text{MeOH}$, 10:1) indicated full conversion of the starting material. The solvent was removed under reduced pressure and the residue purified by preparative RP-HPLC (MeCN and 0.1% TFA in H_2O). The product fractions were lyophilized to give the product **2.27** (8.00 mg, 10.5 μmol , 42%) as a dark purple solid. $^1\text{H-NMR}$ (600 MHz, $\text{DMSO-}d_6$) δ/ppm : 10.51 (s, 1 H), 10.51 (s, 1 H), 8.98 (t, $J = 5.6$ Hz, 1 H), 8.43 (dd, $J = 8.6$ Hz, $J = 1.7$ Hz, 2 H), 8.27 (d, $J = 8.0$ Hz, 1 H), 8.17 (t, $J = 6.3$ Hz, 1 H), 8.06 (d, $J = 8.0$ Hz, 1 H), 7.95 (dd, $J = 8.0$ Hz, $J = 1.8$ Hz, 1 H), 7.47 (d, $J = 8.0$ Hz, 1 H), 7.03-6.93 (m, 6H), 3.67-3.59 (m, 8H), 3.43-3.39 (m, 2H), 3.10-3.05 (m, 2H), 1.20 (t, $J = 6.9$ Hz, 12 H). $^{13}\text{C-NMR}$ (126 MHz, $\text{DMSO-}d_6$) δ/ppm : 192.73, 192.62, 164.72, 157.39, 157.08, 154.99, 148.05, 141.43, 138.54, 137.95, 136.27, 133.11, 132.69, 132.19, 130.70, 130.13, 128.72, 126.52, 125.68, 113.61, 113.44, 95.36, 45.23, 41.66, 40.05, 12.45. LRMS (ESI): $\text{C}_{38}\text{H}_{41}\text{N}_4\text{O}_9\text{S}_2^+$ *calcd.*: 761.2309, *found*: 761.2310 $[\text{M}+\text{H}]^+$. (This compound was synthesized and characterized by Dr. Linna Zhou).



N-Boc protected dabsyl derivative **2.29**: 4-(Dimethylamino)azobenzene-4'-sulfonyl chloride **2.28** (324 mg, 1.00 mmol, 1.00 eq.) and *N*-Boc-ethylenediamine (160 μL , 1.00 mmol, 1.00 eq.) were dissolved in EtOH (30 mL). NEt_3 (278 μL , 2.00 mmol, 1.00 eq.) was added dropwise and the reaction mixture was stirred at room temperature under N_2 atmosphere overnight. The solvent was removed under reduced pressure and the residue purified by flash chromatography ($\text{CH}_2\text{Cl}_2/\text{MeOH}$) to afford the target product **2.29** (240 mg, 537 μmol , 54%) as an orange solid. $^1\text{H-NMR}$ (500 MHz, $\text{DMSO-}d_6$) δ/ppm : 7.91 (s_{br}, 4H), 7.83 (d, $J = 9.1$ Hz, 2H), 7.76 (t, $J = 5.8$ Hz, 1H), 6.86 (d, $J = 9.1$ Hz, 2H), 6.79 (t, $J = 5.8$ Hz, 1H), 3.09 (s, 6H), 2.99-2.95 (m, 2H), 2.82-2.78 (m, 2H), 1.34 (s, 9H). $^{13}\text{C-NMR}$ (101 MHz, $\text{DMSO-}d_6$) δ/ppm : 155.42, 154.46, 153.08, 142.57, 140.13, 127.73, 125.35, 122.21, 111.57, 77.75, 42.25, 39.82, 39.81, 28.13. HRMS (ESI): $\text{C}_{21}\text{H}_{30}\text{N}_5\text{O}_4\text{S}^+$ *calcd.*: 448.2013, *found*: 448.2013 $[\text{M}+\text{H}]^+$. (This compound was synthesized and characterized by Dr. Linna Zhou).



Bis(carbamate) **2.30**: Compound **2.29** (100 mg, 288 μmol , 1.25 eq.) was dissolved in methanol (10 mL) and 4M HCl in 1,4-dioxane (10 mL). The reaction was stirred at room temperature for 4 h and the solvent removed under reduced pressure. The residue was further treated with compound **2.10** (74.0 mg, 231 μmol , 1.00 eq.) and NaBH_3CN (21.0 mg, 346 μmol , 1.50 eq.) in dry MeOH. The reaction mixture was stirred at room temperature overnight and the solvent removed under reduced pressure. The residue was purified by flash chromatography ($\text{CH}_2\text{Cl}_2/\text{MeOH}$) to afford the target product **2.30** (50.0 mg, 76.7 μmol , 27%) as a yellow solid. $^1\text{H-NMR}$ (400 MHz, CDCl_3) δ/ppm : 7.97 (d, $J = 8.6$ Hz, 2H), 7.91-7.89 (m, 4H), 7.65 (s_{br}, 1H), 6.75 (d, $J = 9.2$ Hz, 2H), 3.92-3.88 (m, 2H), 3.81-3.77 (m, 2H), 3.11 (s, 6H), 3.10-3.07 (m, 2H), 2.97-2.91 (m, 1H), 2.82-2.78 (m, 2H), 1.47 (s, 18H). $^{13}\text{C-NMR}$ (101 MHz, CDCl_3) δ/ppm : 157.04, 155.50, 153.04, 143.58, 139.68, 128.04, 125.67, 122.54, 111.44, 82.06, 76.28, 54.73, 45.83, 42.89, 40.29, 28.22. HRMS (ESI): $\text{C}_{29}\text{H}_{46}\text{N}_7\text{O}_8\text{S}^+$ *calcd.*: 652.3123, *found*: 652.3129 $[\text{M}+\text{H}]^+$. (This compound was synthesized and characterized by Dr. Linna Zhou).



Bishydroxylamine **2.31**: Compound **2.30** (25.0 mg, 38.3 μmol , 1.00 eq.) was dissolved in TFA/TIS/ H_2O (95:2.5:2.5) and the reaction mixture was stirred at 0°C for 1h. The solvent was removed under reduced pressure and the residue purified by RP-HPLC (MeCN and 0.1% TFA in H_2O). The product fractions were lyophilized to give the product **2.31** (8.00 mg, 17.7 μmol , 46%) as a yellow solid. $^1\text{H-NMR}$ (600 MHz, $\text{DMSO-}d_6$) δ/ppm : 8.12 (t, $J = 5.8$ Hz, 1H), 8.06-8.03 (m, 4H), 7.93 (d, $J = 9.1$ Hz, 2H), 6.96 (d, $J = 9.2$ Hz, 2H), 4.02 (s_{br}, 4H), 3.85-3.83 (m, 1H), 3.27-3.25 (t, $J = 6.8$ Hz, 2H), 3.19-3.17 (m, 8H). $^{13}\text{C-NMR}$ (126 MHz, $\text{DMSO-}d_6$) δ/ppm : 154.82, 153.20, 142.57, 139.04, 127.97, 125.47, 122.35, 111.60, 70.84, 54.76, 44.77, 40.05, 39.81. HRMS (ESI): $\text{C}_{19}\text{H}_{30}\text{N}_7\text{O}_4\text{S}^+$ *calcd.*: 452.2074, *found*: 452.2072 $[\text{M}+\text{H}]^+$. (This compound was synthesized and characterized by Dr. Linna Zhou).

4.2.2.2 Synthesis of LYRAG pentapeptide hydroxylamine substrates

The LYRAG pentapeptide mono- **2.6** and bishydroxylamine **2.7** were obtained *via* Fmoc-based automated and manual solid phase peptide synthesis (SPPS) on a rink amide AM resin from Novabiochem (0.17 mmol scale). The solid-phase bound LYRAG pentapeptide containing all protecting groups was readily synthesized on a Syro I Peptide Synthesizer (MultiSynTech GmbH, Witten, Germany) according to the following protocol:

- 1) swelling the resin in DMF (1 mL/100 mg) for 12 min.
- 2) Fmoc deprotection with 40% piperidine in DMF for 5 min., repeat with a fresh portion for 10 min.
- 3) wash with DMF 5 x 1 min.
- 4) coupling with 4.0 eq. of Fmoc-Gly-OH dissolved in DMF (0.7 M)/4.0 eq. HCTU in DMF (0.7 M)/4.0 eq. DIPEA in NMP (4.21 M) for 1 h.
- 5) wash with DMF 2 x 2 min.
- 6) capping with DIPEA in NMP (4.21 M)/Ac₂O in DMF (0.44 M) for 21 min.
- 7) wash with DMF 3 x 1 min.
- 8) repeat steps 3-7 using Fmoc-Ala-OH, Fmoc-Arg(Pbf)-OH, Fmoc-Tyr(^tBu)-OH, Fmoc-Leu-OH including a final wash with DMF 5 x 1 min. A small sample of resin (1 mg) was treated with a freshly prepared cleavage cocktail containing TFA/TIPS/H₂O (95:2.5:2.5, 0.2 mL) for 30 min. An aliquot of the cleavage cocktail was analyzed by UPLC-MS which confirmed the peptide mass of H-Gly-Ala-Arg-Tyr-Leu-NHFmoc.

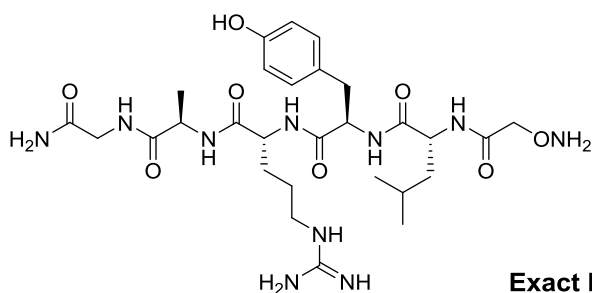
H-Gly-Ala-Arg-Tyr-Leu-NHFmoc: LRMS (ESI): C₄₁H₅₄N₉O₈⁺ *calcd.*: 800.4, *found*: 800.4 [M+H]⁺.

The final hydroxylamine terminated peptides (**2.6** and **2.7**) were manually synthesized in a 2 mL polyethylene syringe equipped with a fritted disk and luer stopper according to the following protocol:

- 1) swelling the LYRAG-containing resin (32 mg for **2.6**, 10 mg for **2.7**) in NMP (2 mL) for 1 h.
- 2) Fmoc deprotection with 40% piperidine in DMF 2 x 10 min.
- 3) wash with DMF/NMP (1:1) 3 x 1 min.
- 4) coupling with 4.0 eq. of Boc-AOAc-OH **1.9** or bishydroxylamine **2.8**/4.0 eq. HATU/4.0 eq. DIPEA in DMF (0.1 M) for 30 min.
- 5) wash with CH₂Cl₂/NMP (1:1) 3 x 1 min.
- 6) wash with CH₂Cl₂ 3 x 1 min.
- 7) peptide cleavage and deprotection of all protecting groups was performed with a freshly prepared cleavage cocktail containing TFA/TIPS/H₂O (95:2.5:2.5, 1 mL) 2 x 30 min. The cleavage solutions containing the peptides were collected in a 2 mL Eppendorf tube. The peptide masses were confirmed by UPLC-MS analysis of the cleavage solutions.

8) the cleavage solutions were concentrated under reduced pressure to ~0.1 mL and the peptides were precipitated with cold Et₂O (1.5 mL). The samples were centrifuged (10,000 rpm, 2 min.) and the supernatant was carefully discarded. The peptides were washed with a fresh portion of Et₂O (1.5 mL), sonicated and centrifuged again (10,000 rpm, 2 min.). This process was repeated once more and the peptide pellets were carefully dried with a gentle nitrogen stream.

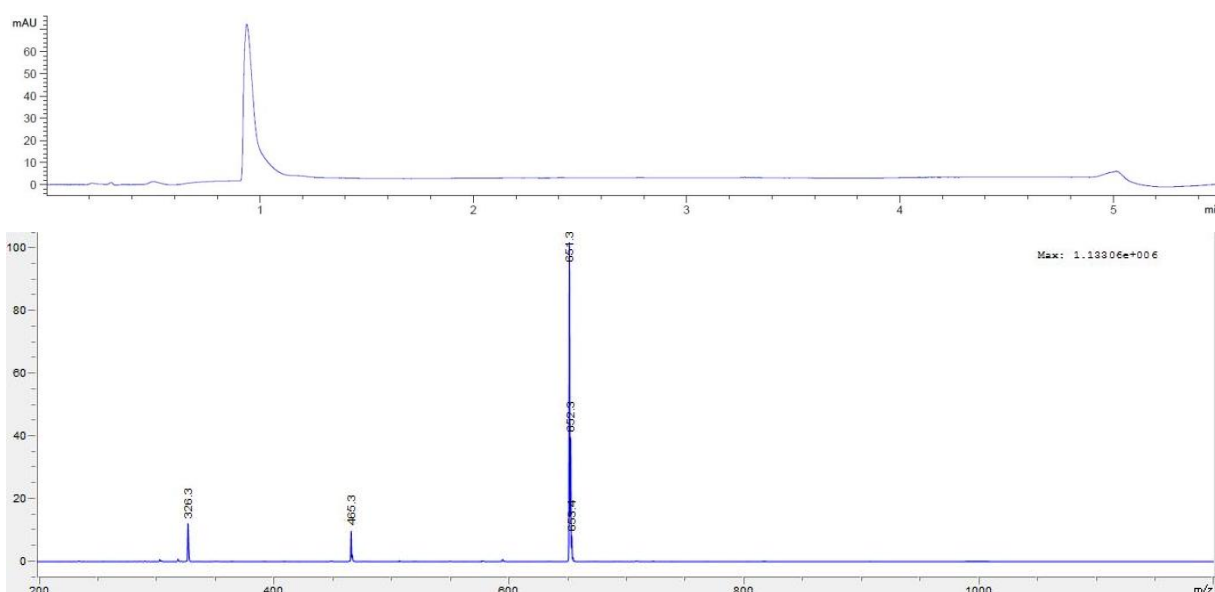
Both **2.6** and **2.7** (dissolved in 200 μ L H₂O) were purified employing preparative RP-HPLC over a C18 column (Gemini NX5u, 110 \AA , AXIA, 250 x 21.2 mm) from Phenomenex (gradient: 0-60% (for **2.6**), 0-40% (for **2.7**) MeCN in H₂O, 1% MeCN, 0.1% formic acid in 25 min.) with a flow rate of 20 mL/min monitoring and collecting the products at 280 nm. The product fractions were re-analyzed by UPLC-MS and lyophilized. Stock solutions were prepared in Milli-Q water and the concentration was determined using a NanoDrop 2000 spectrophotometer from Thermo Scientific with a path length of 1 mm and $\epsilon_{(\text{LYRAG})} = 1490 \text{ M}^{-1} \text{ cm}^{-1}$. All peptide stock solutions were stored at -20°C.

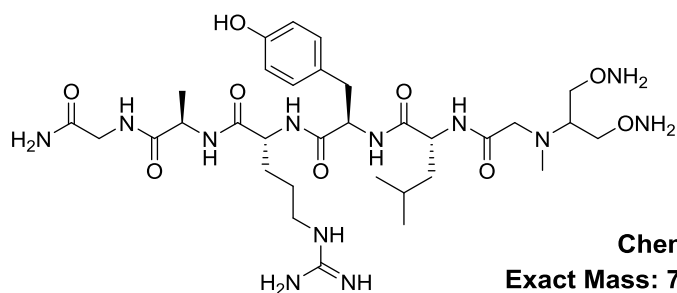


Chemical Formula: C₂₈H₄₆N₁₀O₈;
Exact Mass: 650.3500; Molecular Weight: 650.7380

2.6

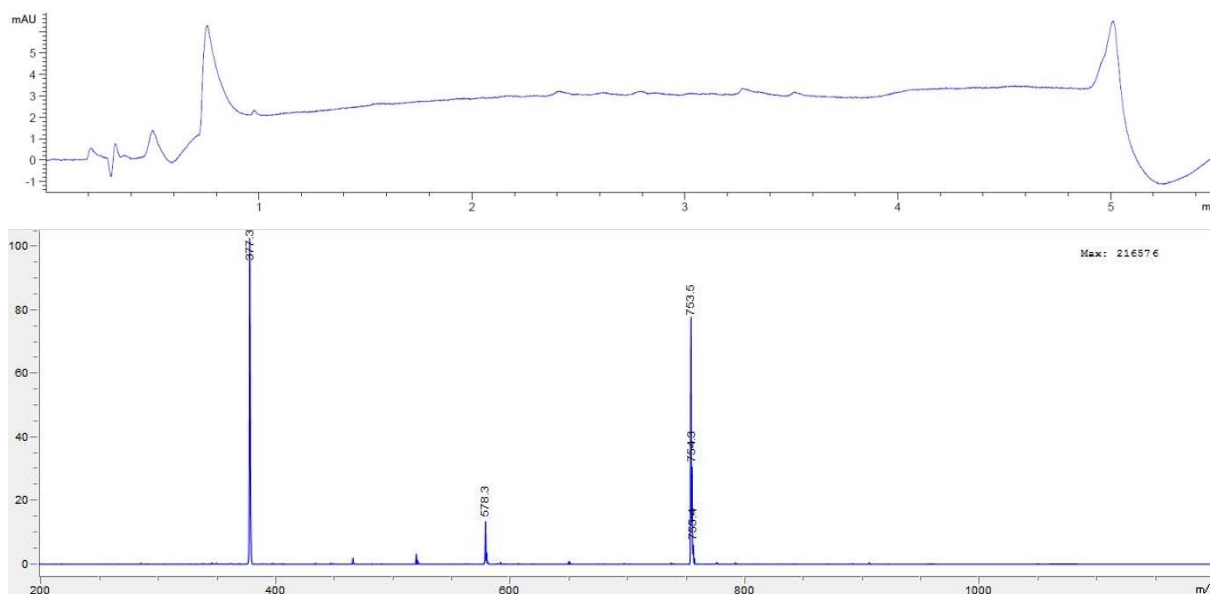
Peptide **2.6**: LRMS (ESI): C₂₈H₄₆N₁₀O₈⁺ *calcd.*: 651.3, *found*: 651.3 [M+H]⁺. t_R = 0.99 min.





2.7

Peptide **2.7**: LRMS (ESI): C₃₂H₅₆N₁₂O₉⁺ *calcd.*: 753.4, *found*: 753.5 [M+H]⁺. t_R = 0.80 min.



4.2.2.3 HPLC assays

For all experiments fresh stock solutions of *ortho*-phthalaldehyde (**2.1**), benzaldehyde, 2-formylbenzoic acid, *O*-benzylhydroxylamine (**2.4**), 3-formyl benzaldehyde, 4-formyl benzaldehyde, 2-acetyl acetophenone and bishydroxylamine **2.15** were prepared in HPLC grade MeCN and directly used in the condensation reactions. Commercial 2-naphthaldehyde (Sigma) was dissolved in MeCN/H₂O (3:2) and directly used in the condensation reactions. As reaction media a 100 mM aqueous KP_i buffer (pH = 7.2) was used. The peptide stock solutions for condensation were allowed to warm to room temperature, vortexed and centrifuged prior to mixing and combined in a PP HPLC vial (BGB, Part Number: PPSV0903K) in the following order: 1) 100 mM KP_i buffer pH = 7.2, 2) *O*-alkylhydroxylamine, 3) L-tryptophan (Sigma) or lysozyme (Roth) and 4) aldehyde. The resulting solution was briefly mixed with a Gilson Pipetman and transferred into a HPLC vial. The reactions (**Table 3.1/E1** entries 1-7) were analyzed by UPLC-MS on an Agilent device using a C18 column (ZORBAX RRHD) 1.8 μ, 2.1 x 50 mm from Agilent (gradient: 5-90% MeCN in H₂O, 1% MeCN,

0.1% formic acid in 3.5 min., flow rate 0.45 mL/min, 40°C) at different time intervals (1 min then every 10 min for 1 h and after 1.5 h) by injecting 4 μ L (100 μ M reactants) or 20 μ L (10 μ M reactants) of the reaction mixture. Reactions (**Table 3.1/E1** entries 8-9 and **Table 3.2/E2** entries 1-6) were followed by RP-HPLC on a Shimadzu device using a C18 column (ECLIPSE XDB) 5 μ m, 4.6 x 150 mm from Agilent (gradient: 2-55% MeCN, 1% H₂O in H₂O, 1% MeCN, 0.1% TFA in 13 min, flow 1.0 mL/min, room temperature) at different time intervals (1 min, 30 min, 1 h and 1.5 h) by injecting 20 μ L (100 μ M reactants) of the reaction mixture. The conversion was determined by integration of the signal at 280 nm of the starting LYRAG pentapeptide hydroxylamine or at 254 nm for all remaining reactions (Note: in cases where the starting materials were not UV active the product formation was monitored). The formation of the corresponding oximes was confirmed by ESI-MS spectra directly extracted from the UPLC-MS runs or by direct injection of the collected product peaks.

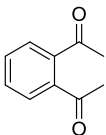
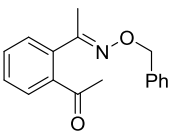
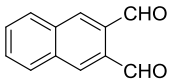
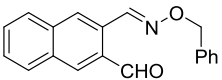
Table E1: Comparison of oxime ligation reactions with different aromatic aldehydes and mono- or bishydroxylamines.

100 or 10 μ M

1 eq. RONH₂
100 mM KPi
pH 7.2
1.5 h

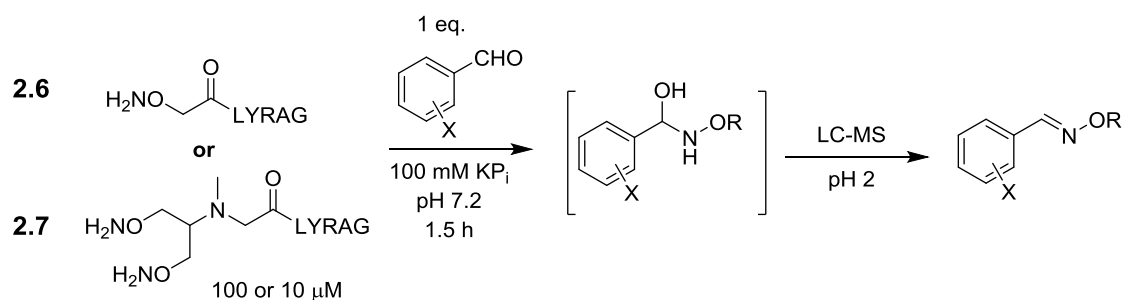
LC-MS
pH 2

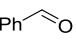
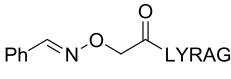
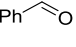
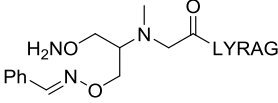
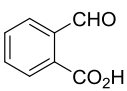
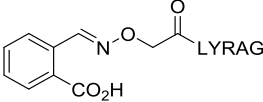
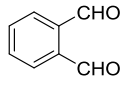
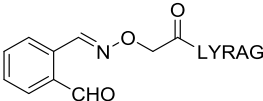
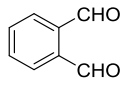
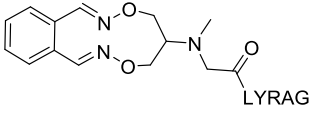
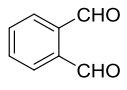
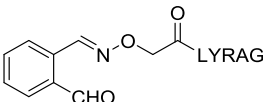
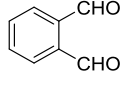
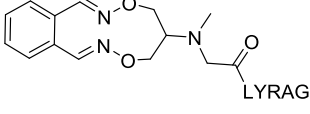
Entry	Aldehyde	RONH ₂	Product (t = 1.5 h)	Product t _R [min]	calc. mass [M+H] ⁺	found mass [M+H] ⁺
1				~[a]	212.1	-
2				2.49 ^[b]	256.1	256.1
3				2.44	205.1	205.1
4				2.84	240.1	240.1
5				2.41/3.12 ^[c]	267.1	267.1/401.2
6				2.82	240.1	240.1
7				2.83	240.1	240.1

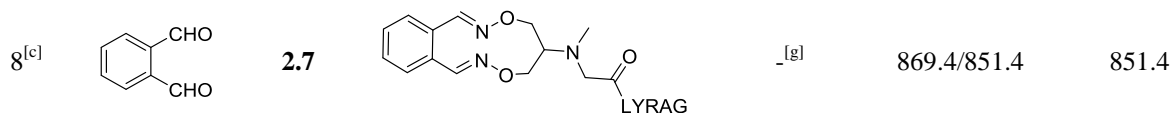
8		$\text{H}_2\text{NO}-\text{CH}_2-\text{Ph}$		- ^[a]	268.1	-
9		$\text{H}_2\text{NO}-\text{CH}_2-\text{Ph}$		18.5 ^[d]	290.1	290.3

[a] No product formation was observed under these conditions after 1.5 h. [b] Conversion less than 10% after 1.5 h. [c] Bis-monooxime (product of two molecules of *ortho*-phthalaldehyde (**2.1**) and one molecule of *O*-benzylhydroxylamine (**2.4**)). [d] Reactions were monitored by RP-HPLC and characterized by ESI-MS direct injection of the collected peaks.

Table E2: Comparison of oxime ligation reactions with peptide substrates.



Entry	Aldehyde	RONH ₂	Product (t = 1.5 h)	Product t _R [min]	calc. mass [M+H] ⁺	found mass [M+H] ⁺
1 ^[a]		2.6		- ^[d]	739.4	-
2 ^[a]		2.7		- ^[d]	840.5/928.5 ^[e]	-
3 ^[a]		2.6		1.38	783.4	783.3
4 ^[a]		2.6		1.52	767.4	767.4
5 ^[a]		2.7		1.41	851.4 ^[f]	851.4
6 ^[b]		2.6		1.52	767.4	767.4
7 ^[b]		2.7		1.44	851.4 ^[f]	851.4



[a] Substrate concentrations: 100 μ M. [b] Substrate concentrations: 10 μ M. [c] Human serum (20% v/v) was added to the reaction mixture; aldehyde concentration in this experiment is 50 μ M. [d] No product formation was observed under these conditions after 1.5 h. [e] Masses for monooxime/bisoxime. [f] Also observed: monooxime ($t_R = 1.20$ min, 869.4 Da) and bis monooxime (peptide/dialdehyde 1:2, $t_R = 1.86$ min, 985.3 Da). [g] Product peak collapses with peaks introduced by the human serum, approximate $t_R = 1.35$ min.

4.2.2.4 $^1\text{H-NMR}$ studies

General Information

All NMR experiments for the mechanistic and kinetic studies were performed at 298.15 K on a BrukerAvance III NMR spectrometer operating at 700.09 MHz, equipped with a $^1\text{H-}^{13}\text{C}/^{15}\text{N-D}$ TCI cryo probe head with z -axis pulsed field gradients. All 1D proton experiments were recorded using exactly the same parameters (256 scans, relaxation delay of 1.5 s and an acquisition time of 2.78 s) and were processed similarly using line broadening of 0.3 Hz and after manual phase correction automated baseline correction was applied. The same integration regions were used for every spectrum and chemical shifts were referenced to the residual solvent peak of MeCN (1.94 ppm) and integrals were referenced to internal TMSP- d_4 (3-(trimethylsilyl)-2,2',3,3'-tetra-deuteriopropionic acid). For every spectrum time points were corrected by half the experiment time, relative to the individual starting time. *Ortho*-phthalaldehyde (**2.1**) was purchased from Acros and *O*-benzylhydroxylamine (**2.4**) was neutralized from its HCl salt according to a published procedure.³⁰⁰ The pH (no correction for deuterium) was adjusted using a 827 pH Lab – Metrohm equipped with a glass minitrode which was pre-rinsed with D_2O .

Experimental

Stock solutions for both *ortho*-phthalaldehyde (**2.1**) and *O*-benzylhydroxylamine (**2.4**) were freshly prepared in CD_3CN . A KPi buffer stock solution was freshly prepared in D_2O adjusting the pH to 7.1 with concentrated DCl from ABCR (DCl, 38% wt% in D_2O , 99.5% atom%D). A TMSP- d_4 stock solution was freshly prepared in D_2O . All experiments were conducted in standard NMR tubes (throw away quality) which were rinsed thoroughly with D_2O and oven dried prior to use. After every addition of substrates the NMR tube was vortexed followed by sonication and finally centrifuged to assure a homogenous mixing prior to the respective NMR experiment. All experiments were setup as follows:

1. 440 μL of KP_i buffer (12.5 mM) were mixed inside of the NMR tube with 50 μL of *O*-benzylhydroxylamine (**2.4**, 1.10 mM) and 10 μL of TMSP-d_4 (0.275 mM). The sample was then locked to MeCN and shimmed before the addition of the OPA.
2. 50 μL of *ortho*-phthalaldehyde (**2.1**, 1.10 mM) was then added and the sample was shimmed again before conducting the first measurement.

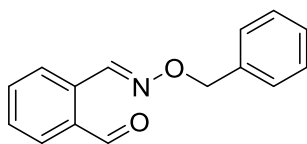
The final volume of the NMR sample was 550 μL with the following final concentrations:

100 μM in each *O*-benzylhydroxylamine (**2.4**) and *ortho*-phthalaldehyde (**2.1**), respectively. 10 mM KP_i buffer and 5 μM TMSP-d_4 with a ratio of 4:1 (D_2O KP_i buffer/ CD_3CN).

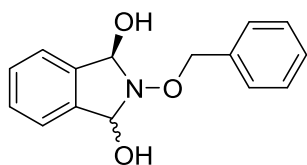
The time dependent ^1H -NMR analysis with a full stack of the spectrum (10.5 – 4.7 ppm) containing all signals of interest is shown in **Figure 3.5**. A mechanistic overview of the processes is shown in **Scheme 3.10**.

Since the IBHA intermediates could not be isolated in a pure form, a preparative scale of the oxime condensation was envisioned for full characterization. The following procedure was followed:

A 10 mL flask under inert atmosphere equipped with a stir bar was charged with *ortho*-phthalaldehyde (53.0 mg, 0.39 mmol, 1.00 eq, 98% purity) dissolved in 1 mL of dry MeCN. To the stirring solution was added *O*-benzylhydroxylamine (48.5 mg, 0.39 mmol, 1.00 eq, 98% purity) as a solution in dry MeCN (0.50 mL) at room temperature. The reaction was stopped as soon as a white solid precipitated (45 seconds) which prevented efficient stirring. The stir bar was removed and washed with MeCN and the solvent was removed under reduced pressure and extensively dried under high vacuum to give 97 mg of a white fluffy solid which turned out to be a 1:1.5 mixture of oxime **2.5** and IBHA **2.16** (as a 9:1 mixture of diastereomers). It is important to mention that this mixture of oxime **2.5** and IBHA **2.16** needs to be stored under inert atmosphere at -20°C since it was found that leaving a sample for several hours at room temperature will lead to full conversion of the IBHA **2.16** to the oxime **2.5**. ^1H (16 scans), ^{13}C (1024 scans) and DEPT135 (128 scans) spectra were recorded in CD_3CN at 298.15 K on a BrukerAvance III NMR spectrometer operating at 500.13 MHz, equipped with a 5mm BBI probe head with *z*-axis pulsed field gradients.



Oxime **2.5**: $^1\text{H-NMR}$ (500 MHz, CD_3CN) δ/ppm : 10.19 (s, 1H), 8.85 (s, 1H), 7.88 (dd, $J = 7.3$ Hz, $J = 1.2$ Hz, 1H), 7.81 (dd, $J = 7.6$ Hz, $J = 0.97$ Hz, 1H), 7.65 (dt, $J = 7.5$ Hz, $J = 1.5$ Hz, 1H), 7.61 (dt, $J = 7.6$ Hz, $J = 1.4$ Hz, 1H), 7.45-7.41 (m, 2H), 7.41-7.37 (m, 2H), 7.36-7.30 (m, 1H), 5.22 (s, 2H). $^{13}\text{C-NMR}$ (126 MHz, CD_3CN) δ/ppm : 193.94, 148.20, 138.75, 135.07, 134.62, 133.61, 132.95, 131.00, 129.42, 129.41, 128.97, 128.88, 77.19.



IBHA **2.16**: $^1\text{H-NMR}$ (500 MHz, CD_3CN) δ/ppm : 7.51-7.46 (m, 2H), 7.41-7.37 (m, 4H, overlapping), 7.36-7.30 (m, 3H, overlapping), 5.57 (d, $J = 8.6$ Hz, 2H), 5.08 (s, 2H), 4.16 (d, $J = 8.5$ Hz, 2H). $^{13}\text{C-NMR}$ (126 MHz, CD_3CN) δ/ppm : 139.04, 138.92, 129.96, 129.73, 129.24, 128.81, 123.85, 90.62, 79.21.

Determining K_{eq} and k_2

To estimate a value for K_{eq} **equation 4** was used.

$$K_{\text{eq}} = \frac{[\text{IBHA}]}{[\text{OPA}] [\text{BnONH}_2]} = \frac{[\text{IBHA}]}{[\text{OPA}]^2} \quad (4)$$

Equation 4: K_{eq} = equilibrium constant [M^{-1}], $[\text{OPA}] = [\text{BnONH}_2]$ [M].

For all $^1\text{H-NMR}$ measurements the corresponding integrals were converted into concentrations with reference to the internal standard TMSP- d_4 . All K_{eq} values (10^7 M^{-1}) were then plotted against the time (sec) and from the steady-state region (between 7000-22000 sec) the average of these values was taken for $K_{\text{eq}} = 2 \times 10^7 \text{ M}^{-1}$ (**Figure E1**, top). This analysis was done using Microsoft Excel 2010.

To determine k_2 a plot of $\ln[\text{oxime}]$ versus the time (sec) was performed where the slope of the straight line is a direct measure for the rate constant (**Figure E1**, bottom). A slight increase in $\ln[\text{oxime}]$ was found in the first 15000 seconds of the reaction which can be attributed to the initial build-up of the IBHA species. Therefore only the linear region (15000-50000 sec) was used for a best fit and the slope of the obtained trend line was determined to be $k_2 = 1.2 \pm 0.2 \times 10^{-5} \text{ s}^{-1}$. The value is an average of two separate $^1\text{H-NMR}$ experiments and was determined using Microsoft Excel 2010.

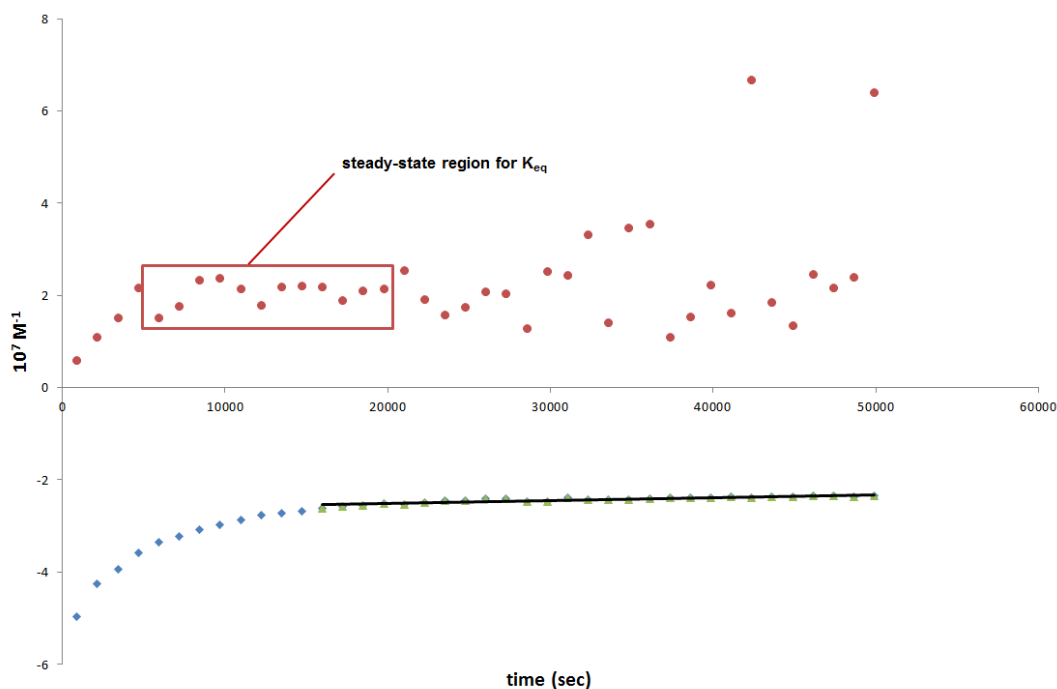


Figure E1: Time course NMR analysis; estimation of K_{eq} and determination of k_2 . **Top:** steady-state region of the reaction allowing for an estimate of K_{eq} . **Bottom:** Best fit of $\ln[\text{oxime}]$ over time in the linear region gives a direct measure of k_2 as the slope.

Equilibrium studies

To determine whether the IBHA **2.16** is in a reversible equilibrium with another *ortho*-dialdehyde time dependent $^1\text{H-NMR}$ spectra were recorded where the naphthalene IBHA **2.20** (see section 4.2.2.1 for synthetic details) was treated with a tenfold excess of *ortho*-phthalaldehyde (**2.1**). The $^1\text{H-NMR}$ spectra were recorded as follows: The corresponding mixture of **2.20** was dissolved in 1:1 (D_2O phosphate buffer/ $\text{DMSO-}d_6$) at 0.1 mM and a proton NMR was recorded. Then OPA (1 mM, 10 eq.) was added and time dependent $^1\text{H-NMR}$ were recorded over 75 min. No interconversion of **2.20** to **2.16** was observed (see **Figure 3.8**, panel D) thus supporting that this reaction is not in equilibrium.

4.2.2.5 Fluorescence quenching assay

The assay and data analysis were performed by Dr. Linna Zhou.

The fluorescence quenching experiments were conducted using a TECAN fluorescence plate reader and data was analyzed with the Megallan software. The fluorescence was monitored at the maximum absorption of lissamine-tagged OPA derivative **2.27** (567 nm) in KP_i buffer (100 mM, pH 7.2). The bleaching effect was monitored at the excitation wavelength (567 nm) at concentrations of 5 μM or 2 μM over 35 minutes. As shown in **Figure E2**, less than 5% and 8% bleaching was observed when quadruple measurements were performed at the concentration of 5 μM and 2 μM respectively. The data is therefore uncorrected for bleaching.

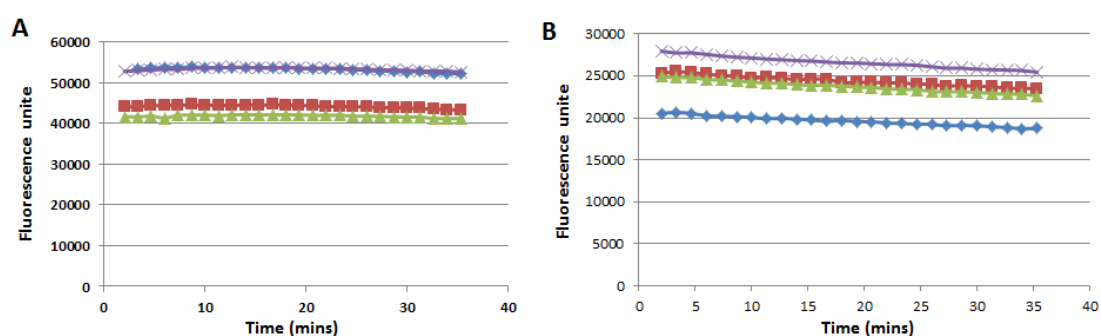


Figure E2: Bleaching effect of lissamine-tagged OPA derivative **2.27** over 35 minutes at 5 μM (A) and 2 μM (B).

The quenching experiments were conducted by mixing 2 μL of lissamine-tagged OPA derivative **2.27** (500 μM or 200 μM , in MeCN) with 2 μL of dabsyl quencher **2.31** (500 μM or 200 μM , in DMSO) in 196 μL KP_i buffer, followed by monitoring the fluorescence at 567 nm. The decrease in concentration over 80 minutes at final concentrations of 5 μM or 2 μM is shown in **Figure E3** and **Figure E4** respectively.

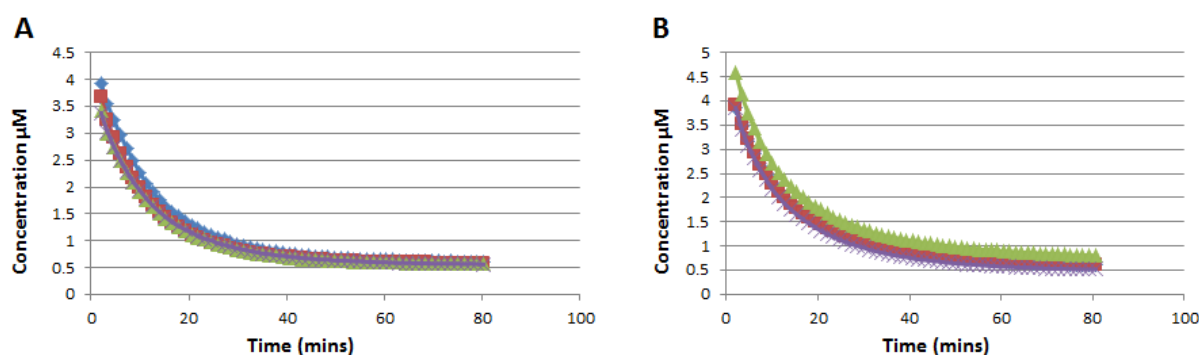


Figure E3: Two independent quadruple quenching experiments with lissamine-tagged OPA derivative **2.27** and dabsyl quencher **2.31** at 5 μM .

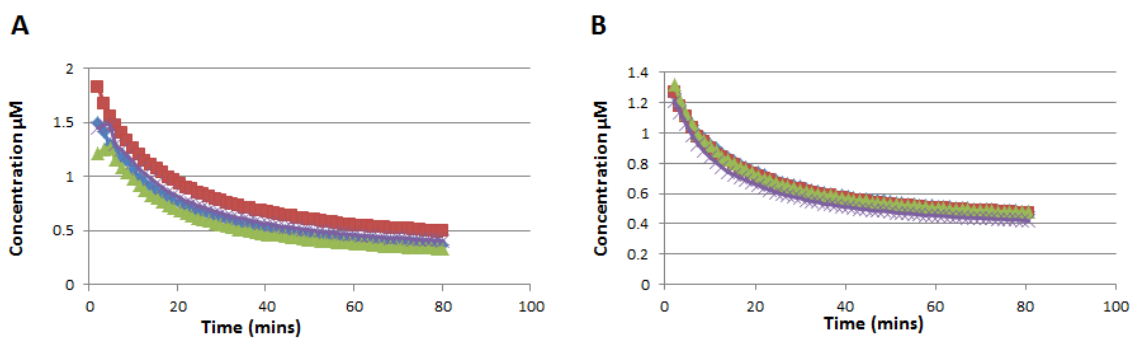


Figure E4: Two independent quadruple quenching experiments with lissamine-tagged OPA derivative **2.27** and dabsyl quencher **2.31** at 2 μM .

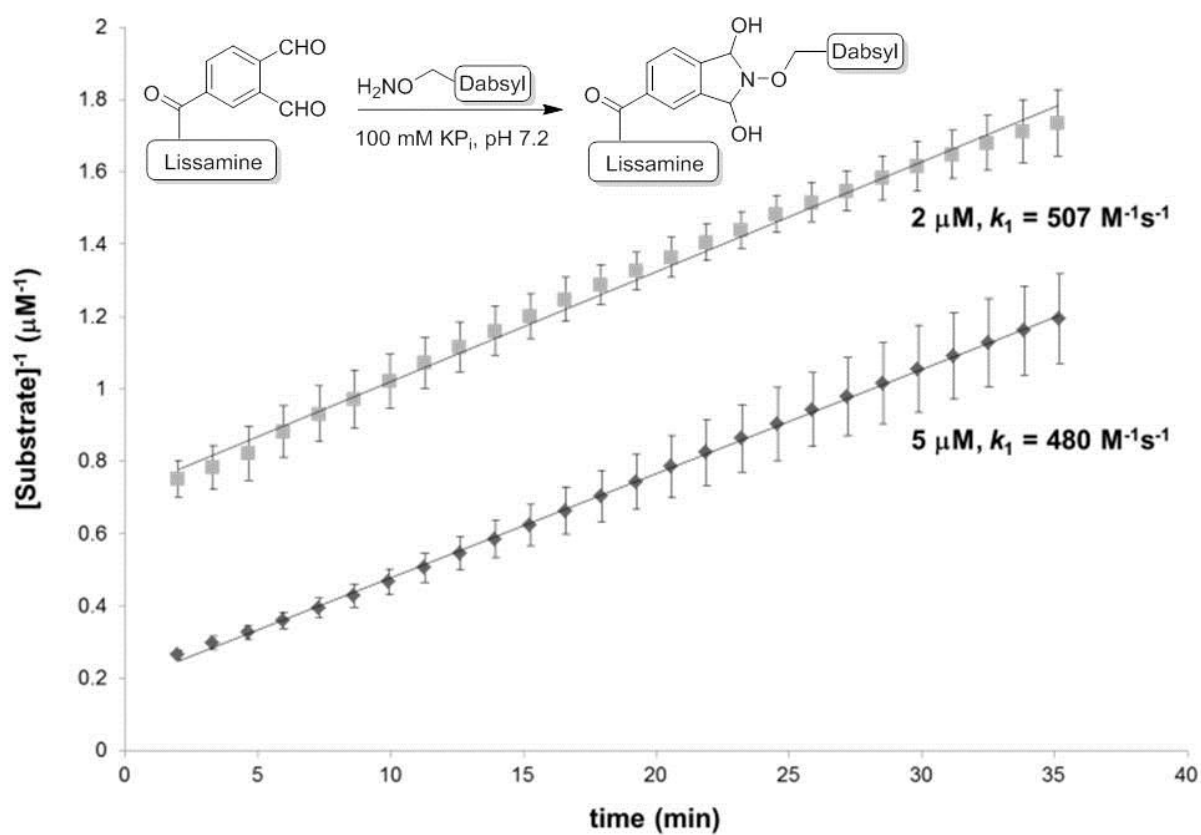


Figure E5: Second order plots at 5 μM and 2 μM , respectively.

HPLC analysis was also conducted and showed $\sim 90\%$ conversion of the starting material after 10 min at 10 μM . Corresponding MS analysis confirmed the formation of the corresponding bisoxime and IBHA.

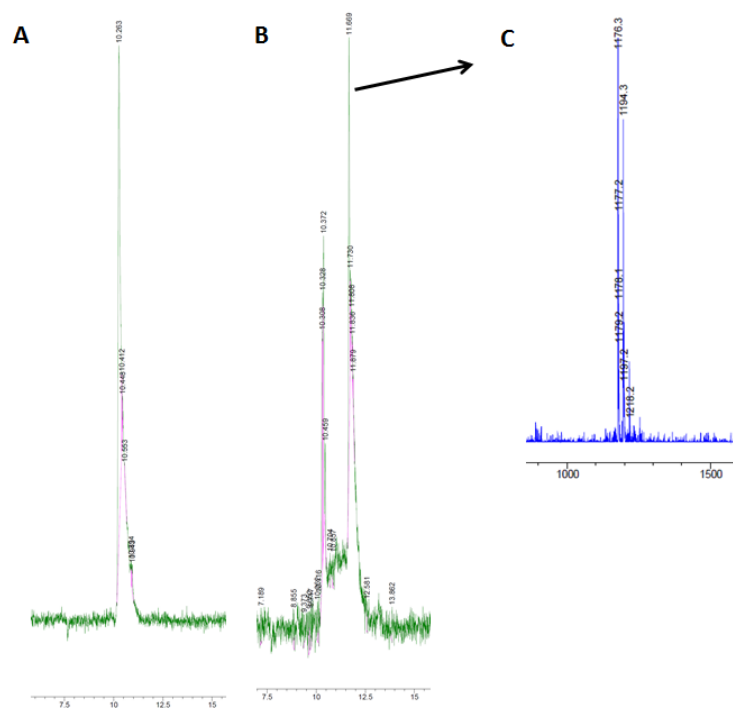


Figure E6: HPLC and MS analysis of the quenching reaction between lissamine-tagged OPA derivative **2.27** and dabsyl quencher **2.31** at 10 μ M. Lissamine-tagged OPA derivative **2.27** has a retention time of around 10.3 min, while the corresponding bisoxime product has a retention time of 11.7 min containing the mass of 1176.3 $[M+H]^+$. The observed mass of 1194.3 ($\Delta M = +18$) is attributed to the IBHA.

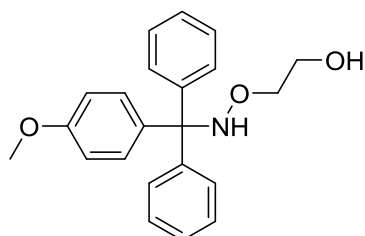
4.2.2.6 DNA bioconjugation

The synthesis and analysis of compounds as well as the DNA bioconjugation assay was performed by Dr. Kiril Tishinov.

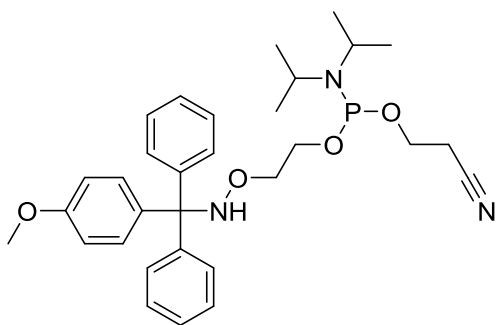
Native polyacrylamide gel electrophoresis (Native PAGE)

Native PAGE was done in 15% gel (29:1 w/w acrylamide/bisacrylamide) in 1×TBE (89 mM Tris-borate, 2 mM EDTA) with Orange G, Bromophenol blue and XylenCynol FF as tracer dyes. The electrophoretic samples were prepared by mixing 5 μL of sample with 2.5 μL 4×TBE in 40% (v/v) glycerol. Five microliters from the resulting mixtures were then applied on the gel without further pre-treatment. Trace dye mixtures were applied on separate wells. The gels were run at 30 V/cm until the Orange G migrated to approximately 1 cm from the end of the gel. The gels were then washed briefly with deionized H_2O and visualized using Bio-Rad ChemiDoc MP system, equipped with Image Lab 5.0 software. The labeled species on the gels were traced by the intrinsic lissamine fluorescence (the device set-up for Blot/Rhodamine or Blot/Alexa488). The gels were then soaked in ethidium bromide solution in H_2O for 15 min and then visualized again (set-up Nucleic Acids/Ethidium bromide) to detect all nucleic acid species present.

Phosphoramidite synthesis



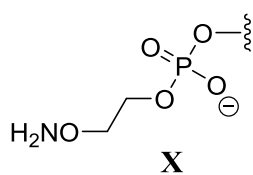
MMT alcohol: *tert*-butyl *N*-(2-hydroxyethoxy)carbamate (310 mg, 1.75 mmol, 1.00 eq.) was dissolved in Et_2O (2 mL), saturated with HCl in Et_2O (6 mL) and the mixture was left at room temperature for 6 h. The white crystalline precipitate that formed was recovered by centrifugation, washed with diethyl ether and dried under high vacuum. It was then dissolved in DMF (5 mL), NEt_3 (1.90 mL, 14.1 mmol, 7.94 eq.) was added and the mixture was stirred under nitrogen at room temperature for 1 h. Monomethoxytrityl chloride (710 mg, 2.30 mmol, 1.31 eq.) as a solution in 2 mL of DMF was added and the mixture stirred at room temperature overnight. The solvent was then removed under reduced pressure and the residue purified by flash chromatography (*n*-pentane/ EtOAc , containing 1% NEt_3) to yield the desired MMT alcohol as a yellow oil (406 mg, 1.16 mmol, 66%). $^1\text{H-NMR}$ (250 MHz, CD_3CN) δ /ppm: 7.18-7.35 (m, 12 H), 6.82-6.88 (m, 3H), 3.76 (s, 3H), 3.64-3.68 (m, 2H), 3.50-3.54 (m, 2H). $^{13}\text{C-NMR}$ (62.5 MHz, CD_3CN) δ /ppm: 159.39, 146.01, 137.72, 131.22, 129.91, 129.87, 128.57, 128.53, 127.68, 113.80, 76.07, 74.21, 61.31, 55.83.



MMT phosphoramidite: The MMT alcohol (220 mg, 630 μmol , 1.00 eq.) was dissolved in CH_2Cl_2 (8 mL) under nitrogen, 3-(bis(diisopropylamino)phosphanyl)oxy)propanenitrile (300 mg, 995 μmol , 1.58 eq.) as a solution in 2 mL of CH_2Cl_2 and diisopropylammonium tetrazolide (61.0 mg, 356 μmol , 0.56 eq.) were added and the mixture was stirred at room temperature overnight.

The solvent was removed under reduced pressure and the residue purified by flash chromatography (*n*-pentane/EtOAc, containing 1% NEt_3) to yield the desired MMT phosphoramidite product as a yellow oil (231 mg, 420 μmol , 67%). $^1\text{H-NMR}$ (250 MHz, CD_3CN) δ/ppm : 7.17-7.34 (m, 12 H), 6.79-6.87 (m, 3H), 3.49-3.81 (m, 11H), 2.50-2.56 (m, 2H), 1.13 (d, $J = 11.1$ Hz, 6H), 1.11 (d, $J = 11.1$ Hz, 6H). $^{13}\text{C-NMR}$ (62.5 MHz, CD_3CN) δ/ppm : 159.39, 146.03, 137.74, 131.21, 129.90, 128.58, 127.69, 118.26, 118.21, 113.81, 74.60, 74.49, 74.15, 62.67, 62.41, 59.54, 59.24, 55.84, 43.90, 43.70, 24.98, 24.85, 21.02, 20.91. $^{31}\text{P}\{^1\text{H}\}$ (CD_3CN) δ/ppm : 147.57. HRMS (ESI): $\text{C}_{31}\text{H}_{40}\text{N}_3\text{NaO}_4\text{P}^+$ *calcd.*: 572.2654, *found*: 572.2659 $[\text{M}+\text{Na}]^+$.

Oligonucleotide synthesis and purification



5'-*O*-alkylhydroxylamine-terminated DNA 41-mer **2.32**: Solid-phase synthesis of d(**X**AG GTG CGA CTT GAT GAA GGA CTA CTG GAT TGA GGC TTA AAC) was carried out on 1- μmol CPG columns using standard phosphoramidite chemistry with 0.3 M 5-benzylthio-1-*H*-tetrazole as activator.

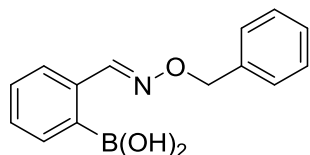
The 5'-hydroxylamine termination (position **X**) was introduced with **MMT phosphoramidite** with an extended coupling cycle (900 s) in DMT-ON regime. The oligonucleotide was cleaved and deprotected as the MMT-derivative. Cleavage of the MMT-group to obtain the free 5'-hydroxylamine was done with 20% (v/v) acetic acid in H_2O for 1 h at room temperature. Semi-preparative HPLC was carried out on a LiChroCART 250-10, packed with Purospher STAR RP-18e (5 μm) in 100 mM triethylammonium acetate, pH 7.0/MeCN gradient: 0-16% MeCN in 15 min, 16-80% MeCN in 5 min; flow rate 5 mL/min, detection by absorption at 254 nm.

Fluorescent labeling with lissamine-tagged OPA derivative **2.27**

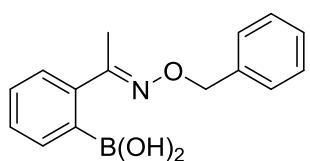
For initial screening of the labeling efficacy 40 μM oligonucleotide **2.32** and 100 μM fluorescent dialdehyde **2.27** (1 mM stock in DMSO) were mixed in H_2O in a final volume of 10 μL and the mixture was left in the dark for 1 h at room temperature, then analyzed by native PAGE. For concentration dependence studies 1, 5, 10, 20 and 40 μM concentrations of oligonucleotide **2.32** were incubated with 100 μM lissamine-tagged OPA derivative **2.27** for 1 h at room temperature in the dark. All reaction mixtures were analyzed by native PAGE (see **Figure 3.10**, right).

4.2.3 Boronic acid studies

4.2.3.1 Synthesis of small molecules

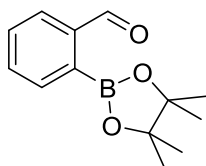


Oxime **2.35**: 2-Formylphenylboronic acid (**2.34**) (49.0 mg, 310 μmol , 1.00 eq.) was dissolved in dry MeOH (3 mL) followed by the addition of *O*-benzylhydroxylamine \cdot HCl (50.0 mg, 310 μmol , 1.00 eq.) which was washed down the flask with another 2 mL of dry MeOH. The progress of the reaction was monitored by UPLC-MS. After 15.5 h full conversion of the starting aldehyde was achieved and the solvent was removed under reduced pressure. The crude was purified employing preparative RP-HPLC (gradient: 5% MeCN in H₂O, 0.1% TFA for 3 min, 5-95% MeCN in H₂O, 0.1% TFA for 25 min) with a flow rate of 20 mL/min monitoring and collecting the product at 254 nm (t_R = 20.7 min). The product fractions were re-analyzed by UPLC-MS and lyophilized. The oxime was obtained as a fluffy white solid (52.0 mg, 203 μmol , 65%). TLC (cyclohexane/EtOAc 1:1) R_f = 0.45. ¹H NMR (400 MHz, CD₃CN) δ /ppm: 8.49 (s, 1H), 7.74-7.70 (m, 1H), 7.63-7.60 (m, 1H), 7.46-7.36 (m, 6H), 7.36-7.31 (m, 1H), 6.49 (s, 2H) 5.17 (s, 2H). It has to be mentioned that the ¹H-NMR spectral data of the boronic acid oxime **2.35** in CDCl₃ contained product signals along with some boroxine or other unidentified boronic acid related signals. Measuring the sample in CD₃CN proved to give a cleaner spectrum with no other species present. ¹³C-NMR (101 MHz, CDCl₃) δ /ppm: 153.93, 138.31, 136.47, 134.99, 133.29, 130.93, 129.97, 128.78, 128.76, 128.67, 128.59, 76.73. ¹¹B-NMR (128 MHz, CDCl₃) δ /ppm: 29.00. ¹¹B-NMR (128 MHz, CD₃CN) δ /ppm: 29.37. HRMS (ESI): C₁₄H₁₄BNNaO₃⁺ *calcd.*: 278.0959, *found*: 278.0963 [M+Na]⁺.

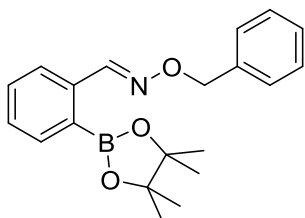


Oxime **2.39**: 2-Acetylphenylboronic acid (21.5 mg, 129 μmol , 1.00 eq.) was dissolved in dry MeOH (1.5 mL) followed by the addition of *O*-benzylhydroxylamine \cdot HCl (21.0 mg, 130 μmol , 1.01 eq.) which was washed down the flask with another 1 mL of dry MeOH. The progress of the reaction was monitored by UPLC-MS. After 18 h full conversion of the starting ketone was achieved and the solvent was removed under reduced pressure. The crude was purified employing preparative RP-HPLC (gradient: 2% MeCN in H₂O, 0.1% TFA for 3 min, 2-80% MeCN in H₂O, 0.1% TFA for 25 min) with a flow rate of 20 mL/min monitoring and collecting the product at 254 nm (t_R = 22.4 min). The product fractions were re-analyzed by UPLC-MS and lyophilized. The oxime **2.39** was obtained as a fluffy white solid (20.0 mg, 74.0 μmol , 58%, 98% purity). TLC (19:1 CH₂Cl₂/MeOH) R_f = 0.36. ¹H-NMR (400 MHz, DMSO-*d*₆) δ /ppm: 7.70-7.60 (m, 1H), 7.47-7.37 (m, 3H), 7.30-7.19 (m, 5H), 5.13 (s, 2H), 2.21 (s, 3H). ¹³C-NMR (101 MHz, DMSO-*d*₆) δ /ppm: 162.62, 139.55, 136.63, 132.02, 129.51, 128.98, 128.32, 128.12, 128.01, 126.43, 75.31, 14.70 (one signal for the carbon atom

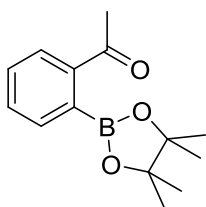
directly attached to the boron was not observed due to the quadrupolar relaxation of the boron atom). ^{11}B -NMR (128 MHz, $\text{DMSO-}d_6$) δ/ppm : 25.15 (after background spectrum subtraction). HRMS (ESI): $\text{C}_{15}\text{H}_{16}\text{BNNaO}_3^+$ *calcd.*: 292.1115, *found*: 292.1120 $[\text{M}+\text{Na}]^+$, $\text{C}_{16}\text{H}_{18}\text{BNNaO}_3^+$ *calcd.*: 306.1272, *found*: 306.1277 $[\text{M}+\text{CH}_2\text{Na}]^+$, $\text{C}_{17}\text{H}_{20}\text{BNNaO}_3^+$ *calcd.*: 320.1428, *found*: 320.1433 $[\text{M}+\text{C}_2\text{H}_4\text{Na}]^+$.



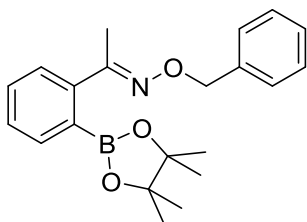
Pinacol ester **2.40**: A 25 mL flask equipped with a Dean-Stark apparatus was charged with 2-formylphenylboronic acid (250 mg, 1.67 mmol, 1.00 eq.) and pinacol (216.7 mg, 1.83 mmol, 1.10 eq.) in benzene (10 mL). The mixture was refluxed for 5 h whereupon a ^1H -NMR aliquot indicated full conversion of the starting boronic acid. The mixture was dried with Na_2SO_4 (~2 g), filtered and washed with benzene. The solvent was removed under reduced pressure to give the pinacol ester **2.40** as light yellow oil (387 mg, 1.67 mmol, quantitative). TLC (cyclohexane/EtOAc 5:1) $R_f = 0.50$. ^1H -NMR (400 MHz, CDCl_3) δ/ppm : 10.54 (s, 1H), 7.97-7.94 (m, 1H), 7.87-7.84 (m, 1H), 7.62-7.53 (m, 2H), 1.40 (s, 12H). ^{13}C -NMR (101 MHz, CDCl_3) δ/ppm : 194.79, 141.39, 135.61, 133.13, 130.88, 128.04, 84.55, 25.02. (one signal for the carbon atom directly attached to the boron was not observed due to the quadrupolar relaxation of the boron atom). ^{11}B -NMR (128 MHz, CDCl_3) δ/ppm : 31.28. HRMS (ESI): $\text{C}_{13}\text{H}_{18}\text{BO}_3^+$ *calcd.*: 233.1344, *found*: 233.1344 $[\text{M}+\text{H}]^+$, $\text{C}_{13}\text{H}_{17}\text{BNaO}_3^+$ *calcd.*: 255.1163, *found*: 255.1164 $[\text{M}+\text{Na}]^+$. (This compound was synthesized and characterized by Cedric Stress).



Oxime **2.41**: Compound **2.40** (25.0 mg, 106 μmol , 1.00 eq.) was dissolved in dry MeOH (2 mL) followed by the addition of *O*-benzylhydroxylamine $\cdot \text{HCl}$ (17.0 mg, 106 μmol , 1.00 eq.) which was washed down the flask with another 1 mL of dry MeOH. The progress of the reaction was monitored by UPLC-MS. After 14.5 h full conversion of the starting aldehyde was achieved and the solvent was removed under reduced pressure. The crude was purified by flash chromatography (10:1 cyclohexane/EtOAc). The oxime **2.41** was obtained as a colorless oil (33.0 mg, 98.0 μmol , 92%, 98% purity). TLC (cyclohexane/EtOAc 5:1) $R_f = 0.63$. ^1H -NMR (400 MHz, CDCl_3) δ/ppm : 8.95 (s, 1H), 7.98-7.95 (m, 1H), 7.86-7.83 (m, 1H), 7.47-7.41 (m, 3H), 7.41-7.35 (m, 3H), 7.35-7.32 (m, 1H), 5.24 (s, 2H), 1.34 (s, 12H). ^{13}C -NMR (101 MHz, CDCl_3) δ/ppm : 150.46, 138.03, 137.97, 136.31, 131.18, 128.84, 128.53, 127.98, 125.45, 84.15, 76.39, 25.01 (HMQC indicated that the protons at 7.47 and 7.37 ppm show a cross peak for the carbon at 128.84 ppm which is an overlay of two carbon signals - one signal for the carbon atom directly attached to the boron was not observed due to the quadrupolar relaxation of the boron atom). ^{11}B -NMR (128 MHz, CDCl_3) δ/ppm : 31.09. HRMS (ESI): $\text{C}_{20}\text{H}_{25}\text{BNO}_3^+$ *calcd.*: 338.1922, *found*: 338.1923 $[\text{M}+\text{H}]^+$, $\text{C}_{20}\text{H}_{24}\text{BNNaO}_3^+$ *calcd.*: 360.1741, *found*: 360.1744 $[\text{M}+\text{Na}]^+$, $\text{C}_{20}\text{H}_{24}\text{BKNO}_3^+$ *calcd.*: 376.1481, *found*: 376.1479 $[\text{M}+\text{K}]^+$.



Pincol ester **2.42**: To a mixture of *bis*-(pinacolato)diboron (280 mg, 1.10 mmol, 1.50 eq.), NaOAc (241 mg, 2.94 mmol, 4.00 eq.) and Pd(PPh₃)₂Cl₂ (25.8 mg, 37.0 μmol, 5 mol%) in 1,4-dioxane (5.0 mL) was added 2-Bromoacetophenone (100 μL, 734 μmol, 1.00 eq.). The resulting mixture was stirred at 90°C for 15 h and the solvent was removed under reduced pressure to give a grey semisolid. The crude was purified by flash chromatography on a Biotage Isolera Four device (5:1 to 4:1 cyclohexane/EtOAc). The product **2.42** was isolated as yellow oil (83 mg, 331 μmol, 45%, 98% purity). TLC (cyclohexane/EtOAc 5:1) *R_f* = 0.18. ¹H-NMR (400 MHz, CDCl₃) δ/ppm: 7.83 (dt, *J* = 7.8, 0.9 Hz, 1H), 7.57-7.49 (m, 2H), 7.47-7.40 (m, 1H), 2.61 (s, 3H), 1.44 (s, 12H). ¹³C-NMR (101 MHz, CDCl₃) δ/ppm: 199.94, 140.63, 132.62, 132.35, 129.00, 128.57, 83.85, 25.63, 25.04 (one signal for the carbon atom directly attached to the boron was not observed due to the quadrupolar relaxation of the boron atom). ¹¹B-NMR (128 MHz, CDCl₃) δ/ppm: 31.26. HRMS (ESI): C₈H₉BNaO₃⁺ *calcd.*: 187.0537, *found*: 187.0540 (free Boronic acid), C₁₄H₁₉BNaO₃⁺ *calcd.*: 269.1319, *found*: 269.1320. LRMS (ESI): 147.1 [M-C₆H₁₁O]⁺, 247.1 [M+H]⁺, 269.2 [M+Na]⁺, 285.1 [M+K]⁺, 515.4 [2M+Na]⁺.



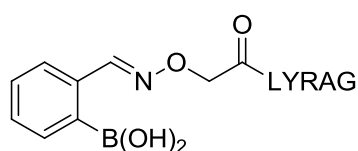
Oxime **2.43**: Compound **2.42** (20.0 mg, 80.0 μmol, 1.00 eq.) was dissolved in dry MeOH (1.5 mL) followed by the addition of *O*-benzylhydroxylamine · HCl (13.0 mg, 81.0 μmol, 1.01 eq.) which was washed down the flask with another 1 mL of dry MeOH. The progress of the reaction was monitored by UPLC-MS. After 18 h full conversion of the starting ketone was achieved and the solvent was removed under reduced pressure. The crude was purified by flash chromatography (6:1 cyclohexane/EtOAc). The early fractions contained 12 mg of desired product. The fractions which had to be eluted with (19:1 CH₂Cl₂/MeOH) didn't contain the free boronic acid product as expected, instead another 10 mg of desired product were isolated. This observation is probably attributed to a charged product species containing an additional methoxy group on the boron atom which changes its polarity significantly. The oxime **2.43** was obtained as colorless oil (22.0 mg, 63.0 μmol, 79%). TLC (6:1 cyclohexane/EtOAc) *R_f* = 0.52. NMR spectroscopy indicated a mixture of stereoisomers of 11:1.

Major stereoisomer:

¹H-NMR (400 MHz, CDCl₃) δ/ppm: 7.72 (dd, *J* = 7.5, 0.9 Hz, 1H), 7.49-7.37 (m, 3H), 7.37-7.26 (m, 4H), 7.25-7.06 (m, 1H), 5.23 (s, 2H), 2.27 (s, 3H), 1.34 (s, 12H). ¹³C-NMR (101 MHz, CDCl₃) δ/ppm: 159.26, 143.32, 138.37, 134.98, 130.44, 128.43, 127.99, 127.72, 127.59, 127.38, 83.95, 75.94, 24.98, 17.11. ¹¹B-NMR (128 MHz, CDCl₃) δ/ppm: 31.65. HRMS (ESI): C₂₁H₂₇BNO₃⁺ *calcd.*: 352.2079, *found*: 352.2085 [M+H]⁺, C₂₁H₂₆BNNaO₃⁺ *calcd.*: 374.1898, *found*: 374.1906 [M+Na]⁺.

Minor stereoisomer:

$^1\text{H-NMR}$ (400 MHz, CDCl_3) δ/ppm : 7.84 (dd, $J = 7.2, 1.0$ Hz, 1H), 7.49-7.37 (m, 3H), 7.37-7.26 (m, 4H), 7.25-7.06 (m, 1H), 5.04 (s, 2H), 2.18 (s, 3H), 1.30 (s, 12H). $^{13}\text{C-NMR}$ (101 MHz, CDCl_3) δ/ppm : 142.84, 138.92, 135.41, 130.94, 128.19, 127.32, 127.96, 127.23, 126.14, 83.88, 75.15, 24.90, 23.02. $^{11}\text{B-NMR}$ (128 MHz, CDCl_3) δ/ppm : 31.65.

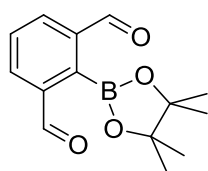


LYRAG pentapeptide oxime **2.44** was exclusively analyzed by LC-

MS:

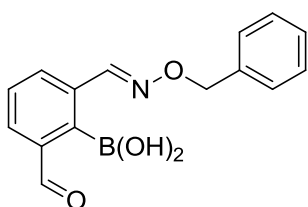
LRMS (ESI): $\text{C}_{35}\text{H}_{52}\text{BN}_{10}\text{O}_{10}^+$ *calcd.*: 783.4, *found*: 783.7 $[\text{M}+\text{H}]^+$.

RP-HPLC: 2-98% MeCN containing 1% H_2O in H_2O containing 1% MeCN over 18 min, 1 mL/min, $t_{\text{R}} = 10.2$ min.



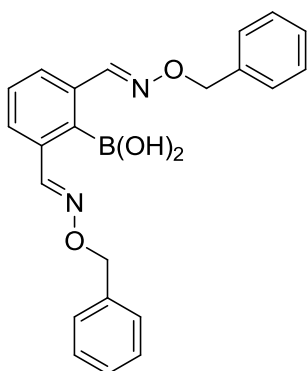
Pinacol ester **2.45**: A flame dried 50 mL flask under argon was charged with 2-bromoisophthalaldehyde (250 mg, 1.16 mmol, 1.00 eq.) and dissolved in 5 mL of 1,4-dioxane. $\text{Pd}(\text{dppf})\text{Cl}_2$ (42.5 mg, 58.0 μmol , 5 mol%), *bis*-(pinacolato)diboron (295 mg, 1.16 mmol, 1.00 eq.) and KOAc (342 mg, 3.49 mmol, 3.00 eq.) were added as

solids. The reagents were washed down the flask with 5 mL of 1,4-dioxane and the mixture heated at 95°C . The mixture was stirred for 6.5 h and allowed to cool down to room temperature. The mixture was filtered over Celite and the cake washed with CH_2Cl_2 (50 mL). The filtrate was concentrated under reduced pressure to give a brown oil which was purified employing preparative RP-HPLC (gradient: 1% MeCN in H_2O , 0.1% TFA for 3 min, 1-50% MeCN in H_2O , 0.1% TFA for 25 min) with a flow rate of 20 mL/min monitoring and collecting the product at 254 nm ($t_{\text{R}} = 8.5$ min). The product fractions were re-analyzed by UPLC-MS and lyophilized to give the product **2.45** as a fluffy white solid (104 mg, 400 μmol , 34%). It is noteworthy to mention that the recorded NMR data suggested a mixture of at least two product species; one which was the pinacol ester **2.45** the other which seemed to be the boronic acid. $^1\text{H-NMR}$ (400 MHz, $\text{DMSO-}d_6$) δ/ppm : 10.07 (2 x s, 2H), 8.26 and 8.19 (2 x d, $J = 7.6$ Hz, 2H), 7.89 and 7.76 (t, $J = 7.7$ Hz, 1H), 3.52 (s_{br} , 2H), 1.41 (s, 12H). $^{13}\text{C-NMR}$ (101 MHz, $\text{DMSO-}d_6$) δ/ppm : 193.49, 193.24, 140.28, 138.91, 136.98, 135.26, 130.34, 128.87, 83.88, 25.24. $^{11}\text{B-NMR}$ (128 MHz, $\text{DMSO-}d_6$) δ/ppm : 31.35. LRMS (ESI): $\text{C}_{14}\text{H}_{18}\text{BO}_4^+$ *calcd.*: 261.1, *found*: 261.1 $[\text{M}+\text{H}]^+$.



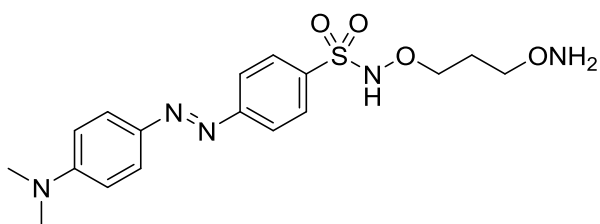
Monooxime **2.46** was exclusively analyzed by LC-MS:

LRMS (ESI): $C_{15}H_{15}BNO_4^+$ *calcd.*: 284.1, *found*: 284.2 $[M+H]^+$. RP-HPLC: 2-98% MeCN containing 1% H_2O in H_2O containing 1% MeCN over 18 min, 1 mL/min. $t_R = 13.8$ min.



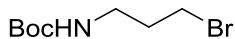
Bisoxime **2.47** was exclusively analyzed by LC-MS:

LRMS (ESI): $C_{22}H_{20}BN_2O_3^+$ *calcd.*: 371.2, *found*: 371.3 $[M-OH]^+$. RP-HPLC: 2-98% MeCN containing 1% H_2O in H_2O containing 1% MeCN over 18 min, 1 mL/min. $t_R = 15.0$ min.



Dabsyl hydroxylamine **2.49**: An oven dried flask under argon was charged with 4-(dimethylamino)azobenzen-4'-sulfonyl chloride (111 mg, 333 μmol , 1.00 eq.), *O,O'*-1,3-propanediylbishydroxylamine dihydrochloride

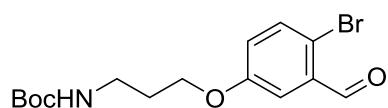
(66.0 mg, 365 μmol , 1.10 eq.) and dry EtOH (12 mL). NEt_3 (170 μL , 1.22 mmol, 3.67 eq.) was added and the resulting mixture was stirred at room temperature for 2 h. The solvent was removed under reduced pressure to give a red solid. The crude was adsorbed onto RP-C18 silica gel and purified by flash chromatography on a Biotage Isolera Four device (gradient: 0% MeCN for 4 min, 0-78% MeCN for 32 min, 78-100% MeCN for 4 min) with a flow rate of 50 mL/min monitoring and collecting the product at 254 nm ($t_R = 27.0$ min). The pure fractions were lyophilized to give dabsyl hydroxylamine **2.49** as an orange crystalline solid (51.0 mg, 130 μmol , 39%). 1H -NMR (400 MHz, $DMSO-d_6$) δ /ppm: 10.46 (s, 1H), 8.00-7.91 (m, 4H), 7.88-7.80 (m, 2H), 6.90-6.82 (m, 2H), 5.92 (s, 2H), 3.93 (t, $J = 6.4$ Hz, 2H), 3.53 (t, $J = 6.4$ Hz, 2H), 3.10 (s, 6H), 1.76 (quint., $J = 6.4$ Hz, 2H). ^{13}C -NMR (101 MHz, $DMSO-d_6$) δ /ppm: 155.25, 153.24, 142.62, 136.80, 129.40, 125.55, 122.01, 111.62, 73.55, 71.30, 39.85, 26.93. HRMS (ESI): $C_{17}H_{24}N_5O_4S^+$ *calcd.*: 394.1544, *found*: 394.1542 $[M+H]^+$, $C_{17}H_{23}N_5NaO_4S^+$ *calcd.*: 416.1363, *found*: 416.1358 $[M+Na]^+$.



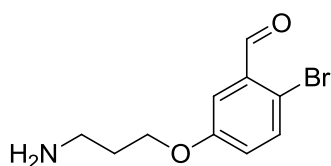
Carbamate **2.51**: 3-bromopropylamine hydrobromide (2.00 g, 8.95 mmol, 1.00 eq.) was added to a solution of di-*tert*-butyl dicarbonate (1.97 g, 8.95 mmol,

1.00 eq.) in CH_2Cl_2 (30 mL) followed by NEt_3 (1.25 mL, 8.95 mmol, 1.00 eq.). The mixture was stirred at room temperature for 1 h and diluted with another 20 mL of CH_2Cl_2 . The mixture was

washed with saturated KHSO₄ (3 x 50 mL, aqueous). The combined organic layers were dried over Na₂SO₄, filtered and concentrated under reduced pressure to give the product **2.51** as a colorless to slightly yellow oil (2.09 g, 8.79 mmol, 98%). ¹H-NMR (400 MHz, CDCl₃) δ/ppm: 4.69 (s_{br}, 1H), 3.43 (t, *J* = 6.6 Hz, 2H), 3.31-3.19 (m, 2H), 2.03 (quint., *J* = 6.6 Hz, 2H), 1.43 (s, 9H). ¹³C-NMR (101 MHz, CDCl₃) δ/ppm: 156.06, 79.53, 39.11, 32.2, 30.93, 28.51. HRMS (ESI): C₈H₁₆BrNNaO₂⁺ *calcd.*: 260.0257, *found*: 260.0258 [M+Na]⁺.

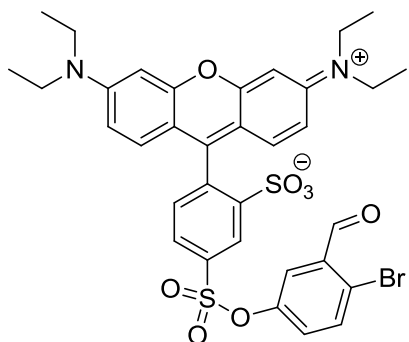


Ether 2.52: An oven dried 25 mL flask equipped with a stir bar was charged with 2-bromo-5-hydroxybenzaldehyde (480 mg, 2.34 mmol, 1.00 eq.), *tert*-butyl (3-bromopropyl)carbamate (**2.51**) (575 mg, 2.37 mmol, 1.01 eq.) which were dissolved in 6 mL of dry DMF. To the stirring solution was added K₂CO₃ (970 mg, 7.02 mmol, 3.00 eq.) whereupon the color turned to bright yellow. The heterogeneous mixture was stirred at 80°C and the progress of the reaction was monitored by UPLC-MS. After 21 h (still starting benzaldehyde derivative) H₂O (50 mL) was added and the mixture extracted with EtOAc (3 x 15 mL). The combined organics were dried over Na₂SO₄, filtered and the solvent removed under reduced pressure to give a slightly orange oil. The crude was purified twice by flash chromatography (5:1 cyclohexane/EtOAc) but the starting benzaldehyde derivative (8% according to ¹H-NMR) could not be removed efficiently from the product. Compound **2.52** was obtained as slightly yellow oil (654 mg, 1.68 mmol, 72%) in 92% purity. TLC (cyclohexane/EtOAc 5:1) R_f = 0.22. ¹H-NMR (400 MHz, CDCl₃) δ/ppm: 10.30 (s, 1H), 7.52 (d, *J* = 8.8 Hz, 1H), 7.40 (d, *J* = 3.2 Hz, 1H), 7.03 (dd, *J* = 8.8, 3.2 Hz, 1H), 4.69 (s_{br}, 1H), 4.05 (t, *J* = 6.0 Hz, 2H), 3.36-3.27 (m, 2H), 1.99 (quint., *J* = 6.3 Hz, 2H), 1.44 (s, 9H). ¹³C-NMR (101 MHz, CDCl₃) δ/ppm: 191.90, 158.60, 156.15, 134.75, 134.09, 123.54, 118.18, 113.51, 79.59, 66.36, 37.91, 29.60, 28.55. HRMS (ESI): C₁₀H₁₃BrNO₂⁺ *calcd.*: 258.0124, *found*: 258.0121 [M-C₅H₇O₂]⁺, C₁₅H₂₀BrNNaO₄⁺ *calcd.*: 380.0468, *found*: 380.0465 [M+Na]⁺, C₁₆H₂₄BrNNaO₅⁺ *calcd.*: 412.0730, *found*: 412.0727 [M+CH₄O]⁺.

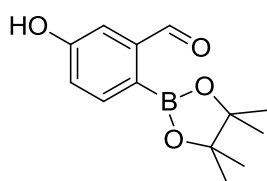


Amine 2.53: A 2.5 mL screw cap vial was charged with **2.52** (70.0 mg, 162 μmol, 1.00 eq.) and dissolved in 250 μL of CH₂Cl₂. To the stirring solution was added 250 μL of TFA whereupon the color changed immediately to light orange/yellow. The mixture was stirred at rt for 1 h (UPLC-MS indicated full conversion to the free amine). The solvent mixture was carefully removed under reduced pressure and co-evaporated once with toluene followed by extensive drying under HV to give 97 mg of an orange oil. The sample was pure enough according to ¹H-NMR and contained around 20% (w/w) of toluene and still 10% (w/w) of unreacted 2-bromo-5-hydroxybenzaldehyde. It was assumed that the TFA salt was obtained since the sample was not neutralized and purified. ¹H-NMR (500 MHz, CDCl₃) δ/ppm: 10.22 (s, 1H), 7.72 (s_{br}, 2H), 7.52 (d, *J* = 8.6 Hz, 1H), 7.37-7.32 (m, 1H), 7.04-7.00 (m, 1H), 4.16 (t, *J* = 5.0 Hz, 2H), 3.40-3.26 (m, 2H), 2.29-2.20 (m, 2H). ¹³C-NMR (126

MHz, CDCl₃) δ /ppm: 192.43, 157.72, 134.98, 133.96, 123.20, 119.12, 113.84, 66.59, 39.04, 26.74. UPLC-MS (ESI): $t_R = 0.925$ min, C₁₀H₁₃BrNO₂⁺ calcd.: 258.0, found: 258.0 [M+H]⁺.

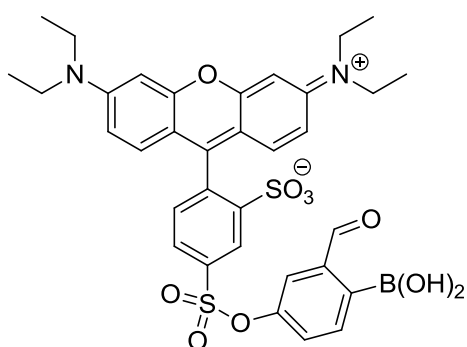


Lissamine aldehyde **2.55**: A 2.5 mL screw cap vial was charged with 2-bromo-5-hydroxybenzaldehyde (20.6 mg, 100 μ mol, 1.00 eq.), NEt₃ (17.0 μ L, 122 μ mol, 1.21 eq.) and DMAP (3.00 mg, 25.0 μ mol, 0.25 eq.) and dissolved in 1 mL of dry CH₂Cl₂. At 0°C lissamine™ rhodamine B sulfonylchloride (**2.54**) (61.0 mg, 100 μ mol, 1.00 eq.) was added as a solid and washed down the flask with another 1 mL of dry CH₂Cl₂. The mixture was allowed to warm to room temperature and the progress of the reaction was monitored by UPLC-MS. After 1.5 h full conversion was observed and the solvent was removed under reduced pressure to give 111 mg of a purple solid. The crude was purified by flash chromatography on a Biotage Isolera Four device (5% MeOH in CH₂Cl₂, isocratic) with a flow rate of 50 mL/min monitoring and collecting the product at 254 nm ($t_R = 3.8$ min). The fractions were re-analyzed by UPLC-MS and pure fractions were combined to give the product **2.55** as a green/purple metallic solid (39.0 mg, 50 μ mol, 50%, 95% purity). ¹H-NMR (400 MHz, MeOD-*d*₄) δ /ppm: 10.25 (s, 1H), 8.63 (d, *J* = 1.8 Hz, 1 H), 8.53 (d, *J* = 1.9 Hz, 1 H), 8.50 (m, 1H), 8.10 (dd, *J* = 8.0, 1.9 Hz, 1 H), 8.06 (dd, *J* = 8.0, 1.9 Hz, 1H), 7.98 (s_{br}, 1H), 7.89 (d, *J* = 8.8 Hz, 1H), 7.67 (d, *J* = 8.7 Hz, 1H), 7.60 (d, *J* = 8.0 Hz, 1H), 7.56 (d, *J* = 8.0 Hz, 1H), 7.54-7.50 (m, 1H), 3.76-3.62 (m, 8H), 1.35-1.26 (m, 24H). The ¹H-NMR spectrum indicated a mixture of rotamers of the aromatic 9-phenylxanthene core and the four ethyl groups since only one aldehyde proton was observed. ¹³C-NMR data could not be recorded in MeOD-*d*₄ since the solubility limit was reached and the product precipitate in the NMR tube. UPLC-MS (ESI): $t_R = 2.800$ min, C₃₄H₃₄BrN₂O₈S₂⁺ calcd.: 741.1, found: 741.1 [M+H]⁺.

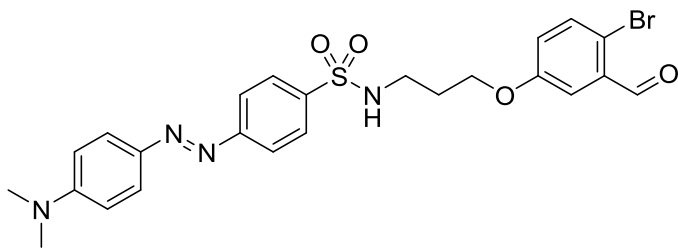


Boronic ester **2.60** was prepared according to a slightly modified literature procedure by SELLA *et al.*³⁰¹ An oven dried 25 mL flask under argon was charged with 2-bromo-5-hydroxybenzaldehyde (253 mg, 1.25 mmol, 1.00 eq.) and dissolved in 4 mL of 1,4-dioxane. Pd(dppf)Cl₂ (92.0 mg, 126 μ mol, 10.1 mol%), *bis*-(pinacolato)diboron (380 mg, 1.50 mmol, 1.20 eq.) and KOAc (367 mg, 3.74 mmol, 3.00 eq.) were added as solids. The reagents were washed down the flask with 2 mL of 1,4-dioxane and the mixture heated at 95°C. The mixture was stirred for 3 h (¹H-NMR aliquot indicated full conversion) and allowed to cool down to room temperature and diluted with 10 mL of CH₂Cl₂. The mixture was washed with H₂O (20 mL) but the phases didn't separate. The organics were removed under reduced pressure and the residue diluted again with 30 mL of CH₂Cl₂. The addition of brine (20 mL) and chloroform (20 mL) didn't improve phase separation and therefore the "bottom" phase was carefully separated while extracting the

“aqueous” phase with chloroform (2 x 20 mL). The combined organics were then treated with activated charcoal (~3 g) and dried over Na₂SO₄, filtered and concentrated under reduced pressure to give a brown oil which was dried extensively under high vacuum overnight. The crude was purified by flash chromatography (cyclohexane/EtOAc, 6:1) to give the product **2.60** as an orange oil which crystallized upon standing (147 mg, 587 μmol, 46%). ¹H-NMR (400 MHz, CDCl₃) δ/ppm: 10.65 (s, 1H), 7.86 (d, *J* = 8.2 Hz, 1H), 7.51 (d, *J* = 2.6 Hz, 1H), 7.10 (dd, *J* = 8.2, 2.6 Hz, 1H), 5.95 (s_{br}, 1H), 1.37 (s, 12H). ¹³C-NMR (101 MHz, CDCl₃) δ/ppm: 195.32, 158.52, 143.68, 138.59, 120.55, 113.33, 84.36, 25.01 (one signal for the carbon atom directly attached to the boron was not observed due to the quadrupolar relaxation of the boron atom). ¹¹B-NMR (128 MHz, CDCl₃) δ/ppm: 30.93. HRMS (ESI): C₁₃H₁₇BNaO₄⁺ *calcd.*: 271.1112, *found*: 271.1111 [M+Na]⁺.

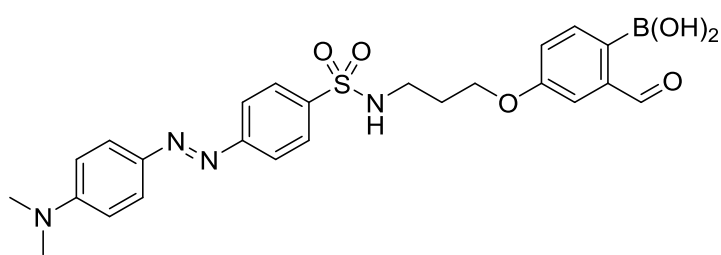


Lissamine boronic acid **2.61**: A flame dried 5 mL flask was charged with lissamine™ rhodamine B sulfonylchloride (**2.54**) (50.0 mg, 82.0 μmol, 1.00 eq.) and dissolved in 2 mL of dry CH₂Cl₂. Boronic acid pinacol ester **2.60** (23.8 mg, 86.0 μmol, 1.05 eq.) was added followed by NEt₃ (13.0 μL, 93.0 μmol, 1.13 eq.). The progress of the reaction was monitored by UPLC-MS. After a total of 17 h at room temperature the reaction was stopped and the solvent was removed under reduced pressure to give 81 mg of a purple solid. The crude was purified by flash chromatography on a Biotage Isolera Four device (0-8% MeOH in CH₂Cl₂) with a flow rate of 25 mL/min monitoring and collecting the product at 254 nm (*t_R* = 10.5 min). The fractions were re-analyzed by UPLC-MS but were found to be still impure containing a major impurity with the mass of 679 Da. The crude (35 mg) was purified employing preparative RP-HPLC (gradient: 5% MeCN in H₂O, 0.1% TFA for 3 min, 5-95% MeCN in H₂O, 0.1% TFA for 30 min) with a flow rate of 20 mL/min monitoring and collecting the product at 254 nm (*t_R* = 22.8 min). The product fractions were re-analyzed by UPLC-MS and lyophilized to give the product **2.61** as a purple film (3.00 mg, 3.80 μmol, 4%, 97% purity). Characterization by ¹H and ¹³C-NMR failed in various solvents (DMSO-*d*₆, CDCl₃ and MeOD-*d*₄). It is noteworthy to mention that the isolated product **2.61** was pure according to UPLC-MS containing the desired mass. The boronic acid moiety however was found to be oxidized within days to give the corresponding aromatic alcohol **2.62** (679 Da). UPLC-MS (ESI): *t_R* = 2.394 min, C₃₄H₃₆BN₂O₁₀S₂⁺ *calcd.*: 707.2, *found*: 707.2 [M+H]⁺.



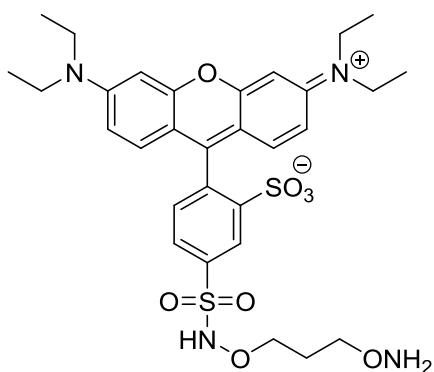
Dabsyl bromide **2.64**: Compound **2.52** (113 mg, 284 μmol , 1.00 eq., 90% purity) was dissolved in dry CH_2Cl_2 (2 mL) followed by the addition of TFA (0.50 mL). The mixture was stirred at room temperature and the progress of the

reaction was monitored by UPLC-MS. After 25 min full conversion of the starting material was observed. The solvents were removed under reduced pressure to give a orange oil which was extensively dried under high vacuum. The mass balance was too high which was attributed to residual TFA in the sample. Without further purification the crude TFA salt of the free amine was dissolved in dry EtOH (10 mL) and cooled to 0°C . To the stirring solution was added dabsyl chloride (123 mg, 323 mmol, 1.00 eq., 97.5% purity) followed by NEt_3 (2 mL). It has to be noticed that the excess of base was chosen to neutralize the TFA salt of the free amine as well as the residual TFA which could not be removed by high vacuum treatment. The mixture was allowed to warm to room temperature and the progress of the reaction was monitored by UPLC-MS. The starting amine was still present after 18 h at which point the reaction was stopped and the solvent was removed under reduced pressure. The crude was purified by flash chromatography on a Biotage Isolera Four device (3:1 cyclohexane/EtOAc, isocratic). The product was isolated as a red solid (41.0 mg, 69.2 μmol , 21%, 92% purity). An analytical sample was purified employing preparative RP-HPLC (gradient: 20% MeCN in H_2O , 0.1% TFA for 3 min, 20-95% MeCN in H_2O , 0.1% TFA for 25 min) with a flow rate of 20 mL/min monitoring and collecting the product at 254 nm ($t_{\text{R}} = 23.9$ min). The product fractions were re-analyzed by UPLC-MS and lyophilized to give **2.64** as a dark red crystalline solid. TLC (cyclohexane/EtOAc 1:1) $R_f = 0.55$. $^1\text{H-NMR}$ (400 MHz, CDCl_3) δ/ppm : 10.24 (s, 1H), 7.96-7.89 (m, 4H), 7.88-7.82 (m, 2H), 7.49 (d, $J = 8.8$ Hz, 1H), 7.30 (d, $J = 3.2$, 1H), 6.95 (dd, $J = 8.8, 3.2$ Hz, 1H), 6.82-6.76 (m, 2H), 4.80 (t, $J = 6.6$ Hz, 1H), 3.98 (t, $J = 5.8$ Hz, 2H), 3.23 (q, $J = 6.2$ Hz, 2H), 3.14 (s, 6H), 1.97 (quint., $J = 6.2$ Hz, 2H). $^{13}\text{C-NMR}$ (101 MHz, CDCl_3) δ/ppm : 191.78, 158.21, 155.17, 153.44, 143.54, 139.23, 134.78, 134.05, 128.18, 126.37, 123.36, 122.59, 118.37, 113.46, 112.00, 65.81, 40.63, 40.61, 29.16. HRMS (ESI): $\text{C}_{24}\text{H}_{26}\text{BrN}_4\text{O}_4\text{S}^+$ *calcd.*: 545.0853, *found*: 545.0842 $[\text{M}+\text{H}]^+$, $\text{C}_{24}\text{H}_{25}\text{BrN}_4\text{NaO}_4\text{S}^+$ *calcd.*: 567.0672, *found*: 567.0666 $[\text{M}+\text{Na}]^+$, $\text{C}_{25}\text{H}_{29}\text{BrN}_4\text{NaO}_5\text{S}^+$ *calcd.*: 599.0934, *found*: 599.0929 $[\text{M}+\text{CH}_4\text{NaO}]^+$.



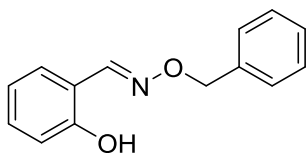
Dabsyl boronic acid **2.65**: A flame dried 5 mL Schlenk tube under argon equipped with a stir bar was charged with compound **2.64** (9.00 mg, 17.0 mmol, 1.00 eq.) and dissolved in 1 mL of freshly distilled 1,4-dioxane. To the

stirring solution was added *bis*-(pinacolato)diboron (8.60 mg, 34.0 mmol, 2.05 eq.), NaOAc (4.30 mg, 52 mmol, 3.18 eq.) and Pd(PPh₃)₂Cl₂ (1.20 mg, 2.0 mmol, 10 mol%) and washed down the pressure tube with 0.5 mL of 1,4-dioxane. The pressure tube was closed and the mixture heated to 90°C. The progress of the reaction was monitored by UPLC-MS and after 16 h the mixture was allowed to cool to room temperature and filtered over a plug of cotton. The solvent was removed under reduced pressure to give 23 mg of a crude orange residue. The crude was purified employing preparative RP-HPLC (gradient: 10% MeCN in H₂O, 0.1% TFA for 13 min, 10-98% MeCN in H₂O, 0.1% TFA for 30 min) with a flow rate of 20 mL/min monitoring and collecting the product at 254 nm (*t_R* = 31.4 min). The product fractions were re-analyzed by UPLC-MS and lyophilized to give **2.65** as a fluffy dark red solid (3.7 mg, 6.25 μmol, 38%). ¹H-NMR (400 MHz, DMSO-*d*₆) δ/ppm: 10.18 (s, 1H), 7.94-7.85 (m, 4H), 7.85-7.76 (m, 3H), 7.58 (d, *J* = 8.1 Hz, 1H), 7.32 (d, *J* = 2.5 Hz, 1H), 7.14 (dd, *J* = 8.3, 2.5 Hz, 1H), 6.88-6.84 (m, 2H), 4.03 (t, *J* = 6.2 Hz, 2H), 3.09 (s, 6H), 3.01-2.93 (m, 2H), 1.89-1.80 (m, 2H). ¹³C-NMR (101 MHz, DMSO-*d*₆) δ/ppm: 194.22, 159.14, 154.49, 153.14, 142.62, 141.35, 140.17, 135.58, 127.80, 125.44, 122.27, 119.61, 112.99, 111.63, 64.77, 39.88, 39.35 (overlapping with DMSO signal - identified by DEPT135), 28.79 (one signal for the carbon atom directly attached to the boron was not observed due to the quadrupolar relaxation of the boron atom). ¹¹B-NMR (128 MHz, DMSO-*d*₆) δ/ppm: 20.11 (measured in a 701-PQ NMR tube using 2048 scans and after background spectrum subtraction). HRMS (ESI): C₂₄H₂₈BN₄O₆S⁺ *calcd.*: 511.1817, *found*: 511.1826 [M+H]⁺, C₂₅H₃₀BN₄O₆S⁺ *calcd.*: 525.1974, *found*: 525.1979 [M+CH₃]⁺, C₂₄H₂₇BN₄NaO₆S⁺ *calcd.*: 533.1637, *found*: 533.1638 [M+Na]⁺.



Lissamine hydroxylamine **2.66**: An oven dried 10 mL flask under argon was charged with *O,O'*-1,3-propanediylbishydroxylamine dihydrochloride (13.0 mg, 72.0 μmol, 1.10 eq.) and dry EtOH (4 mL). The suspension was cooled to 0°C before NEt₃ (46 μL, 330 μmol, 5.00 eq.) was added. After 5 min lissamine™ rhodamine B sulfonylchloride (**2.54**) (40.0 mg, 66.0 μmol, 1.00 eq.) was added as a solid and the reaction allowed to warm to room temperature. The mixture was stirred for 2 h and UPLC-MS indicated a product peak (647.3 Da) along with a peak corresponding to the dimer (1187.3 Da). The solvent was removed under reduced pressure to give a purple solid (86 mg). The crude was purified employing preparative RP-HPLC (gradient: 25% MeCN

in H₂O, 0.1% TFA for 3 min, 25-80% MeCN in H₂O, 0.1% TFA for 25 min) with a flow rate of 20 mL/min monitoring and collecting the product at 254 nm (*t_r* = 13.0 min). The product fractions were re-analyzed by UPLC-MS and lyophilized to give **2.66** as a dark purple fluffy solid (11.6 mg, 18.0 μmol, 27%). ¹H-NMR (400 MHz, DMSO-*d*₆) δ/ppm: 10.78 (s, 1H), 10.50 (s_{br}, 2H), 8.50 (d, *J* = 1.9 Hz, 1H), 8.01 (dd, *J* = 8.0, 1.9 Hz, 1H), 7.57 (d, *J* = 8.0 Hz, 1H), 7.06 (dd, *J* = 9.5, 2.4 Hz, 2H), 6.96 (d, *J* = 2.4 Hz, 2H), 6.93 (d, *J* = 9.4 Hz, 2H), 4.07-4.00 (m, 4H), 3.70-3.58 (m, 8H), 1.94 (quint., *J* = 6.2 Hz, 2H), 1.21 (t, *J* = 7.0 Hz, 12H). ¹³C-NMR (101 MHz, DMSO-*d*₆) δ/ppm: 157.08, 156.76, 155.04, 147.51, 138.12, 134.29, 132.41, 130.83, 127.52, 113.77, 113.34, 95.47, 72.80, 71.26, 45.27, 26.32, 12.48. HRMS (ESI): C₃₀H₃₉N₄O₈S₂⁺ *calcd.*: 647.2204, *found*: 647.2206 [M+H]⁺, C₃₀H₃₈N₄NaO₈S₂⁺ *calcd.*: 669.2023, *found*: 669.2021 [M+Na]⁺.



Oxime **2.68**: Salicylaldehyde (31.0 mg, 249 μmol, 1.00 eq.) was dissolved in dry MeOH (3 mL) followed by the addition of *O*-benzylhydroxylamine · HCl (40.0 mg, 0.248 mmol, 1.00 eq.) which was washed down the flask with another 2 mL of dry MeOH. The progress of the reaction was monitored by UPLC-MS. After 21 h full conversion of the starting aldehyde was achieved and the solvent was removed under reduced pressure. The crude was passed through a short plug of silica eluting the desired compound with cyclohexane/EtOAc (6:1). The oxime **2.68** was obtained as colorless oil which crystallized upon drying under high vacuum (56.0 mg, 248 μmol, 99%). TLC (cyclohexane/EtOAc 6:1) *R_f* = 0.59. ¹H-NMR (400 MHz, CDCl₃) δ/ppm: 9.80 (s, 1H), 8.22 (s, 1H), 7.44-7.32 (m, 5H), 7.30-7.24 (m, 1H), 7.14 (dd, *J* = 7.7, 1.6 Hz, 1H), 6.99-6.94 (m, 1H), 6.92-6.87 (dt, *J* = 7.6, 1.1 Hz, 1H), 5.18 (s, 2H). ¹³C-NMR (101 MHz, CDCl₃) δ/ppm: 157.56, 152.05, 136.66, 131.41, 130.93, 128.77, 128.74, 128.54, 119.73, 116.88, 116.44, 77.02. HRMS (ESI): C₁₄H₁₄NO₂⁺ *calcd.*: 228.1019, *found*: 228.1021.

4.2.3.2 ¹H-NMR studies

General Information

The NMR experiments on boron-assisted oxime formation were performed at 288 K on a BrukerAvance III NMR spectrometer operating at 600.27 MHz, equipped with a ¹H-¹³C/¹⁵N/¹⁹F-D cryogenic QCI probe head with z-axis pulsed field gradients. All 1D proton experiments were recorded using exactly the same parameters (relaxation delay of 0.5 s and an acquisition time of 2.0 s). The data was processed using TopSpin software from Bruker with a line broadening of 0.5 Hz and manually baseline corrected. Chemical shifts were referenced to the residual solvent peak of MeCN (1.94 ppm) and TMSP-d₄ (3-(trimethylsilyl)-2,2',3,3'-tetradeuteriopropionic acid) was used as an internal standard. 2-FPBA **2.34** was purchased from ABCR and *O*-benzylhydroxylamine (**2.4**) was neutralized from its HCl salt according to a published procedure.³⁰⁰ The pH (no correction for deuterium) was adjusted using a 827 pH Lab – Metrohm equipped with a glass minitrode which was pre-rinsed with D₂O.

The NMR experiments on the stability and reversibility of oxime **2.35** were performed at 298 K on a BrukerAvance III NMR spectrometer operating at 600.13 MHz and equipped with a direct observe 5-mm BBFO smart probe. All 1D proton experiments were recorded using exactly the same parameters (256 scans, relaxation delay of 4.0 s and an acquisition time of 2.00 s) and were processed using TopSpin software from Bruker using line broadening of 0.5 Hz and after manual phase correction automated baseline correction was applied. Chemical shifts were referenced to the residual solvent peak of MeCN (1.94 ppm) and TMSP-d₄ (3-(trimethylsilyl)-2,2',3,3'-tetradeuteriopropionic acid) was used as an internal standard. The pH (no correction for deuterium) was adjusted using a 827 pH Lab – Metrohm equipped with a glass minitrode which was pre-rinsed with D₂O. (These experiments were performed by Cedric Stress)

Experimental – boron-assisted oxime formation

Stock solutions for both 2-FPBA **2.34** and *O*-benzylhydroxylamine (**2.4**) were freshly prepared in CD₃CN. A KP_i buffer stock solution was freshly prepared in D₂O adjusting the pH to 7.2 with concentrated DCl from ABCR (DCl, 38% wt% in D₂O, 99.5% atom%D). A TMSP-d₄ stock solution was freshly prepared in D₂O. All experiments were conducted at 15°C (288 K) in standard NMR tubes (throw away quality) which were rinsed thoroughly with D₂O and oven dried prior to the respective NMR experiment.

Setup for the $^1\text{H-NMR}$ experiment at 10 μM :

1. 440 μL of KP_i buffer (12.5 mM) were mixed inside the NMR tube with 50 μL of *O*-benzylhydroxylamine (**2.4**, 110 μM) and 10 μL of TMSP-d_4 (0.275 mM). The sample was then locked to MeCN and shimmed before the addition of the 2-FPBA **2.34**.
2. 50 μL of 2-FPBA (**2.4**, 110 μM) were then added and the reaction followed by $^1\text{H-NMR}$ (32 scans) without additional shimming. The time between adding 2-FPBA **2.34** to the NMR tube and recording of the last scan was determined to be ~ 3.5 min.

The final volume of the NMR sample was 550 μL with the following final concentrations:

10 μM in each *O*-benzylhydroxylamine (**2.4**) and 2-FPBA **2.34**, respectively. 10 mM KP_i buffer and 5 μM TMSP-d_4 with a ratio of 4:1 (10 mM KP_i in $\text{D}_2\text{O}/\text{CD}_3\text{CN}$).

For comparison a reference spectrum of 2-FPBA **2.34** was recorded at 10 μM with the same solvent ratio of 4:1 (10 mM KP_i in $\text{D}_2\text{O}/\text{CD}_3\text{CN}$). The setup for the $^1\text{H-NMR}$ experiment at 1 μM was identical using the same stock solutions except that the final solvent ratio was 54:1 (10 mM KP_i in $\text{D}_2\text{O}/\text{CD}_3\text{CN}$) and scans were increased to 128. The time between adding 2-FPBA **2.34** to the NMR tube and recording of the last scan was determined to be ~ 8.5 min. An overview of the three $^1\text{H-NMR}$ spectra (selected region of 10.2 – 6.9 ppm) is shown in **Figure 3.12**.

Stability assay

A stock solution of oxime **2.35** was freshly prepared in CD_3CN . A KP_i buffer stock solution was freshly prepared in D_2O adjusting the pH to 7.20 with concentrated DCl from ABCR (DCl, 38% wt% in D_2O , 99.5% atom%D). A TMSP-d_4 stock solution was freshly prepared in D_2O . All experiments were conducted at 298 K in standard NMR tubes (throw away quality) which were rinsed thoroughly with D_2O and oven dried prior to the respective NMR experiment.

Setup for the $^1\text{H-NMR}$ stability experiment at 100 μM :

1. 430 μL of KP_i buffer (12.8 mM) were mixed inside the NMR tube with 110 μL of oxime **2.35** (500 μM) and 10 μL of TMSP-d_4 (275 μM). The sample was then locked to MeCN and shimmed before recording the first $^1\text{H-NMR}$ spectrum.

The final volume of the NMR sample was 550 μL with the following final concentrations:

100 μM of oxime **2.35**, 10 mM KP_i buffer and 5 μM TMSP-d_4 with a ratio of 4:1 (10 mM KP_i in $\text{D}_2\text{O}/\text{CD}_3\text{CN}$).

The stability of oxime **2.35** was followed by recording $^1\text{H-NMR}$ spectra every 7 h for the first day and then one spectrum every day for another two days. The integration of the oxime proton (blue) was compared to the internal standard (pink) integral at 1, 24, 48 and 72 h (see **Figure 3.16**).

Reversibility assay

Stock solutions of oxime **2.35** (in CD_3CN) and Methoxyamine hydrochloride (Supelco) in D_2O were freshly prepared the day they were used. A KPi buffer stock solution was freshly prepared in D_2O adjusting the pH to 7.20 with concentrated DCl from ABCR (DCl , 38% wt% in D_2O , 99.5% atom%D). A TMSP-d_4 stock solution was freshly prepared in D_2O . All experiments were conducted at 298 K in standard NMR tubes (throw away quality) which were rinsed thoroughly with D_2O and oven dried prior to use.

Setup for the $^1\text{H-NMR}$ reversibility experiment at 100 μM :

1. 420 μL of KPi buffer (13.1 mM) were mixed inside the NMR tube with 110 μL of oxime **2.35** (500 μM), 10 μL of TMSP-d_4 (275 μM) and 10 μL of Methoxyamine hydrochloride (27.5 mM). The sample was then sonicated, locked to MeCN and shimmed before recording the first $^1\text{H-NMR}$ spectrum.

The final volume of the NMR sample was 550 μL with the following final concentrations:

100 μM of oxime **2.35**, 10 mM KPi buffer, 5 μM TMSP-d_4 and 500 μM of Methoxyamine hydrochloride with a ratio of 4:1 (10 mM KPi in $\text{D}_2\text{O}/\text{CD}_3\text{CN}$).

The reversibility of oxime **2.35** was followed by recording $^1\text{H-NMR}$ spectra every 2 h for a total of 30 measurements (60 h) tracing the oxime protons H_a and H_b (see **Figure 3.17**, panel A). A stack of selected $^1\text{H-NMR}$ spectra is presented in panel B of **Figure 3.17** and shows the process of oxime interconversion which reaches equilibrium between 9 and 19 h. The final ratio of the newly formed oxime **2.68** and oxime **2.35** was found to be 3:1.

For establishing the equilibration pathway oxime **2.35** was treated with a fivefold excess of aldehyde **2.69** in a NMR tube as described above. Final reaction conditions: 100 mM **2.35**, 500 mM **2.68**, 5 μM TMSP-d_4 , 4:1 (10 mM KPi in $\text{D}_2\text{O}/\text{CD}_3\text{CN}$).

The interconversion of oxime **2.35** to **2.69** was followed by recording $^1\text{H-NMR}$ spectra every 2 h for a total of 24 h at 298 K (**Figure 3.18**). A stack of selected $^1\text{H-NMR}$ spectra is presented in panel B of **Figure 3.18**. According to the respective integrals the equilibration process was reached after 10 h.

The integral values were converted into a concentration and a first order plot (using OriginPro 8 software) for the reverse reaction was performed to determine k_{-1} (**Figure E7**).

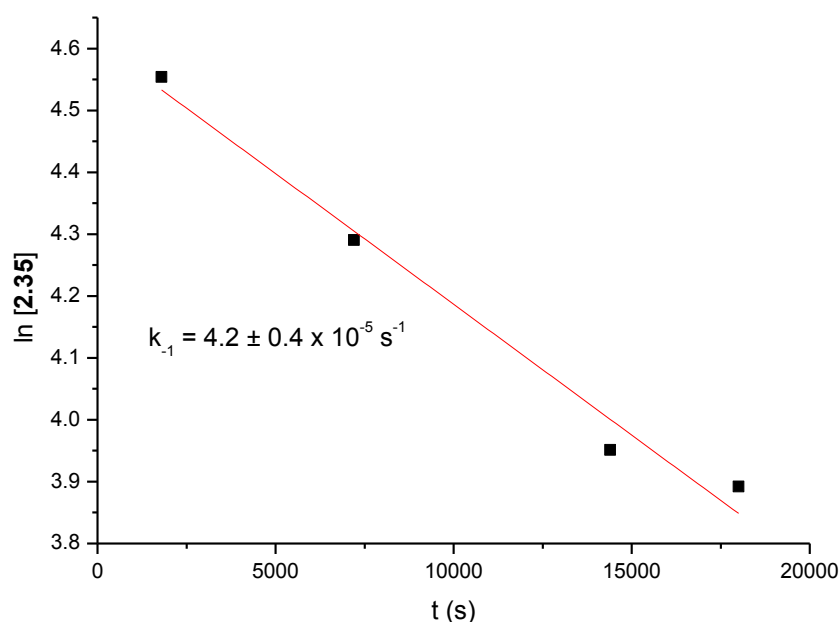


Figure E7: Plot of $\ln[2.35]$ (determined from the oxime proton H_a integral values) versus time. To evaluate the rate constant k_{-1} for the reverse reaction only time points between 0.5 and 5 h were considered.

The slope of the trend line (—) represents the rate constant k_{-1} for the reverse reaction of **2.35**. Its value of $4.2 \pm 0.4 \times 10^{-5} \text{ s}^{-1}$ is obtained directly from the graph along with the standard error. Using **equations 5** and **6** the equilibrium constant K_{eq} and its uncertainty can be calculated inserting the following values:

$$k_1 = 11113 \pm 284 \text{ M}^{-1} \text{ s}^{-1} \text{ (see section 4.2.3.4), } k_{-1} = 4.2 \pm 0.4 \times 10^{-5} \text{ s}^{-1}$$

$$K_{\text{eq}} = \frac{k_1}{k_{-1}} \quad (5)$$

$$\Delta K_{\text{eq}} = K_{\text{eq}} \times \sqrt{\left(\frac{\Delta k_1}{k_1}\right)^2 + \left(\frac{\Delta k_{-1}}{k_{-1}}\right)^2} \quad (6)$$

Equation 5 and 6: Calculating K_{eq} = equilibrium constant [M^{-1}] and its uncertainty Δk [M^{-1}].

This gives an equilibrium constant $K_{\text{eq}} = 2.6 \pm 0.3 \times 10^8 \text{ M}^{-1}$ for this particular type of oxime formation which clearly emphasizes the equilibrium being almost exclusively on the side of the product.

4.2.3.3 HPLC studies

Boron-accelerated oxime formation

All substrate stock solutions were prepared in HPLC grade MeCN except for the LYRAG pentapeptide monohydroxylamine **2.6** which was prepared in Milli-Q water and stored at -20°C. The concentration of the peptide was determined using a NanoDrop 2000 spectrophotometer from Thermo Scientific with a path length of 1 mm and $\epsilon_{(\text{LYRAG } 280 \text{ nm})} = 1490 \text{ M}^{-1} \text{ cm}^{-1}$. The different stock solutions for condensation were allowed to warm to room temperature, vortexed and centrifuged prior to mixing and combined in the following order in a PP HPLC vial (BGB, Part Number: PPSV0903K): 1) 100 mM KP_i buffer pH = 7.2, 2) *O*-alkylhydroxylamine, 3) aldehyde or ketone. The resulting solution was briefly mixed with a Gilson Pipetman before injection (time between mixing and injection was determined to be around 30 seconds). The reactions (**Table 3.4** entries 1-9) were followed by RP-HPLC on a Shimadzu Prominence UFLC Liquid Chromatograph using a C18 column (Eclipse XDB, 5 μm , 4.6 x 150 mm) from Agilent (gradient: 2-98% MeCN containing 1% H_2O in H_2O containing 1% MeCN over 18 min, flow rate 1 mL/min, room temperature, injection volume of 20 μL , neutral conditions) monitoring and collecting the products at 254 nm or 280 nm if not otherwise specified. It is noteworthy to mention that *O*-benzylhydroxylamine (**2.4**) was not UV active and could not be monitored under these HPLC conditions. The slight excess of 1.10 eq. is used to discriminate pipetting errors from the establishment of an equilibrium; a small excess will not affect the equilibrium but will negate the possibility of small pipetting errors leading to incomplete conversion. All conversion numbers are related to the disappearance of the peak area of the aldehyde species at 254 nm or the pentapeptide monohydroxylamine **2.6** at 280 nm on the first injection after ~1 min.

Boron-assisted ligation in complex media

Stock solutions of 2-FPBA **2.34** and *O*-benzylhydroxylamine (**2.4**) were prepared in HPLC grade MeCN. Stock solutions of L-glutathione (reduced, Sigma Aldrich), sucrose (Fluka) and lysozyme (hen eggwhite, Roth) were prepared in Milli-Q water. The lysozyme concentration was determined using a NanoDrop 2000 spectrophotometer from Thermo Scientific with a path length of 1 mm and $\epsilon_{(\text{lysozyme oxidized cystein } 280 \text{ nm})} = 37970 \text{ M}^{-1} \text{ cm}^{-1}$. Human Serum (male) type AB was purchased from Sigma Aldrich and stored at -20°C. The different stock solutions for condensation were allowed to warm to room temperature, vortexed and centrifuged prior to mixing and combined in the following order in a PP HPLC vial (BGB, Part Number: PPSV0903K): 1) 100 mM KP_i buffer pH = 7.2, 2) *O*-benzylhydroxylamine (**2.4**), 3) interfering additive 4) 2-FPBA **2.34**. The resulting solution was briefly mixed with a Gilson Pipetman before injection (time between mixing and injection was determined to be around 30 seconds). The reactions (**Table 3.5** entries 1-5) were analyzed by RP-HPLC on a Shimadzu Prominence UFLC Liquid Chromatograph using a C18 column (Eclipse XDB, 5 μm , 4.6 x

150 mm) from Agilent (gradient: 2-98% MeCN containing 1% H₂O in H₂O containing 1% MeCN over 18 min, flow rate 1 mL/min, room temperature, neutral conditions) monitoring and collecting the products at 254 nm.

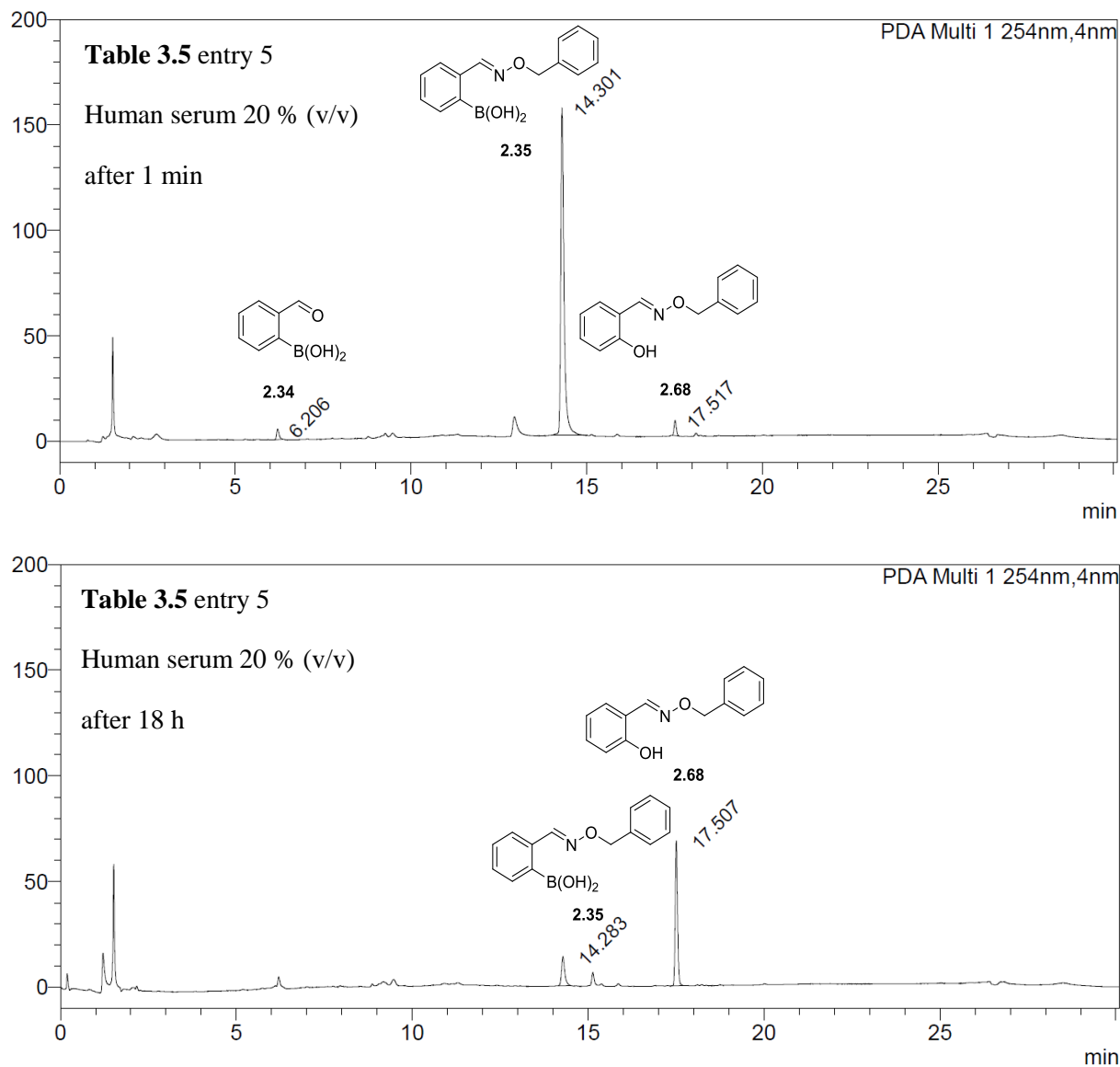


Figure E8: Top: Chromatogram of the reaction mixture of 100 μ M 2-FPBA (**2.34**) and 110 μ M *O*-benzylhydroxylamine (**2.4**) containing Human serum (20% v/v) as interfering additive in 100 mM KP_i, pH 7.20 recorded at 254 nm after 1 min under neutral HPLC conditions. The conversion of 2-FPBA is >98% and the peak at $t_R = 17.5$ min is the oxidation product **2.68**. **Bottom:** Chromatogram of the reaction mixture recorded after 18 h; clearly the oxime **2.35** gets continuously oxidized in human serum and oxime **2.68** is the major product.

The reaction with interfering lysozyme additive was also analyzed by UPLC-MS under acidic conditions (0.1% formic acid additive in the elution buffer) which showed no protein modification even after 12 h and complete conversion to the oxime **2.35** (see **Figure E9** and **Figure E10**).

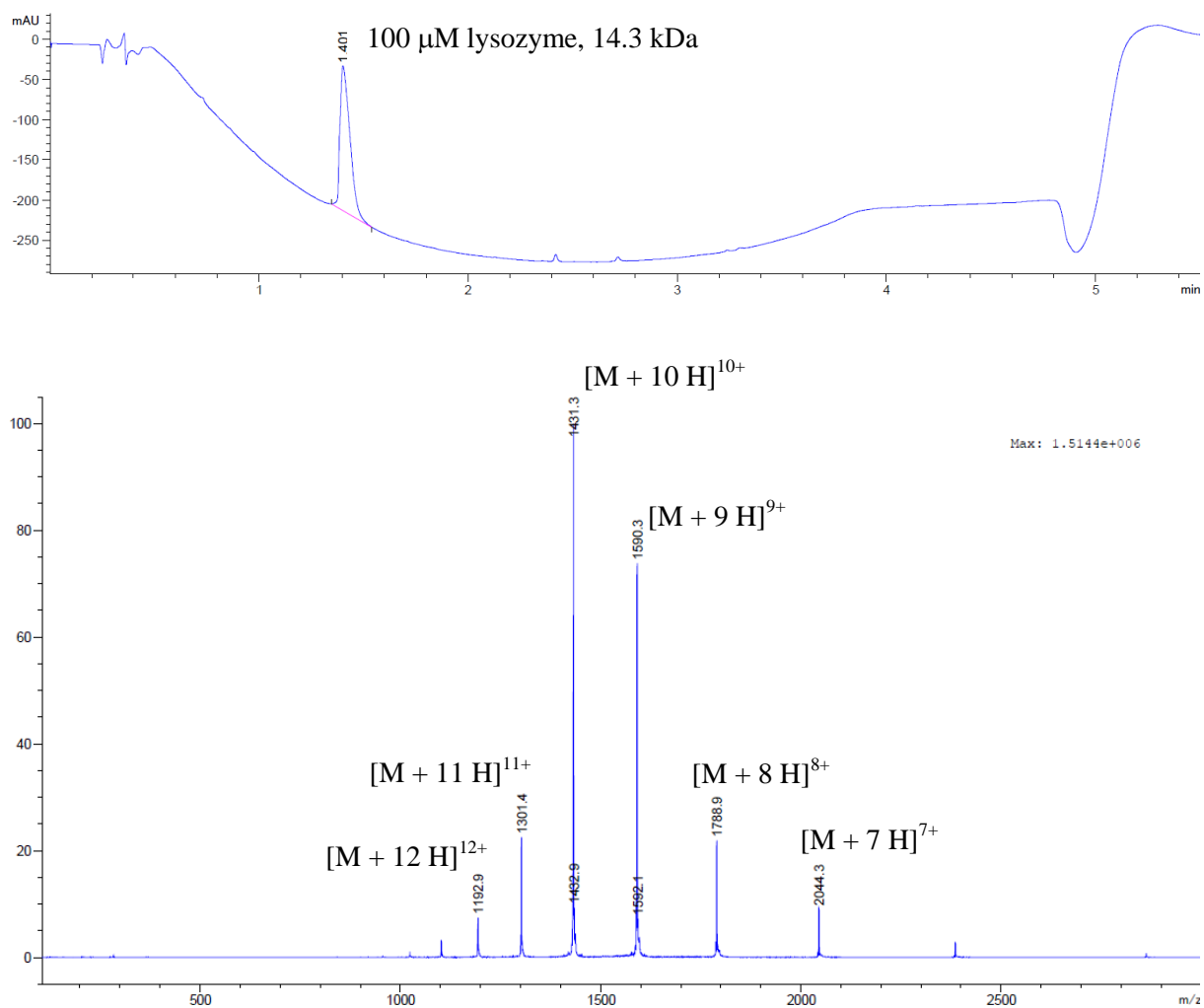


Figure E9: Top: Chromatogram of a 100 μ M lysozyme solution in 100 mM KP_i , pH 7.20 recorded at 254 nm under acidic UPLC-MS conditions. **Bottom:** ESI-MS spectra of the unmodified lysozyme peak at $t_R = 1.401$ min containing the masses for the molecular ions with different protonation states.

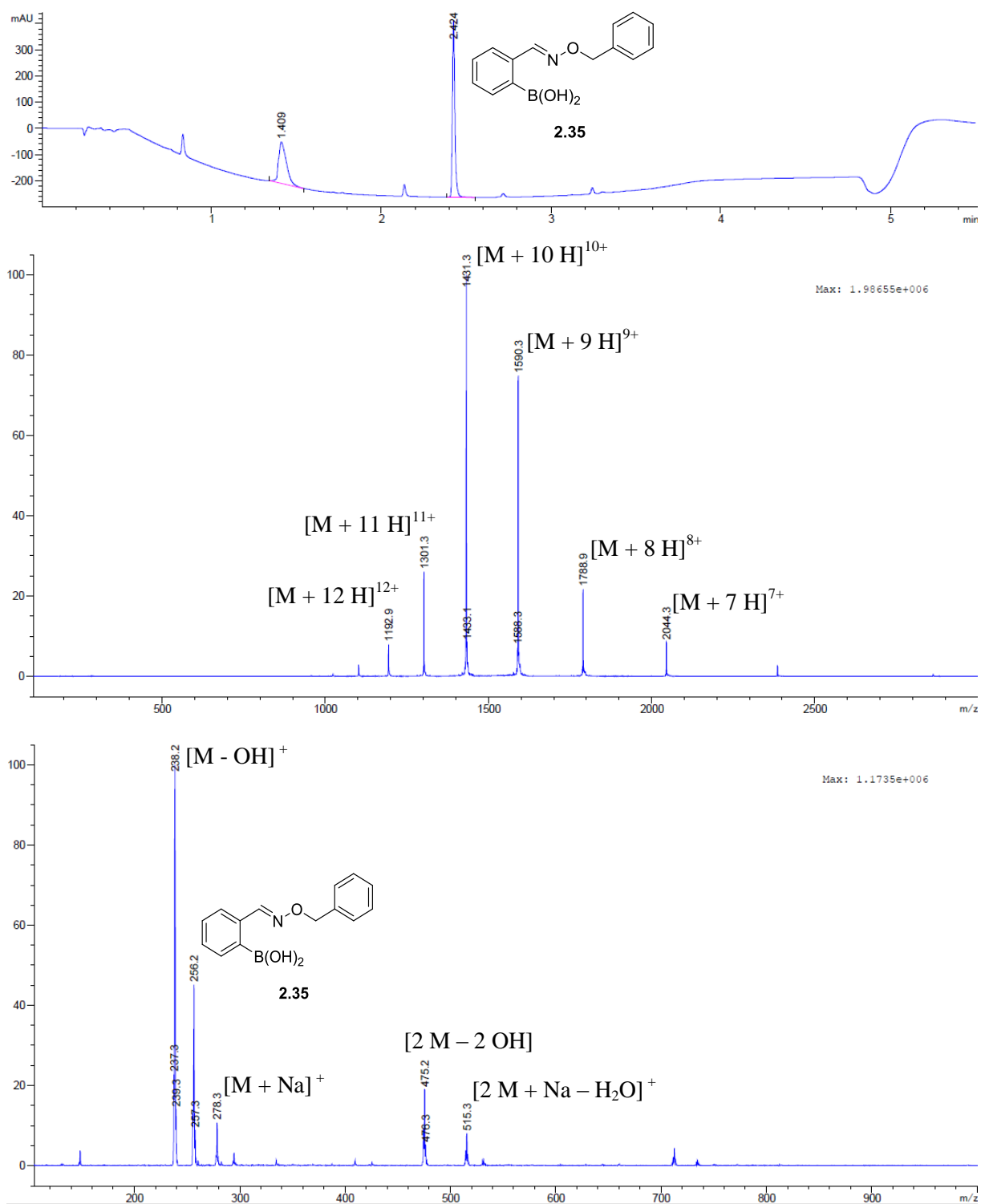


Figure E10: Top: Chromatogram of the reaction mixture of 100 μ M 2-FPBA **2.34** and 110 μ M *O*-benzylhydroxylamine (**2.4**) containing 100 μ M of lysozyme as interfering additive in 100 mM KP_i , pH 7.20 recorded at 254 nm after 12 h under acidic UPLC-MS conditions. **Middle:** ESI-MS spectra of the unmodified lysozyme peak at $t_R = 1.409$ min. **Bottom:** ESI-MS spectra of the oxime **2.35** peak at $t_R = 2.424$ min and its characteristic ionization adducts.

4.2.3.4 Fluorescence quenching assay

General Information

The fluorescence quenching experiments were conducted using a TECAN Infinite M1000 PRO fluorescence plate reader and the data was analyzed with the TECAN i-control software. All experiments were performed using a Nunclon flat black 96-well Microplate from Thermo Scientific. The fluorescence was monitored at the maximum absorption of lissamine derivative **2.66** (566 nm) in KP_i buffer (100 mM, pH 3.02, 3.89, 4.49, 5.00, 5.53, 6.14, 7.20 and 8.05). Stock solutions of the reaction partners in DMSO were freshly prepared and data was recorded the same day. The higher concentrated stock solutions were stored at -20°C and wrapped in aluminum foil to minimize bleaching. Prior to analysis all samples were gently allowed to warm up to room temperature in the absence of light and vortexed for 30 seconds to allow homogeneity.

Validation of oxime formation

In a scouting experiment dabsyl hydroxylamine **2.49** was mixed with an equimolar amount of 2-FPBA tagged lissamine **2.61** and the mixture analyzed after 10 min by UPLC-MS. The oxime product **2.63** could clearly be identified along with its oxidized form (**Figure E11**).

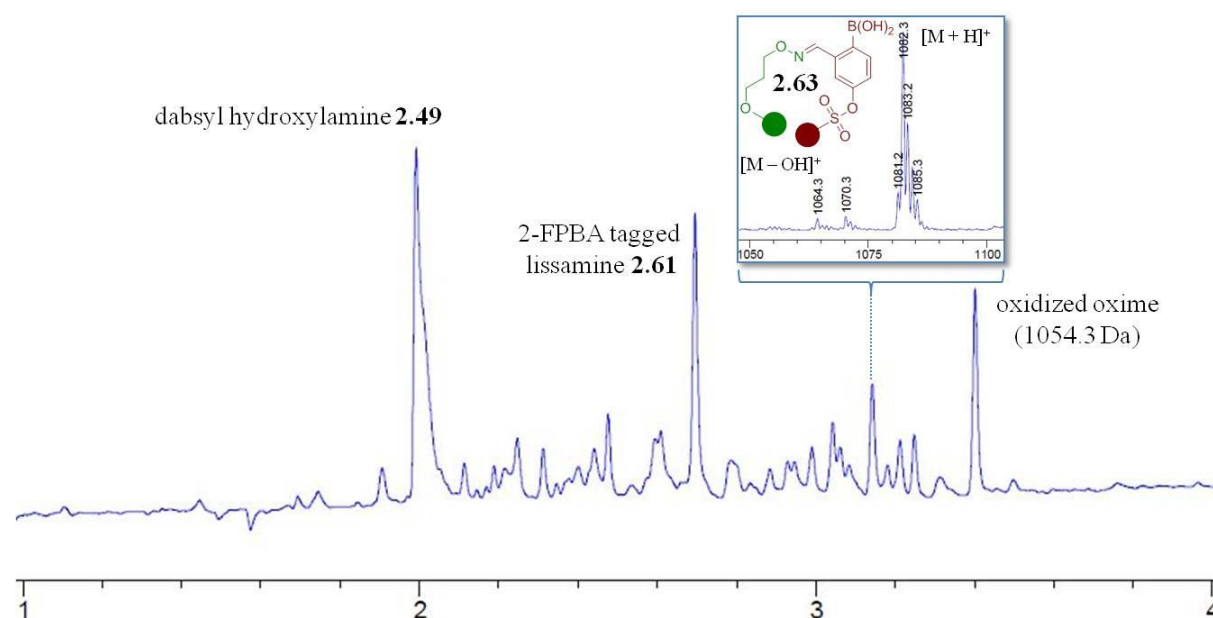


Figure E11: UPLC chromatogram of the reaction mixture after 10 min. The number in parenthesis indicates the mass observed by ESI-MS after elution of the respective UV peak. The axis represents the retention time in minutes. The extracted mass spectrometry data of oxime **2.63** is shown as a zoom for clear visualization.

Experimental

2 μL of a lissamine derivative **2.66** stock solution (50 μM or 10 μM , in DMSO) were added to a well filled with 196 μL of KP_i solution (100 mM) with the respective pH followed by 2 μL of a dabsyl derivative **2.65** stock solution (50 μM or 10 μM , in DMSO) to give a final volume of 200 μL (500 nM or 100 nM). The mixture was immediately mixed with a pipette to ensure homogeneity followed by monitoring the fluorescence at 566 nm. The control experiment was set up in analogy by adding 2 μL of a lissamine derivative **2.66** stock solution (50 μM or 10 μM , in DMSO) to a well filled with 196 μL of KP_i solution (100 mM, pH = 5.00) followed by 2 μL of a dabsyl derivative **2.65** stock solution (10 μM in DMSO). The mixture was immediately mixed with a pipette to ensure homogeneity followed by monitoring the fluorescence at 566 nm and 26°C. Both wells were analyzed simultaneously over a period of 7 minutes with data points recorded every 15 seconds. The time delay between mixing the samples and recording the first data point was determined to be 30 seconds.

Data processing

All experiments were triplicates and the data was processed in Microsoft Excel 2010 and plotted in OriginPro 8. The collected readout (fluorescence signal) was corrected by subtracting the control measurement with lissamine derivative **2.49** as well as for the 30 seconds delay time (see **Figure 3.14**, panel B). The corrected readout was then converted into a concentration [Lissamine] and the triplicate average of $1/[\text{Lissamine}]$ in μM^{-1} was plotted against the corrected time points in seconds. Only data points which lie within the linear region of the plot were considered (435 seconds for 0.1 μM). All error bars represent the standard deviation of the respective data series and were determined with OriginPro 8. The value for k_1 [$\text{M}^{-1} \text{s}^{-1}$] was determined as the slope of the linear fit of the respective graph.

Determining k_1

The reaction from **Figure 3.15** shows second order behavior up to 405 seconds and excellent linearity in inverse concentration plot (**Figure E12**). The collected data is corrected for the time and the control measurement.

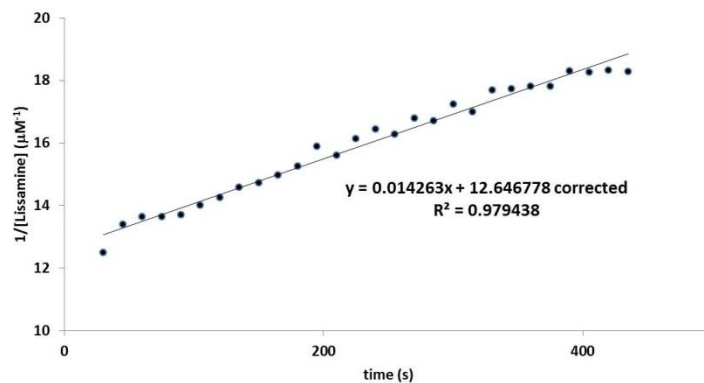


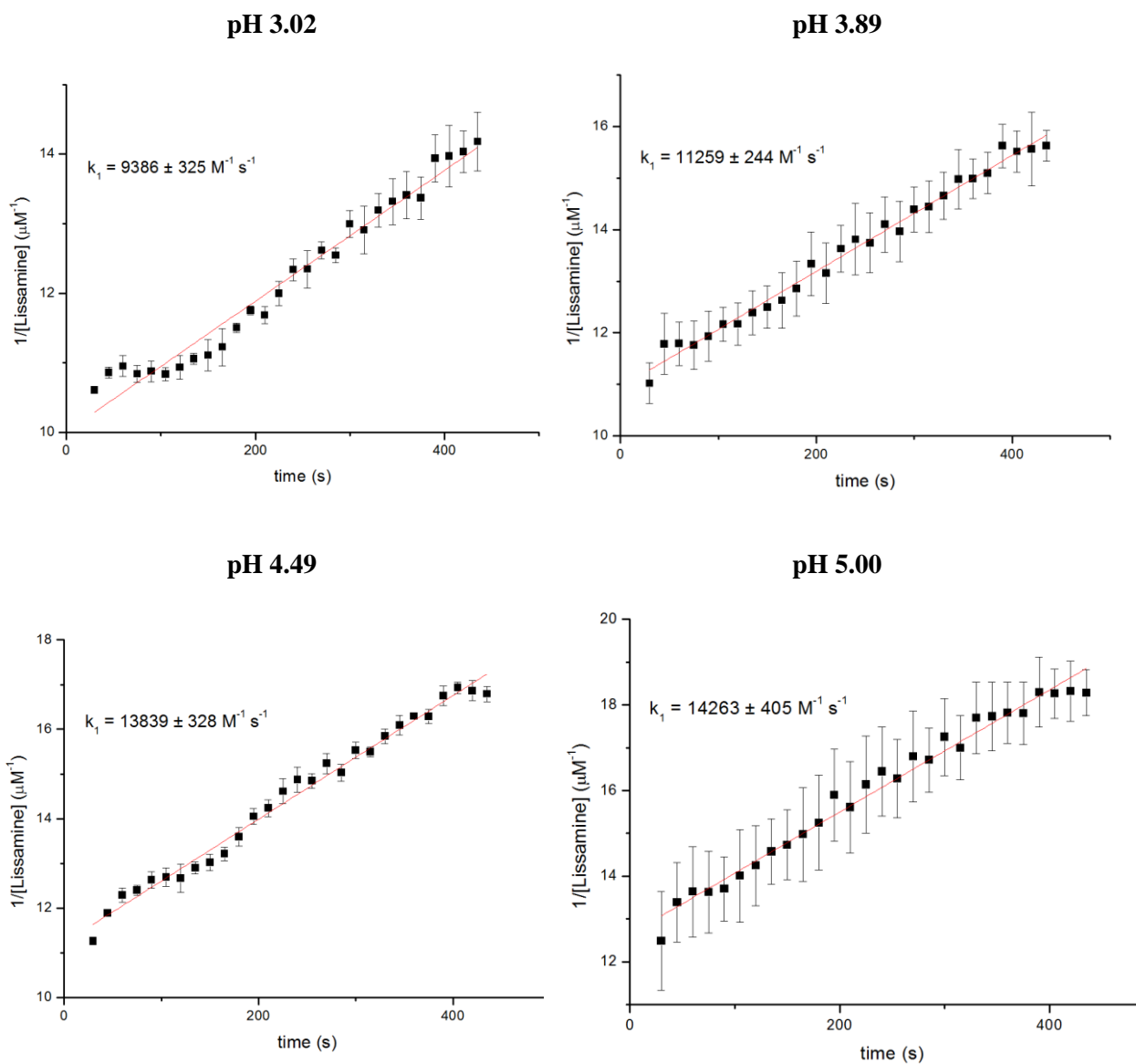
Figure E12: Fluorescence quench assay at 100 nM in 100 mM KP_i at pH 5.00 and 26°C. • Data points (corrected for time and the control measurement) recorded over 435 seconds are fitted by a trend line (—). The slope multiplied by 10^6 gives the rate constant k_1 [$\text{M}^{-1} \text{s}^{-1}$] for this particular oxime condensation reaction at the respective pH.

All pH profile measurements were evaluated in Microsoft Excel 2010 and plotted in OriginPro 8. All data presented is the average of triplicates and the error represents the standard error [$\text{M}^{-1} \text{s}^{-1}$]. Values for k_1 [$\text{M}^{-1} \text{s}^{-1}$] represent the slope of the trend line which was obtained from the average data points collected in the first 405 seconds. **Table E3** summarizes the results for the kinetic pH dependency of the oxime formation. These results are additionally plotted in a graph for better visualization (**Figure E13**).

Table E3: Results of the pH profile measurements at 100 nM. Values determined from triplicate measurements at 26°C.

pH	k_1 [$\text{M}^{-1} \text{s}^{-1}$]	standard error [$\text{M}^{-1} \text{s}^{-1}$]
3.02	9386	± 325
3.89	11259	± 244
4.49	13839	± 328
5.00	14263	± 405
5.53	12161	± 377
6.14	11181	± 360
7.20	11113	± 284
8.05	10180	± 310

The following eight inverse concentration plots (pH 3.02 – 8.05) were generated in OriginPro 8 from processing raw data in Microsoft Excel 2010. Average data points ■ include standard error bars and a trend line (—). The slope represents the rate constant [$\mu\text{M}^{-1} \text{s}^{-1}$] and is multiplied by a factor of 10^6 to obtain the final magnitude for k_1 [$\text{M}^{-1} \text{s}^{-1}$]. The standard error in k_1 is evaluated in the same manner.



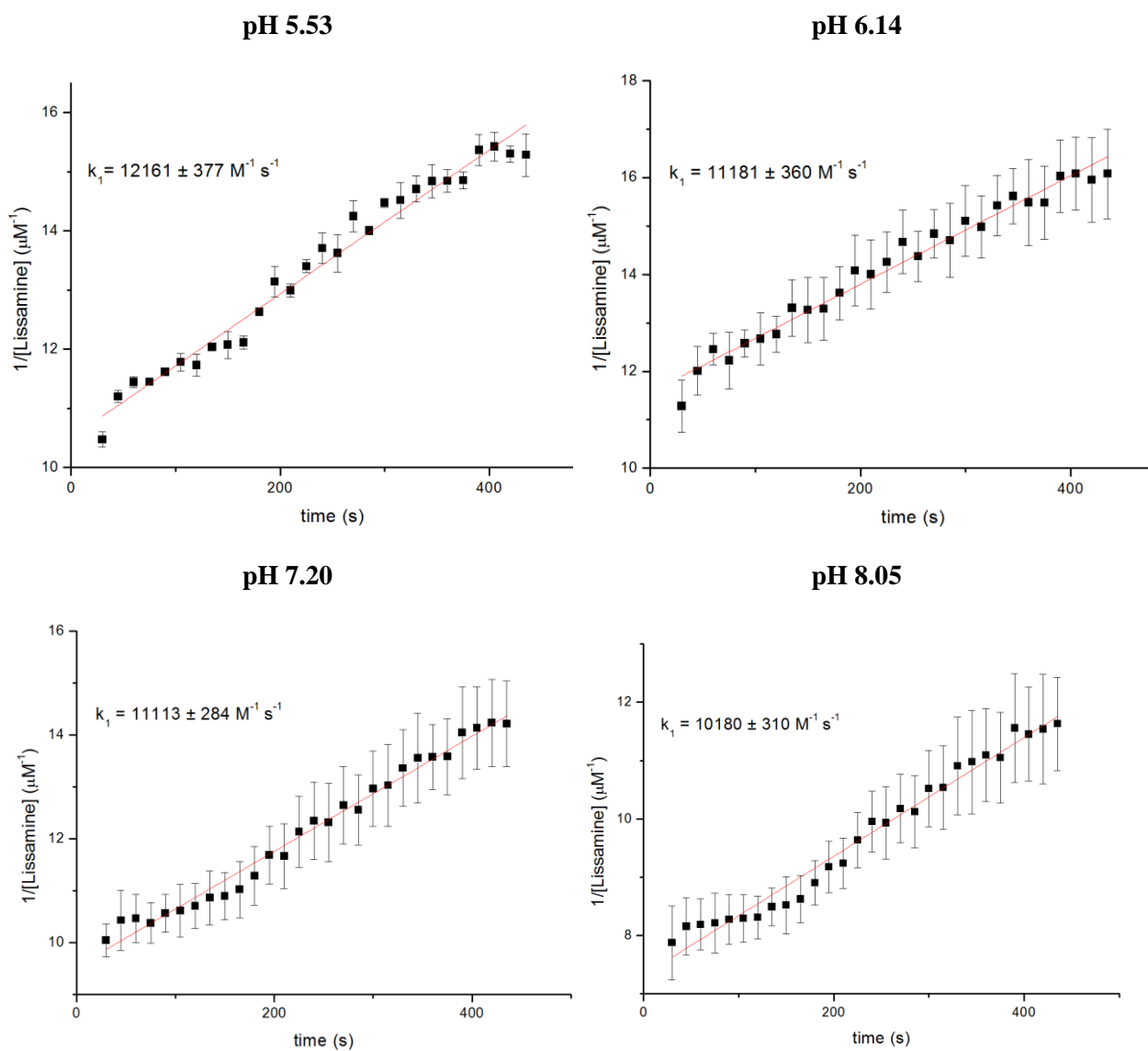
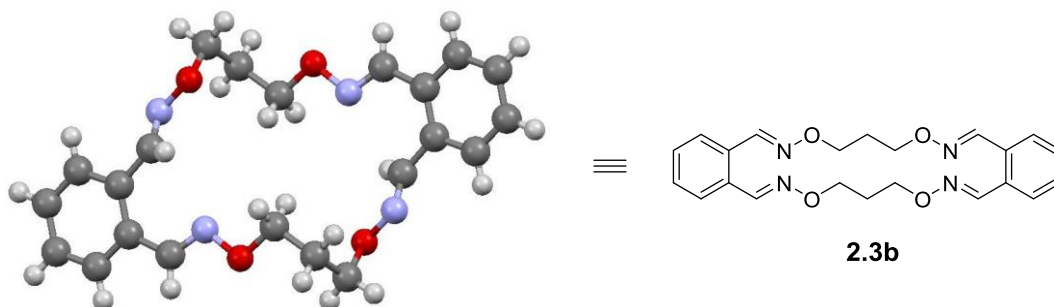


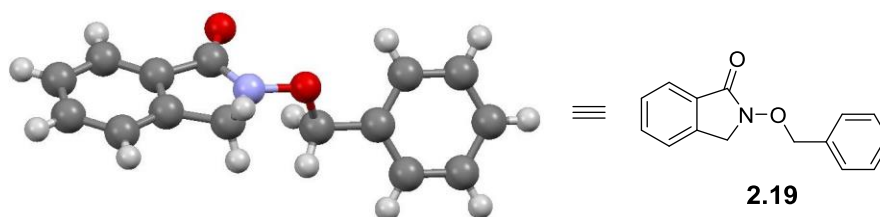
Figure E13: pH dependence of the rate constant at 100 nM. Inverse concentration plots obtained from triplicate measurements including the standard errors and the trendline.

4.3 Appendix

4.3.1 X-ray data

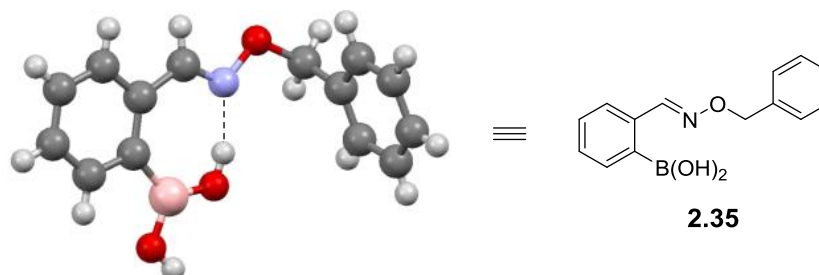


Crystal data for **2.3b**: formula $C_{22}H_{24}N_4O_4$, $M = 408.46$, $F(000) = 432$, colorless needle, size $0.030 \cdot 0.050 \cdot 0.270 \text{ mm}^3$, monoclinic, space group $P 2_1/n$, $Z = 2$, $a = 14.0072(10) \text{ \AA}$, $b = 4.5247(3) \text{ \AA}$, $c = 15.7406(11) \text{ \AA}$, $\alpha = 90^\circ$, $\beta = 90.463(3)^\circ$, $\gamma = 90^\circ$, $V = 997.58(12) \text{ \AA}^3$, $D_{\text{calc.}} = 1.360 \text{ Mg} \cdot \text{m}^{-3}$. The crystal was measured on a Bruker Kappa Apex2 diffractometer at 123K using graphite-monochromated Cu K_α -radiation with $\lambda = 1.54178 \text{ \AA}$, $\Theta_{\text{max}} = 69.073^\circ$. Minimal/maximal transmission 0.96/0.98, $\mu = 0.782 \text{ mm}^{-1}$. The Apex2 suite has been used for datacollection and integration. From a total of 7553 reflections, 1808 were independent (merging $r = 0.023$). From these, 1783 were considered as observed ($I > 2.0\sigma(I)$) and were used to refine 136 parameters. The structure was solved by other methods using the program Superflip. Least-squares refinement against F was carried out on all non-hydrogen atoms using the program CRYSTALS. $R = 0.0308$ (observed data), $wR = 0.0329$ (all data), $\text{GOF} = 1.1123$. Minimal/maximal residual electron density = $-0.17/0.25 \text{ e \AA}^{-3}$. Chebychev polynomial weights were used to complete the refinement. Plots were produced using CAMERON.



Crystal data for **2.19**: formula $C_{15}H_{13}N_1O_2$, $M = 239.27$, $F(000) = 252$, colorless plate, size $0.010 \cdot 0.130 \cdot 0.190 \text{ mm}^3$, triclinic, space group $P -1$, $Z = 2$, $a = 5.8350(3) \text{ \AA}$, $b = 7.7208(4) \text{ \AA}$, $c = 13.5719(7) \text{ \AA}$, $\alpha = 106.446(3)^\circ$, $\beta = 92.161(3)^\circ$, $\gamma = 92.767(3)^\circ$, $V = 584.88(5) \text{ \AA}^3$, $D_{\text{calc.}} = 1.359 \text{ Mg} \cdot \text{m}^{-3}$. The crystal was measured on a Bruker Kappa Apex2 diffractometer at 123K using graphite-monochromated Cu K_α -radiation with $\lambda = 1.54178 \text{ \AA}$, $\Theta_{\text{max}} = 68.712^\circ$. Minimal/maximal transmission 0.91/0.99, $\mu = 0.731 \text{ mm}^{-1}$. The Apex2 suite has been used for datacollection and integration. From a total of 5236 reflections, 1993 were independent (merging $r = 0.020$). From these, 1822 were considered as observed ($I > 2.0\sigma(I)$) and were used to refine 163 parameters. The structure was solved

by other methods using the program Superflip. Least-squares refinement against F was carried out on all non-hydrogen atoms using the program CRYSTALS. R = 0.0347 (observed data), wR = 0.0457 (all data), GOF = 1.1138. Minimal/maximal residual electron density = -0.17/0.21 e Å⁻³. Chebychev polynomial weights were used to complete the refinement. Plots were produced using CAMERON.



Crystal data for **2.35**: formula C₁₄H₁₄B₁N₁O₃, M = 255.08, F(000) = 2144, colourless block, size 0.100 · 0.120 · 0.140 mm³, monoclinic, space group C 2/c, Z = 16, a = 18.5248(15) Å, b = 15.2275(12) Å, c = 18.9615(16) Å, α = 90°, β = 94.102(4)°, γ = 90°, V = 5335.1(5) Å³, D_{calc.} = 1.270 Mg · m⁻³. The crystal was measured on a Bruker Kappa Apex2 diffractometer at 123K using graphite-monochromated Cu K_α-radiation with λ = 1.54178 Å, Θ_{max} = 68.196°. Minimal/maximal transmission 0.88/0.93, μ = 0.718 mm⁻¹. The Apex2 suite has been used for datacollection and integration. From a total of 17258 reflections, 4673 were independent (merging r = 0.020). From these, 4673 were considered as observed (I > 2.0σ(I)) and were used to refine 427 parameters. The structure was solved by other methods using the program Superflip. Least-squares refinement against Fsqd was carried out on all non-hydrogen atoms using the program CRYSTALS. R = 0.0386 (observed data), wR = 0.0884 (all data), GOF = 0.8971. Minimal/maximal residual electron density = -0.20/1.03 e Å⁻³. Chebychev polynomial weights were used to complete the refinement. Plots were produced using CAMERON.

4.3.2 License details for reference #173

The original publication entitled “Modular Ligands for Dirhodium Complexes Facilitate Catalyst Customization” can be found on **Wiley Online Library**:

<http://onlinelibrary.wiley.com/doi/10.1002/adsc.201500050/abstract>

This Agreement between Pascal Schmidt ("You") and John Wiley and Sons ("John Wiley and Sons") consists of your license details and the terms and conditions provided by John Wiley and Sons and Copyright Clearance Center.

License Number	3662980557175
License date	Jul 06, 2015
Licensed Content Publisher	John Wiley and Sons
Licensed Content Publication	Advanced Synthesis & Catalysis
Licensed Content Title	Modular Ligands for Dirhodium Complexes Facilitate Catalyst Customization
Licensed Content Author	Daniel G. Bachmann, Pascal J. Schmidt, Stefanie N. Geigle, Antoinette Chougnet, Wolf-Dietrich Woggon, Dennis G. Gillingham
Licensed Content Date	May 1, 2015
Pages	6
Type of use	Dissertation/Thesis
Requestor type	Author of this Wiley article
Format	Print and electronic
Portion	Full article
Will you be translating?	No
Title of your thesis / dissertation	New Strategies in Bioconjugation Chemical Modification of Nucleic Acids and Peptides
Expected completion date	Sep 2015
Expected size (number of pages)	180
Requestor Location	Pascal Schmidt St. Johannis-Ring 19 3rd floor - 308 Basel, Switzerland 4056 Attn: Pascal Schmidt
Billing Type	Invoice
Billing Address	Pascal Schmidt

St. Johannis-Ring 19
3rd floor - 308
Basel, Switzerland 4056
Attn: Pascal Schmidt

Total 0.00 EUR

4.3.3 License details for reference #213

The original publication entitled "Dialdehydes Lead to Exceptionally Fast Bioconjugations at Neutral pH by Virtue of a Cyclic Intermediate" can be found on **Wiley Online Library**:

<http://onlinelibrary.wiley.com/doi/10.1002/anie.201406132/abstract>

This Agreement between Pascal Schmidt ("You") and John Wiley and Sons ("John Wiley and Sons") consists of your license details and the terms and conditions provided by John Wiley and Sons and Copyright Clearance Center.

License Number	3662930960404
License date	Jul 06, 2015
Licensed Content Publisher	John Wiley and Sons
Licensed Content Publication	Angewandte Chemie
Licensed Content Title	Dialdehydes Lead to Exceptionally Fast Bioconjugations at Neutral pH by Virtue of a Cyclic Intermediate
Licensed Content Author	Pascal Schmidt, Linna Zhou, Kiril Tishinov, Kaspar Zimmermann, Dennis Gillingham
Licensed Content Date	Aug 22, 2014
Pages	4
Type of use	Dissertation/Thesis
Requestor type	Author of this Wiley article
Format	Print and electronic
Portion	Full article
Will you be translating?	No
Title of your thesis / dissertation	New Strategies in Bioconjugation Chemical Modification of Nucleic Acids and Peptides
Expected completion date	Sep 2015
Expected size (number of pages)	180
Requestor Location	Pascal Schmidt

	St. Johannis-Ring 19
	3rd floor - 308
	Basel, Switzerland 4056
	Attn: Pascal Schmidt
Billing Type	Invoice
Billing Address	Pascal Schmidt
	St. Johannis-Ring 19
	3rd floor - 308
	Basel, Switzerland 4056
	Attn: Pascal Schmidt
Total	0.00 EUR

5 References

- (1) Kalia, J.; Raines, R. T. *Curr Org Chem* **2010**, *14*, 138.
- (2) Hermanson, G. T. *Bioconjugate Techniques*; 2nd Ed.; ELSEVIER, **2008**.
- (3) Lim, S. I.; Kwon, I. *Critical Reviews in Biotechnology* **2015**, *1*.
- (4) Nie, S. M.; Xing, Y.; Kim, G. J.; Simons, J. W. *Annu Rev Biomed Eng* **2007**, *9*, 257.
- (5) Ostler, E. L. *Chem Cent J* **2007**, *1*, 5.
- (6) Sletten, E. M.; Bertozzi, C. R. *Angew Chem Int Ed* **2009**, *48*, 6974.
- (7) Saito, F.; Noda, H.; Bode, J. W. *Acs Chem Biol* **2015**, *10*, 1026.
- (8) Fancy, D. A. *Curr Opin Chem Biol* **2000**, *4*, 28.
- (9) Tiefenbrunn, T. K.; Dawson, P. E. *Biopolymers* **2010**, *94*, 95.
- (10) Brinkley, M. *Bioconjugate Chem* **1992**, *3*, 2.
- (11) Wedekind, F.; Baerpontzen, K.; Balamohan, S.; Choli, D.; Zahn, H.; Brandenburg, D. *Biol Chem H-S* **1989**, *370*, 251.
- (12) Sletten, E. M.; Bertozzi, C. R. *Accounts Chem Res* **2011**, *44*, 666.
- (13) Persch, E.; Dumele, O.; Diederich, F. *Angew Chem Int Ed* **2015**, *54*, 3290.
- (14) Nay, S. L.; O'Connor, T. R. *New Research Directions in DNA Repair*; 1st Ed.; InTech, **2013**.
- (15) Mishina, Y.; Duguid, E. M.; He, C. *Chem Rev* **2006**, *106*, 215.
- (16) Siede, W.; Doetsch, P. W. *DNA Damage Recognition*; CRC Press, **2005**.
- (17) Lawley, P. D.; Brookes, P. *Biochem J* **1963**, *89*, 127.
- (18) Maxam, A. M.; Gilbert, W. *P Natl Acad Sci USA* **1977**, *74*, 560.
- (19) Huppert, J. L. *Chem Soc Rev* **2008**, *37*, 1375.
- (20) Hayatsu, H.; Wataya, Y.; Kai, K.; Iida, S. *Biochemistry-Uts* **1970**, *9*, 2858.
- (21) Shapiro, R.; Servis, R. E.; Welcher, M. *J Am Chem Soc* **1970**, *92*, 422.
- (22) Frommer, M.; McDonald, L. E.; Millar, D. S.; Collis, C. M.; Watt, F.; Grigg, G. W.; Molloy, P. L.; Paul, C. L. *P Natl Acad Sci USA* **1992**, *89*, 1827.
- (23) Hayatsu, H. *P Jpn Acad B-Phys* **2008**, *84*, 321.
- (24) Solomon, J. J.; Segal, A. *Environ Health Persp* **1985**, *62*, 227.

- (25) Capaldi, D. C.; Gans, H.; Krotz, A. H.; Arnold, J.; Carty, R. L.; Moore, M. N.; Scozzari, A. N.; Lowery, K.; Cole, D. L.; Ravikumar, V. T. *Org Process Res Dev* **2003**, *7*, 832.
- (26) Tsunoda, H.; Kudo, T.; Ohkubo, A.; Seio, K.; Sekine, M. *Molecules* **2010**, *15*, 7509.
- (27) Li, T. H.; Zeng, Q. P.; Rokita, S. E. *Bioconjugate Chem* **1994**, *5*, 497.
- (28) Pande, P.; Shearer, J.; Yang, J. H.; Greenberg, W. A.; Rokita, S. E. *J Am Chem Soc* **1999**, *121*, 6773.
- (29) Veldhuyzen, W. F.; Pande, P.; Rokita, S. E. *J Am Chem Soc* **2003**, *125*, 14005.
- (30) Liu, Y.; Rokita, S. E. *Biochemistry-Us* **2012**, *51*, 1020.
- (31) Deans, A. J.; West, S. C. *Nat Rev Cancer* **2011**, *11*, 467.
- (32) Sherman, S. E.; Lippard, S. J. *Chem Rev* **1987**, *87*, 1153.
- (33) Neog, B.; Sinha, S.; Bhattacharyya, P. K. *Comput Theor Chem* **2013**, *1018*, 19.
- (34) Tomasz, M. *Chem Biol* **1995**, *2*, 865.
- (35) Cimino, G. D.; Gamper, H. B.; Isaacs, S. T.; Hearst, J. E. *Annu Rev Biochem* **1985**, *54*, 1151.
- (36) Tishinov, K.; Schmidt, K.; Haussinger, D.; Gillingham, D. G. *Angew Chem Int Ed* **2012**, *51*, 12000.
- (37) Beltrao, P.; Bork, P.; Krogan, N. J.; van Noort, V. *Mol Syst Biol* **2013**, *9*, 1.
- (38) Gurd, F. R. N. *Methods in Enzymology*; Academic Press: New York, **1967**; Vol. 11.
- (39) Cole, R. D.; Stein, W. H.; Moore, S. *J Biol Chem* **1958**, *233*, 1359.
- (40) Kaiser, E. T.; Lawrence, D. S. *Science* **1984**, *226*, 505.
- (41) Goddard, D. R.; Michaelis, L. *J Biol Chem* **1935**, *112*, 361.
- (42) Lundell, N.; Schreitmuller, T. *Anal Biochem* **1999**, *266*, 31.
- (43) Sechi, S.; Chait, B. T. *Anal Chem* **1998**, *70*, 5150.
- (44) Ghosh, S. S.; Kao, P. M.; Mccue, A. W.; Chappelle, H. L. *Bioconjugate Chem* **1990**, *1*, 71.
- (45) Schelte, P.; Boeckler, C.; Frisch, B.; Schuber, F. *Bioconjugate Chem* **2000**, *11*, 118.
- (46) Masri, M. S.; Friedman, M. *J Protein Chem* **1988**, *7*, 49.
- (47) Morpurgo, M.; Veronese, F. M.; Kachensky, D.; Harris, J. M. *Bioconjugate Chem* **1996**, *7*, 363.
- (48) Bell, S. J.; Fam, C. M.; Chlipala, E. A.; Carlson, S. J.; Lee, J. I.; Rosendahl, M. S.; Doherty, D. H.; Cox, G. N. *Bioconjugate Chem* **2008**, *19*, 299.
- (49) Junutula, J. R.; Bhakta, S.; Raab, H.; Ervin, K. E.; Eigenbrot, C.; Vandlen, R.; Scheller, R. H.; Lowman, H. B. *J Immunol Methods* **2008**, *332*, 41.

- (50) Smith, M. E. B.; Schumacher, F. F.; Ryan, C. P.; Tedaldi, L. M.; Papaioannou, D.; Waksman, G.; Caddick, S.; Baker, J. R. *J Am Chem Soc* **2010**, *132*, 1960.
- (51) Ryan, C. P.; Smith, M. E. B.; Schumacher, F. F.; Grohmann, D.; Papaioannou, D.; Waksman, G.; Werner, F.; Baker, J. R.; Caddick, S. *Chem Commun* **2011**, *47*, 5452.
- (52) Kim, Y. G.; Ho, S. O.; Gassman, N. R.; Korlann, Y.; Landorf, E. V.; Collart, F. R.; Weiss, S. *Bioconjugate Chem* **2008**, *19*, 786.
- (53) Lyon, R. P.; Setter, J. R.; Bovee, T. D.; Doronina, S. O.; Hunter, J. H.; Anderson, M. E.; Balasubramanian, C. L.; Duniho, S. M.; Leiske, C. I.; Li, F.; Senter, P. D. *Nat Biotechnol* **2014**, *32*, 1059.
- (54) Pollack, S. J.; Schultz, P. G. *J Am Chem Soc* **1989**, *111*, 1929.
- (55) Ellman, G. L. *Arch Biochem Biophys* **1959**, *82*, 70.
- (56) Ellman, G. L.; Courtney, K. D.; Andres, V.; Featherstone, R. M. *Biochem Pharmacol* **1961**, *7*, 88.
- (57) Bheda, P.; Swatkoski, S.; Fiedler, K. L.; Boeke, J. D.; Cotter, R. J.; Wolberger, C. *P Natl Acad Sci USA* **2012**, *109*, E916.
- (58) Markoutsas, S.; Bahr, U.; Papisotiriou, D. G.; Hafner, A. K.; Karas, M.; Sorg, B. L. *Proteomics* **2014**, *14*, 659.
- (59) Smith, H. T.; Staudenmayer, N.; Millett, F. *Biochemistry-U.S.* **1977**, *16*, 4971.
- (60) Ng, S.; Smith, M. B.; Smith, H. T.; Millett, F. *Biochemistry-U.S.* **1977**, *16*, 4975.
- (61) Tuls, J.; Geren, L.; Millett, F. *J Biol Chem* **1989**, *264*, 16421.
- (62) Nakamura, T.; Kawai, Y.; Kitamoto, N.; Osawa, T.; Kato, Y. *Chem Res Toxicol* **2009**, *22*, 536.
- (63) Gavriluk, J.; Ban, H.; Nagano, M.; Hakamata, W.; Barbas, C. F. *Bioconjugate Chem* **2012**, *23*, 2321.
- (64) Kawakami, T.; Akaji, K.; Aimoto, S. *Org Lett* **2001**, *3*, 1403.
- (65) Chelius, D.; Shaler, T. A. *Bioconjugate Chem* **2003**, *14*, 205.
- (66) Witus, L. S.; Moore, T.; Thuronyi, B. W.; Esser-Kahn, A. P.; Scheck, R. A.; Iayarone, A. T.; Francis, M. B. *J Am Chem Soc* **2010**, *132*, 16812.
- (67) Tam, J. P.; Yu, Q. T.; Miao, Z. W. *Biopolymers* **1999**, *51*, 311.
- (68) Li, X. F.; Zhang, L. S.; Hall, S. E.; Tam, J. P. *Tetrahedron Lett* **2000**, *41*, 4069.
- (69) Dawson, P. E.; Muir, T. W.; Clarklewis, I.; Kent, S. B. H. *Science* **1994**, *266*, 776.
- (70) Staudinger, H.; Meyer, J. *Helv. Chim. Act.* **1919**, *2*, 635.
- (71) Saxon, E.; Bertozzi, C. R. *Science* **2000**, *287*, 2007.
- (72) Nilsson, B. L.; Kiessling, L. L.; Raines, R. T. *Org Lett* **2000**, *2*, 1939.
- (73) Saxon, E.; Armstrong, J. I.; Bertozzi, C. R. *Org Lett* **2000**, *2*, 2141.

- (74) van Berkel, S. S.; van Eldijk, M. B.; van Hest, J. C. M. *Angew Chem Int Ed* **2011**, *50*, 8806.
- (75) Schilling, C. I.; Jung, N.; Biskup, M.; Schepers, U.; Brase, S. *Chem Soc Rev* **2011**, *40*, 4840.
- (76) Gothelf, K. V.; Jorgensen, K. A. *Chem Rev* **1998**, *98*, 863.
- (77) Kolb, H. C.; Finn, M. G.; Sharpless, K. B. *Angew Chem Int Ed* **2001**, *40*, 2004.
- (78) Rostovtsev, V. V.; Green, L. G.; Fokin, V. V.; Sharpless, K. B. *Angew Chem Int Ed* **2002**, *41*, 2596.
- (79) Tornøe, C. W.; Christensen, C.; Meldal, M. *J Org Chem* **2002**, *67*, 3057.
- (80) Worrell, B. T.; Malik, J. A.; Fokin, V. V. *Science* **2013**, *340*, 457.
- (81) Thirumurugan, P.; Matosiuk, D.; Jozwiak, K. *Chem Rev* **2013**, *113*, 4905.
- (82) Nwe, K.; Brechbiel, M. W. *Cancer Biother Radio* **2009**, *24*, 289.
- (83) Best, M. D. *Biochemistry-US* **2009**, *48*, 6571.
- (84) McKay, C. S.; Finn, M. G. *Chem Biol* **2014**, *21*, 1075.
- (85) Sauer, J.; Wiest, H. *Angew Chem Int Ed* **1962**, *74*, 353.
- (86) Blackman, M. L.; Royzen, M.; Fox, J. M. *J Am Chem Soc* **2008**, *130*, 13518.
- (87) Devaraj, N. K.; Weissleder, R.; Hilderbrand, S. A. *Bioconjugate Chem* **2008**, *19*, 2297.
- (88) Taylor, M. T.; Blackman, M. L.; Dmitrenko, O.; Fox, J. M. *J Am Chem Soc* **2011**, *133*, 9646.
- (89) Darko, A.; Wallace, S.; Dmitrenko, O.; Machovina, M. M.; Mehl, R. A.; Chin, J. W.; Fox, J. M. *Chem Sci* **2014**, *5*, 3770.
- (90) Knall, A. C.; Slugovc, C. *Chem Soc Rev* **2013**, *42*, 5131.
- (91) Devaraj, N. K.; Weissleder, R. *Accounts Chem Res* **2011**, *44*, 816.
- (92) Lang, K.; Chin, J. W. *Acs Chem Biol* **2014**, *9*, 16.
- (93) Rashidian, M.; Mahmoodi, M. M.; Shah, R.; Dozier, J. K.; Wagner, C. R.; Distefano, M. D. *Bioconjugate Chem* **2013**, *24*, 333.
- (94) Axup, J. Y.; Bajjuri, K. M.; Ritland, M.; Hutchins, B. M.; Kim, C. H.; Kazane, S. A.; Halder, R.; Forsyth, J. S.; Santidrian, A. F.; Stafin, K.; Lu, Y. C.; Tran, H.; Seller, A. J.; Biroce, S. L.; Szydlak, A.; Pinkstaff, J. K.; Tian, F.; Sinha, S. C.; Felding-Habermann, B.; Smider, V. V.; Schultz, P. G. *P Natl Acad Sci USA* **2012**, *109*, 16101.
- (95) Ferris, D. P.; McGonigal, P. R.; Witus, L. S.; Kawaji, T.; Algaradah, M. M.; Alnajadah, A. R.; Nassar, M. S.; Stoddard, J. F. *Org Lett* **2015**, *17*, 2146.
- (96) Crisalli, P.; Hernandez, A. R.; Kool, E. T. *Bioconjugate Chem* **2012**, *23*, 1969.
- (97) Dahlhoff, G.; Barsnick, U.; Hölderich, W. F. *Appl Catal a-Gen* **2001**, *210*, 83.

- (98) Mahal, L. K.; Yarema, K. J.; Bertozzi, C. R. *Science* **1997**, *276*, 1125.
- (99) Byeon, J. Y.; Limpoco, F. T.; Bailey, R. C. *Langmuir* **2010**, *26*, 15430.
- (100) Dirksen, A.; Yegneswaran, S.; Dawson, P. E. *Angew Chem Int Ed* **2010**, *49*, 2023.
- (101) Egholm, M.; Buchardt, O.; Christensen, L.; Behrens, C.; Freier, S. M.; Driver, D. A.; Berg, R. H.; Kim, S. K.; Norden, B.; Nielsen, P. E. *Nature* **1993**, *365*, 566.
- (102) Nielsen, P. E.; Egholm, M.; Berg, R. H.; Buchardt, O. *Science* **1991**, *254*, 1497.
- (103) Moser, H. E.; Dervan, P. B. *Science* **1987**, *238*, 645.
- (104) Hoogsteen, K. *Acta Crystallographica* **1963**, *16*, 907.
- (105) Nielsen, P. E. *Chem Biodivers* **2010**, *7*, 786.
- (106) Egholm, M.; Buchardt, O.; Nielsen, P. E.; Berg, R. H. *J Am Chem Soc* **1992**, *114*, 1895.
- (107) Merrifield, R. B. *J Am Chem Soc* **1963**, *85*, 2149.
- (108) Rozners, E. *Journal of Nucleic Acids* **2012**, *8*.
- (109) Nielsen, P. E.; Egholm, M. *Current Issues in Molecular Biology* **1999**, *1*, 89.
- (110) Jensen, K. K.; Orum, H.; Nielsen, P. E.; Norden, B. *Biochemistry-Us* **1997**, *36*, 5072.
- (111) Leijon, M.; Graslund, A.; Nielsen, P. E.; Buchardt, O.; Norden, B.; Kristensen, S. M.; Eriksson, M. *Biochemistry-Us* **1994**, *33*, 9820.
- (112) Nielsen, P. E.; Egholm, M.; Buchardt, O. *J. Mol. Recognit.* **1994**, *7*, 164-170.
- (113) Nielsen, P. E.; Christensen, L. *J Am Chem Soc* **1996**, *118*, 2287.
- (114) Lohse, J.; Dahl, O.; Nielsen, P. E. *P Natl Acad Sci USA* **1999**, *96*, 11804.
- (115) Ortega, J. A.; Blas, J. R.; Orozco, M.; Grandas, A.; Pedroso, E.; Robles, J. *Org Lett* **2007**, *9*, 4503.
- (116) Chenna, V.; Rapireddy, S.; Sahu, B.; Ausin, C.; Pedroso, E.; Ly, D. H. *Chembiochem* **2008**, *9*, 2388.
- (117) Bohler, C.; Nielsen, P. E.; Orgel, L. E. *Nature* **1995**, *376*, 578.
- (118) Rosenbaum, D. M.; Liu, D. R. *J Am Chem Soc* **2003**, *125*, 13924.
- (119) Janssen, P. G. A.; Meeuwenoord, N.; van der Marel, G.; Jabbari-Farouji, S.; van der Schoot, P.; Surin, M.; Tomovic, Z.; Meijer, E. W.; Schenning, A. P. H. J. *Chem Commun* **2010**, *46*, 109.
- (120) Koppitz, M.; Nielsen, P. E.; Orgel, L. E. *J Am Chem Soc* **1998**, *120*, 4563.
- (121) Mattes, A.; Seitz, O. *Chem Commun* **2001**, *20*, 2050.
- (122) Kazane, S. A.; Axup, J. Y.; Kim, C. H.; Ciobanu, M.; Wold, E. D.; Barluenga, S.; Hutchins, B. A.; Schultz, P. G.; Winssinger, N.; Smider, V. V. *J Am Chem Soc* **2013**, *135*, 340.

- (123) Singh, Y.; Murat, P.; Defrancq, E. *Chem Soc Rev* **2010**, *39*, 2054.
- (124) Crick, F. *Nature* **1970**, *227*, 561.
- (125) Yin, H. F.; Lu, Q. L.; Wood, M. *Mol Ther* **2008**, *16*, 38.
- (126) Bendifallah, N.; Rasmussen, F. W.; Zachar, V.; Ebbesen, P.; Nielsen, P. E.; Koppelhus, U. *Bioconjugate Chem* **2006**, *17*, 750.
- (127) Shiraishi, T.; Hamzavi, R.; Nielsen, P. E. *Nucleic Acids Res* **2008**, *36*, 4424.
- (128) Orum, H.; Nielsen, P. E.; Egholm, M.; Berg, R. H.; Buchardt, O.; Stanley, C. *Nucleic Acids Res* **1993**, *21*, 5332.
- (129) Reller, M. E.; Mallonee, A. B.; Kwiatkowski, N. P.; Merz, W. G. *J Clin Microbiol* **2007**, *45*, 3802.
- (130) Kurupati, P.; Tan, K. S. W.; Kumarasinghe, G.; Poh, C. L. *Antimicrob Agents Ch* **2007**, *51*, 805.
- (131) Patureau, B. M.; Hudson, R. H. E.; Damha, M. J. *Bioconjugate Chem* **2007**, *18*, 421.
- (132) Debaene, F.; Da Silva, J. A.; Pianowski, Z.; Duran, F. J.; Winssinger, N. *Tetrahedron* **2007**, *63*, 6577.
- (133) Katritzky, A. R.; Narindoshvili, T. *Org Biomol Chem* **2008**, *6*, 3171.
- (134) Debaene, F.; Winssinger, N. *Org Lett* **2003**, *5*, 4445.
- (135) Pothukanuri, S.; Pianowski, Z.; Winssinger, N. *Eur J Org Chem* **2008**, *18*, 3141.
- (136) Goodwin, T. E.; Holland, R. D.; Lay, J. O.; Raney, K. D. *Bioorg Med Chem Lett* **1998**, *8*, 2231.
- (137) Sarin, V. K.; Kent, S. B. H.; Merrifield, R. B. *J Am Chem Soc* **1980**, *102*, 5463.
- (138) Rodionov, I. L.; Peshenko, I. A.; Baidakova, L. K.; Ivanov, V. T. *Int J Pept Res Ther* **2007**, *13*, 161.
- (139) Gupta, A.; Lee, L. L.; Roy, S.; Tanious, F. A.; Wilson, W. D.; Ly, D. H.; Armitage, B. A. *Chembiochem* **2013**, *14*, 1476.
- (140) Panagene - Guidelines on PNA oligomers,
http://www.panagene.com/bbs/ndata/pnk_guide/pnk_guide_1239068147.pdf.
- (141) Lee, H. N.; Jeon, J. H.; Lim, J. C.; Choi, H.; Yoon, Y. H.; Kim, S. K. *Org Lett* **2007**, *9*, 3291.
- (142) Paulissen, R.; Reimlinger, H.; Hayez, E.; Hubert, A. J.; Teyssié, P. *Tetrahedron Lett* **1973**, 2233.
- (143) Yates, P. *J Am Chem Soc* **1952**, *74*, 5376.
- (144) Pirrung, M. C.; Morehead, A. T. *J Am Chem Soc* **1996**, *118*, 8162.
- (145) Gillingham, D.; Fei, N. *Chem Soc Rev* **2013**, *42*, 4918.

- (146) Koizumi, Y.; Kobayashi, H.; Wakimoto, T.; Furuta, T.; Fukuyama, T.; Kan, T. *J Am Chem Soc* **2008**, *130*, 16854.
- (147) Zhang, X. M.; Ma, M.; Wang, J. B. *Arkivoc* **2003**, *ii*, 84.
- (148) Salzmann, T. N.; Ratcliffe, R. W.; Christensen, B. G.; Bouffard, F. A. *J Am Chem Soc* **1980**, *102*, 6161.
- (149) Doyle, M. P.; Hu, W. H.; Timmons, D. J. *Org Lett* **2001**, *3*, 933.
- (150) Lian, Y. J.; Davies, H. M. L. *J Am Chem Soc* **2010**, *132*, 440.
- (151) Schwartz, B. D.; Denton, J. R.; Lian, Y. J.; Davies, H. M. L.; Williams, C. M. *J Am Chem Soc* **2009**, *131*, 8329.
- (152) Davies, H. M. L.; Clark, T. J.; Church, L. A. *Tetrahedron Lett* **1989**, *30*, 5057.
- (153) Davies, H. M. L.; Lee, G. H. *Org Lett* **2004**, *6*, 1233.
- (154) Doyle, M. P.; Morgan, J. P.; Fettinger, J. C.; Zavalij, P. Y.; Colyer, J. T.; Timmons, D. J.; Carducci, M. D. *J Org Chem* **2005**, *70*, 5291.
- (155) Antos, J. M.; Francis, M. B. *J Am Chem Soc* **2004**, *126*, 10256.
- (156) Antos, J. M.; McFarland, J. M.; Iavarone, A. T.; Francis, M. B. *J Am Chem Soc* **2009**, *131*, 6301.
- (157) Popp, B. V.; Ball, Z. T. *J Am Chem Soc* **2010**, *132*, 6660.
- (158) Chen, Z.; Popp, B. V.; Bovet, C. L.; Ball, Z. T. *Acs Chem Biol* **2011**, *6*, 920.
- (159) Kundu, R.; Ball, Z. T. *Chem Commun* **2013**, *49*, 4166.
- (160) Ball, Z. T. *Accounts Chem Res* **2013**, *46*, 560.
- (161) Lifetechnologies - PNA Oligomer Quick Reference Card,
https://www3.appliedbiosystems.com/cms/groups/mcb_support/documents/generaldocuments/cms_040636.pdf.
- (162) PNA Bio Inc. - Guidelines for PNA oligomers,
http://www.pnabio.com/pdf/PNA%20oligomer%20handling_PNABio.pdf.
- (163) Braasch, D. A.; Corey, D. R. *Methods* **2001**, *23*, 97.
- (164) Tackett, A. J.; Corey, D. R.; Raney, K. D. *Nucleic Acids Res* **2002**, *30*, 950.
- (165) Singh, S. K.; Nielsen, P.; Koshkin, A. A.; Wengel, J. *Chem Commun* **1998**, 455.
- (166) Zaykov, A. N.; MacKenzie, K. R.; Ball, Z. T. *Chem-Eur J* **2009**, *15*, 8961.
- (167) Tam, J. P.; Lu, Y. A. *J Am Chem Soc* **1995**, *117*, 12058.
- (168) Mergler, M.; Durieux, J. P.; 2nd Ed.; Bachem AG: Bubendorf, **2005**.
- (169) Walker, J. M. *The Protein Protocols Handbook*; 1st Ed.; Humana Press, **1996**.
- (170) Kalia, J.; Raines, R. T. *Angew Chem Int Ed* **2008**, *47*, 7523.

- (171) Neuner, P.; Gallo, P.; Orsatti, L.; Fontana, L.; Monaci, P. *Bioconjugate Chem* **2003**, *14*, 276.
- (172) Shao, J.; Tam, J. P. *J Am Chem Soc* **1995**, *117*, 3893.
- (173) Bachmann, D. G.; Schmidt, P. J.; Geigle, S. N.; Chougnet, A.; Woggon, W.-D.; Gillingham, D. G. *Adv Synth Catal* **2015**, *357*, 2033.
- (174) Espino, C. G.; Fiori, K. W.; Kim, M.; Du Bois, J. *J Am Chem Soc* **2004**, *126*, 15378.
- (175) Bickley, J.; Bonar-Law, R.; McGrath, T.; Singh, N.; Steiner, A. *New J Chem* **2004**, *28*, 425.
- (176) Sasmal, P. K.; Carregal-Romero, S.; Han, A. A.; Streu, C. N.; Lin, Z. J.; Namikawa, K.; Elliott, S. L.; Koster, R. W.; Parak, W. J.; Meggers, E. *Chembiochem* **2012**, *13*, 1116.
- (177) Sasmal, P. K.; Streu, C. N.; Meggers, E. *Chem Commun* **2013**, *49*, 1581.
- (178) Volker, T.; Dempwolff, F.; Graumann, P. L.; Meggers, E. *Angew Chem Int Ed* **2014**, *53*, 10536.
- (179) Wilson, Y. M.; Durrenberger, M.; Nogueira, E. S.; Ward, T. R. *J Am Chem Soc* **2014**, *136*, 8928.
- (180) Sadhu, K. K.; Winssinger, N. *Chem-Eur J* **2013**, *19*, 8182.
- (181) Davies, H. M. L.; Kong, N. *Tetrahedron Lett* **1997**, *38*, 4203.
- (182) Chifotides, H. T.; Dunbar, K. R. *Accounts Chem Res* **2005**, *38*, 146.
- (183) Bickley, J. F.; Bonar-Law, R. P.; Femoni, C.; MacLean, E. J.; Steiner, A.; Teat, S. J. *J Chem Soc Dalton* **2000**, *22*, 4025.
- (184) Bonar-Law, R. P.; McGrath, T. D.; Singh, N.; Bickley, J. F.; Femoni, C.; Steiner, A. *J Chem Soc Dalton* **2000**, *23*, 4343.
- (185) Bonar-Law, R. P.; McGrath, T. D.; Singh, N.; Bickley, J. F.; Steiner, A. *Chem Commun* **1999**, *24*, 2457.
- (186) Taber, D. F.; Meagley, R. P.; Louey, J. P.; Rheingold, A. L. *Inorg Chim Acta* **1995**, *239*, 25.
- (187) Candeias, N. R.; Carias, C.; Gomes, L. F. R.; Andre, V.; Duarte, M. T.; Gois, P. M. P.; Afonso, C. A. M. *Adv Synth Catal* **2012**, *354*, 2921.
- (188) Sahu, B.; Sacui, I.; Rapireddy, S.; Zanutti, K. J.; Bahal, R.; Armitage, B. A.; Ly, D. H. *J Org Chem* **2011**, *76*, 5614.
- (189) Zhang, A. J.; Russell, D. H.; Zhu, J. P.; Burgess, K. *Tetrahedron Lett* **1998**, *39*, 7439.
- (190) Cotton, F. A.; Felthouse, T. R. *Inorg Chem* **1980**, *19*, 323.
- (191) Cotton, F. A.; Felthouse, T. R. *Inorg Chem* **1980**, *19*, 2347.
- (192) Cotton, F. A.; Dikarev, E. V.; Petrukhina, M. A.; Stiriba, S. E. *Inorg Chem* **2000**, *39*, 1748.

- (193) Lo Schiavo, S.; Serroni, S.; Puntoriero, F.; Tresoldi, G.; Piraino, P. *Eur J Inorg Chem* **2002**, 79.
- (194) Christoph, G. G.; Koh, Y. B. *J Am Chem Soc* **1979**, 101, 1422.
- (195) Padwa, A.; Austin, D. J. *Angewandte Chemie-International Edition in English* **1994**, 33, 1797.
- (196) Felczak, K.; Miazga, A.; Poznanski, J.; Bretner, M.; Kulikowski, T.; Dzik, J. M.; Golos, B.; Zielinski, Z.; Ciesla, J.; Rode, W. *J Med Chem* **2000**, 43, 4647.
- (197) Gjonaj, L.; Roelfes, G. *Org Biomol Chem* **2015**, 13, 6059.
- (198) Brown, D. M.; Schell, P. *J Chem Soc* **1965**, 208.
- (199) Oka, Y.; Takei, F.; Nakatani, K. *Chem Commun* **2010**, 46, 3378.
- (200) Politzer, P.; Murray, J. S. *The Chemistry of Hydroxylamines, Oximes and Hydroxamic Acids*; John Wiley & Sons, **2011**; Vol. 2.
- (201) Jencks, W. P. *Prog Phys Org Chem* **1964**, 2, 63.
- (202) Rossi, S.; Salvatori, A.; Peruzzi, G. *Farmaco-Ed Sci* **1979**, 34, 486.
- (203) Chen, Y. L.; Chen, I. L.; Lu, C. M.; Tzeng, C. C.; Tsao, L. T.; Wang, J. P. *Bioorgan Med Chem* **2003**, 11, 3921.
- (204) Maly, D. J.; Choong, I. C.; Ellman, J. A. *P Natl Acad Sci USA* **2000**, 97, 2419.
- (205) Dirksen, A.; Hackeng, T. M.; Dawson, P. E. *Angew Chem Int Ed* **2006**, 45, 7581.
- (206) Jencks, W. P. *J Am Chem Soc* **1959**, 81, 475.
- (207) Cordes, E. H.; Jencks, W. P. *J Am Chem Soc* **1962**, 84, 826.
- (208) Dirksen, A.; Dawson, P. E. *Bioconjugate Chem* **2008**, 19, 2543.
- (209) Crisalli, P.; Kool, E. T. *J Org Chem* **2013**, 78, 1184.
- (210) Crisalli, P.; Kool, E. T. *Org Lett* **2013**, 15, 1646.
- (211) Kool, E. T.; Park, D. H.; Crisalli, P. *J Am Chem Soc* **2013**, 135, 17663.
- (212) Kool, E. T.; Crisalli, P.; Chan, K. M. *Org Lett* **2014**, 16, 1454.
- (213) Schmidt, P.; Zhou, L. N.; Tishinov, K.; Zimmermann, K.; Gillingham, D. *Angew Chem Int Ed* **2014**, 53, 10928.
- (214) EnCor Biotechnology Inc. - <http://encorbio.com/protocols/Prot-MW-Abs.htm>.
- (215) Kurian, J. R.; Bajad, S. U.; Miller, J. L.; Chin, N. A.; Trepanier, L. A. *J Pharmacol Exp Ther* **2004**, 311, 1171.
- (216) Wang, K.; Guengerich, F. P. *Chem Res Toxicol* **2013**, 26, 993.
- (217) Akine, S.; Sairenji, S.; Taniguchi, T.; Nabeshima, T. *J Am Chem Soc* **2013**, 135, 12948.

- (218) Anbu, S.; Kamalraj, S.; Varghese, B.; Muthumary, J.; Kandaswamy, M. *Inorg Chem* **2012**, *51*, 5580.
- (219) Akine, S.; Sunaga, S.; Nabeshima, T. *Chem-Eur J* **2011**, *17*, 6853.
- (220) Klima, J.; Polasek, M.; Ludvik, J.; Urban, J. *J Heterocyclic Chem* **2012**, *49*, 1202.
- (221) Kulla, E.; Zuman, P. *Org Biomol Chem* **2008**, *6*, 3771.
- (222) K. Bowden, F. A. E.-K., N. S. Nadvi *J. Chem. Soc., Perkin Trans. 2* **1979**, *5*, 642.
- (223) Wolfenden, R.; Jencks, W. P. *J Am Chem Soc* **1961**, *83*, 2763.
- (224) Walter, N. G.; Burke, J. M. *Rna* **1997**, *3*, 392.
- (225) Lewis, W. G.; Magallon, F. G.; Fokin, V. V.; Finn, M. G. *J Am Chem Soc* **2004**, *126*, 9152.
- (226) Johansson, M. K.; Cook, R. M. *Chem-Eur J* **2003**, *9*, 3466.
- (227) Koenig, K.; Schneckenburger, H. *Journal of Fluorescence* **1994**, *4*, 17.
- (228) Hayashida, O.; Kaku, Y. *J Org Chem* **2013**, *78*, 10437.
- (229) Patterson, D. M.; Nazarova, L. A.; Prescher, J. A. *Acs Chem Biol* **2014**, *9*, 592.
- (230) Selvaraj, R.; Fox, J. M. *Curr Opin Chem Biol* **2013**, *17*, 753.
- (231) Arnold, Z.; Budesinsky, M. *J Org Chem* **1988**, *53*, 5352.
- (232) Budesinsky, M.; Fiedler, P.; Arnold, Z. *Synthesis-Stuttgart* **1989**, 858.
- (233) Adams, C. M.; Schemenaur, J. E.; Crawford, E. S.; Joslin, S. A. *Synthetic Commun* **1992**, *22*, 1385.
- (234) Liffourrena, A. S.; Lucchesi, G. I. *Int Biodeter Biodegr* **2014**, *90*, 88.
- (235) Schmidt, P.; Stress, C.; Gillingham, D. *Chem Sci* **2015**, *6*, 3329.
- (236) Maly, D. J.; Allen, J. A.; Shokat, K. M. *J Am Chem Soc* **2004**, *126*, 9160.
- (237) Statsuk, A. V.; Maly, D. J.; Seeliger, M. A.; Fabian, M. A.; Biggs, W. H.; Lockhart, D. J.; Zarrinkar, P. P.; Kuriyan, J.; Shokat, K. M. *J Am Chem Soc* **2008**, *130*, 17568.
- (238) Collins, B. E.; Sorey, S.; Hargrove, A. E.; Shabbir, S. H.; Lynch, V. M.; Anslyn, E. V. *J Org Chem* **2009**, *74*, 4055.
- (239) Ni, W. J.; Kaur, G.; Springsteen, G.; Wang, B. H.; Franzen, S. *Bioorg Chem* **2004**, *32*, 571.
- (240) Adamczyk-Wozniak, A.; Borys, K. M.; Madura, I. D.; Pawelko, A.; Tomecka, E.; Zukowski, K. *New J Chem* **2013**, *37*, 188.
- (241) Liu, C. T.; Tomsho, J. W.; Benkovic, S. J. *Bioorgan Med Chem* **2014**, *22*, 4462.
- (242) Smoum, R.; Rubinstein, A.; Dembitsky, V. M.; Srebnik, M. *Chem Rev* **2012**, *112*, 4156.

- (243) Chalker, J. M.; Wood, C. S. C.; Davis, B. G. *J Am Chem Soc* **2009**, *131*, 16346.
- (244) Yusop, R. M.; Unciti-Broceta, A.; Johansson, E. M. V.; Sanchez-Martin, R. M.; Bradley, M. *Nat Chem* **2011**, *3*, 239.
- (245) Dowlut, M.; Hall, D. G. *J Am Chem Soc* **2006**, *128*, 4226.
- (246) Pal, A.; Berube, M.; Hall, D. G. *Angew Chem Int Ed* **2010**, *49*, 1492.
- (247) Ellis, G. A.; Palte, M. J.; Raines, R. T. *J Am Chem Soc* **2012**, *134*, 3631.
- (248) Chang, M. C. Y.; Pralle, A.; Isacoff, E. Y.; Chang, C. J. *J Am Chem Soc* **2004**, *126*, 15392.
- (249) Dickinson, B. C.; Chang, C. J. *J Am Chem Soc* **2008**, *130*, 9638.
- (250) Hutin, M.; Bernardinelli, G.; Nitschke, J. R. *Chem-Eur J* **2008**, *14*, 4585.
- (251) Arnal-Herault, C.; Pasc, A.; Michau, M.; Cot, D.; Petit, E.; Barboiu, M. *Angew Chem Int Ed* **2007**, *46*, 8409.
- (252) Perez-Fuertes, Y.; Kelly, A. M.; Johnson, A. L.; Arimori, S.; Bull, S. D.; James, T. D. *Org Lett* **2006**, *8*, 609.
- (253) Tickell, D. A.; Mahon, M. F.; Bull, S. D.; James, T. D. *Org Lett* **2013**, *15*, 860.
- (254) Cal, P. M. S. D.; Frade, R. F. M.; Chudasama, V.; Cordeiro, C.; Caddick, S.; Gois, P. M. P. *Chem Commun* **2014**, *50*, 5261.
- (255) Cal, P. M. S. D.; Vicente, J. B.; Pires, E.; Coelho, A. V.; Veiros, L. F.; Cordeiro, C.; Gois, P. M. P. *J Am Chem Soc* **2012**, *134*, 10299.
- (256) Dewar, M. J. S.; Dougherty, R. C. *J Am Chem Soc* **1964**, *86*, 433.
- (257) Dunn, H. E.; Catlin, J. C.; Snyder, H. R. *J Org Chem* **1968**, *33*, 4483.
- (258) Mears, R. J.; Sailes, H. E.; Watts, J. P.; Whiting, A. *J Chem Soc Perk T 1* **2000**, *19*, 3250.
- (259) Li, M.; Ge, H. B.; Arrowsmith, R. L.; Mirabello, V.; Botchway, S. W.; Zhu, W. H.; Pascu, S. I.; James, T. D. *Chem Commun* **2014**, *50*, 11806.
- (260) Carey F. A.; Sundberg R. J. *Advanced Organic Chemistry*; 5th Ed.; Springer: New York, **2007**.
- (261) Hine, J.; Zeigler, J. P.; Johnston, M. *J Org Chem* **1979**, *44*, 3540.
- (262) Achilli, C.; Ciana, A.; Fagnoni, M.; Balduini, C.; Minetti, G. *Cent Eur J Chem* **2013**, *11*, 137.
- (263) Yuen, A. K. L.; Hutton, C. A. *Tetrahedron Lett* **2005**, *46*, 7899.
- (264) Hall, D. G. *Boronic Acids - Preparation and Applications in Organic Synthesis, Medicine and Materials*; 2nd Ed.; Wiley-VCH: Weinheim, **2011**.
- (265) Song, Y. L.; Morin, C. *Synlett* **2001**, *2*, 266.

- (266) Coutts, S. J.; Adams, J.; Krolikowski, D.; Snow, R. J. *Tetrahedron Lett* **1994**, *35*, 5109.
- (267) Cruse J. M.; E, L. R. *Atlas of Immunology*; 3rd Ed.; CRC Press: Florida, **2010**.
- (268) Ryu, Z. H.; Lee, S. W.; D'Souza, M. J.; Yaakoubd, L.; Feld, S. E.; Kevill, D. N. *Int J Mol Sci* **2008**, *9*, 2639.
- (269) Spivey, A. C.; Arseniyadis, S. *Angew Chem Int Ed* **2004**, *43*, 5436.
- (270) Dean J. A. *Lange's Handbook of Chemistry*; 15th Ed.; McGraw-Hill, Inc.: New York, **1998**.
- (271) Ishiyama, T.; Murata, M.; Miyaura, N. *J Org Chem* **1995**, *60*, 7508.
- (272) Christophersen, C.; Begtrup, M.; Ebdrup, S.; Petersen, H.; Vedso, P. *J Org Chem* **2003**, *68*, 9513.
- (273) Molander, G. A.; Trice, S. L. J.; Kennedy, S. M.; Dreher, S. D.; Tudge, M. T. *J Am Chem Soc* **2012**, *134*, 11667.
- (274) Henderson, J. N.; Ai, H. W.; Campbell, R. E.; Remington, S. J. *P Natl Acad Sci USA* **2007**, *104*, 6672.
- (275) Adamczyk-Wozniak, A.; Borys, K. M.; Czerwinska, K.; Gierczyk, B.; Jakubczyk, M.; Madura, I. D.; Sporzynski, A.; Tomecka, E. *Spectrochim Acta A* **2013**, *116*, 616.
- (276) Rose, K. *J Am Chem Soc* **1994**, *116*, 30.
- (277) Kitov, P. I.; Vinals, D. F.; Ng, S.; Tjhung, K. F.; Derda, R. *J Am Chem Soc* **2014**, *136*, 8149.
- (278) Kowada, T.; Maeda, H.; Kikuchi, K. *Chem. Soc. Rev.* **2015**, *44*, 4953.
- (279) Loudet, A.; Burgess, K. *Chem Rev* **2007**, *107*, 4891.
- (280) Boens, N.; Leen, V.; Dehaen, W. *Chem Soc Rev* **2012**, *41*, 1130.
- (281) Gagnon, P.; Huang, X. C.; Therrien, E.; Keillor, J. W. *Tetrahedron Lett* **2002**, *43*, 7717.
- (282) Lou, Y.; Remarchuk, T. P.; Corey, E. J. *J Am Chem Soc* **2005**, *127*, 14223.
- (283) Lelais, G.; Campo, M. A.; Kopp, S.; Seebach, D. *Helv Chim Acta* **2004**, *87*, 1545.
- (284) Bitan, G.; Muller, D.; Kasher, R.; Gluhov, E. V.; Gilon, C. *J Chem Soc Perk T 1* **1997**, *10*, 1501.
- (285) Kurosawa, W.; Kan, T.; Fukuyama, T. *Org. Synth.* **2002**, *79*, 186.
- (286) Bialy, L.; Diaz-Mochon, J. J.; Specker, E.; Keinicke, L.; Bradley, M. *Tetrahedron* **2005**, *61*, 8295.
- (287) Sakaguchi, H.; Tokuyama, H.; Fukuyama, T. *Org Lett* **2008**, *10*, 1711.
- (288) Grover, G. N.; Lee, J.; Matsumoto, N. M.; Maynard, H. D. *Macromolecules* **2012**, *45*, 4958.

- (289) Cheng, Y. A.; Chen, T.; Tan, C. K.; Heng, J. J.; Yeung, Y. Y. *J Am Chem Soc* **2012**, *134*, 16492.
- (290) Fruit, C.; Muller, P. *Helv Chim Acta* **2004**, *87*, 1607.
- (291) Dillon, B. R.; Roberts, D. F.; Entwistle, D. A.; Glossop, P. A.; Knight, C. J.; Laity, D. A.; James, K.; Praquin, C. F.; Strang, R. S.; Watson, C. A. L. *Org Process Res Dev* **2012**, *16*, 195.
- (292) Brodsky, B. H.; Du Bois, J. *Chem Commun* **2006**, *45*, 4715.
- (293) Hoffman, R. V.; Huizenga, D. J. *J Org Chem* **1991**, *56*, 6435.
- (294) Roßbach, J.; Baumeister, J.; Harms, K.; Koert, U. *Eur J Org Chem* **2013**, *4*, 662.
- (295) Qi, H. Z.; Li, X. Y.; Xu, J. X. *Org Biomol Chem* **2011**, *9*, 2702.
- (296) Choi, M. K. W.; Yu, W. Y.; Che, C. M. *Org Lett* **2005**, *7*, 1081.
- (297) Avitabile, C.; Moggio, L.; D'Andrea, L. D.; Pedone, C.; Romanelli, A. *Tetrahedron Lett* **2010**, *51*, 3716.
- (298) Su, W.; Mishra, R.; Pfeuffer, J.; Wiesmuller, K. H.; Ugurbil, K.; Engelmann, J. *Contrast Media Mol I* **2007**, *2*, 42.
- (299) Haris, S. P.; Zhang, Y.; Le Bourdonnec, B.; McCurdy, C. R.; Portoghese, P. S. *J Med Chem* **2007**, *50*, 3392.
- (300) Nieto, L.; Mascaraque, A.; Miller, F.; Glacial, F.; Martinez, C. R.; Kaiser, M.; Brun, R.; Dardonville, C. *J Med Chem* **2011**, *54*, 485.
- (301) Sella, E.; Shabat, D. *Org Biomol Chem* **2013**, *11*, 5074.